

GEOLOGICA ULTRAIECTINA

Mededelingen van de
Faculteit Aardwetenschappen der
Rijksuniversiteit te Utrecht

No. 101

**THE BAMBLE AMPHIBOLITE TO GRANULITE FACIES
TRANSITION ZONE, NORWAY**

T.G. Nijland

GEOLOGICA ULTRAIECTINA

Mededelingen van de
Faculteit Aardwetenschappen der
Rijksuniversiteit te Utrecht

No. 101

THE BAMBLE AMPHIBOLITE TO GRANULITE FACIES TRANSITION ZONE, NORWAY

CIP-GEGEVENS KONINKLIJKE BIBLIOTHEEK, DEN HAAG

Nijland, Teunis Gerrit

The Bamble amphibolite to granulite facies transition zone, Norway / Teunis Gerrit Nijland. - Utrecht :
Faculteit Aardwetenschappen der Rijksuniversiteit Utrecht.
- (Geologica Ultraiectina, ISSN 0072-1026 ; no. 101)
Proefschrift Rijksuniversiteit Utrecht. - Met lit. op. -
Met samenvatting in het Nederlands
ISBN 90-71577-56-2
Trefw.: Noorwegen; geologie.

THE BAMBLE AMPHIBOLITE TO GRANULITE FACIES TRANSITIONS ZONE, NORWAY

**DE BAMBLE AMFIBOLIET NAAR GRANULIET FACIES OVERGANGSZONE,
NOORWEGEN**

(MET EEN SAMENVATTING IN HET NEDERLANDS)

PROEFSCHRIFT

**TER VERKRIJGING VAN DE GRAAD VAN DOCTOR
AAN DE RIJSUNIVERSITEIT TE UTRECHT
OP GEZAG VAN DE RECTOR MAGNIFICUS, PROF.DR. J.A. VAN GINKEL,
INGEVOLGE HET BESLUIT VAN HET COLLEGE VAN DEKANEN
IN HET OPENBAAR TE VERDEDIGEN OP MAANDAG
17 MEI 1993 DES NAMIDDAGS OM 12.45 UUR**

DOOR

**TEUNIS GERRIT NIJLAND
GEBOREN OP 11 JANUARI 1967, TE ZWOLLE**

PROMOTOR:
CO-PROMOTOR:

PROF.DR. R.D. SCHUILING
DR. C. MAIJER

EXAMINING COMMITTEE:

PROF. DR. T. ANDERSEN (Oslo)
PROF. DR. V.I. FONAREV (Chernogolovka, Moscow)
PROF. DR. I.S. OEN (Amsterdam)
DR. I.C. STARMER (London)
PROF. DR. J.L.R. TOURET (Amsterdam)

CONTENTS

Chapter 1. Some introductory remarks on the geology of the Baltic Shield	10
1.1 Precambrian geology	10
1.2 Southwestern Scandinavia	11
1.3 The Bamble Sector: In geological focus since Viking times	17
1.4 The Central Bamble Sector	17
1.4.1 Lithological relationships	17
1.4.2 Metamorphic petrology and geochemistry	21
Appendix to chapter 1. Coordinates of critical exposures	22
Chapter 2. Sveconorwegian granulite facies metamorphism of polyphase migmatites and basic dikes, South Norway	23
Abstract	23
2.1 Introduction and geological setting	23
2.2 Relations between migmatization and deformation	25
2.3 Metamorphic aspects	30
2.4 P-T estimates	30
2.4.1 Method	30
2.4.2 Mineral chemistry	32
2.4.3 Results	32
2.5 Discussion and conclusions	33
Chapter 3. The regional amphibolite to granulite facies transition at Arendal, Norway: Evidence for a thermal dome	36
Abstract	36
3.1 Introduction	37
3.2 Regional petrology	37
3.3 Metamorphic index minerals	40
3.3.1 Orthopyroxene	40
3.3.2 Cordierite	41
3.3.3 Allanite and titanite	42
3.3.4 Kyanite	43
3.3.5 Sillimanite	44
3.3.6 Other high grade index minerals and chemical fossils	45
3.3.7 Index minerals in calcsilicate and carbonate rocks	45
3.3.8 Index minerals in late Sveconorwegian granitic sheets	45
3.3.9 Index minerals of low grade metamorphism	46
3.4 P-T distribution	47
3.4.1 Temperature	48
3.4.2 Pressure	57
3.4.3 P-T gradients	60
3.5 Discussion	61
3.5.1 The nature of granulite facies metamorphism	61
3.5.2 Age and geotectonic considerations	64
3.6 Conclusions	65
Chapter 4. Halogen geochemistry of fluid during amphibolite-granulite metamorphism as indicated by apatite and hydrous silicates in basic rocks from the Bamble Sector, South Norway	66
Abstract	66
4.1 Introduction and geological background	66
4.1.1 Halogen geochemistry and petrology	66
4.1.2 The Bamble Sector	68

4.2 Analytical methods	70
4.3 Results	70
4.3.1 Apatite	70
4.3.2 Biotite	80
4.3.3 Amphibole	80
4.3.4 Titanite	81
4.4 Discussion	81
4.4.1 Halogen behaviour in apatite	81
4.4.2 Halogen distribution among apatite and hydrous silicates	82
4.4.3 Halogen fugacities	83
4.4.4 Fluorine and chlorine patterns	84
4.4.5 Implications for amphibolite-granulite transition	88
4.5 Conclusions	89
Chapter 5. Crystal chemistry of hornblende and biotite as indicators of metamorphic conditions in the Bamble Sector, South Norway	91
Abstract	91
5.1 Introduction	91
5.1.1 Amphibole and biotite	91
5.1.2 The Bamble Sector	92
5.2 Method	93
5.3. Results	93
5.3.1 Hornblende chemistry	93
5.3.2 Hornblende chemistry versus metamorphic grade	95
5.3.3 Biotite chemistry	99
5.3.4 Biotite chemistry versus metamorphic grade	101
5.3.5 Fe ²⁺ -Mg and Ti distribution between hornblende and biotite	101
5.4 Discussion	105
5.5 Conclusions	107
Chapter 6. Metamorphic petrology of the Froland corundum-bearing rocks: The cooling and uplift history of the Bamble Sector, South Norway	108
Abstract	108
6.1 Introduction	108
6.2 Petrography	110
6.2.1 Oldest mineral assemblage (M I)	110
6.2.2 Kyanite-bearing veinlets (M II)	110
6.2.3 Margaritization reaction (M III)	113
6.2.4 Low grade assemblages (M IV)	113
6.2.5 Lowest grade alteration (M V)	113
6.3 Mineral chemistry	115
6.3.1 Aluminum silicates	115
6.3.2 Corundum	115
6.3.3 Biotite	117
6.3.4 Margarite	117
6.3.5 Muscovite s.l.	117
6.3.6 Plagioclase and scapolite	118
6.3.7 Rutile	118
6.3.8 Chlorite	118
6.4 Reaction history and P-T path	118
6.4.1 Thermal climax (M I)	118
6.4.2 Initial cooling (M II)	119
6.4.3 Uplift and further cooling (M III)	120
6.4.4 Late stage cooling (MIV & M V)	122
6.4.5 Retrograde P-T path	122
6.5 Time constraints	124

6.6 Tectonic history	125
Chapter 7. Nature and heat source of metamorphism in the Bamble Sector, South Norway, and implications for the geodynamic evolution of the Southwest Scandinavian Domain	127
7.1 Nature and heat source of metamorphism in Bamble	127
7.2 The Bamble Sector in relation to the geodynamic evolution of the Southwest Scandinavian Domain	131
7.2.1 Pre-Gothian to Early Gothian: Deposition and subduction	133
7.2.2 Mid to Late Gothian: Metamorphism below and deposition above	135
7.2.3 Late to Post-Gothian: Metamorphism in formerly upper segments	135
7.2.4 Gothian-Sveconorwegian interlude	136
7.2.5 Main Sveconorwegian: Renewed subduction, deposition and metamorphism	136
7.2.6 Late Sveconorwegian: Post-tectonic intrusions	137
References	139
Appendix	157
Summary	161
Samenvatting	162
Acknowledgements	164
Chapter 2 has been published in the Journal of Geology, vol. 99, p. 515–525. Co-author: A. Senior.	
Chapter 3 with parts of chapter 5 has been accepted for publication by the Neues Jahrbuch für Mineralogie. Co-author: C. Maijer.	
Chapter 4 has been accepted for publication by Lithos. Co-authors: J.B.H. Jansen and C. Maijer.	
Chapter 6 has been accepted for publication by Norges geologiske undersøkelse Bulletin. Co-authors: F. Liauw, D. Visser, C. Maijer and A. Senior.	

*... waar het wereldstof
aanvankelijk gestrooid en zwevend was
in doffen stilstand of al aangevat
door plotseling bezinken schoksgewijs
bijeën liep en ging vloeien ...*

Leopold

SOME INTRODUCTORY REMARKS ON THE GEOLOGY OF THE BALTIC SHIELD

1.1

Precambrian geology

The Baltic Shield is one of the large Precambrian cratons that still constitute the cores of present day continents. The Precambrian (Prior to 0.59 Ga) cratons are of great importance in unravelling the early history of the earth. Another interesting aspect of these cratons is that they provide us with sections through the roots of orogens, whereas younger mountain chains usually only display higher level sections.

One of the main questions regarding Precambrian geology is to what extent its features may be explained in terms of present day plate tectonic processes. The absence of direct evidence for the closure of oceanic basins, the obduction of ophiolites and HP-LT metamorphic assemblages lead many to reject plate collision models for pre-Eocambrian times (e.g. Baer 1981, Etheridge et al. 1987). However, the presence of Proterozoic (2.7 - 0.59 Ga) blueschists has since been demonstrated (e.g. Liou et al. 1990), while ophiolite slices have also been identified (e.g. Park 1983, Kontinen 1987, Vuollo and Piirianen 1989, Dobretsov et al. 1992). Although similar tectonic processes may have been operative in Proterozoic and Phanerozoic (Post 0.59 Ga) times, crustal formation seems to have been different in Proterozoic belts: In contrast to most of their Phanerozoic counterparts, which are mainly made up by reworked crust, the Proterozoic belts contain large volumes of juvenile crust in restricted regions, whereas sutures have been obscured or transformed, and ophiolites occupy within terrane positions rather than being situated along sutures (Samson and Patchett 1991).

HP metamorphic assemblages have not been reported from southern Scandinavia up to now, but relic eclogites of Grenvillian (1.25-0.9 Ga) age occur in Scotland (Sanders et al. 1984, Sanders 1989) and the Grenville Province (Grant 1989, Indares 1992), and have also been reported from the contemporaneous Llano Orogen in Texas (Wilkerson et al. 1988). Evidence for their former existence in southern Norway may have been wiped out by subsequent granulite facies metamorphism and slow uplift after prolonged burial.

Palaeomagnetic data for the Mid Proterozoic have been interpreted in terms of one Proterozoic supercontinent (Piper 1982, 1992), but may alternatively be interpreted in terms of colliding plates (cf. Gaál and Gorbatshev 1987). It has been suggested that the Grenville Province, the Sveconorwegian (1.25-0.9 Ga) linear belts of southern Norway and

contemporaneous mobile belts elsewhere represent essentially mega shear zones due to the drift of a supercontinent over subcontinental hot spots (Wynne-Edwards 1976, Davis and Windley 1976). Alternatively, Dewey and Burke proposed a model of Tibetan-like continental collision as early as 1973.

It has been suggested that the P-T-t path which represents the process of basin closure, continental collision and uplift in southern Scandinavia, comprised a much larger time span than observed in modern style plate tectonics: After Gothian continental collision (Demaiffe and Michot 1985, Visser and Senior 1990) following subduction (Smalley and Field 1985), the Bamble Sector sustained prolonged burial until its final uplift during the second part of the Sveconorwegian (ch. 6). Such periods of prolonged burial have recently also been found for other Precambrian terranes (e.g. Enderby Land, Antarctica, Sandiford 1985; Mount Stafford area, Australia, Vernon et al. 1990).

1.2

Southwestern Scandinavia

The Bamble Sector is part of the Southwest Scandinavian Domain (cf. Gaál and Gorbatshev 1987) of the Baltic Shield (Figs. 1.1,4). The Baltic Shield, comprising mainland Norway, Sweden, Finland, the Kola peninsula and Karelia, was mainly accreted between 3.1 and 1.5 Ga. The oldest well established ages are about 3.1 Ga, but Sm-Nd systematics indicate that crustal material was separated from the mantle 3.5 Ga ago or even earlier (Kröner et al. 1981, Jahn et al. 1984). In addition, Svecofennian quartzites contain 3.3 - 3.4 Ga old detrital zircons (Claesson et al. 1991) and Svecofennian lead ores contain a 3.6 Ga old component (Rickard 1978). If the Caledonides are left out of consideration, the Baltic Shield shows an overall younging from NE to SW. This younging is accompanied by a decrease in $^{207}\text{Pb}/^{206}\text{Pb}$ isotopic ratios (Rickard 1978). The evolution of the Baltic Shield is summarized in table 1.1.

The Southwest Scandinavian Domain comprises those parts of southern Norway and Sweden that were mainly accreted / reworked during the Gothian (1.75 - 1.5 Ga) and Sveconorwegian orogenies (1.25 - 0.9 Ga). It was part of the cratonic landmass NENA (Northern Europe - North America; Gower et al. 1990), which comprised not only the Mid Proterozoic terrains of North America and the Baltic Shield, but also parts of Scotland, Ireland, and the Rockall Bank in the Atlantic Ocean (Fig. 1.1). Correlations between southern Norway and the North American Grenville Province have already been suggested by Barth and Dons in 1960, and became gradually better established (e.g. Gower and Owen 1984, Gower 1985, 1990). NENA probably evolved as one single craton since the amalgamation of Archean microcontinents during the Svecofennian (2.0 - 1.8 Ga; Hoffman 1988, Gower et al. 1990). The North American and Baltic terrains show roughly contemporaneous orogenic events. Separate phases of activity have been recognized in both the Grenvillian and Sveconorwegian orogenies. Moore and Thompson (1980) divided the Grenvillian into the Elzevirian and Ottawa orogenies, which were separated by deposition of the Flinton Group sediments. This Flinton Group may be equivalent to the Dal Group and Jotnian supracrustals in Southwest Sweden (cf. Verschure 1985); both orogenies may be correlated with the two orogenic phases of the Sveconorwegian



Fig. 1.1 NENA with its constituting segments. The B denotes Bamble. Modified after Gower et al. (1990).

identified by Starmer (1991).

In the Southwest Scandinavian Domain, the relationship between the Bamble, Kongsberg and Østfold-Stora Le-Marstrand Sectors is nowadays obscured by the Oslo Rift, whereas the Bamble Sector and the Telemark Basement Gneiss Complex are separated by co-located mylonite zones and brittle faults. In the north, the Kongsberg Sector passes into the Telemark Basement Gneiss Complex without any discontinuity. Whereas several authors maintain that the Bamble Sector originally constituted one continuous terrain with the Kongsberg and Østfold-Stora Le-Marstrand Sectors and the Telemark Basement Gneiss Complex (cf. Hageskov 1980, Starmer 1985a, 1990a, 1991), others propose that the terrain west

Table 1.1 Summarized evolution of the Baltic Shield, mainly after Verschure (1985), Gorbatshev and Gaál (1987), Gaál and Gorbatshev (1987) and Krauss and Lindh (1990), with adaptations for the Porsanger (Daly et al. 1991), Eocambrian (Ramberg and Barth 1966, Verschure et al. 1983), Finnmarkian (Sturt et al. 1978), Scandian (Dallmeyer et al. 1988) and Oslo Rifting (Neumann et al. 1986). North American correlations after Gower (1985, 1990) and Rivers and Nunn (1985). Hyphenated dates denote episodes that are not well defined. For discussion of the Hallandian, see Gaál and Gorbatshev (1987). The Porsanger may be correlated with the Grenvillian, but this is not established with certainty (Daly et al. 1991). (Lindh 1982, 1987). This westward younging is also reflected in the K-Ar biotite cooling ages (Fig. 1.2). The geochronology of Southwest Scandinavia is summarized in fig. 1.2.

Episode	Timespan (Ga)	Main features	Metamorphism	North American equivalent	Synonyma
Saamian	3.1 - 2.9	Tonalitic-trondhjemitic intrusions, greenstones			
Lopian	2.9 - 2.65	Tonalitic-trondhjemitic intrusions, greenstones, large volumes added to the crust	LP amphibolite, locally M/HP granulite		Karelia: Rebolian
Supracrustals:					
Karelian					
Lapponian	2.75- 2.45				
SumiSarolian	2.6 - 2.3				
Jatulian	2.5 - 2.3				
Svecofennian	2.0 - 1.8	Tholeiitic volcanics, obducted ophiolites, calcalkaline magmatism	Amphibolite, locally granulite, locally HP	Makkovik	North America: Hudsonian Greenland: Ketilidian Scandinavia: Svecokarelian
TransScandinavian Igneous Belt	1.78- 1.65	Felsic volcanics, monzonitic-granitic plutonics		Trans Labrador Batholith	Scandinavia: Trans Scandinavian Granite Porphyry Belt
Gothian	1.75- 1.5	Mafic and charnockitic intrusions, calcalkaline magmatism	Amphibolite (in W) to greenschist (in E), locally granulite	Labradorian	Scandinavia: Kongsbergian
"Hallandian"	1.5 - 1.4	Mafic intrusions and sporadic granitic magmatism			
Sveconorwegian	1.25- 0.9	Large scale reworking, plate rotation	Amphibolite, locally granulite	Grenvillian	Scandinavia: Dalslandian
"Porsanger"	> 0.8	Magmatism			
Eocambrian (fen)	≈ 0.6	Carbonatitic magmatism			
Caledonian		Nappe tectonics			
Finmarkian	0.54- 0.49				
Scandian	0.43- 0.4				
Oslo Rift	0.3 - 0.24	Rifting, magmatism.			

of the present day Oslo Rift was originally situated north to the terrain east of the Oslo Rift (Torske 1985).

The oldest rocks present in the Southwest Scandinavian Domain are the supracrustals. The Stora Le-Marstrand amphibolites, which were interpreted by the authors to be syndeositional, have a Sm-Nd whole rock age of 1.76 Ga (Åhäll and Daly 1989). O'Nions and Heier (1972) obtained a 1.76 Ga Rb-Sr whole rock reference line for the Håv Formation in the Kongsberg Sector. The Southwest Scandinavian Domain shows an overall E to W younging in the ages of plutonic rocks, which is accompanied by an increase in the $^{87}\text{Sr}/^{86}\text{Sr}$ initial ratios

The depositional environment and tectonic setting of the supracrustal rocks in the Southwest Scandinavian Domain remains rather controversial. Åhäll and Daly (1989) inferred an arc setting for the Østfold-Stora Le-Marstrand supracrustals, which interpretation is supported by the presence of probably bimodal volcanics, turbiditic metagreywacke-like rocks, and pillow lavas (Åhäll 1984). Starmer (1985a) suggested that the Bamble supracrustals were deposited in a basin marginal to the Svecofennian craton, while in contrast Smalley and Field (1985) considered the Telemark supracrustals to have been deposited on oceanic crust.

Almost the entire Southwest Scandinavian domain was accreted and enjoyed metamorphism and deformation during the Gothian (1.75 - 1.5 Ga) Orogeny. This Gothian Orogeny finds its North American counterpart in the Labradorian Orogeny (e.g. Thomas et al. 1985, Rivers and Nunn 1985), and has also been recognized in the Atlantic Ocean, where granulites drilled from the middle of the Rockall Bank yield an age of 1.6 Ga (Roberts et al. 1973, Morton and Taylor 1991). In most of the Southwest Scandinavian Domain, this gneiss forming event occurred at upper amphibolite facies conditions (e.g. Starmer 1985a, 1990a, 1991, Åhäll et al. 1990, Nijland and Senior 1991).

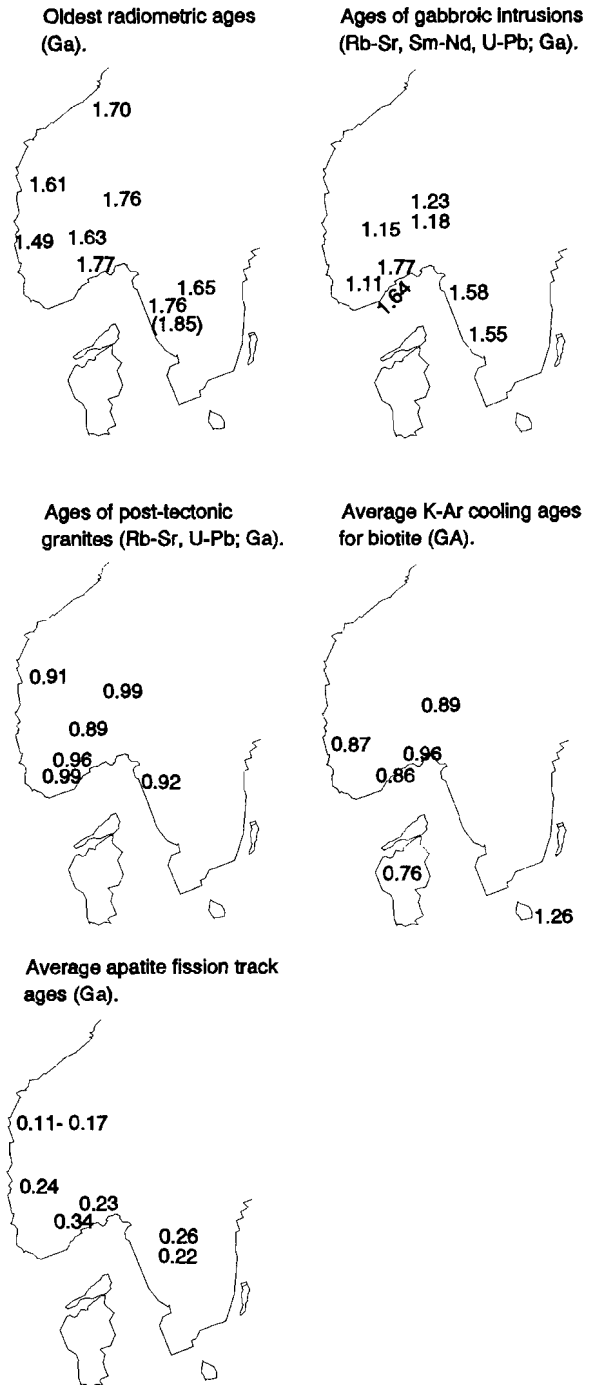
The Gothian terrain extends far north below the Caledonian nappe pile in Norway (e.g. Gorbatshev 1985, Schouenborg et al. 1991). Until recently, it was thought that the Svecofennian terrain of Central Sweden and southern Finland was not reworked during the Gothian Orogeny. Recent age determinations, however, indicate significant Gothian ultramylonitic deformation in southern Finland (Ploegsma 1991). Most of the Gothian basement below the Caledonides was not reworked during the Sveconorwegian Orogeny, but recent age determinations indicate that in Central Norway it was intruded by granitic plutons at c. 1.36 Ga (Fossen and Nissen 1991), i.e. during the period of post-Gothian anorogenic magmatism in the Southwest Scandinavian Domain. In addition, Sveconorwegian rocks are present in some of the Caledonian nappes (Reymer et al. 1980).

Subsequently, the Southwest Scandinavian Domain was variably reworked during the Sveconorwegian Orogeny (1.25 - 0.9 Ga), of which the North American counterpart is the Grenville Orogeny (e.g. Barth and Dons 1960, Gower 1985). Granulites drilled from the southern part of the Rockall Bank have an age of 0.95 Ga (Miller et al. 1973), indicating that the Sveconorwegian front intersects this landmass. Sveconorwegian events also affected northwestern Scotland (Brook et al. 1976, 1977, van Breemen et al. 1978, Brewer et al. 1979, Sanders et al. 1984).

The grade of Sveconorwegian metamorphism in the Southwest Scandinavian Domain has been hotly debated during the last decade (e.g. Field and Råheim 1979, 1981, 1983, Weis and Demaiffe 1983, Field et al. 1985, Kullerud and Dahlgren 1990, Maijer 1990, Kullerud and

Fig. 1.2 Summary of the geochronology of the Southwest Scandinavian Domain.

Compilation of data from the following authors: Oldest ages: Priem et al. (1973), Andresen et al. (1974), Pasteels and Michot (1975), Skjernaas and Pedersen (1982), Mearns (1986), Hansen et al. (1989), Åhäll and Daly (1989), de Haas et al. (1993a). Gabbros: Jacobsen and Heier (1978), Welin et al. (1980), Morvik (1987), Åhäll et al. (1990), Dahlgren et al. (1990), de Haas et al. (1993a). Granites: Brueckner (1972), Priem et al. (1973, 1976), Killeen and Heier (1975ab), Pedersen and Maaløe (1990), Eliasson and Schöberg (1991), Kullerud and Machado (1991). Cooling ages: Kulp and Neumann (1961), O'Nions et al. (1969a), Priem et al. (1970), Larsen (1971), Verschure et al. (1980), de Haas et al. (1992a). Fission tracks: van den Haute (1977), Bos and Andriessen (1985), van Haren and Röhrman (1988), Zeck et al. (1988), Hansen et al. (1989).



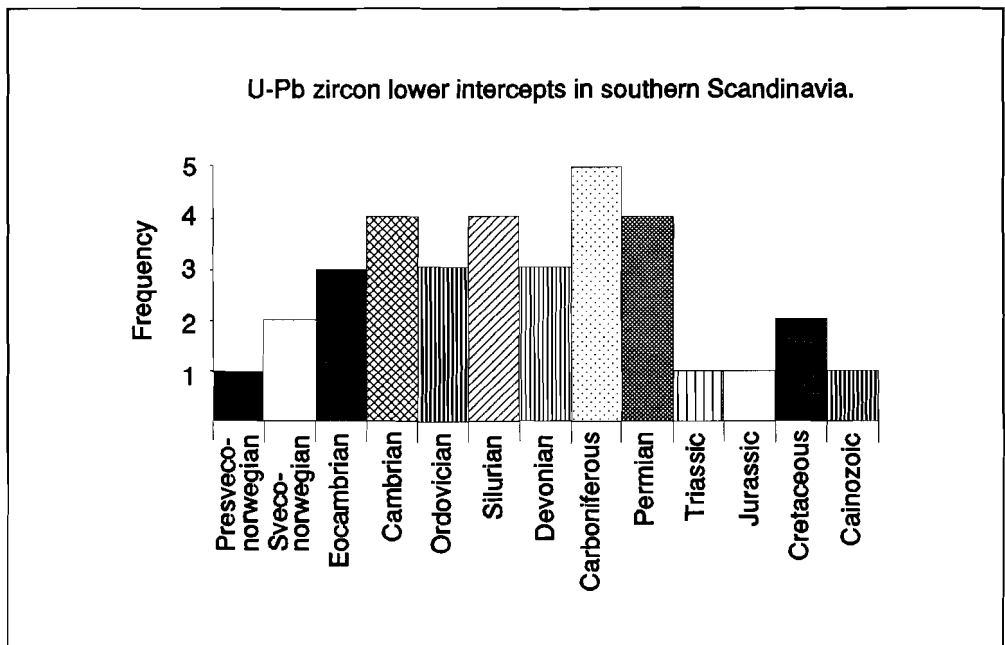


Fig. 1.3 Histogram of the lower intercepts of U-Pb discordia for zircons in the Southwest Scandinavian Domain. Compilation from the following sources: Pasteels and Michot (1975), Welin and Kähr (1980), Wielens et al. (1981), Persson et al. (1983), Lindh and Schöberg (1987, 1988), Johansson and Larsen (1989), Hansen et al. (1989), Johansson (1990), Åhäll (1990), Åhäll et al. (1990), Kullerud and Machado (1991), L. Kullerud (pers. com. 1991), Mansfield (1991).

Machado 1991, Nijland and Senior 1991, Nijland et al. 1991). The high grade nature has been clear in the most western part of the Southwest Scandinavian Domain, the Rogaland Sector (e.g. Maijer et al. 1981). Recently, both structural (Hagelia 1989, Nijland and Senior 1991) and geochronological evidence (Kullerud and Dahlgren 1990, 1993, Johansson et al. 1991) has been provided that the Sveconorwegian reworking involved regional upper amphibolite and granulite facies metamorphism in various parts of the more eastern sectors of the Southwest Scandinavian Domain.

Ultrapotassic magmatism occurred during the late Sveconorwegian (Dahlgren 1991), and during the late Precambrian the crust of southern Norway was penetrated by explosive volcanism related to the Fen peralkaline carbonatite complex (Verschure et al. 1983, 1989). The northern parts of the domain also suffered from Caledonian activity, featured by localized disturbance of isotopic systems and new growth of green biotite (Verschure et al. 1980, Verschure 1982, Sauter et al. 1983). The prehnite-pumpellyite facies overprint present in most of southern Norway is, however, most likely not related to the Caledonian Orogeny, but due to prolonged cooling during post-Sveconorwegian times (Nijland et al. 1993a, ch. 6). Lower U-Pb intercepts of the discordia for zircons from the Southwest Scandinavian Domain do not show preferential resetting during the Caledonian (Fig. 1.3). The major resetting seems to be due to

formation of the Oslo Rift. Limited igneous activity related to the magmatism in the Oslo Rift occurred in the sectors adjacent to the rift (e.g. Bamble, Halvorsen 1970; Kongsberg, Ihlen et al. 1984).

1.3 The Bamble Sector: In geological focus since Viking times.

The Bamble Sector has attracted geological attention since Viking times, when iron and copper ores from the area were already mined; modern geological interest dates back to the mid nineteenth century. The area became known for its iron ores (Kjerulf and Dahll 1861), nickel deposits (A. Bugge 1922), and many apatite mines (Helland 1874, Brøgger and Reusch 1875, Sjögren 1883, Solly 1892) like the Ødegårdens Verk, which was exploited jointly by the Compagnie Française de Mines de Bamle and Bamble A.S. (cf. C. Bugge 1922). An elaborate iron industry was operating around the change of century, but the oldest iron works date back to about 1540 (Vogt 1908). In 1975, Bråstad was the last iron mine to be closed. Many other minerals were also exploited (cf. J. A. W. Bugge 1978). King Christian IV exploited a gold mine at Hisøy (Daubrée 1843, C. Bugge 1934). Radioactive minerals, which were partly sold to Madame Curie, were mined from several pegmatites (Solås 1990). But interest went far beyond the economic aspects of geology, and the area was an object for study by many of the great international geologists of that time, like Scheerer (1848), Michel-Lévy (1878ab) and Lacroix (1889).

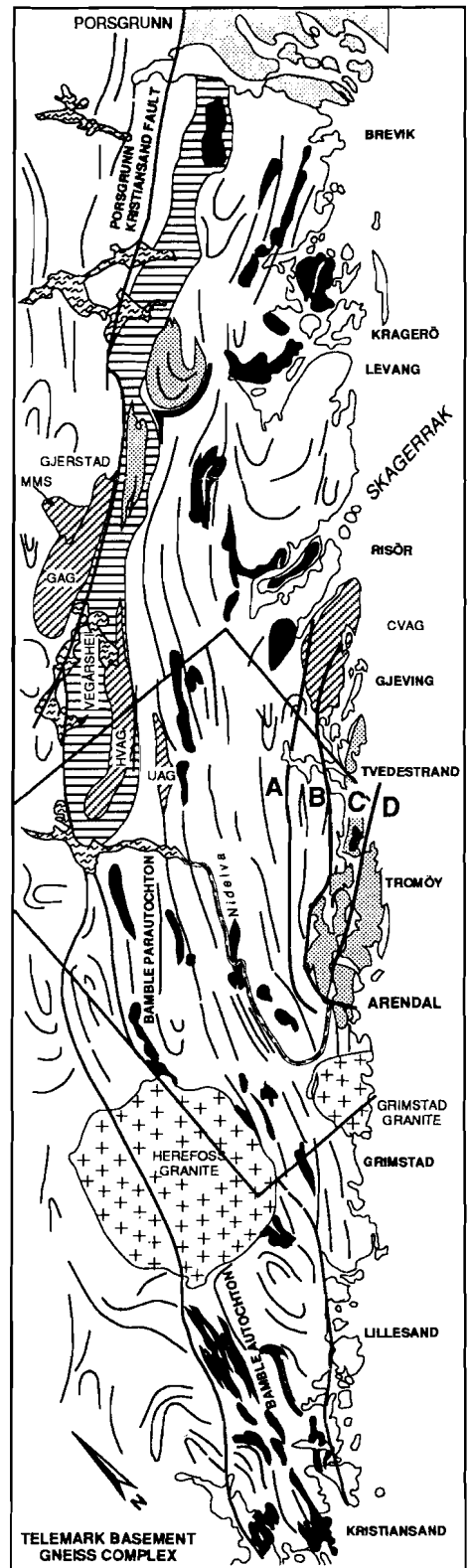
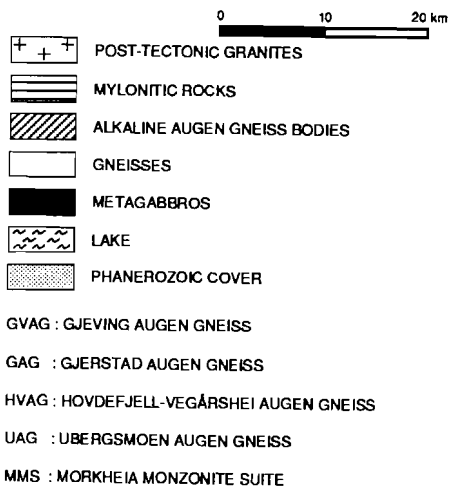
During the first half of this century, the sector was the domain of four Norwegian geologists who made it one of the classical amphibolite - granulite facies transitional terrains, and whose names start with the B of Bamble: Brøgger (1906, 1934ab), Barth (1925, 1928, 1947), A. Bugge (1928, 1936) and J. A. W. Bugge (1940, 1943, 1945). In the same period, the first age estimates were obtained, based on lead abundances (Bakken and Gleditsch 1938). Radiometric age determinations became available as early as the mid-fifties (Holmes et al. 1955). After the second world war, the sector became under investigation by the French (e.g. Touret 1962, 1968, 1971ab, 1985, Moine et al. 1972) and Nottingham/London schools, notably D. Field and I. C. Starmer and coworkers (e.g. Burrell 1966, Starmer 1969, 1972, 1985ab, 1991, Field and Clough 1976, Field et al. 1980, 1985, Lamb et al. 1986), but many individuals worked on their own.

1.4 The Central Bamble Sector

1.4.1 Lithological relationships

Elaborate reviews of the geology of the Bamble Sector have recently been given by Starmer (1985a, 1990, 1991), and there is no point in duplicating his work. However, to

Fig. 1.4 Geological sketch map of the Bamble Sector, modified after Starmer (1985a).



the introduce the reader to the part of the Bamble Sector which is subject of this thesis (Fig. 1.4), i.e. covering the area between Nelaug, Ubergsmoen and Arendal, with Froland in its centre, and the islands of Tromøy, Hisøy and Merdøy, and to report some new aspects of the geology of this area, the lithological relationships as deduced from field work will briefly be outlined below. Superscripts refer to the list of coordinates of critical and/or characteristic exposures attend of this chapter.

The oldest rocks present in the area are the supracrustals. These comprise at least three different suites, whose interrelations could not be established: 1) the Nidelva Quartzite Complex (Nijland et al. 1992a), 2) the Selås Banded Gneisses (Touret 1966), and 3) the Vrakevika-Merdøy Supracrustal Complex. The Nidelva Quartzite Complex consists of variably pure quartzites, amphibolites, sillimanite-bearing nodular gneisses with minor lenses of marbles, Na-rich calcsilicate rocks and cordierite-orthoamphibole rocks, which are commonly considered to represent metaevaporites (Touret 1979, Beeson 1988, Hulzebos-Sijen et al. 1990, Visser et al. 1991) on ground of their chemistry. Pure quartzites have rarely preserved different types of cross bedding ¹, ripple marks and mudcracks ², whereas intraformational, monomict conglomerates ³ also occur (Nijland and Maijer 1991, Nijland et al. 1992a). The more easterly situated Selås Banded Gneisses may represent metamorphosed greywackes ⁴ (Touret 1966). In some of the intercalated amphibolites ⁵, a relic porphyric texture may be recognized (A. Senior pers. com. 1990). The third supracrustal complex is exposed near Vrakevika, on the southeastern edge of Hisøya, and on Merdøya ⁶. The supracrustal rocks on the northwestern tip of Tromøy may also belong to this complex. This complex is characterized by the relatively frequent occurrence of a few cm thick sillimanite-biotite-garnet layers in the quartzites, which may represent old soils (cf. Fujimori and Fyfe 1984). Metaevaporites also occur among these supracrustals (Visser et al. 1991).

Touret (1969) inferred a turbiditic origin for the Selås Banded Gneisses in the Bamble Sector, while Starmer (1985a) suggested that the Bamble supracrustals were deposited in a basin marginal to the Svecofennian craton. In contrast to these marine environments, primary sedimentary structures in the Nidelva Quartzite Complex, and the presence of small occurrences of alleged metaevaporites led Nijland et al. (1992a) to propose a near shore or inland continental basin under (semi) arid conditions as depositional environment for the Nidelva Quartzite Complex. The interpretation of the corundum-bearing gneisses occurring north of Froland (Ofstedahl 1963, Nijland et al. 1993a, ch. 6) as metamorphosed kaolinite-bauxite weathering crusts (Serdyuchenko 1968) may support the inferred depositional environment.

The depositional age of the supracrustals is uncertain. Except the fact that this age has to be older than that of the oldest intruding magmas, the only available estimate is a 1.51 ± 0.06 Ga Pb model age obtained by Moorbath and Vokes (1963) for galenas from the Etedal Pb-Zn-Ag deposit (Krijgsman 1991ab); U-Pb systematics of zircons from quartzites in the same area indicate deposition before 1.4 Ga (Swainbank 1965). The inferred paleoenvironment of the Nidelva Quartzite Complex would hence require the existence of continental crust in this part of southern Scandinavia prior to 1.5 Ga.

The supracrustals have been intruded by granites, tonalites and charno-enderbites. The magmatic origin of many of the latter rocks, the "arendalites" of Bugge (1940), is however

disputed (cf. Moine et al. 1972, Visser et al. 1991). Charno-enderbites at Tromøy are K-depleted. Tonalites have been dated at 1.62 ± 0.22 Ga (Rb-Sr whole rock, Ubergsmoen, Hagelia 1989), whereas the "charno-enderbites" have been dated at 1.59–1.54 Ga (U-Pb zircon, Tromøya, A. Råheim unpubl. data in Lamb et al. 1986; U-Pb zircon, Fløstaøya, Kullerud and Machado 1991).

Both supracrustals and orthogneisses were intruded by monzodioritic magmas like the Vimme amphibolite ⁷. These intrusions cut across the foliation in the gneisses, but are themselves entirely metamorphosed. The supracrustals and gneisses were subsequently intruded by gabbroic magmas like the Jåmmåsknutene ⁸ en Fløsta ⁹ gabbros, which have been dated at 1.77 and 1.64 Ga respectively, but with a large error of c. 0.2 Ga (Sm-Nd whole rock, de Haas et al. 1993a).

Two kinds of ultramafic rocks occur in the area: 1) Those directly related to gabbroic plutons, and 2) Isolated bodies. Isolated ultramafic rocks ¹⁰ occurring in the area are discordant with respect to the main foliation, but otherwise, their relative age remains unclear. They are entirely metamorphosed (Krijgsman 1991c).

Several augen gneiss bodies are present. They are discordant with respect to the two oldest phases of migmatization and deformation (Nijland and Senior 1991, ch. 2). These augen gneisses may have been emplaced around 1.25 Ga (See discussion in Nijland and Senior (1991)). The augen gneisses are mainly situated in the strongly sheared zone at the contact between the Bamble and Telemark Sectors. However, the Ubergsmoen Augen Gneiss may be traced much farther to the southwest ¹¹ than previously thought, at least to the west of the Vestre Dale Gabbro ¹². The augen gneisses contain xenoliths of tonalitic gneisses, amphibolites and layered metagabbro.

Basic dykes cutting both across the two oldest migmatizations and deformation structures outside, and across the augen fabric inside the augen gneisses, occur in the Ubergsmoen Augen Gneiss ¹³ and its contact aureole ¹⁴ (Nijland and Senior 1991, Nijland et al. 1991). Similar basic dykes occur in the Gjeving Augen Gneiss near Risør (Nijland et al. 1991). The dykes have olivine-tholeiitic affinities. A metamorphosed tonalitic dyke has been found in the southwestern extension of the Ubergsmoen Augen Gneiss ¹⁵. This dyke cuts across the augen fabric, but has been folded itself; a new axial cleavage has been developed, which is cut by a late pegmatite.

Large, discordant, northeast-southwest trending bodies of granitic gneisses, often rich in magnetite, Na and K, and low in Ca, occur in the area west of the Nidelva. These granitic gneisses contain large boudins of layered metagabbro ¹⁶. They may either be correlated with the augen gneisses, or with the Holt granite, which is in fact a gneissoid granite. This brackets their age between 1.25 Ga (the assumed age of the augen gneisses) and 1.1 Ga, the whole rock age of the Holt granite (Rb-Sr whole rock, C. Maijer pers. com. 1989). Both the augen gneisses and granitic gneisses follow the main structural trend in the area, whereas the Holt granite is a highly discordant body. Therefore correlation between the first two lithologies seems most likely.

Young gabbros intrude both the older rocks and these granitic gneisses. They have a virtually unmetamorphosed core, and a (garnet)-amphibolitized margin. One of these gabbros, the Vestre Dale Gabbro ¹² has been dated at 1.20 ± 0.01 Ga (Sm-Nd whole rock + Pl + Cpx, de

Haas et al. 1992a). If the small, relatively round outcrop and the absence of magmatic layering may serve as criteria to correlate other gabbros with the Vestre Dale gabbro ¹² (de Haas et al. 1992b), then the Tromøy ¹⁷ and Arendal ¹⁸, Skibbevig ¹⁹ and Klådeborg ²⁰ gabbros probably belong to the same suite; they are discordant with respect to the main foliation.

Discordant basic dykes, preserving a relic ophitic texture and occasionally a flow lamination, have been found in the Blengsvatn and Jåmmåsknutene gabbros ²¹. These olivine-microdolerites have been metamorphosed under upper greenschist to lower amphibolite facies conditions, which resulted in the replacement of almost all mafic minerals by actinolitic hornblende. The age of these dykes is uncertain, but the grade of metamorphism makes it likely that they are older than the low grade metamorphic granitic sheets.

Especially at Tromøya and Hisøya ²², the high grade rocks have been intruded by granitic to granodioritic sheets. These have been dated by Field and Råheim (1979; Rb-Sr whole rock) at 1.06 ± 0.02 Ga. They have only been metamorphosed at low grade (new growth of muscovite; Nijland and Maijer 1992, 1993, ch. 3).

Two types of pegmatites occur in the area: 1) Large, irregular bodies like the Gloshei pegmatite ²³, and 2) Low angle pegmatites (LAP), which are much smaller, usually less than 2 m thick, and intruded along a joint system; these LAP's cut across the granitic sheets ²⁴, and are consequently younger. Type 1) pegmatites have been dated radiometrically. Baadsgaard et al. (1984) obtained an age of 1.06 ± 0.01 Ga (U-Pb euxenite and Rb-Sr whole rock) for the Gloshei pegmatite, seemingly contemporaneous with the granitic sheets, and Neumann (1960) reported U-Pb cleveite ages of 1.09 Ga for the Auselmyra pegmatite, even older than the granitic sheets. The pegmatites, however, do not show any signs of metamorphism.

A discordant leucocratic dyke of tonalitic composition occurs near Øyestad ²⁵. This dyke bears no evidence for metamorphism.

One example of ultrapotassic magmatism, a lamproite dyke, has been found and dated at 1.03 Ga (U-Pb zircon, Dahlgren 1991). The well known Herefoss and Grimstad post tectonic granitic plutons respectively intruded at 0.96 ± 0.06 (Rb-Sr whole rock, Brueckner 1972) and 0.99 ± 0.01 Ga (U-Pb zircon, Kullerud and Machado 1991). During the late Precambrian and Phanerozoic, lamprophyric and microdoleritic dykes have been intruded. A fault breccia of unknown age occurs at Hisøya and Tromøya ²⁶.

1.4.2 Metamorphic petrology and geochemistry

A well developed amphibolite to granulite facies transition zone is situated in the area outlined above (e.g. Bugge 1940, 1943, Touret 1971a). The metamorphic isograd sequence in this transition zone is elaborately dealt with in chapter 3, and includes separate orthopyroxene- in isograds for felsic and basic rocks. The isograd sequence is accompanied by a shift in the composition of fluid inclusions from H₂O to CO₂ in felsic gneisses (Touret 1971b, 1985).

Granulite facies rocks, especially those not directly related to major plutons, attract still increasing amounts of attention, because they are generally considered to represent slices of formerly lower to middle continental crust. The processes resulting in granulite petrogenesis

are still hotly debated, and have recently been reviewed by several authors (e.g. Bohlen 1987, 1991, Harley 1989, Newton 1990, Ashwal et al. 1992). The main processes proposed to be involved are: I. Extraction of water by anatectic melts. II. Dilution of aqueous fluids by the introduction of other species, notably carbon dioxide. III. Metamorphism of already dry rocks. IV. Heating by underplating basic magmas. V. Heating due to crustal doubling by simple shear thrusting during continental collision. VI. Any combination of the fore mentioned processes.

To unravel the different contributions made by the different processes in different terrains, amphibolite to granulite facies transition zones may provide critical information not easily obtained from within large granulite facies areas or from granulitic xenoliths. Therefore, the study of small changes over such a transition zone will be valuable. Oddly, except elaborate fluid inclusion work (Touret 1971b, 1972, 1985), studies of the transition zone in the Bamble Sector almost solely focused on whole rock features like LILE and REE chemistry (Moine et al. 1972, Field and Clough 1976, Cooper and Field 1977, Clough and Field 1980, Field et al. 1980, Smalley et al. 1983a) and stable isotopic systematics (Andreae 1974, Hoefs and Touret 1975, Pineau et al. 1981, Broekmans et al. 1992, 1993, van den Kerkhof et al. 1993). Changes in mineral chemistry over the transition zone have not been investigated, and all major geothermobarometric studies were confined to the granulite facies part of the transition zone. This thesis aims to fill this gap, and to use mineral distributions, chemistry, and relationships to quantify the transition from upper amphibolite to granulite facies rocks in the Bamble Sector, to subsequently attempt to unveil its cause, and finally consider the geological evolution and plate tectonic setting of the transition zone.

Acknowledgements - This paper benefitted from the constructive criticism of G.J.L.M. de Haas, C. Maijer and R.D. Schuiling. Financial support was provided by AWON (NWO 751.353.023).

Appendix to chapter 1. Coordinates of critical exposures.

1 32VMK712926, 701922, 698900, 902893, 692693	14 32VML850024, 854030
2 32VMK715931	15 32VMK823986
3 32VMK767832	16 32VMK732878
4 32VML878075	17 32VMK894795
5 32VML829010	18 32VMK891816
6 32VMK368762, 880762	19 32VMK914843
7 32VML806027	20 32VMK843785
8 32VMK775986	21 32VMK776988, 3777990, 698895
9 32VMK953870	22 32VMK903809
10 32VMK828909, 747995, 815865	23 32VMK841886
11 32VMK823986, 796929, 782907	24 32VMK851783
12 32VMK770894	25 32VMK804748
13 32VML876053	26 32VMK862794, 875796

De draad is zoekgeraakt; het labyrint is ook verdwenen. Nu weten wij zelfs niet of ons een labyrint, een geheime kosmos of een willekeurige chaos omringt. Onze schone plicht is ons in te beelden dat er een labyrint is en een draad.

Borges

SVECONORWEGIAN GRANULITE FACIES METAMORPHISM OF POLYPHASE MIGMATITES AND BASIC DIKES, SOUTH NORWAY

Abstract - Migmatites in the Nelaug-Krossvatnet-Ubergsmoen area in the amphibolite facies part of the Bamble Sector were intruded by the Ubergsmoen Augen Gneiss (UAG) and by younger basic dikes. Both are critical time markers and show that the area underwent two phases of deformation and migmatization during the Gothian Orogeny (1600–1500 Ma) before emplacement of the augen gneiss, and four subsequent phases of deformation during the Sveconorwegian Event (1200–950 Ma), accompanied by amphibolite facies metamorphism and a minor third migmatization. Mineral assemblages in the basic dikes and in the migmatites indicate local granulite facies conditions resulting from lowered aH_2O at nearly constant temperature of $\approx 750^\circ\text{C}$ at 8.7 kb. It is suggested that this granulite facies overprinting was due to the introduction of fluids released during the crystallization of another charnockitic magma at a deeper level.

2.1

Introduction and geological setting

The Bamble Sector along the Skagerrak coast of southern Norway is part of the Mid-Proterozoic of the Baltic shield. The area studied (Fig. 2.1) is within part of the Bamble Sector traditionally regarded as an amphibolite facies terrain in the northwest, with a transition to granulite conditions towards the southeast (Smalley et al. 1983a).

The Bamble Sector was metamorphosed during two orogenies. The first, the Gothian (Kongsbergian) Event, took place between 1600 and 1500 Ma (Starmer 1985a), and was overprinted by the Sveconorwegian Event, which lasted from 1200 to 950 Ma (Field and Råheim 1979, Verschure 1985). The latter has been correlated with the Grenville Province in North America (e.g. Barth and Dons 1960, Gower 1985). A Labradorian Orogeny, contemporaneous with the Gothian Event in southern Scandinavia has recently been recognized in the Grenville Province (Thomas et al. 1985, Gower 1990). In southern Norway, both events were accompanied by the intrusion of basic magmas (de Haas et al. 1990).

Gupta and Johannes (1982) proposed a genetic model for the stromatic migmatites

along the shores of Krossvatnet. The "Nelaug migmatites" were considered to be virtually undeformed to gently deformed and to have formed at 650°C at a presumed pH_2O of 5 kb (Gupta and Johannes 1982, Johannes 1985). They did not mention different phases of migmatization, but the present paper provides evidence for three generations of migmatites. The migmatites may be the migmatized equivalents of the metasedimentary Selås banded gneisses (Touret 1966). The migmatites, of granodioritic to tonalitic composition, contain concordant intercalations of differentiated amphibolite layers and lenses, and small calcsilicate nodules.

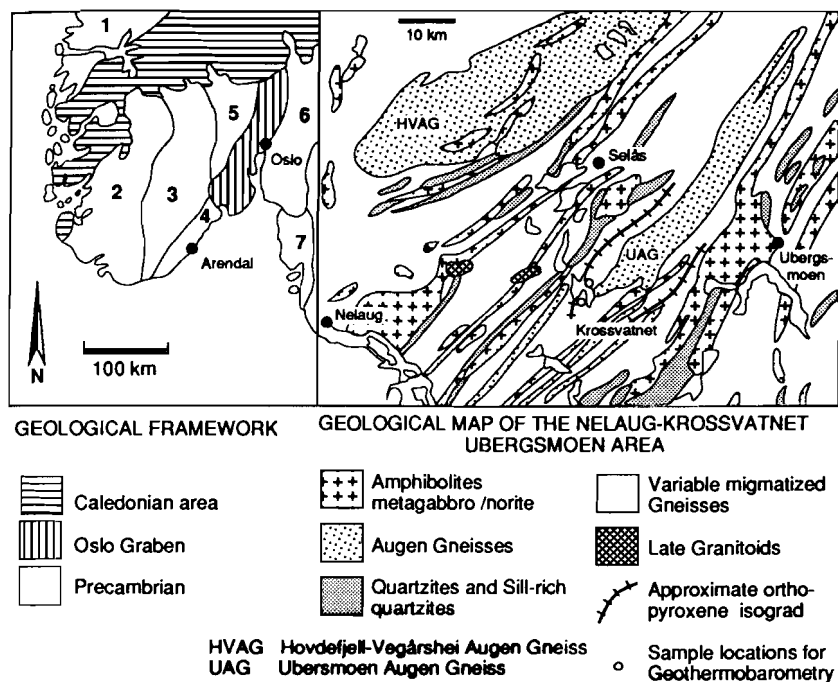


Fig. 2.1 The geological framework of southern Norway (Modified after Verschure (1985)) and a simplified geological map of the Nelaug-Krossvatn-Ubergsmoen area (Mainly after Starmer (1985b) with minor modifications after Hagelia (1989) and Nijland (1989).

The migmatites were intruded by the granitic-charnockitic Ubergsmoen Augen Gneiss (UAG), and by later basic dikes. Radiometric data available for the UAG and similar augen gneiss bodies show three groups of ages: (1) ≈ 1275 Ma, (2) ≈ 1150 Ma, and (3) ≈ 1050 Ma. The UAG yields a Rb-Sr whole rock age of 1143 ± 30 Ma (Hagelia 1989), but a U-Pb zircon age of 1275 Ma (R. Chessex unpub. data quoted in Maijer and Padget (1987)). Migmatites surrounding the UAG give a Rb-Sr age of 1501 ± 63 Ma (Hagelia 1989).

The nearby Hovdefjell-Vegårshei Augen Gneiss (HVAG) yields U-Pb zircon ages of

1127 Ma (R. Chessex unpub. data quoted in Maijer and Padget (1987)) and 1168 ± 2 Ma (A. Råheim unpub. data quoted in Hagelia (1989)), and a Rb-Sr whole rock age of 1276 ± 105 Ma (Field et al. 1985). Model ages of ≈ 1500 Ma have been obtained for the HVAG by Ploquin (1980), who thought them of dubious significance. The Gjerstad Augen Gneiss (GAG) gives a Rb-Sr age of 1237 ± 53 (Smalley et al. 1983b), which was considered by the authors to reflect closure of the Rb-Sr system following high temperature deformation shortly after intrusion. Younger Rb-Sr whole rock ages for the GAG of ≈ 1050 Ma have been interpreted as due to resetting (Smalley et al. 1983b). The Gjeving Augen Gneiss near Risør, considered to be equivalent to the augen gneisses mentioned above (Touret 1968, Starmer 1985a) gives similar reset Rb-Sr ages (1023 ± 90 Ma; Field and Råheim 1979). In this augen gneiss, basic dikes intersecting the augen fabric have also been observed (T.G. Nijland unpubl. data). The Ubergsmoen Augen Gneiss (UAG) and later basic dikes are critical time markers that cut across earlier deformational and migmatitic structures. They provide evidence for two high-grade events in the Nelaug-Ubergsmoen area.

2.2 Relations between migmatization and deformation

The sequence of events is summarized in fig. 2.2. The first generation of leucosomes (MIG 1) is stromatic. The leucosomes are composed of quartz, K-feldspar and plagioclase and are generally bordered by well developed melanosomes, consisting mainly of biotite. In the leucosomes septae of biotite are present, representing relict melanosomes (Gupta and Johannes 1982). The leucosomes have not broken through these septae, which indicates an in situ formation (Gupta and Johannes 1982, Johannes 1988) and immobility of the melts.

The fact that oriented biotite was present prior to the formation of the leucosomes provides evidence for a deformation phase, D 1, preceding this migmatization, although MIG 1 leucosomes and this foliation are now parallel. This D 1 deformation phase caused the development of an S 1 foliation. Some F 1 isoclinal folds have been preserved, and deform compositional layering of possibly sedimentary origin (Touret 1968).

A D 2 deformation folded the S 1 and MIG 1 leucosomes. In the more felsic gneisses, the F 2 folds are isoclinal, while in the more micaceous gneisses they were developed as close to isoclinal chevron folds. Both types of folds are symmetric. A new S 2 foliation was developed, and along axial planes to F 2 folds, new leucosomes were developed (Fig. 2.3). The mineralogical composition and grain size of these MIG 2 leucosomes is similar to that of MIG 1. Away from the fold hinges, these MIG 2 leucosomes are parallel to the MIG 1 leucosomes, and to S 1 and S 2. All of them trend NE-SW and dip steeply. In the intercalated concordant amphibolites a weakly developed L 2 amphibole-lineation is present.

During D 2 rigid blocks, which are internally strongly folded and bounded at their margins by S 2, developed at different scales (at least on outcrop scale, but probably also on a regional scale). All later deformation was concentrated at the margins of such blocks. Due to later flattening, S 2 foliation planes are more closely spaced along these margins.

Boudinage of amphibolites during plastic deformation of their host rocks gave rise to

the formation of agmatite-like structures similar to those described from other parts of the Bamble Sector (A. Bugge 1936, J.A.W. Bugge 1943), due to the accumulation of melt in low stress areas. In zones with less melting, boudinaged amphibolites preserve original fold structures (Fig. 2.4).

At the eastern end of Krossvatnet, a granitic off-shoot of the UAG intruded the migmatites. The contact is diffuse, but clearly cuts D 2 structures. The augen gneiss contains xenoliths of F 2 folded gneiss and of amphibolite. In large parts of the UAG, an S 3 b augen gneiss fabric was developed, but in the southern part only a widely spaced discontinuous S 3 a foliation was developed. The relation between these two parallel fabrics has not yet been established with certainty, but the S 3 b augen gneiss foliation is considered to be a more strongly developed stage of the widely spaced discontinuous S 3 a foliation. In the migmatites, an S 3 b mylonitic foliation has been observed only in discrete zones.

Ga	Deformation		Migmatization	Metamorphism		
1.5	D1 F1 Isoclinal S1 Gneissic		MIG1 Stromatic	Amphibolite	Gothian	
	D2aF2 Isoclinal S2 Gneissic		MIG2 Stromatic			
	D2b Boudinage		MIG2 Agmatic			
1.5						
1.25		Ubergsmoen augen gneiss		Amphibolite	Sveconorwegian	
	D3 S3a Discontinuous S3b Augen/mylonitic					Granulite
		Basic dikes				
	D4 F4 tight S4 Gneissic		MIG3			
1.05	D5 F5 open S5 Crenulation					
	D6 Faulting					

Fig 2.2 Schematic presentation of the sequence of events in the Nelaug-Krossvatn-Ubergsmoen area. For discussion and references of ages, see text.

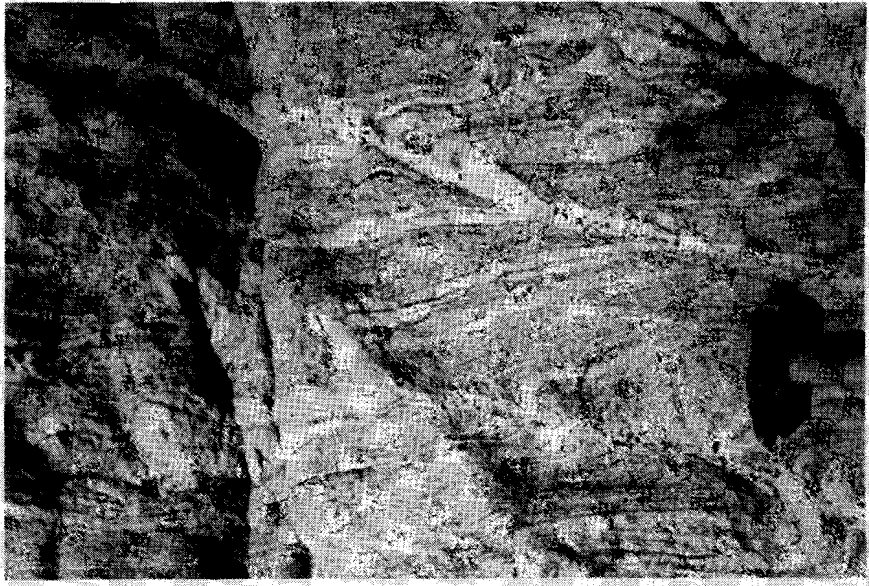


Fig. 2.3 F 2 fold in the migmatites at Krossvatnet with an MIG 2 leucosome parallel to the axial plane.



Fig. 2.4 Boudinaged amphibolite intercalated in the migmatites preserving the outlines of an original fold structure (Krossvatnet).

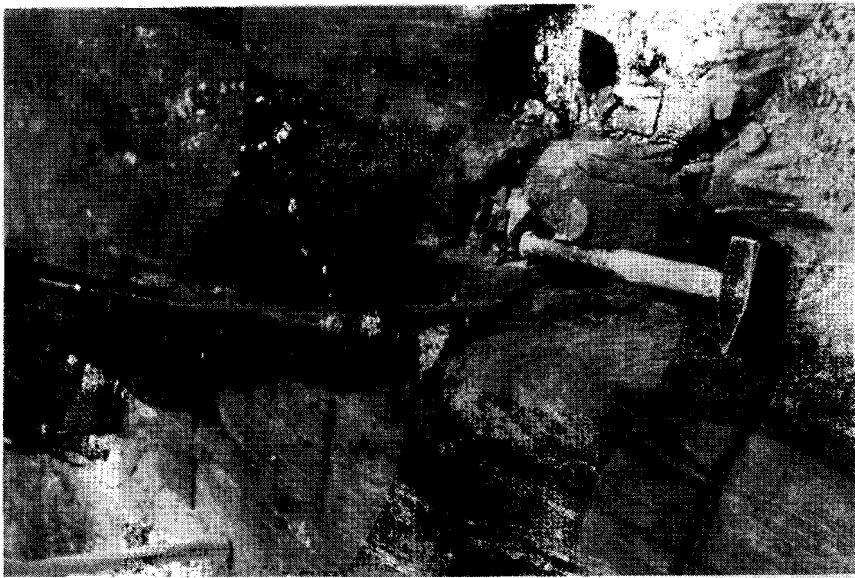
Tight F 4 folds of the S 3 augen gneiss foliation have been observed to the north along the strike of the UAG (R. Vogels pers. com.). In the migmatites, tight folds which fold S 2 and F 2, are occasionally developed, but have not been observed folding the S 3 b foliation. These tight folds and associated cleavage are considered to be D 4 structures. The axial planes trend more NNE-SSW than those of F 2. An axial planar cleavage is only sporadically present and is more widely spaced than S 2.

Fine-grained amphibolite dikes cut S 2 and F 2 (Fig. 2.5) at several places around Krossvatnet and also cut across the S 3 b augen gneiss foliation in the UAG near Ubergsmoen (Fig. 2.6). Flattening caused the development of a foliation in the dikes parallel to their margins. Tight folds of some of these dikes have been observed. The basic dikes therefore intruded between the D 3 and D 4 deformational events. Ptygmatic folds of leucocratic material cut across the structures in the migmatites and the discordant contacts with the basic dikes (Fig. 2.7) and represent a minor third migmatization MIG 3.

Open D 5 folding of previous structures occurred locally, and a 1 cm. wide spaced S 5 crenulation cleavage is sporadically present in the more biotite-rich rocks.

The tectonic history was terminated by a brittle D 6 deformation characterized by small-scale faulting.

Fig. 2.5 Basic dike cutting across D 2 folds in the migmatites at Krossvatnet.



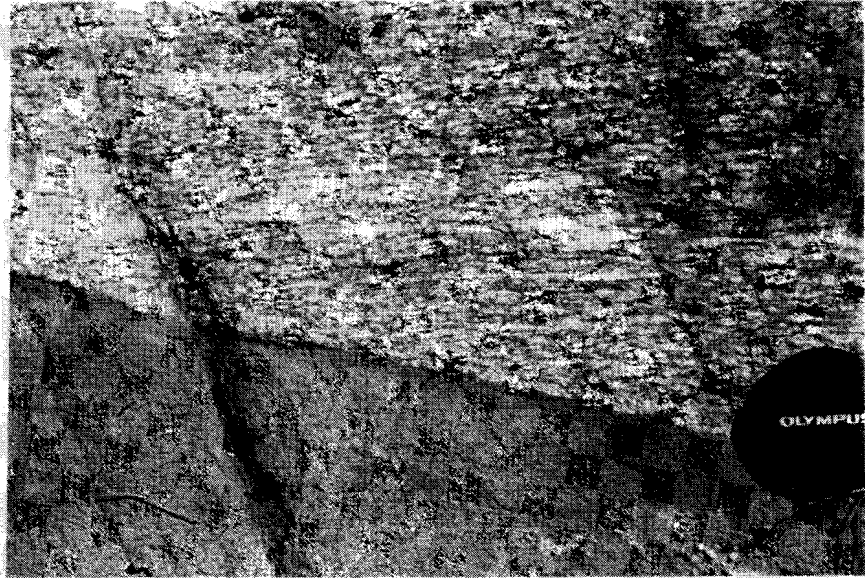


Fig. 2.6 Basic dike intersecting the S 3 b augen gneiss foliation in the UAG at Rambergsfjellet, Ubergsmoen.



Fig. 2.7 Ptygmatic folded leucocratic veins (MIG 3) cutting across the contact between the migmatites and a basic dike at Krossvatnet.

2.3

Metamorphic aspects

All the migmatites exhibit a well developed biotite foliation which is often overgrown by garnet. Garnets are also present in MIG 1 and 2 leucosomes of suitable composition and in the UAG, in which they overgrew the S 3 b.

Adjacent to the UAG (Fig. 2.1), clino- and orthopyroxene grew over the foliation in the migmatites and in the intercalated amphibolites. In the basic dikes, clino- and orthopyroxene (assemblage [II]) overgrew a foam textured green hornblende- plagioclase assemblage [I]. Garnet-clinopyroxene-quartz symplectites [III] grew at the expense of the orthopyroxene-bearing assemblage [II]. The symplectite growth was very localized and was not even homogeneous in a single dike. A rim of cummingtonite is sporadically present between orthopyroxene and hornblende, and clearly grows at the expense of orthopyroxene.

The northwestern part of the UAG is characterized by a charnockitic mineral assemblage of ortho- and clinopyroxene plus hornblende, quartz, feldspars and accessory biotite. Late post foliation garnet is occasionally present. Both clino- and orthopyroxene were stable during D 3 deformation, and recrystallized during the formation of the S 3 b augen gneiss fabric. They do not exhibit relicts of a magmatic texture and according to Touret (1967), they often enclose flakes of biotite. In aggregates of pyroxene and hornblende, no replacement relations could be established (cf. Touret 1967).

The southeastern part of the body has a mineral assemblage of hastingsitic hornblende, biotite, K-feldspar, plagioclase and quartz. Late garnet also occurs in this zone. Xenoliths of metagabbro are rarely present.

2.4

P-T estimates

2.4.1

Method

Coexisting minerals in three samples from the basic dikes were analyzed by electron microprobe in order to establish temperatures and pressures of the local granulite facies metamorphism around the UAG. Samples were analyzed for major elements, and Cr, Cl and F, using a Jeol JXA 8600 Superprobe at the Department of Geochemistry, Utrecht University. Cr, Mn, Na, Cl and F were analyzed by WDS, the other elements by EDS. Spot size was 5 μm .

Table 2.1 Selected analyses from minerals in the Krossvatn dikes.

Mineral	Grt3/2	Hbl61	Cpx5	Opx9	Pl11
Sample	AS2191	AS2191	TN16	TN16	TN16
SiO ₂	37.88	43.81	51.72	49.92	57.86
TiO ₂	0.00	1.80	0.15	0.26	0.00
Al ₂ O ₃	21.52	10.69	1.32	0.75	26.38
Cr ₂ O ₃	0.02	0.06	0.05	0.08	0.01
FeO	28.17	17.65	13.65	32.97	0.00
MnO	1.39	0.10	0.19	0.52	0.02
MgO	4.34	10.17	11.47	14.66	0.00
CaO	6.93	10.80	21.31	0.08	8.57
Na ₂ O	0.00	1.46	0.37	0.00	7.01
K ₂ O	0.10	0.81	0.00	0.00	0.07
P ₂ O ₅	0.00	0.00	0.00	0.00	0.00
Cl	0.00	0.00	0.00	0.01	0.00
F	0.00	0.06	0.00	0.00	0.00
Total	100.35	97.49	100.23	99.97	99.92
O	12	23	6	6	8
Si	2.98	6.59	1.96	1.97	2.60
Ti	0.00	0.20	0.01	0.01	0.00
Al	1.99	1.89	0.06	0.04	1.39
Cr	0.00	0.01	0.00	0.03	0.00
Fe	1.85	2.22	0.43	1.09	0.00
Mn	0.10	0.01	0.01	0.02	0.00
Mg	0.51	2.28	0.65	0.86	0.00
Ca	0.59	1.75	0.87	0.03	2.97
Na	0.00	0.43	0.03	0.00	5.02
K	0.01	0.16	0.00	0.00	0.04
P	0.00	0.00	0.00	0.00	0.00
Cl	0.00	0.00	0.00	0.00	0.00
F	0.00	0.03	0.00	0.00	0.00

2.4.2

Mineral chemistry

Plagioclases (normalized to 8 oxygens) have anorthite contents of 38 to 40 % (TN16, AS2191) and 46.5 to 49 % (TN17) and $K \leq 0.03$.

Hornblendes (normalized to 23 oxygens) have Mg-numbers ($Mg\# = 100 * Mg / (Fe + Mn + Mg)$) ranging from 46.2 to 50.9 with one exception ($Mg\# = 55.0$). Ti varies between 0.19 and 0.25, and $Cr \leq 0.01$. Ca varies between 1.75 and 1.88, while Na and K range from 0.40 to 0.49 and 0.14 to 0.21 respectively. An exception is the amphibole with $Mg\# = 55$, which has a Na content of 0.26. Chlorine and fluorine are less than 0.01 and 0.09 respectively.

Garnets (normalized to 12 oxygens) have $Mg\#$ of 16.7 - 20.8. Grossular component varies between 19.0 and 20.1 %. Ti, Cr, Na and $K \leq 0.01$.

Orthopyroxenes (normalized to 6 oxygens) have $Mg\#$ of 43.1 - 47.7. Al, Mn and $Ca \leq 0.03$, and Ti, Cr and Na are absent.

Assemblage [II] clinopyroxenes (normalized to 6 oxygens) have $Mg\#$ of 59.1 - 62.6 and low Al-contents (≤ 0.07). Ca is ≈ 0.88 . Ti, Mn and Na are ≤ 0.03 , and Cr is absent. Assemblage [III] clinopyroxenes have $Mg\#$ of 57.6 - 59.6. Ca varies between 0.79 and 0.90. Ti, Mn and Na ≤ 0.03 and Al ≤ 0.06 . Cr is absent.

2.4.3

Results

To estimate the P-T conditions of the granulite facies metamorphism, several geothermometers have been applied to the basic dikes. The hornblende-plagioclase geothermometer (Blundy and Holland 1990) was applied to assemblages [I], [II] and [III] and gave results ranging from 728°C to 788°C, with an average of 749°C and no systematic differences between the assemblages.

The two pyroxene geothermometers were applied to assemblage [II], and yielded an average temperature of 802°C (range 789-814°C) using the method of Wood and Banno (1973) and 846°C (range 828-862°C) using the method of Wells (1977). The graphical method of Lindsley (1983) yields much lower temperatures of 540-640°C.

For assemblage [III], the garnet-clinopyroxene geothermometer (Powell 1985) yielded an average temperature of 697°C (range 714-678°C) and the garnet-hornblende geothermometer (Powell 1985) yielded 614°C (range 601-643°C). The garnet-clinopyroxene-plagioclase-quartz geobarometer (Eckert et al. 1989, Newton and Perkins 1982) was applied to assemblage [III] and gave 8.75 kb at 700°C, using the revised calibration of Eckert et al. (1989), whilst the original calibration of Newton and Perkins gave 6.29 kb at the same temperature. This difference of $\pm 2\frac{1}{2}$ kb between the two calibrations is predictable (Eckert et al. 1989).

The temperatures obtained for assemblage [II] from the Lindsley two pyroxene geothermometer are $\approx 50^\circ\text{C}$ lower than expected considering the fact that the other versions of the two pyroxene geothermometer yield temperatures which are ± 50 to 100°C too high for most granulite facies terrains. However, if the accuracy of the Lindsley method is estimated at

$\pm 100^{\circ}\text{C}$ (Lindsley 1983), there is no significant difference in the temperatures obtained for assemblage [II] and the garnet-clinopyroxene temperatures for assemblage [III]. The hornblende-plagioclase temperatures fall within the same range.

2.5

Discussion and conclusions

The MIG 1 and 2 provide evidence for at least one upper-amphibolite facies event in this part of the Bamble Sector before emplacement of the Ubergsmoen Augen Gneiss. The D 1 and D 2 as well as MIG 1 and 2 are older than the UAG and thus record a Gothian event (1600–1500 Ma). Observations regarding the MIG 1 do not contradict the *in situ* migmatization model of Gupta and Johannes (1982), but the presence of MIG 2 leucosomes parallel to those of MIG 1 indicates that the model should be considered carefully before being applied to the entire migmatite complex. The MIG 2 leucosomes imply synkinematic mobility of melts, as they do not fulfil the criteria for migmatites produced by metamorphic differentiation, which should be coarse grained to pegmatitic (Yardley 1978).

The radiometric age determinations of the UAG show two age groups, (1) around 1275 Ma and (2) around 1140 Ma. Group (1) for the UAG are U-Pb zircon ages and could be interpreted as the time of emplacement. Group (2) Rb-Sr whole rock ages would then record an ≈ 1140 Ma event which reset the Rb-Sr system. In contrast, the U-Pb zircon ages for the HVAG belong to group (2) and Rb-Sr ages to group (1), which would indicate Pb loss from zircon while the Rb-Sr system remained closed during the ≈ 1140 Ma event, if ≈ 1275 Ma is considered to be the age of emplacement. This is unlikely and therefore both isotopic systems have probably been reset and group (1) as well as group (2) ages represent post emplacement disturbances of the isotopic systems.

The Bamble Augen Gneisses have been correlated with the 1450 Ma old Varberg charnockite in Southwest Sweden by Starmer (1990b), who interpreted group (1) ages from Bamble as representing resettings of originally similar intrusion ages. No direct isotopic data supporting this interpretation are available from the Bamble Augen Gneisses. Therefore, the real age of emplacement of the UAG remains uncertain, but lies between the Gothian and early stages of the Sveconorwegian Orogeny and is thus probably older than ≈ 1250 Ma.

The age of emplacement of the basic dikes is more uncertain, but they may be correlated with other basic dike swarms in the Sveconorwegian province, such as the Lysekil-Marstrand dikes that were emplaced between 1510 and 1220 Ma and have similar structural relations (Park et al. 1987).

Amphibolitization of the dikes intruded after the emplacement of the augen gneiss implies regional amphibolite facies conditions contemporaneous with or shortly after the emplacement of the UAG.

Orthopyroxene in the Ubergsmoen Augen Gneiss was stable during D 3, but is not present everywhere in the body. Small variations in pH_2O within the solidifying magma probably resulted in charnockitic and granitic domains in the UAG, which were preserved through D 3. If group (1) ages have any geological significance, they may represent resetting

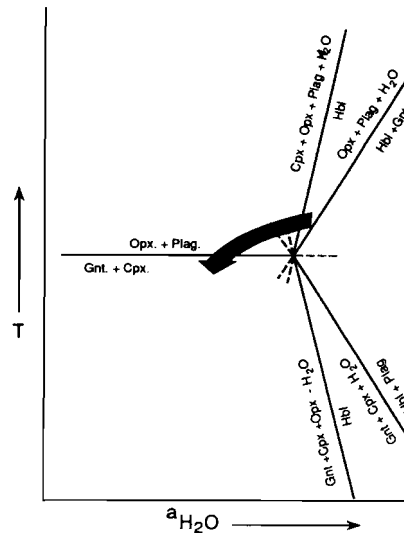
of the isotopic systems due to D 3 shearing.

The presence of ortho- and clinopyroxenes in the migmatites and in the basic dikes around the augen gneiss provide evidence for local granulite facies conditions after emplacement of the UAG. The metamorphism of the dikes can be described in terms of the CMASH system (Fig. 2.8). The partial replacement of [I] by [II] cannot be explained by a near isobaric increase in temperature, as there are no significant temperature differences between these assemblages. Instead, dehydration of amphibole could be achieved by changing fluid composition at nearly constant P and T. Water activities must have been already rather low to shift the invariant point towards the temperatures indicated by geothermometry for the assemblages [I], [II] and [III]. Slight lowering of water activity due to the introduction of small amounts of volatiles, possibly, CO_2 , may account for the observed reaction sequence.

Pressures calculated for assemblage [III] were lower than the theoretical stability field of clinopyroxene + garnet + quartz (Wells 1978). However, increased proportions of Fe will shift this stability field towards lower pressures (Wells 1978), whereas addition of Na will counter this effect. The transition from [II] to [III] resulted from cooling at conditions of near constant $a_{\text{H}_2\text{O}}$ (Fig. 2.8). The same event that caused pyroxene blastesis in the dikes and neighbouring migmatites was probably responsible for resetting of the isotopic system in the augen gneiss which resulted in group (2) ages. This implies that the change in fluid composition probably took place before 1140 Ma.

Pyroxene blastesis is spatially related to the UAG. This implies that the fluids that

Fig. 2.8 Isobaric diagram of T versus $a_{\text{H}_2\text{O}}$ (modified after Bradshaw (1989)) showing the development of the basic dikes after their initial amphibolitization: dehydration in response to lower $a_{\text{H}_2\text{O}}$ in the fluid at nearly constant temperature.



caused a decrease in water activity migrated outward from the UAG. At the time of pyroxene blastesis, however, the UAG was already solidified. It is suggested that the carbonic fluids originated from crystallization of deeper seated charnockitic magmas, and migrated upward

along the sheared UAG and its contacts.

After intrusion of the basic dikes, the area underwent two phases of ductile deformation. These phases occurred before 1060 Ma, the age of intrusion of undeformed granitic sheets and pegmatites (Field and Råheim 1979, Baadsgaard et al. 1984), which is similar to group (3) ages in the Bamble Augen Gneisses.

It is concluded that the Nelaug-Krossvatnet-Ubergsmoen area underwent upper-amphibolite facies regional metamorphic–deformational events during both the Gothian and the Sveconorwegian orogenies. Additionally, the country rocks around the Ubergsmoen Augen Gneiss underwent granulite facies overprinting due to small variations in fluid composition resulting from the crystallization of a charnockitic magma at deeper levels. This counters recent claims that the Bamble Sector escaped any Sveconorwegian high-grade metamorphism (Field and Råheim 1983), and affirms the high-grade polyorogenic nature of the Bamble belt (Starmer 1972a, 1985a).

Acknowledgements - Financial support of AWON/NWO (NWO grant 751-353-023, TGN) is gratefully acknowledged. C. Maijer assisted with part of the field work and sampling, R.P.E. Poorter assisted with the microprobe analyses. C. Maijer and J.B.H. Jansen critically read earlier drafts of this paper, while G.J.L.M. de Haas, D.J. Liefink and D. Visser contributed useful comments. The paper also benefitted from the constructive criticism of three anonymous reviewers.

**THE REGIONAL AMPHIBOLITE TO GRANULITE FACIES TRANSITION AT
 ARENDAL, NORWAY: EVIDENCE FOR A THERMAL DOME**

Abstract - A refinement of the metamorphic zoneography of the Proterozoic amphibolite-granulite facies transition zone at Arendal in the Bamble Sector of the Baltic Shield is presented together with the first set of P-T data covering the entire transition zone. The regional amphibolite to granulite facies transition zone at Arendal is characterized by the following south facing isograd sequence:

- Ms Muscovite-out in metapelitic rocks.
- +Crd Cordierite-in in metapelitic rocks.
- +Opx(1) Orthopyroxene-in in amphibolites.
- +Opx(2) Orthopyroxene-in in acidic gneisses.
- All Allanite-out in gneisses, metapelites and amphibolites.
- Ttn Titanite-out in gneisses, metapelites and amphibolites.

These isograds are cross cut by a possible south facing

- Ky Kyanite-in isograd in metapelites and cordierite-orthoamphibole rocks.

Cordierite and orthopyroxene-in isograds should be located several kilometres to the northwest of the presently existing ones. The isograds are accompanied by increasing recrystallization of sillimanite and an overall increase in the titanium content of hornblende in amphibolites.

Temperature estimates are $752 \pm 34^\circ\text{C}$ (range $710\text{--}780^\circ\text{C}$) for the amphibolite facies zone at 7.1 ± 0.4 kb (range $6.5\text{--}7.6$ kb). Granulites of zone B + C show an average temperature of $836^\circ \pm 49^\circ\text{C}$ at 7.7 ± 0.3 kb; surprisingly, the peak thermal area is situated on the mainland, and temperatures start towards decrease to the Skagerrak: those in zone D yielded slightly lower P-T estimates: $797^\circ \pm 15^\circ\text{C}$ at 7.2 ± 0.5 kb. All granulite facies samples together yield $822^\circ \pm 40^\circ\text{C}$ (range $770\text{--}890^\circ\text{C}$) at 7.4 ± 0.5 kb (range $6.6\text{--}8.1$ kb). Based on the structural trend, isograd pattern and temperature distribution it is tentatively suggested that the metamorphic complex represents a thermal dome. Increased heat flow in the centre of the dome caused a temperature gradient. At the same time, $P_{\text{H}_2\text{O}}$ was significantly lowered in the centre of the dome, while P_{Tot} remained roughly constant. Different cooling paths are established for the area along the Porsgrunn-Kristiansand Fault and the remaining part of the investigated area.

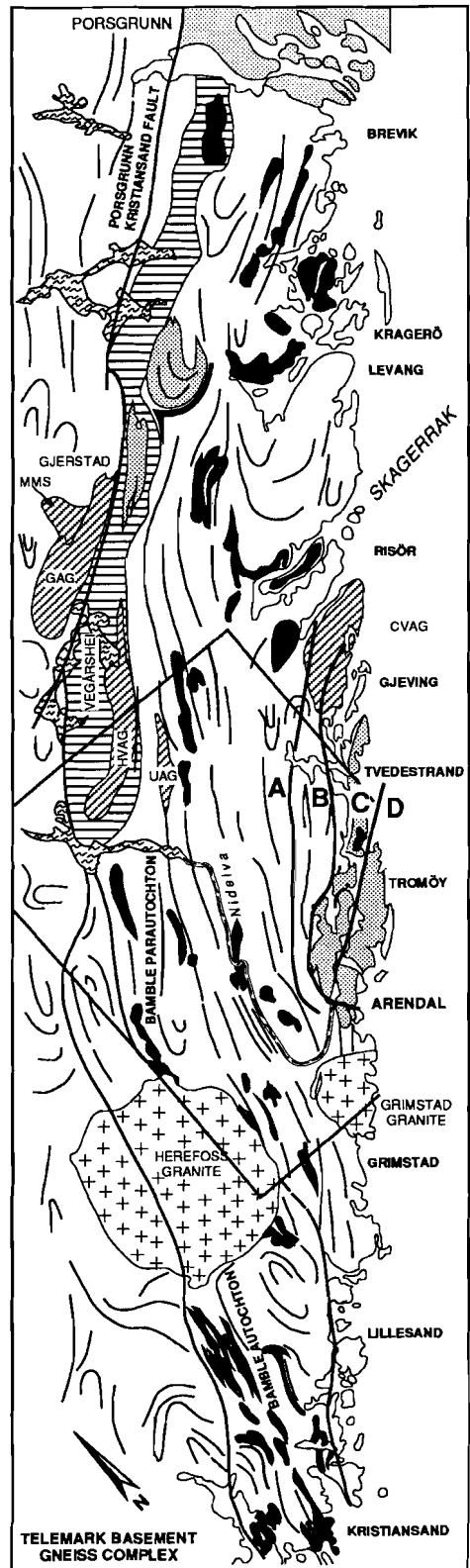
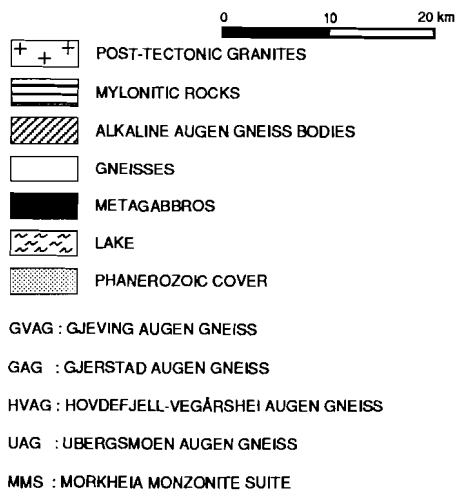
The importance of the distribution of metamorphic index minerals has been recognized since Barrow's (1893) pioneering work in the Scottish Highlands. Mineral isograds and tectonic units reveal the basic architecture of an orogen. Therefore, their exact location is the foundation on which more detailed studies have to be built. The high grade metamorphic terrain between Nelaug and Arendal in the Bamble Sector of the Baltic Shield (Fig. 3.1) is one of the classic amphibolite to granulite facies transition zones (Bugge 1940, 1943). Such terrains attract still increasing attention, as they are crucial to elucidate the petrogenesis of granulite facies rocks, which remains controversial in many areas (cf. Harley 1989, Newton 1990). The significance of granulites from a more general point of view lies in the fact that they are, in almost all currently accepted geophysical interpretations, the best candidates to be the major constituents of the lower continental crust. The polymetamorphic nature of many of the terrains in which granulites occur obscures the features diagnostic of their petrogenesis. The nature of the orthopyroxene isograd in such terrains is considered to be diagnostic for the mechanism of granulite petrogenesis (cf. Newton 1990).

In the Nelaug-Arendal area, an isograd sequence has been established two decades ago by Touret (1971a) and has since only been slightly adapted (Field et al. 1980, Smalley et al. 1983a). Newton (1990) considered the isograd pattern in the area as diagnostic for carbonic metamorphism. The aim of this paper is to place constraints on granulite petrogenesis in the Bamble Sector. Therefore, we conducted a new study of metamorphic index minerals, accompanied them by a new, consistent set of P-T estimates, as previous P-T surveys were almost entirely restricted to the granulite facies areas, and will discuss them in relation to structures, age determinations and geotectonics in the area.

The Bamble Sector (Fig. 3.1) is part of the Southwest Scandinavian Domain of the Baltic Shield (Gaál and Gorbatshev 1987) and has been in international petrological focus since the second half of the nineteenth century. The belt is constituted by an early Gothian supracrustal suite that was metamorphosed and intruded by basic and acidic magmas during the Gothian (Kongsbergian, 1.75-1.5 Ga) and Sveconorwegian (Grenvillian, 1.25-0.9 Ga) orogenies (Verschure 1985, Starmer 1985a, 1990a, 1991). Visser and Senior (1990) established a clockwise prograde P-T path for the area, which was followed by prolonged isobaric cooling and final uplift (Touret and Olsen 1985, Touret 1985, Visser and Senior 1990, Nijland et al. 1993a, ch. 6).

Touret (1971a) was the first to map a set of isograds in the Nelaug-Arendal area (from north to south): (1) Muscovite-out (-Ms), (2) Cordierite-in (+Crd), (3) Orthopyroxene-in (+Opx), (4) Cordierite-out (-Crd). The latter was due to a lack of suitable lithologies in the highest grade part of the area (Touret and Falkum 1987). In addition, Moine et al. (1972)

Fig. 3.1 Geological sketch map of the Bamble Sector (Modified after Starmer 1985a).



recognized the LILE-depleted nature of some of the granulites, and divided them in a strongly depleted Tromøya-Arendal association and a non-depleted Dypvåg-Flostaøya association. Andreae (1974) postulated that the transition from amphibolite to granulite facies in the area was also accompanied by the formation of perthites and myrmekites and by a change in the colour of hornblende.

Field and coworkers (Field and Clough 1976, Cooper and Field 1977, Clough and Field 1980, Field et al. 1980, Smalley et al. 1983a) confirmed the LILE-depleted nature of Tromøya rocks, but mapped the boundary between the depleted and non-depleted granulites in the Tromøysundet between Tromøy, Hisøy and the mainland. Based upon this boundary, and separated orthopyroxene-in isograds for basic and acidic rocks, the Nelaug-Arendal area was split up into four zones (Field et al. 1980, Smalley et al. 1983a): Zone A - upper amphibolite facies; zone B - orthopyroxene in basic rocks; zone C - orthopyroxene in basic and acidic rocks; zone D - LILE and LREE-depleted granulite facies rocks, nearly devoid of K-feldspar, hornblende and biotite. Touret and Falkum (1987) pointed out that the boundary between zones C and D is a tectonic line with minor regional significance. Although they did not establish a discrete isograd, Touret and Falkum (1987) suggested an eastward increase in pressure, featured by the presence of kyanite.

P-T determinations were almost entirely restricted to the granulite facies zones. These are summarized in table 3.1. Generally, temperature and pressure were estimated at ≈ 800 °C and 7-8 kb. for the granulite facies area. Lamb et al. (1986) obtained a P-T box of 800 ± 60 °C and 7.3 ± 0.5 kb. Based solely upon granulite facies data, these authors concluded that no pressure or temperature gradient existed over the transition zone, and attributed the transition to variation in carbon dioxide activity, as proposed by Touret (1971b).

Table 3.1 Previous P-T determinations. Zones are after Smalley et al. (1983a), mineral abbreviations after Kretz (1983).

P (kb)	T (°C)	Zone	Method	Reference
6-7	700-800	BCD	Mineral assemblage	Touret (1971a)
	740-830	D	Ilm-Mag	Comin Chiaramonti (1974)
8-9	725-820	D	Mineral assemblage	Comin Chiaramonti and Frangipane (1974)
6-8	700-900	B	Grt-Bt, Grt-Crd, Grt-Opx-Pl-Qtz	Jansen et al. (1985)
7.3 ± 0.5	800 ± 60	BCD	Opx-Cpx, Grt-Opx-Pl-Qtz, Grt-Opx, Grt-Cpx, Grt-Cpx-Pl-Qtz, Grt-Pl-Sil-Qtz	Lamb et al. (1986)
7	750-800	A	Grt-Bt, Grt-Crd	Visser and Senior (1990)

About 2000 thin sections of all major rock types were studied by optical microscopy. The following rock types were considered: Amphibolites (no different response could be observed between quartz-free and quartz-bearing ones), metagabbros, gneisses (covering the entire range from granitic to tonalitic gneisses), cordierite-orthoamphibole rocks, metapelites, and the late 1.06 Ga granitic sheets of Field and Råheim (1979). Quartzites were excluded because of their limited response to changing metamorphic conditions. Calcsilicate and carbonate rocks are not very useful because they are confined to two narrow zones, but some observations will be reported. In order to keep the regional transition zone between Nelaug and Arendal clear in the picture, the Hovdefjell-Vegårsheia and Ubergsmoen Augen Gneisses and their surrounding aureoles were not considered in this study; details on these areas may be found in Hagelia (1989), and in Nijland and Senior (1991). Sample localities are shown in fig. 3.2.

3.3.1

Orthopyroxene

The distribution of metamorphic orthopyroxene in amphibolites and acidic gneisses is shown in fig. 3.3. The shape of the isograds is roughly similar to those of Field and coworkers (Field et al. 1980, Smalley et al. 1983a), but both isograds have to be shifted several kilometres at the expense of the amphibolite facies zone. In amphibolites, orthopyroxene usually occurs in a foam texture with clinopyroxene, hornblende and plagioclase, \pm biotite and opaque minerals. Sporadically, ortho- and clinopyroxene have overgrown hornblende, or occur in small discrete bands in the amphibolites. A specific type of orthopyroxene occurrence is provided by so-called "dehydration bands" at the contacts of amphibolites with gneisses, in which it occurs together with clinopyroxene and plagioclase (e.g. Visser et al. 1991). In acidic gneisses, orthopyroxene occurs usually in bands with mafic minerals, like biotite, ilmenite and magnetite. Relationships with hornblende are variable. Both orthopyroxene and hornblende may overgrow each other.

A few occurrences of metamorphic orthopyroxene have been found in the area north of the orthopyroxene-in isograds. Non-cronitic orthopyroxene overgrowing hornblende occurs in the Jåmmåsknutene, Vestre Dale, Ripåsen en Östeböfjellet metagabbros. Orthopyroxene also occurs in lenses of cordierite-orthoamphibole rocks at Niksjå (J. Kihle, pers. com. 1991), near Östeböfjellet and Fidalskjerret. At the latter two localities, orthopyroxene postdates the first generation of cordierite and orthoamphibole, but precedes a second generation of these minerals.

Two metapelite occurrences also contain orthopyroxene north of the isograds (Fig. 3.2). In the first one, situated on the shore of Hauglandsvatn, biotite and quartz broke down to orthopyroxene, K-feldspar and melt; subsequently, spinel and sapphirine have been developed (Vogels and Nijland 1991, Nijland et al. in prep.). The second occurrence is in a metapelite

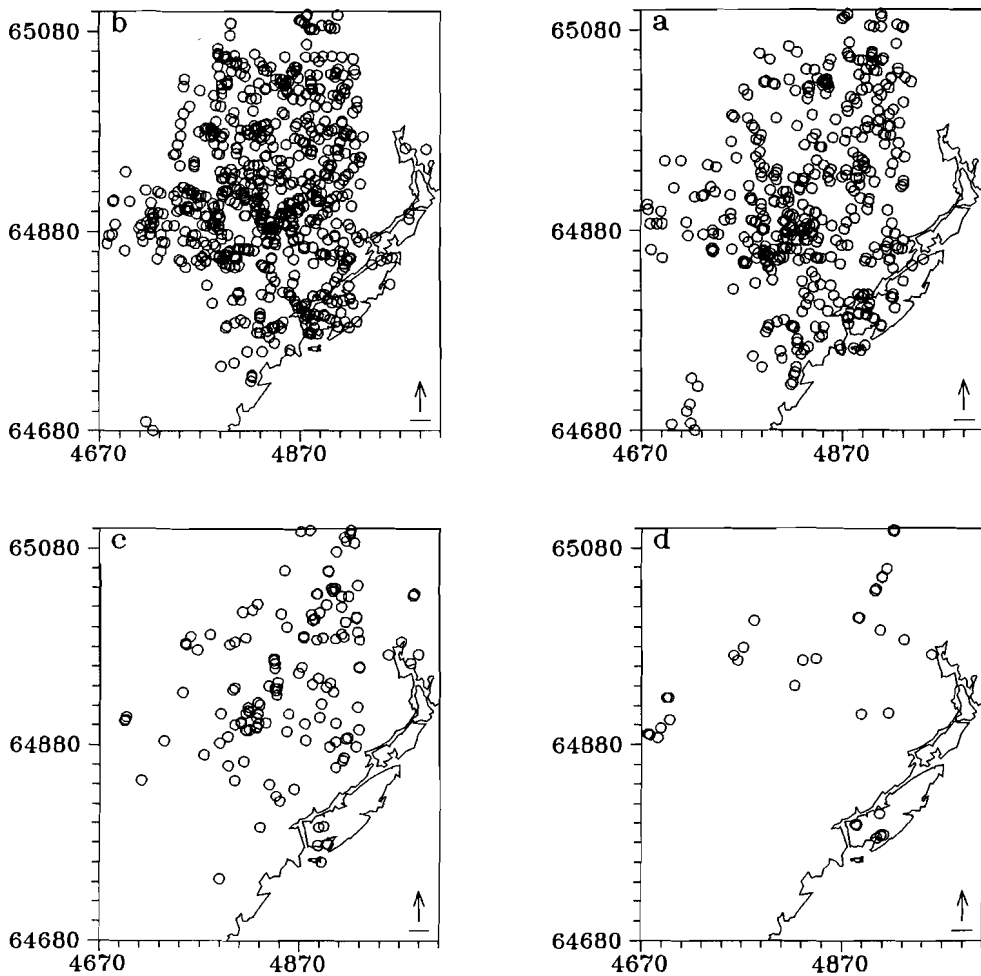


Fig. 3.2 Sample localities. Coordinates refer to the 1:50,000 map sheets of Norges Geografiske Oppmåling. Scale bar is 1 km. **Upper left:** gneisses; **upper right:** amphibolites; **lower left:** pelites; **lower right:** cordierite-orthoamphibole rocks.

band near the Gloserhei pegmatite, and contains the assemblage orthopyroxene-garnet-biotite-cordierite-sillimanite-plagioclase.

3.3.2

Cordierite

The distribution of cordierite in metapelites is shown in fig. 3.4. The +Crd isograd of Touret (1971a) is largely confirmed, although it has to be shifted to the northwest like the +Opx isograds. We observed no cordierite in metapelites from Tromøya and Hisøya, i.e. in

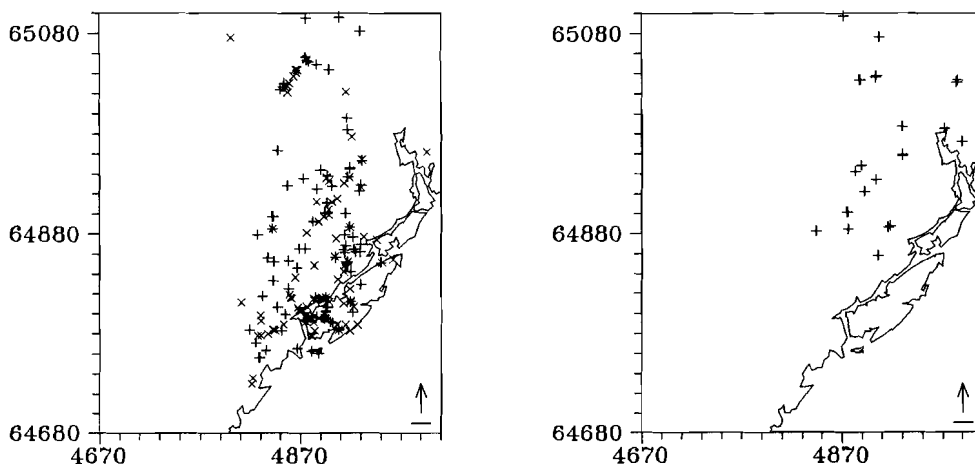


Fig. 3.3 (Left) Distribution of orthopyroxene in amphibolites (+) and gneisses (x).

Fig. 3.4 (Right) Distribution of cordierite in metapelites. Cordierite occurrences in the northeast are related to the Ubergsmoen and Hovdefjell Augen Gneisses and not considered here.

zone D, but this may be due to unsuitable whole rock composition. Cordierite generally occurs in domains between the foliation in the metapelites, which is usually made up by biotite and sillimanite.

Cordierite-orthoamphibole rocks have been described as small lenses from many localities in the Bamble Sector (Brøgger 1934b, Bugge 1943, Beeson 1976, Visser and Senior 1990). In these lenses, cordierite is present irrespective of their position with respect to the +Crd isograd for metapelitic rocks.

3.3.3

Allanite and titanite

The occurrence of allanite and titanite in amphibolites, gneisses and metapelites is shown in fig. 3.5. Two roughly coinciding out isograds, -All and -Tit, are situated on the mainland near Arendal. Allanite is also absent from in skarns on Tromøya, but titanite is found (M. Broekmans pers. com. 1990). Outside the isograds, allanites usually occur as small isolated grains, or as inclusions in other minerals like hornblende or biotite. In microfolded metapelites, allanite tends to accumulate in the fold hinges. Most grains are zoned, and often metamict. Overgrowths of epidote and clinozoisite are common. Allanite is present in samples from granitic sheets which intrude the granulite facies gneisses on Tromøya and Hisøya, and have been dated at 1.06 Ga (Rb-Sr whole rock; Field & Råheim (1979)).

We suggest that the -All isograd is the real boundary between zones C and D. As allanite is a LREE-bearing epidote, it could be assumed that this isograd is related to depletion

of the granulites, thus confirming older conclusions of Moine et al. (1972) that depletion is not restricted to Tromøya and Hisøya. Preliminary whole rock chemical data (T.G. Nijland unpubl. data) confirm the latter observation, but preclude the possibility that the -All isograd is related to the depletion, as they indicate non-depleted, granulite facies metabasic rocks occur in both zones.

Titanite occurs as small isolated grains, or associated with ilmenite and biotite. In the latter cases, it is occasionally present as overgrowths. Although the -Ttn isograd is not based on these overgrowths, they have not been observed at the -Ttn side. The disappearance of titanite in charnockitic rocks has also been noticed by Touret (1968). Titanites tend to display more intense absorption colours with increasing metamorphic gradient.

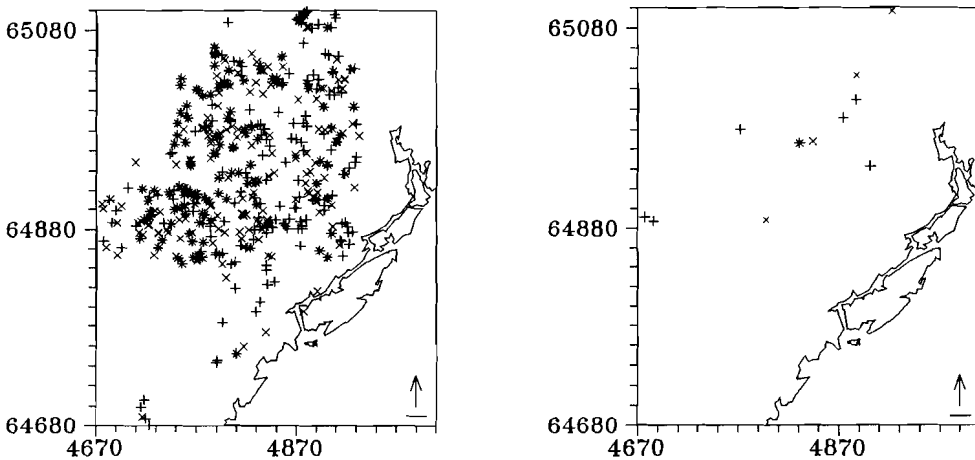


Fig. 3.5 (Left) Distribution of allanite (+) and titanite (x) in amphibolites, gneisses and metapelites.

Fig. 3.6 (Right) Distribution of old (+) and young (x) kyanite in metapelites and cordierite-orthoamphibole rocks.

3.3.4

Kyanite

During this century, kyanite has been considered as a rare mineral in the Bamble Sector. However, both recent observations and forgotten publications report kyanite from all over the Bamble Sector: Nesodden (Broch 1926, this study), Bamble (Weibye 1847, 1849), Bjordammen (Touret 1979, Visser and Senior 1991), Kragerö (Weibye 1847, Touret and Falkum 1987, this study), Risør (Forbes 1857), Söndeled and Gjerstad (D. Visser pers. com. 1990, 1992), Tvedestrand (D. Visser pers. com. 1993), Hovdefjell (Hagelia 1989), Ubergsmoen (this study), Froland (Oftedal 1963, Visser and Senior 1990, 1991, Nijland et al. 1993a, this study) and near Kristiansand, just out of the Bamble Sector (A.C. Tobi in Jansen et al. 1985).

Kyanite occurs in both metapelites and cordierite–orthoamphibole rocks from the present area (Fig. 3.5). As kyanite has since long been known from the eastern part of the Bamble Sector, Touret and Falkum (1987) suggested the possibility of a pressure increase towards the east. The recently reported occurrences do not support this hypothesis.

Visser and Senior (1990) provided evidence for the presence of two generations of kyanite, and considered the oldest of Gothian age, and the younger one of Sveconorwegian age. Both generations are confined to the northern part of the area. We do not know if this possible Ky isograd might be extended east and westwards, but as kyanite also occurs in the coastal strip around Kragerö, it seems possible that the Ky isograd follows the trend set by the +Opx isograds and bends towards the Skagerrak. Especially for the old kyanite, this isograd should probably be interpreted as a south facing kyanite–out isograd, due to increasing temperature at roughly equal pressure, as the old kyanite was the result of M2 metamorphism and is replaced by M3 sillimanite (Visser and Senior 1990).

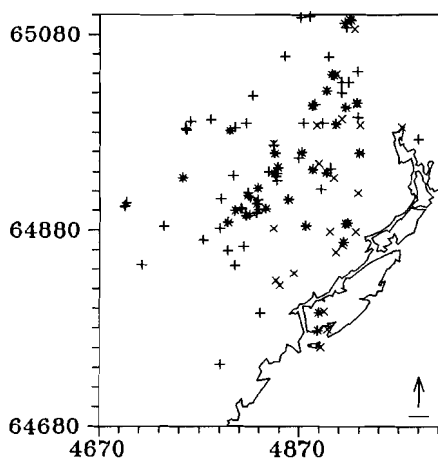


Fig. 3.6 Distribution of fibrolite (+) and euhedral sillimanite (x) in metapelites.

3.3.5

Sillimanite

Two types of sillimanite occur throughout the area: (1) fibrolite, and (2) sub- to euhedral, prismatic sillimanite. Fibrolite usually constitutes the foliation together with biotite, or is present as inclusions in garnet, quartz, tourmaline or feldspars. When both types of sillimanite occur together, it is not always possible to infer their relative age. In cases when this is possible, two textures dominate: (a) A preserved fibrolite foliation occurs in garnet, whereas outside, the main foliation is constituted by prismatic sillimanite. (b) Both types occur in the same main foliation, but crystal faces of prismatic sillimanite truncate the fibrolite. Both textures indicate that prismatic sillimanite is the youngest, and probably in most cases a recrystallization of fibrolite. The spatial distribution of both types of sillimanite (Fig.

3.6) shows increasing dominance of prismatic sillimanite over fibrolite with increasing metamorphic grade.

3.3.6 Other high grade index minerals and chemical fossils

We tried to identify isograds based on what may be called "chemical fossils". Exsolution textures may indicate the existence of high temperature phases that have fallen apart due to a low temperature immiscibility gap. Andreae (1974) claimed that the formation of myrmekite, perthite and antiperthite coincides with the +Opx isograd, whereas the colour of hornblende changed abruptly from green to brown. No systematic distribution of myrmekite or antiperthite could be observed. Perthite is almost absent in zone D, but this is obviously related to the K-deficient nature of the rocks present. A discrete hornblende colour isograd, which has been observed and mapped in some other amphibolite-granulite facies transition zones (e.g. Rogaland: Dekker 1978) is not present in the area. However, a general increase exists in the presence of brown over green hornblende with the metamorphic gradient.

All reported sapphirine occurrences are restricted to the granulite facies zones (Touret and de la Roche 1971, Lamb 1981a). We only found one occurrence outside the +Opx isograds; this is the same as the Hauglandsvatn orthopyroxene locality (See above). Kornerupine has only been found at two localities on Tromøya (Hulzebos-Sijen et al. 1990, Visser et al. 1991, this study), and one locality in the amphibolite facies terrain near Bøylefoss. No systematic distribution is present in the sparse occurrences of staurolite or andalusite. Clinopyroxene is abundant, but does not show any variation with the metamorphic gradient.

3.3.7 Index minerals in calcisilicate and carbonate rocks

Clinopyroxene (hedenbergite-diopside), tremolitic amphibole, hornblende, scapolite, epidote, phlogopite and titanite are common at all localities (Bugge 1940, 1945, this study). Vesuvianite has been observed in both the granulite (Arendal: Bugge 1940, 1943, Barth 1963, this study) and amphibolite facies (Froland: Barth 1963) areas. Grossular-andradite (Arendal and Tromøya) and spinel (Arendal skarns, Tromøya marbles) have only been observed in exposures in the granulite facies terrain. Olivine occurs in marbles near Løddesøl, at the margin of the granulite facies area (Bugge 1945), at Arendal (Bugge 1943) and on Tromøya.

3.3.8 Index minerals in late Sveconorwegian granitic sheets

Granitic sheets at Tromøya and Hisøya postdate the peak of metamorphism (Field and Råheim 1979), and may provide information about conditions during the latest stage of the

Sveconorwegian orogeny. Metamorphism of these sheets is limited to the growth of poikiloblastic muscovite at the expense of feldspars and to the alteration of biotite to chlorite. It is unclear whether this biotite is primary or of metamorphic origin. Garnet has been observed in one sheet.

3.3.9

Index minerals of low grade metamorphism

Late muscovite is common in many metapelites, and has developed at expense of sillimanite. It either occurs as fine grained aggregates replacing fibrolite aggregates or as large unoriented poikiloblasts. Sporadically pseudomorphs after prismatic sillimanite or kyanite occur. Fine grained sericite developed in plagioclase in many samples. Green biotite is rare, but chlorite is common.

The low grade index mineral assemblages prehnite-pumpellyite, pumpellyite-actinolite and epidote-actinolite occur throughout the entire area. Prehnite occurs usually as lenses in biotite, and more rarely in thin veinlets or aggregates of euhedral crystals. Pumpellyite and epidote also occur as small lenses in biotite, but commonly developed at the expense of plagioclase, hornblende or allanite. Other Ca-minerals also occurring as lenses in biotite are F-OH-andradite, calcite and fluorite. Scapolite is not bound to the metamorphic grade, but in specific areas it is significantly more abundant.

Summarized, the regional amphibolite to granulite facies transition zone at Arendal is characterized by the following south facing isograd sequence (Fig. 3.8):

-Ms	Muscovite-out in quartzites (Touret 1971a).
+Crd	Cordierite-in in metapelitic rocks.
+Opx(1)	Orthopyroxene-in in amphibolites.
+Opx(2)	Orthopyroxene-in in acidic gneisses.
-All	Allanite-out in gneisses, metapelites and amphibolites.
-Ttn	Titanite-out in gneisses, metapelites and amphibolites.

These isograds are cross cut by a possible south facing

-Ky	Kyanite-in isograd in metapelites and cordierite-orthoamphibole rocks.
-----	--

The isograds are accompanied by increasing recrystallization of sillimanite and increasing dominance of brown over green hornblende, which correlates with increasing titanium contents of hornblende in amphibolites.

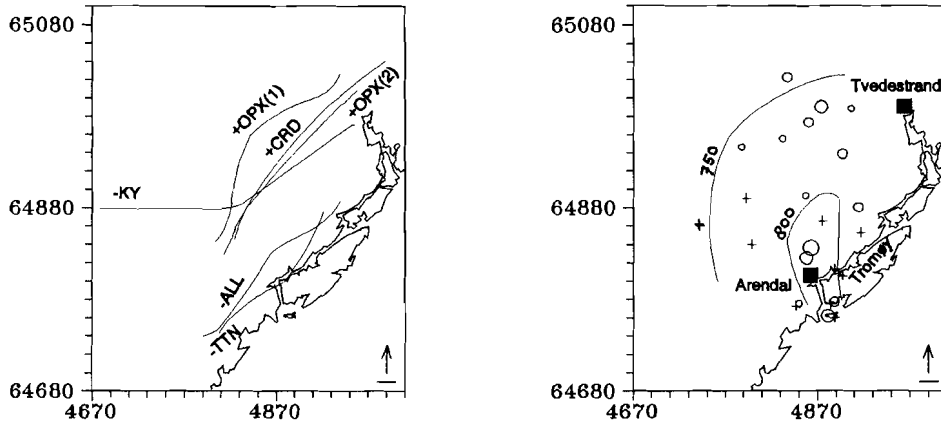


Fig. 3.8 a (Left) Metamorphic zoneography of the Nelaug-Arendal area of the Bamble Sector: +Opx(1): Opx-in isograd for basic rocks; +Opx(2): Opx-in isograd for gneisses; +Crd: Crd-in isograd for metapelites; -Ky: Ky-out isograd for old kyanite in metapelites and orthoamphibole rocks; -All & -Ttn: All-out and Ttn-out isograds for gneisses, metapelites and amphibolites. **b (Right)** Isotherms for 750°C and 800°C, and pressure estimates. Samples which were used for geothermometry are indicated with a +; samples which were used for geobarometry are indicated with circles of increasing size, representing the intervals $P < 7$ kb, $7 \leq P < 7.5$ kb, $7.5 \leq P < 8$ kb, $P \geq 8$ kb. Used temperatures are the best core estimates in °C; the anomalously high temperature of TN250 is left out of consideration.

3.4 P-T distribution

Selected amphibolite and metapelite samples were analyzed by a Jeol JXA 8600 electron microprobe at the Department of Geochemistry, Utrecht University, in order to obtain a set of P-T estimates for the various parts of the transition zone. Running conditions were 15 keV and 10 nA, at a counting time of 30 sec. Analyses were checked against synthetic and natural standards and corrected with a Tracor Northern PROZA correction program. A concise description of the samples is given in the appendix. Selected mineral analyses are given in table 3.2 for the amphibolites and in table 3.3 for the metapelites. Average P-T estimates for the amphibolites are presented in table 3.4 (cores) and 3.5 (rims). Pressure estimates for the metapelites are presented in table 3.6.

The garnet-hornblende (Powell 1985) and hornblende-plagioclase (Blundy and Holland 1990) geothermometers were applied to all samples, except in two cases. The garnet-hornblende-plagioclase geobarometer (Kohn and Spear 1990) was applied to the quartz-bearing samples to obtain pressure estimates. Garnet-biotite (Thompson 1976, Perchuk 1981)

and orthopyroxene-clinopyroxene (Wells 1977, Fonarev and Graphikov 1987) geothermometers were also applied to samples with a suitable mineralogy. All methods yielded consistent pressures and temperatures within each sample. The garnet-plagioclase- Al_2SiO_5 -quartz geobarometer (Newton and Haselton, 1981) was applied to the metapelites, using the newly determined anorthite breakdown reaction of Koziol and Newton (1988).

3.4.1

Temperature

Generally, the highest temperatures are those obtained from hornblende-plagioclase pairs (Table 3.4). The Hbl-Pl temperatures may be slightly higher or lower than Wells' Opx-Cpx temperatures. They tend to be 50-100° higher than Fonarev and Graphikov Opx-Cpx temperatures, and 100-150 °C higher than Grt-Hbl temperatures, which is larger than the uncertainty in the Hbl-Pl calibration (Blundy and Holland 1990). The Hbl-Pl temperatures of 710-890 °C are in fair agreement with the mineral assemblages that were considered to represent the thermal metamorphic climax (Visser and Senior 1990).

The calibration of Fonarev and Graphikov (1987) yields Opx-Cpx temperatures which are roughly one hundred degrees lower than the Wells calibration. This was expected by Fonarev and Graphikov (1990) who concluded that the calibration of Wells (1977) is the only older calibration consistent with recent experimental data, but yields temperatures that are 60-100°C too high. The error (1σ) in the average temperatures of the Fonarev and Graphikov (1987) calibration is similar to the accuracy of 20° estimated by these authors.

The Opx-Cpx temperatures obtained from the Fonarev and Graphikov (1987) calibration cluster around c. 670°C, and coincide with the 600-700°C Grt-Hbl (Powell 1985) and 650-700°C Grt-Bt (Thompson 1976, Perchuk 1981) temperatures (Table 3.4). Grt-Hbl temperatures seem to preserve a relic increasing distribution, similar to those of the Hbl-Pl temperatures.

Table 3.2 Selected analyses for the amphibolites. Nd: not determined. Normalization to number of oxygens: Bt 22, Cpx 6, Grt 12, Hbl 23, Opx 6, Pl 8.

Sample Mineral	TN 19				TN 142				TN 146			
	Bt	Grt	Hbl	Pl	Bt	Grt	Hbl	Pl	Bt	Grt	Hbl	Pl
SiO2	35.43	36.99	42.34	63.24	36.50	37.58	41.98	57.86	35.41	37.68	42.68	57.16
TiO2	1.48	0.08	1.52	0.01	1.85	0.06	1.45	0.00	1.67	0.03	0.95	0.01
Al2O3	16.53	21.26	11.45	22.14	16.49	21.15	11.83	26.41	16.68	20.81	12.85	26.57
Cr2O3	nd	nd	nd	nd	nd	nd	nd	nd	nd	nd	nd	nd
FeO	21.69	28.97	19.28	0.30	20.37	30.27	19.49	0.36	20.56	30.24	18.85	0.01
MnO	0.02	1.68	0.37	0.01	0.00	1.13	0.00	0.00	0.07	1.20	0.10	0.01
MgO	10.13	4.29	8.74	0.01	11.60	5.39	9.04	0.00	11.34	5.15	9.07	0.01
CaO	0.01	5.22	10.17	3.35	0.15	5.51	11.08	8.13	0.01	4.56	10.56	7.82
Na2O	0.31	0.01	1.74	9.70	0.30	0.00	1.33	7.11	0.35	0.00	1.25	7.18
K2O	8.76	0.07	0.70	0.07	8.81	0.00	0.97	0.00	8.60	0.09	0.49	0.13
P2O5	0.01	0.01	0.01	0.01	0.00	0.00	0.00	0.00	0.01	0.00	0.01	0.01
SO3	nd	nd	nd	nd	nd	nd	nd	nd	nd	nd	nd	nd
Cl	0.47	0.06	0.14	0.04	0.07	0.00	0.09	0.00	0.16	0.00	0.07	0.01
F	0.39	0.01	0.45	0.11	0.25	0.13	0.24	0.14	0.36	0.17	0.28	0.23
Total	95.23	98.65	96.91	98.99	96.39	101.22	97.50	100.01	95.22	99.93	97.16	99.15
Si	5.47	2.97	6.47	2.82	5.51	2.95	6.39	2.59	5.43	2.99	6.45	2.58
Ti	0.17	0.01	0.18	0.00	0.21	0.01	0.17	0.00	0.19	0.00	0.11	0.00
Al	3.01	2.01	2.06	1.16	2.93	1.95	2.12	1.39	3.01	1.94	2.29	1.42
Cr	nd	nd	nd	nd	nd	nd	nd	nd	nd	nd	nd	nd
Fe	2.80	1.94	2.46	0.01	2.57	1.98	2.48	0.01	2.63	2.01	2.38	0.00
Mn	0.00	0.12	0.05	0.00	0.00	0.08	0.00	0.00	0.01	0.08	0.01	0.00
Mg	2.33	0.51	1.99	0.00	2.61	0.63	2.05	0.00	2.59	0.61	2.04	0.00
Ca	0.00	0.45	1.66	0.16	0.03	0.46	1.81	0.39	0.00	0.39	1.71	0.38
Na	0.09	0.00	0.51	0.84	0.09	0.00	0.38	0.62	0.11	0.00	0.36	0.63
K	1.73	0.01	0.13	0.01	1.70	0.00	0.18	0.00	1.68	0.01	0.09	0.01
P	0.00	0.00	0.00	0.00	0.00	0.00	0.00	0.00	0.00	0.00	0.00	0.00
S	nd	nd	nd	nd	nd	nd	nd	nd	nd	nd	nd	nd
Cl	0.12	0.01	0.04	0.00	0.02	0.00	0.03	0.00	0.05	0.00	0.02	0.00
F	0.20	0.01	0.22	0.02	0.12	0.03	0.12	0.02	0.18	0.04	0.14	0.03
Mg#	0.45	0.20	0.44		0.50	0.24	0.45	0.50	0.23	0.46		

Table 3.2 Continued.

Sample Mineral	TN 201				TN 202				TN 204			
	Bt	Grt	Hbl	Pl	Bt	Grt	Hbl	Pl	Bt	Grt	Hbl	Pl
SiO2	35.44	38.14	42.13	56.18	35.32	38.29	42.47	58.47	36.13	37.95	42.59	59.00
TiO2	1.26	0.07	1.20	0.00	1.08	0.06	1.35	0.01	2.22	0.06	1.57	0.01
Al2O3	17.65	21.79	12.44	27.21	16.93	21.20	13.42	25.43	16.27	21.58	13.28	26.34
Cr2O3	nd	nd	nd	nd	nd	nd	nd	nd	nd	nd	nd	nd
FeO	18.29	28.19	15.42	0.00	19.44	29.82	17.97	0.15	20.02	28.64	16.54	0.01
MnO	0.11	1.09	0.26	0.00	0.04	1.79	0.18	0.01	0.06	1.51	0.27	0.01
MgO	12.33	7.08	10.66	0.00	13.03	5.04	9.05	0.01	11.71	6.15	9.52	0.01
CaO	0.00	4.05	10.50	9.21	0.16	4.49	10.84	7.50	0.01	4.48	10.89	8.28
Na2O	0.19	0.00	1.77	6.73	0.23	0.01	1.60	7.60	0.23	0.01	1.89	7.16
K2O	9.47	0.00	0.27	0.06	8.66	0.01	0.52	0.10	8.99	0.01	0.49	0.01
P2O5	0.00	0.00	0.28	0.00	0.01	0.01	0.01	0.01	0.01	0.01	0.01	0.01
SO3	nd	nd	nd	nd	nd	nd	nd	nd	nd	nd	nd	nd
Cl	0.14	0.00	0.07	0.00	0.23	0.04	0.22	0.01	0.29	0.01	0.24	0.01
F	0.10	0.05	0.27	0.09	0.34	0.01	0.20	0.01	0.22	0.20	0.28	0.07
Total	94.98	100.46	95.27	99.48	95.47	100.77	97.83	99.31	96.16	100.61	97.57	100.92
Si	5.40	2.97	6.40	2.54	5.37	3.00	6.36	2.63	5.47	2.96	6.38	2.61
Ti	0.15	0.01	0.14	0.00	0.12	0.01	0.15	0.00	0.26	0.01	0.18	0.00
Al	3.17	2.00	2.23	1.45	3.03	1.96	2.37	1.35	2.91	1.99	2.34	1.38
Cr	nd	nd	nd	nd	nd	nd	nd	nd	nd	nd	nd	nd
Fe	2.34	1.83	1.96	0.00	2.48	1.95	2.25	0.01	2.54	1.87	2.07	0.00
Mn	0.02	0.07	0.04	0.00	0.01	0.12	0.03	0.00	0.01	0.10	0.04	0.00
Mg	2.80	0.82	2.41	0.00	2.95	0.59	2.03	0.00	2.64	0.72	2.12	0.00
Ca	0.00	0.34	1.71	0.45	0.03	0.38	1.74	0.36	0.00	0.38	1.74	0.39
Na	0.06	0.00	0.53	0.59	0.07	0.00	0.47	0.67	0.07	0.00	0.54	0.62
K	1.85	0.00	0.06	0.01	1.68	0.00	0.11	0.01	1.73	0.00	0.09	0.00
P	0.00	0.00	0.04	0.00	0.00	0.00	0.00	0.00	0.00	0.00	0.00	0.00
S	nd	nd	nd	nd	nd	nd	nd	nd	nd	nd	nd	nd
Cl	0.04	0.00	0.02	0.00	0.06	0.01	0.05	0.00	0.07	0.00	0.06	0.00
F	0.05	0.01	0.13	0.01	0.17	0.01	0.10	0.00	0.11	0.05	0.14	0.01
Mg#	0.54	0.30	0.55		0.54	0.22	0.47		0.51	0.27	0.50	

Table 3.2 Continued.

Sample	TN 209				TN 226				TN 227			
Mineral	Bt	Grt	Hbl	Pl	Bt	Cpx	Grt	Hbl	Opx	Pl	Cpx	Grt
SiO2	36.63	37.72	43.18	58.88	34.25	50.06	37.35	39.86	49.53	54.75	51.09	36.84
TiO2	3.03	0.06	1.43	0.01	5.49	0.21	0.06	2.71	0.06	0.01	0.26	0.08
Al2O3	15.51	21.71	12.49	25.47	13.60	1.81	21.37	12.26	0.55	27.91	2.15	20.61
Cr2O3	nd	nd	nd	nd	nd	nd	nd	nd	nd	nd	nd	nd
FeO	19.86	30.39	18.40	0.25	19.39	12.31	27.70	18.40	31.24	0.25	14.37	28.89
MnO	0.02	1.45	0.13	0.01	0.08	0.22	1.33	0.01	0.50	0.01	0.22	0.90
MgO	11.87	5.07	9.51	0.01	10.13	11.52	4.38	9.05	15.55	0.01	10.16	2.80
CaO	0.01	4.66	10.70	7.22	0.01	21.41	6.77	11.09	0.55	9.85	21.39	9.09
Na2O	0.30	0.01	1.73	7.63	0.07	0.36	0.01	1.51	0.01	5.77	0.36	0.01
K2O	9.34	0.01	0.70	0.07	9.62	0.01	0.01	1.90	0.01	0.31	0.01	0.13
P2O5	0.01	0.01	0.01	0.01	0.01	0.01	0.27	0.01	0.01	0.01	0.01	0.01
SO3	nd	nd	nd	nd	nd	nd	nd	nd	nd	nd	nd	nd
Cl	0.13	0.02	0.10	0.01	0.16	0.01	0.01	0.15	0.01	0.01	0.01	0.01
F	0.29	0.01	0.11	0.01	0.39	0.28	0.10	0.35	0.22	0.09	0.19	0.13
Total	97.00	101.12	98.44	99.58	93.20	98.21	99.36	97.30	98.24	98.98	100.22	99.50
Si	5.51	2.95	6.44	2.64	5.42	1.94	2.96	6.13	1.97	2.49	1.95	2.96
Ti	0.34	0.01	0.16	0.00	0.65	0.01	0.01	0.31	0.00	0.00	0.01	0.01
Al	2.75	2.00	2.20	1.35	2.53	0.08	2.00	2.22	0.03	1.50	0.10	1.95
Cr	nd	nd	nd	nd	nd	nd	nd	nd	nd	nd	nd	nd
Fe	2.49	1.99	2.30	0.01	2.57	0.40	1.84	2.37	1.04	0.01	0.46	1.94
Mn	0.00	0.09	0.02	0.00	0.01	0.01	0.09	0.00	0.02	0.00	0.01	0.06
Mg	2.66	0.59	2.12	0.00	2.38	0.67	0.52	2.08	0.92	0.00	0.58	0.33
Ca	0.00	0.39	1.71	0.35	0.00	0.89	0.58	1.83	0.02	0.48	0.87	0.78
Na	0.09	0.00	0.50	0.66	0.02	0.03	0.00	0.44	0.00	0.51	0.03	0.00
K	1.79	0.00	0.13	0.01	1.94	0.00	0.00	0.37	0.00	0.02	0.00	0.01
P	0.00	0.00	0.00	0.00	0.00	0.00	0.02	0.00	0.00	0.00	0.00	0.00
S	nd	nd	nd	nd	nd	nd	nd	nd	nd	nd	nd	nd
Cl	0.04	0.01	0.03	0.00	0.05	0.00	0.00	0.04	0.00	0.00	0.00	0.00
F	0.14	0.01	0.05	0.00	0.20	0.04	0.00	0.17	0.03	0.01	0.02	0.03
Mg#	0.52	0.22	0.48		0.48	0.62	0.21	0.47	0.47		0.55	0.14

Table 3.2 Continued.

Sample	TN 227		TN 250			TN 258				TN 291		
Mineral	Hbl	Pl	Grt	Hbl	Pl	Grt	Hbl	Opx	Pl	Grt	Hbl	Pl
SiO ₂	39.71	54.92	37.93	41.01	57.08	37.74	41.91	49.63	56.07	38.32	42.53	56.93
TiO ₂	2.78	0.01	0.06	1.45	0.01	0.06	2.53	0.13	0.01	0.00	1.67	0.00
Al ₂ O ₃	12.40	28.30	21.46	13.53	26.43	21.14	12.07	1.02	27.83	20.78	11.28	26.93
Cr ₂ O ₃	nd	nd	nd	nd	nd	nd	nd	nd	nd	nd	nd	nd
FeO	19.82	0.01	28.20	17.15	0.35	29.07	18.44	32.21	0.22	29.54	19.31	0.00
MnO	0.01	0.01	1.52	0.19	0.01	1.42	0.15	0.52	0.01	1.48	0.22	0.00
MgO	7.74	0.01	6.67	9.63	0.01	4.10	8.62	15.98	0.01	4.89	9.72	0.00
CaO	11.34	10.48	4.11	10.59	8.65	6.98	11.31	0.91	9.68	5.76	9.85	9.46
Na ₂ O	1.40	5.43	0.01	1.81	6.78	0.06	1.93	0.02	6.08	0.00	1.52	6.09
K ₂ O	1.84	0.24	0.01	0.59	0.01	0.01	0.78	0.01	0.10	0.00	0.72	0.20
P ₂ O ₅	0.01	0.01	0.15	0.01	0.01	0.01	0.01	0.01	0.01	0.00	0.00	0.00
SO ₃	nd	nd	nd	nd	nd	nd	nd	nd	nd	0.00	0.00	0.00
Cl	0.01	0.01	0.01	0.63	0.01	0.01	0.03	0.02	0.01	0.00	0.06	0.00
F	0.37	0.24	0.22	0.31	0.01	0.22	0.28	0.06	0.01	0.00	0.00	0.00
Total	97.43	99.67	100.35	96.90	99.36	100.82	98.06	100.52	100.04	100.77	96.88	99.61
Si	6.13	2.48	2.96	6.23	2.58	2.97	6.33	1.94	2.52	3.01	6.48	2.56
Ti	0.33	0.00	0.01	0.16	0.00	0.01	0.29	0.00	0.00	0.00	0.19	0.00
Al	2.26	1.51	1.97	2.42	1.41	1.96	2.15	0.05	1.48	1.92	2.03	1.43
Cr	nd	nd	nd	nd	nd	nd	nd	nd	nd	nd	nd	nd
Fe	2.56	0.00	1.84	2.18	0.01	1.91	2.33	1.05	0.01	1.94	2.46	0.00
Mn	0.00	0.00	0.10	0.03	0.00	0.10	0.02	0.02	0.00	0.10	0.03	0.00
Mg	1.78	0.00	0.77	2.18	0.00	0.48	1.94	0.93	0.00	0.57	2.21	0.00
Ca	1.87	0.51	0.34	1.72	0.42	0.59	1.83	0.04	0.47	0.49	1.61	0.46
Na	0.43	0.48	0.00	0.53	0.59	0.01	0.56	0.00	0.53	0.00	0.46	0.53
K	0.37	0.02	0.00	0.11	0.00	0.00	0.15	0.00	0.01	0.00	0.15	0.01
P	0.00	0.00	0.01	0.00	0.00	0.00	0.00	0.00	0.00	0.00	0.00	0.00
S	nd	nd	nd	nd	nd	nd	nd	nd	nd	0.00	0.00	0.00
Cl	0.00	0.00	0.00	0.16	0.00	0.00	0.01	0.00	0.00	0.00	0.02	0.00
F	0.18	0.04	0.06	0.15	0.00	0.06	0.14	0.01	0.00	0.00	0.00	0.00
Mg#	0.41		0.29	0.50		0.19	0.45	0.47		0.22	0.47	

Table 3.2 Continued.

Sample Mineral	TN 294						TN 309					TN 402
	Bt	Cpx	Grt	Hbl	Opx	Pl	Bt	Cpx	Hbl	Opx	Pl	Cpx
SiO2	36.05	50.75	38.74	40.67	50.85	53.83	36.69	51.22	43.07	51.88	60.86	50.77
TiO2	4.99	0.15	0.02	2.22	0.05	0.00	5.02	0.13	1.87	0.07	0.00	0.10
Al2O3	14.36	2.15	21.05	12.24	1.19	28.66	14.00	1.57	9.73	0.85	24.34	1.04
Cr2O3	nd	nd	nd	nd	nd	nd	nd	nd	nd	nd	nd	0.00
FeO	18.01	10.27	27.51	16.84	28.23	0.48	13.10	10.19	16.09	25.50	0.00	17.19
MnO	0.06	0.40	2.32	0.19	0.84	0.04	0.08	0.62	0.34	1.36	0.01	0.76
MgO	11.89	12.05	5.57	9.63	18.54	0.00	14.97	13.35	11.61	19.80	0.00	8.95
CaO	0.11	23.18	6.84	12.01	0.45	11.92	0.00	22.04	10.79	0.41	6.37	21.17
Na2O	0.08	0.34	0.00	1.46	0.00	4.84	0.00	0.59	1.66	0.00	7.97	0.47
K2O	10.03	0.00	0.00	2.24	0.00	0.16	10.12	0.00	1.26	0.07	0.81	0.00
P2O5	0.00	0.00	0.00	0.00	0.00	0.00	0.00	0.00	0.21	0.00	0.00	0.00
SO3	0.22	0.27	0.00	0.00	0.00	0.00	0.00	0.00	0.15	0.00	0.00	nd
Cl	0.03	0.00	0.00	0.04	0.00	0.00	0.02	0.00	0.06	0.01	0.01	0.00
F	0.31	0.00	0.00	0.13	0.00	0.00	0.51	0.03	0.19	0.00	0.00	0.00
Total	96.14	99.56	102.05	97.67	100.15	99.93	94.51	99.70	97.03	99.95	100.37	100.45
Si	5.45	1.93	1.50	6.20	1.95	2.44	5.55	1.94	6.52	1.97	2.71	1.96
Ti	0.57	0.01	0.00	0.26	0.00	0.00	0.57	0.00	0.21	0.00	0.00	0.00
Al	2.56	0.10	0.96	2.20	0.05	1.53	2.50	0.07	1.73	0.04	1.28	0.05
Cr	nd	nd	nd	nd	nd	nd	nd	nd	nd	nd	nd	0.00
Fe	2.28	0.33	0.89	2.14	0.91	0.02	1.66	0.32	2.04	0.81	0.00	0.56
Mn	0.01	0.01	0.08	0.03	0.03	0.00	0.01	0.02	0.05	0.04	0.00	0.03
Mg	2.68	0.68	0.32	2.19	1.06	0.00	3.37	0.75	2.62	1.21	0.00	0.52
Ca	0.02	0.94	0.28	1.96	0.02	0.58	0.00	0.89	1.75	0.02	0.31	0.88
Na	0.02	0.02	0.00	0.44	0.00	0.43	0.00	0.05	0.49	0.00	0.69	0.04
K	1.93	0.00	0.00	0.44	0.00	0.01	1.95	0.00	0.24	0.01	0.05	0.00
P	0.00	0.00	0.00	0.00	0.00	0.00	0.00	0.00	0.03	0.00	0.00	0.00
S	0.02	0.01	0.00	0.00	0.00	0.00	0.00	0.00	0.02	0.00	0.00	nd
Cl	0.01	0.00	0.00	0.01	0.00	0.00	0.01	0.00	0.02	0.00	0.00	0.00
F	0.15	0.00	0.00	0.06	0.00	0.00	0.25	0.01	0.09	0.00	0.00	0.00
Mg#	0.54	0.67	0.25	0.50	0.53		0.67	0.69	0.56	0.57		0.47

Table 3.2 Continued.

Sample Mineral	TN 402			TN 420			TN 430			
	Hbl	Opx	Pl	Grt	Hbl	Pl	Cpx	Hbl	Opx	Pl
SiO2	39.83			38.36	43.39	56.03	50.98	41.89	49.76	60.57
TiO2	2.07	0.08	0.02	0.00	1.38	0.00	0.15	2.09	0.07	0.02
Al2O3	11.70	0.55	24.34	21.11	11.83	27.11	1.47	10.69	0.36	24.36
Cr2O3	0.00	0.00	0.00	0.00	0.00	0.16	nd	nd	nd	nd
FeO	22.68	37.96	0.00	29.80	18.55	0.00	14.73	20.88	34.44	0.14
MnO	0.39	1.55	0.00	1.18	0.09	0.00	0.46	0.17	0.96	0.00
MgO	6.91	11.09	0.00	5.21	10.53	0.00	10.10	7.88	13.89	0.00
CaO	11.32	0.77	6.13	5.74	10.63	9.49	20.69	10.97	0.81	6.18
Na2O	1.73	0.00	8.10	0.00	1.64	6.28	0.57	1.79	0.00	8.10
K2O	1.81	0.00	0.53	0.00	0.27	0.08	0.06	1.18	0.00	0.37
P2O5	0.00	0.00	0.00	0.00	0.00	0.00	0.00	0.00	0.00	0.00
SO3	nd	nd	nd	nd	nd	nd	0.00	0.00	0.00	0.00
Cl	0.14	0.00	0.00	0.00	0.01	0.00	0.01	0.06	0.00	0.00
F	0.50	0.00	0.00	0.00	0.22	0.00	0.00	0.00	0.00	0.00
Total	99.08	100.93	100.31	101.40	98.54	99.15	99.22	97.60	100.29	99.74
Si	6.15	1.97	2.72	2.99	6.46	2.54	1.97	6.44	1.97	2.72
Ti	0.24	0.00	0.00	0.00	0.16	0.00	0.01	0.24	0.00	0.00
Al	2.13	0.03	1.27	1.94	2.08	1.45	0.07	1.94	0.02	1.28
Cr	0.00	0.00	0.00	0.00	0.00	0.01	nd	nd	nd	nd
Fe	2.93	1.27	0.00	1.95	2.31	0.00	0.48	2.69	1.14	0.01
Mn	0.05	0.05	0.00	0.08	0.01	0.00	0.01	0.02	0.03	0.00
Mg	1.59	0.66	0.00	0.60	2.33	0.00	0.58	1.80	0.82	0.00
Ca	1.88	0.03	0.29	0.48	1.70	0.46	0.86	1.81	0.03	0.30
Na	0.52	0.00	0.70	0.00	0.47	0.55	0.04	0.54	0.00	0.70
K	0.35	0.00	0.03	0.00	0.05	0.01	0.01	0.24	0.00	0.02
P	0.00	0.00	0.00	0.00	0.00	0.00	0.00	0.00	0.00	0.00
S	nd	nd	nd	nd	nd	nd	0.00	0.00	0.00	0.00
Cl	0.04	0.00	0.00	0.00	0.00	0.00	0.00	0.02	0.00	0.00
F	0.24	0.00	0.00	0.00	0.11	0.00	0.00	0.00	0.00	0.00
Mg#	0.35	0.33			0.23	0.50		0.54	0.40	0.41

Table 3.2 Continued.

Sample	TN 431				
Mineral	Bt	Grt	Hbl	Opx	Pl
SiO2	34.91	37.97	40.65	49.78	57.29
TiO2	3.62	0.02	2.12	0.00	0.00
Al2O3	15.21	20.73	12.02	1.04	26.68
Cr2O3	0.00	0.00	0.00	0.00	0.00
FeO	22.08	30.12	19.72	33.60	0.24
MnO	0.03	1.34	0.12	0.45	0.09
MgO	8.72	3.91	7.61	14.48	0.00
CaO	0.00	6.58	11.07	0.76	8.94
Na2O	0.09	0.00	1.55	0.00	6.51
K2O	9.29	0.00	1.59	0.00	0.24
P2O5	0.00	0.00	0.00	0.00	0.00
SO3	nd	nd	nd	nd	nd
Cl	0.04	0.00	0.00	0.00	0.00
F	0.04	0.00	0.06	0.06	0.00
Total	94.03	100.67	96.51	100.17	99.99
Si	5.50	3.00	6.31	1.96	2.57
Ti	0.43	0.00	0.25	0.00	0.00
Al	2.83	1.93	2.20	0.05	1.41
Cr	0.00	0.00	0.00	0.00	0.00
Fe	2.90	1.99	2.56	1.11	0.01
Mn	0.00	0.09	0.02	0.01	0.00
Mg	2.04	0.46	1.76	0.85	0.00
Ca	0.00	0.56	1.84	0.03	0.43
Na	0.02	0.00	0.47	0.00	0.57
K	1.87	0.00	0.32	0.00	0.02
P	0.00	0.00	0.00	0.00	0.00
S	nd	nd	nd	nd	nd
Cl	0.01	0.00	0.00	0.00	0.00
F	0.02	0.00	0.03	0.01	0.00
Mg#	0.41	0.18	0.41	0.43	

Table 3.3 Selected mineral analyses for the metapelites. Garnets (Grt) were normalized to 12 oxygens, plagioclase (Pl) to 8.

CM 407		CM 454		EJ 10		MR 35
Grt	Pl	Grt	Pl	Grt	Pl	Grt
39.11	59.82	38.40	62.64	38.44	54.70	38.44
0.01	0.01	0.01	0.01	0.01	0.01	0.01
22.54	25.34	21.63	23.51	22.69	25.49	21.86
nd	nd	nd	nd	nd	nd	nd
22.07	0.01	30.32	0.01	28.69	0.01	31.61
0.45	0.01	0.88	0.01	0.26	0.01	0.47
9.48	0.01	8.09	0.01	9.53	0.01	6.90
1.41	6.88	0.83	5.47	1.26	7.32	1.97
0.02	7.75	0.01	8.76	0.11	7.66	0.02
0.11	0.29	0.13	0.41	0.01	0.08	0.01
0.01	0.24	0.01	0.01	0.01	0.01	0.01
nd	nd	nd	nd	nd	nd	nd
0.01	0.01	0.01	0.01	0.08	0.02	0.01
0.09	0.01	0.02	0.01	0.01	0.01	0.02
100.21	100.11	100.31	100.84	101.01	100.07	101.30
2.99	2.66	2.99	2.76	2.94	2.65	2.98
0.00	0.00	0.00	0.00	0.00	0.00	0.00
2.03	1.32	1.98	1.22	2.05	1.34	2.00
nd	nd	nd	nd	nd	nd	nd
1.73	0.00	1.97	0.00	1.83	0.00	2.05
0.03	0.00	0.06	0.00	0.02	0.00	0.03
1.08	0.00	0.94	0.00	1.08	0.00	0.80
0.12	0.33	0.07	0.26	0.10	0.35	0.16
0.00	0.67	0.00	0.75	0.02	0.66	0.00
0.01	0.02	0.01	0.02	0.00	0.01	0.00
0.00	0.01	0.00	0.00	0.00	0.00	0.00
nd	nd	nd	nd	nd	nd	nd
0.00	0.00	0.01	0.00	0.01	0.00	0.00
0.02	0.00	0.01	0.00	0.01	0.00	0.01
0.38		0.32		0.37		0.28

Table 3.3 Continued.

Sample Mineral	MR 35 Pl	MR 75 Grt	Pl	NS 19 Grt	Pl	WT 66 Grt	Pl
SiO2	55.54	38.02	57.83	38.55	58.81	37.82	58.53
TiO2	0.01	0.01	0.01	0.01	0.01	0.26	0.01
Al2O3	27.38	22.26	27.13	22.07	26.40	21.71	25.64
FeO	0.22	27.85	0.01	28.86	0.01	30.70	0.25
MnO	0.01	0.62	0.01	0.53	0.01	0.80	0.01
MgO	0.01	8.49	0.01	8.37	0.01	7.00	0.01
CaO	10.24	2.73	8.66	1.89	7.85	1.87	7.54
Na2O	5.84	0.04	6.66	0.01	7.17	0.01	7.36
K2O	0.29	0.01	0.10	0.01	0.20	0.01	0.20
P2O5	0.01	0.01	0.01	0.01	0.10	0.01	0.01
Cl	0.01	0.01	0.01	0.02	0.10	0.03	0.01
F	0.01	0.01	0.05	0.01	0.10	0.01	0.01
Total	99.55	100.04	100.43	100.31	100.48	100.19	99.56
Si	2.52	2.94	2.58	2.98	2.62	2.96	2.63
Ti	0.00	0.00	0.00	0.00	0.00	0.02	0.00
Al	1.46	2.03	1.43	2.01	1.38	2.00	1.36
Fe	0.01	1.81	0.00	1.87	0.00	2.01	0.01
Mn	0.00	0.04	0.00	0.03	0.00	0.05	0.00
Mg	0.00	0.98	0.00	0.97	0.00	0.82	0.00
Ca	0.50	0.23	0.41	0.16	0.37	0.16	0.36
Na	0.51	0.01	0.57	0.00	0.62	0.00	0.64
K	0.02	0.00	0.01	0.00	0.01	0.00	0.01
P	0.00	0.00	0.00	0.00	0.00	0.00	0.00
Cl	0.00	0.00	0.01	0.01	0.00	0.01	0.00
F	0.00	0.01	0.01	0.01	0.00	0.01	0.00
Mg#		0.35		0.34		0.28	

So two temperature estimates rival to represent the thermal conditions of granulite facies metamorphism: The c. 800°C (or higher) obtained from Hbl-Pl thermometry, and from Opx-Cpx thermometry according to Wells (1977), and the c. 670°C obtained from Grt-Hbl thermometry, Grt-Bt thermometry, and Opx-Cpx thermometry according to Fonarev and Graphikov (1987). Grt-Bt temperatures are commonly regarded as closure temperatures, especially in areas which underwent prolonged (near) isobaric cooling, which is the case in the Bamble Sector (Touret and Olsen 1985, Visser and Senior 1990, Nijland et al. 1993a, ch. 6). The Grt-Bt temperatures show homogenization over the entire area, which supports their interpretation as closure temperatures resulting from isobaric cooling.

The temperature of the allanite- and titanite-out isograds may elucidate which of the two temperatures is the real estimate for the highest grade area. The upper stability of allanite is not well defined. Critical saturation temperatures in felsic magmas are c. 800°C (Chesner and Ettliger 1989). Bingen (1988, 1989) observed the disappearance of allanite during amphibolite to granulite facies transition in augen gneisses from Rogaland, SW Norway. Temperature estimates by both feldspar and two pyroxene thermometry are 700–800°C for the zone in which allanite disappeared (Bingen 1988, Bingen et al. 1990). Titanite is stable up to at least c. 700–750°C, depending on fluid composition (Schuiling and Vink 1967, Hunt and Kerrick 1977, Gibert et al. 1990). The absence of allanite and titanite indicates that a temperature of c. 670°C is too low for the highest grade zone. We therefore consider the temperature obtained from the Hbl-Pl and Wells Opx-Cpx thermometers to be the best estimate for granulite facies conditions. Nevertheless, it should be realized that these estimates are also blocking temperatures, and hence provide minima (cf. Frost and Chacko 1989).

The core and rim temperatures for Hbl-Pl, Opx-Cpx and Grt-Bt pairs generally coincide within error (Compare tables 3.4 and 3.5). Samples from the amphibolite facies area along the Porsgrunn-Kristiansand Fault display higher Grt-Hbl temperatures for the rims of mineral pairs than for their cores. Corresponding Grt-Hbl-Pl-Qtz pressures are also higher for the rims (See below). In contrast, Grt-Hbl temperatures are lower for the rims of mineral pairs than for the cores in samples from the coastal area. Grt-Hbl-Pl-Qtz pressures are also slightly lower or equal (See below).

3.4.2

Pressure

The Grt-Hbl-Pl-Qtz geobarometer (Tables 3.4 and 3.5) was applied to quartz-bearing samples whose garnet, hornblende and plagioclase fulfilled the criteria of Kohn and Spear (1990). The pressures were calculated at the obtained Grt-Hbl temperature. They can therefore not be considered to directly represent P_{Tot} during peak metamorphism. However, the first stage of the cooling and uplift path of the Bamble Sector was essentially isobaric down to approximately 500 °C (Touret and Olsen 1985, Visser and Senior 1990, Nijland et al. 1993a, ch. 6). For this reason, we consider the Grt-Hbl-Pl-Qtz pressures to be indicative of P_{Tot} during the peak of metamorphism.

Table 3.4 P-T estimates for the cores of minerals. Temperatures and pressures reported as the average $\pm 1\sigma$. Pressures are reported as averages of Fe and Mg exchange reactions, which usually differ less than 0.2-0.3 kb. Temperatures were calculated at 7.5 kb.

Sample	Hbl-Pl	Opx-Cpx	Grt-Hbl Pl-Qtz	Grt-Hbl- Pl-Qtz	Grt-Bt		
	Blundy & Holland (1990)	Wells (1977)	Fonarev & Graphikov (1987)	Powell (1985)	Kohn & Spear (1990)	Thompson (1976)	Perchuk (1981)
TN 19	712° \pm 19°			619° \pm 11°	7.3 \pm 0.2 kb	675° \pm 12°	698° \pm 9°
TN 142	777° \pm 12°			674° \pm 12°		662° \pm 8°	688° \pm 6°
TN 146	780° \pm 18°			616° \pm 16°	6.5 \pm 0.2 kb	650° \pm 29°	680° \pm 22°
TN 201				651° \pm 43°		722° \pm 27°	732° \pm 19°
TN 202	735° \pm 20°			633° \pm 16°		620° \pm 18°	659° \pm 13°
TN 204	751° \pm 21°			656° \pm 13°		722° \pm 10°	731° \pm 7°
TN 209	758° \pm 15°			617° \pm 21°	6.9 \pm 0.3 kb	627° \pm 21°	662° \pm 16°
TN 226	880° \pm 30°	835° \pm 35°	662° \pm 16°	696° \pm 6°		647° \pm 20°	677° \pm 15°
TN 227	870° \pm 13°			704° \pm 6°	7.6 \pm 0.1 kb		
TN 250	810° \pm 14°			714° \pm 30°	7.0 \pm 0.4 kb		
TN 258	823° \pm 7°			686° \pm 23°			
TN 291	796° \pm 14°			654° \pm 15°	6.6 \pm 0.2 kb		
TN 294	886° \pm 13°	714° \pm 56°	666° \pm 22°			646° \pm 19°	674° \pm 14°
TN 309	730° \pm 7°	784° \pm 60°	739° \pm 55°				
TN 402	752° \pm 4°	794° \pm 17°	717° \pm 21°				
TN 420	771° \pm 7°						
TN 430	747° \pm 10°	804° \pm 34°	692° \pm 10°				
TN 431	807° \pm 11°			696° \pm 13°	7.9 \pm 0.2 kb	784° \pm 27°	728° \pm 19°

Table 3.5 P-T estimates for the rims of minerals. Temperatures and pressures are reported as averages $\pm 1\sigma$. Pressures (kb) are reported as the average of both Fe and Mg exchange reactions, which usually differ less than 0.2-0.3 kb. Temperatures were calculated at 7.5 kb.

Sample	Hbl-Pl	Opx-Cpx	Grt-Hbl	Grt-Hbl-Pl-Qtz	Grt-Bt		
	Blundy & Holland (1990)	Wells (1977)	Fonarev & Graphikov (1987)	Powell (1985)	Kohn & Spear (1990)	Thompson (1976)	Perchuk (1981)
TN 19	726° \pm 18°			654° \pm 3°	7.6 \pm 0.3 kb	673° \pm 12°	696° \pm 8°
TN 142	766° \pm 8°			707° \pm 6°		661° \pm 21°	689° \pm 14°
TN 146	762° \pm 11°			642° \pm 14°	6.6 \pm 0.2 kb	656° \pm 21°	684° \pm 15°
TN 201				682° \pm 57°		657° \pm 11°	685° \pm 8°
TN 202				604° \pm 14°		643° \pm 7°	674° \pm 6°
TN 204	773° \pm 4°			632° \pm 21°		697° \pm 27°	713° \pm 19°
TN 209	723° \pm 28°			552° \pm 11°	6.5 \pm 0.2 kb	565° \pm 14°	615° \pm 11°
TN 226	876° \pm 4°	825° \pm 11°	649° \pm 6°	637° \pm 8°		588° \pm 11°	633° \pm 9°
TN 227	899° \pm 3°			693° \pm 1°			
TN 250	803° \pm 19°			685° \pm 30°	7.2 \pm 0.4 kb		
TN 258	815° \pm 11°			674° \pm 18°			
TN 291	793° \pm 14°			627° \pm 7°	6.6 \pm 0.2 kb		
TN 294	878° \pm 14°	783° \pm 60°	676° \pm 21°			659° \pm 24°	683° \pm 17°
TN 309	737° \pm 19°	834° \pm 27°	700° \pm 30°				
TN 402	770° \pm 15°	818° \pm 28°	703° \pm 14°				
TN 420	752° \pm 16°						
TN 430	747° \pm 10°	843° \pm 29°	690° \pm 19°				
TN 431	795° \pm 6°			674° \pm 14°	7.8 \pm 0.2 kb	734° \pm 34°	693° \pm 24°

To obtain a larger data set and to check for a possible gradient in P_{Tot} , seven metapelites were selected for garnet-plagioclase-aluminum silicate-quartz geobarometry. The obtained pressures range from 6.8 to 8.1 kb (Table 3.6), which is comparable to Grt-Hbl-Pl-Qtz pressures that vary between 6.5 and 7.9 kb (Table 3.4). Throughout the entire area, Grt-Als-Pl-Qtz pressure are equal for the cores and rims of mineral assemblages, or slightly lower for the latter. Grt-Hbl-Pl-Qtz pressures are higher for rims than for corresponding cores in the north of the amphibolite facies area, but equal or lower in the coastal area.

Table 3.6 Grt-Pl-Sil/Ky-Qtz pressure estimates (Newton and Haselton 1981) for metapelites. Pressures were calculated at 750°C and are reported at $\pm 1 \sigma$. As pressure estimates are equal for both cores and rims of CM454, EJ10, MR35, and WT66, only the average of both is reported.

Sample	Core	Rim
CM407	8.1 \pm 0.1	7.6 \pm 0.1
CM454	7.1 \pm 0.1	
EJ10	7.5 \pm 0.2	
MR35	6.8 \pm 0.2	
MR73	7.6 \pm 0.0	6.8 \pm 0.3
NS19	7.3 \pm 0.4	6.9 \pm 0.1
WT66	6.8 \pm 0.4	

3.4.3

P-T gradients

Contrary to the claim of Lamb et al. (1986), temperature estimates show a increase with metamorphic gradients, with the highest temperatures in the granulite facies area (table 3.4). An exception to the regional pattern is sample TN 250, which yields a Hbl-Pl temperature of 810°C. The reason of this elevated temperature is unclear; it may either be related to a local anomaly as metamorphic orthopyroxene has been found in a metagabbro in its direct vicinity, or to the elevated chlorine content of the rock (up to 0.80 wt.% Cl in hornblende). The amount of titanium in hornblende increases with increasing temperature (e.g. Otten 1984). Indeed isopleths for Ti in hornblende (0.1 and 0.2 Ti atoms per formula unit) divide the area, and Ti increases with increasing metamorphic gradient in the Nelaug-Arendal area (See chapter 5, Fig. 5.2). This provides an independent argument for a temperature increase over the transition zone. A gradient in P_{Tot} seems not to be present, although maximum pressures are higher in the granulite facies area.

P_{H_2O} was almost certainly significantly lower than the P_{Tot} estimated from barometry. This is strongly suggested by the CO₂-rich fluid inclusions in the granulite facies area (Touret 1971b, 1985). In addition, detailed PT and fluid inclusion studies on one of the two metapelitic granulite occurrences north of the Opx-isograds indicate a P_{H_2O} of about $\frac{1}{4} P_{Tot}$, although CO₂

seems to be absent (Nijland et al. in prep.).

Temperature estimates are $752 \pm 34^{\circ}\text{C}$ (range $710\text{--}780^{\circ}\text{C}$) for the amphibolite facies zone at 7.1 ± 0.4 kb (range $6.5\text{--}7.6$ kb). Granulites of zone B + C have an average temperature of $836^{\circ} \pm 49^{\circ}\text{C}$ at 7.7 ± 0.3 kb. Surprisingly, those in zone D yielded slightly lower P-T estimates: $797^{\circ} \pm 15^{\circ}\text{C}$ at 7.2 ± 0.5 kb. All granulite facies samples together yield $822^{\circ} \pm 40^{\circ}\text{C}$ (range $770\text{--}890^{\circ}\text{C}$) at 7.4 ± 0.5 kb (range $6.6\text{--}8.1$ kb).

3.5

Discussion

3.5.1

The nature of granulite facies metamorphism

Surprisingly, the temperature estimates are lower for what was traditionally regarded as the most high grade part of the transition zone (zone D) than for the mainland granulite facies terrain (zones B + C). The P-T study of Lamb et al. (1986) was based on eight samples only, and the difference is not directly evident in their data. However, their Grt-Cpx temperatures (Dahl's (1980) and Saxena's (1979) calibrations) also show higher averages for the combined zones B + C ($820^{\circ} \pm 31^{\circ}\text{C}$ and $865^{\circ} \pm 17^{\circ}\text{C}$ respectively, $n=8$) than for zone D ($788^{\circ} \pm 9^{\circ}$ and $837^{\circ} \pm 5^{\circ}\text{C}$ respectively, $n=2$). Peterson and Valley (in prep.) conducted a detailed P-T study on Tromøya (zone D) and concluded that temperatures were c. 850°C in the north of the island, i.e. near zone C, and c. 750°C in the southeast. Hence, it appears to be a consistent image that the highest temperature areas were not Tromøya, Hisøya and Merdøya, but that the peak thermal area was situated on the mainland and perhaps the northernmost part of Tromøya.

The Bamble Sector constitutes a separate, NW-SE trending structural domain in the generally N-S trending Sveconorwegian part of south Norway (e.g. Falkum and Petersen 1980). The structural trend in the parautochthon of the Bamble Sector (Starmer 1990a, 1991) is concave with respect to the present day coast line. The established isograd sequence is also concave to the coast. In the east, orthopyroxene and cordierite isograds bend towards the coast. In the west, they are truncated by the post-tectonic Grimstad granite, but here too, they head for the sea, as no orthopyroxene and cordierite have been reported west of the granite.

Both the structural trend and the isograd pattern define the one half of an oval. It may be assumed that the half oval exposed on the mainland is completed by one situated in the Skagerrak. The highest temperatures occur in the centre of the exposed half oval. Away from the centre of the oval, temperatures are lower; this holds for both the amphibolite facies area to the northwest, and for Tromøya, Hisøya and Merdøya to the southeast: temperatures are distributed in a more or less oval way. This would indicate that the exposed metamorphic terrain is in fact half of a thermal dome complex. Whereas most thermal domes, like the dome de l'Agout, France (Schuiling 1960) and the dome on Naxos (Jansen and Schuiling 1976, Schuiling and Kreulen 1979) have a migmatitic core, the Bamble thermal dome has a granulite core.

Unfortunately, little is known about the deep geology below the Skagerrak. A positive gravity anomaly, which is concave toward the coast, is present below the Skagerrak (Smithson 1963). This anomaly was explained by a greater density contrast near the coast, or by a body with a density close to that of a gabbro. Alternatively, the anomaly may be explained as an offshore continuation of the granulite complex, as granulites have densities slightly higher than gabbros, whereas the density of quartz-garnet-sillimanite gneisses is slightly lower (cf. Holbrook 1989). With its concave boundary, this interpretation would be in agreement with the concept of a dome structure. The first data about the Precambrian basement in the southeast are provided by a few deep boreholes in Denmark (Noe-Nygaard 1963, Larsen 1971). In Central Jutland, these yielded muscovite free, biotite, garnet and hornblende-bearing gneisses, i.e. amphibolite facies rocks; low grade phyllitic gneisses occur in northern Jutland. It is, however, unclear to what extent this terrain is continuous with the Bamble Sector. In addition, present day geology has largely been influenced by the Permian Oslo Rift.

Ore types are often bound to specific rock types, and usually not to metamorphic gradients. However, certain ore types in the Bamble Sector seem to be related to the thermal dome structure, although this may be a mere coincidence. Whereas iron and pyrite-chalcopyrite deposits occur in the entire area, Ni and Zn-Pb deposits do not occur in the centre of the dome (See map of Lindahl and Gust 1987). No relationship between metamorphic grade and the occurrence of Fe-Ti and rutile deposits is observed.

Two results from this study are not explained by the thermal dome concept: 1) the cross cutting nature of some isograds, and 2) the increasing P-T conditions indicated by the rims of mineral pairs in the area along the boundary between the Bamble and Telemark Sectors, the Porsgrunn-Kristiansand Fault (PKF).

Two cross cutting relationships are present. The allanite and titanite-out isograds intersect each other. This may be due to the fact that both minerals only occur as accessories in most rocks. This inevitably introduces a limited uncertainty in the exact location of both isograds. Therefore, the intersection may be an artefact. The intersection of the kyanite-out isograds and the cordierite and orthopyroxene in-isograds may also be an artefact, as kyanite occurs in relatively few samples. In addition, both old and young kyanite are restricted to the north side of isograd. It is possible, however, that the intersection has geological significance for the old kyanite. The -Ky isograd may be an old relic isograd. In the amphibolite facies area, the initial high pressure stage of metamorphism was followed by a heating stage which resulted in the growth of sillimanite (cf. Visser and Senior 1990). This obviously explains the -Ky isograd. This may be related to Gothian upper amphibolite facies metamorphism. However, recrystallization of sillimanite indicates another heating event and it is conceivable that the +Crd and especially the +Opx isograds are related to this heating event, and are thus younger. This would imply two separate metamorphic sequences: In the coastal area (Arendal plus islets), Gothian high pressure metamorphism was followed by Gothian upper amphibolite facies metamorphism, and overprinted by granulite facies metamorphism related to thermal doming. In the northwestern area (PKF-Nelaug-Froland), Gothian high pressure metamorphism and subsequent upper amphibolite facies metamorphism were overprinted by a second phase of upper amphibolite facies metamorphism related to the thermal dome.

Some samples from the area along the boundary between the Bamble and Telemark

Sectors (PKF) indicate slightly higher P-T conditions of equilibration for the rims of mineral pairs than for their cores (TN 19, TN 146), where samples from the more southern amphibolite facies area (TN 209, 250) and granulite facies area (TN 291, TN 431) yield higher or equal pressures and temperatures. These indicate slightly different cooling paths for these areas (Fig. 3.9). Two explanations are possible: 1) The increased conditions displayed by rims are related to the second amphibolite facies event, whereas the cores provide information about the first. 2) The increased rim conditions reflect an event that only occurred in that part of the Bamble Sector. In case of 1), the topographically restricted occurrence is not explained. It would be expected that amphibolite facies samples nearer to the high temperature area show increased rim conditions. In case of 2), the increased rim conditions may be related to mylonitic deformation and the emplacement of the various augen gneiss complexes in the area along the PKF (See below). It is well established that these augen gneisses have granulite facies contact aureoles (Touret 1968, Hagelia 1989, Nijland and Senior 1991). This thermal disturbance may have been larger: Outside the granulite facies aureole, it enhanced amphibolite facies conditions.

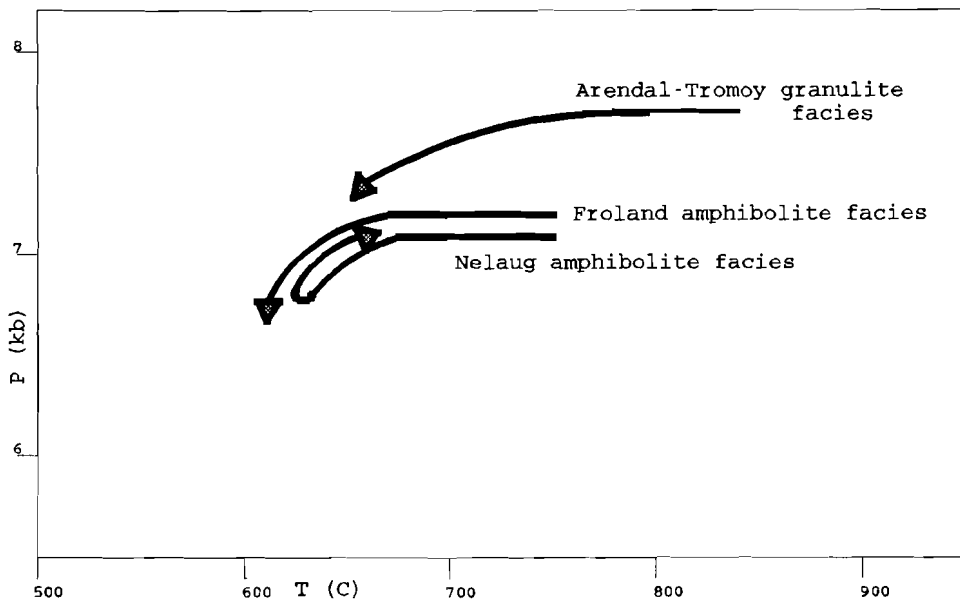


Fig. 3.9 Cooling path deduced from thermobarometry. Average P-T vectors for each area were constructed using 1) Hbl-Pl and Opx-Cpx core temperatures with Grt-Hbl-Pl-Qtz and Grt-Al₂SiO₅-Pl-Qtz core pressures; 2) Grt-Hbl core temperatures and Grt-Hbl-Pl-Qtz core pressures; 3) Grt-Hbl rim temperatures and Grt-Hbl-Pl-Qtz rim pressures. The Nelaug amphibolite facies area is situated along the Porsgrunn-Kristiansand Fault, the Froland amphibolite facies area between the Nelaug area and the granulite facies area in the southeast.

Sm-Nd ages recently obtained by Kullerud and Dahlgren (1990, 1993) for the granulite facies mineral assemblages, indicate closure of the mineral isotopic systems at c. 1.08 Ga. This indicates that thermal doming had ceased around this time. When the dome was initiated, it is less evident. Visser and Senior (1990) claimed that high grade metamorphism in the area started as result of Gothian continental collision, and continued during prolonged cooling until late Sveconorwegian times. Several felsic granulites yield c. 1.5 Ga Gothian Rb-Sr whole rock ages with low Sr_1 ratio's (Field and Råheim 1979, Field et al. 1985), indicating that the Rb-Sr isotopic system was not disturbed afterwards. This may be explained by the absence of subsequent high grade metamorphism, as favoured by Field and co-workers (Field and Råheim 1979, Field et al. 1985), but may alternatively be explained if subsequent metamorphism was featured by low water activities, which prohibited whole rock scale Rb-Sr redistribution (Maijer 1990). Sm-Nd whole rock + granulite facies mineral ages obtained by Kullerud and Dahlgren (1990, 1992) indicate closure of that isotopic system during the second half of the Sveconorwegian orogeny; this seems to favour the second explanation. However, no evidence exists for uplift or retrogression between the Gothian and Sveconorwegian periods. This may indicate that the thermal dome became active during the late Gothian and existed until c. 1.15 Ga, or was initiated somewhere in between.

Sveconorwegian deformation was most intense along the border between the Bamble and Telemark Sectors. Mylonitic deformation was thus concentrated at the margin of the thermal dome. Several granitic-charnockitic augen gneiss complexes have been emplaced in this margin. If emplacement of these magmas was related to formation of the dome, then the dome was probably initiated between c. 1.27 and 1.23, because these are the most probable emplacement ages for some of these complexes (Smalley et al. 1983b, 1988). The thermal dome probably moved from east to west, as K-Ar biotite cooling ages become systematically younger in this direction. They are 0.96 ± 0.05 Ga in the eastern part of the Bamble Sector ($n=26$, O'Nions et al. 1969a), 0.86 ± 0.05 Ga in the part of the Bamble Sector investigated in this study ($n=13$, Kulp and Neumann 1961, de Haas et al. 1992a).

Thermal doming may have been due to elevation of the asthenosphere below the area and/or thinning of lithosphere itself. This envisages two mechanisms for the formation of the dome:

I. Doming may have been related to attempted rifting, for which Starmer (1990a) found possible evidence in flow textures probably resulting from transtensional tectonism. The granitic-charnockitic augen gneisses show alkaline affinities and the related Morkheia Monzonite Complex shows anorthositic affinities (Milne and Starmer 1982, Starmer 1990ab). These intrusions have an anorogenic signature, and therefore fit with an extensional setting. The Grenville Province in North America has commonly been thought to be continuous and cogenetic with the post-Svecofennian terrain in southern Norway and Sweden (e.g. Barth and Dons 1960, Gower and Owen 1984). For this terrain, Emslie and Hunt (1990) also suggested that the Grenville thermal regime resulted from thinned lithosphere and/or magmatism rather than a subduction related event.

II. Thermal doming may have been related to elevation of the asthenosphere magmas below the overriding plate in response to subduction and subsequent continental collision in a setting analogous to the Lepontine dome in the Alps, but at a deeper level. A destructive plate marginal setting would be in agreement with the geochemical signature of volcanics that were deposited around 1.16 Ga in the Telemark area (Atkin and Brewer 1990). Provided that the subduction zone was situated in the present day west, it would also fit with the presence of calcalkaline intrusions to the west (Rogaland; Bingen et al. 1990) and with 1.08 Ga eclogites in Scotland (Sanders et al. 1984), which was situated to the west of South Norway at that time.

For the period which saw most likely the formation of the thermal dome, i.e. 1.27 to 1.23 Ga, Pesonen and Torsvik (1990) inferred a rather slow plate drift velocity. They based their conclusions on palaeomagnetic data, from which they deduced a strongly increased plate drift velocity during the period from c. 1.4 to 1.3 Ga. This is likely to be related to rifting. This would imply that, provided that doming started somewhere between 1.27 and 1.23 Ga, it may be probably explained by the second concept.

3.6

Conclusion

It is concluded that amphibolite to granulite facies transition in the Nelaug-Arendal area of the Bamble Sector was related to thermal doming, which resulted in renewed metamorphism of rocks that were already metamorphosed under upper amphibolite facies conditions. Increased heat flow in the centre of the dome caused a temperature gradient. At the same time, P_{H_2O} was significantly lowered in the centre of the dome, while P_{Tot} remained roughly constant. Doming ceased at c. 1.15 Ga, and is likely to have started between 1.27 and 1.23 Ga, although an earlier onset can not be excluded.

Acknowledgements - All those who participated in the Bamble Project of the Dept. of Geochemistry, Univ. of Utrecht, are thanked for the use of their samples and J. de Groot and his crew for producing over two thousand thin sections. We are grateful to Blakstad Yrkeskole for lodging during field work. R.P.E. Poorter and T. Bouten assisted in the microprobe analyses. A. Moerenhout and E.J. Kornman did some of the analyses. Prof. V.I. Fonarev provided the TPF program for the Fonarev & Graphikov Opx-Cpx geothermometer. Financial support from AWON (NWO 751.353.023) is gratefully acknowledged. G.J.L.M. de Haas, J.B.H. Jansen and R.D. Schuiling critically read the manuscript. The paper benefitted from a constructive review by J.L.R. Touret.

**HALOGEN GEOCHEMISTRY OF FLUID DURING AMPHIBOLITE-GRANULITE
METAMORPHISM AS INDICATED BY APATITE AND HYDROUS SILICATES IN
BASIC ROCKS FROM THE BAMBLE SECTOR, SOUTH NORWAY.**

Abstract - Halogen chemistry of apatites, biotites, amphiboles and titanites from metabasites in the Proterozoic Bamble Sector amphibolite-granulite facies transition zone has been studied to elucidate the behaviour of halogens during original magmatism and subsequent metamorphism. Three groups could be recognized: I. F-OH-apatites with more than 50 mole % F and virtually no Cl. II. F-OH-apatites with up to 15 mole % of Cl. III. Cl-rich apatites with up to 6.73 wt.% Cl. The latter are the most Cl-rich metamorphic apatites ever reported. The F-contents of biotite do not follow this division, but their Cl-contents do. $\log(f\text{HF}/f\text{H}_2\text{O})$ values for the coexisting fluid phase calculated from biotite are slightly lower than those calculated from apatite, while $\log(f\text{HCl}/f\text{H}_2\text{O})$ values calculated from biotite are substantially higher than those calculated from apatite. The $\log(f\text{HF}/f\text{H}_2\text{O})$ values reflect the composition of the peak metamorphic fluid phase. The apatites show three kinds of patterns of F-contents: 1). W-shaped, 2). Rimward increasing, and 3) Rimward decreasing. Pattern 2) reflects progressive metamorphism. Pattern 3) is thought to reflect growth starting near peak metamorphism and going on during retrograde dilution of the peak metamorphic fluid by a newly introduced aqueous one. Some apatites show local resorption effects along cracks. No regional trend in calculated $\log(f\text{HF}/f\text{H}_2\text{O})$ values is present. As different from other granulite terrains, the Bamble biotites and amphiboles from granulite facies samples have halogen-contents similar to those from the amphibolite facies area. The samples show that halogen bearing fluids were controlled at a very restricted scale during peak as well as retrograde metamorphism.

4.1 Introduction and geological background

4.1.1 Halogen geochemistry and petrology

The fluid evolution in metamorphic terrains may be recorded by fluid inclusions and chemical mineral equilibria. Hydroxyl-bearing silicates like micas, amphiboles and titanite, and phosphates like apatite incorporate halogens. Especially amphibolites contain a number of such minerals and are therefore suitable for studying fluid evolution.

Although synthetic apatites have been studied to understand the incorporation of halogens in their crystal structure (e.g. Morton 1961, Ekström 1973a, Ruzsala and Kostiner 1975, Latil and Maury 1977, Baumer and Argiolas 1981, Maiti and Freund 1981), only limited data are yet available on the behaviour of halogens in metamorphic apatites (cf. Nash 1984), especially when they are mixtures of end members. Chlorine tends to enlarge the crystal lattice of apatite, whereas fluorine contracts it (Hughes et al. 1989). Halogens are strongly fractionated into apatite with respect to amphiboles and micas (Ekström 1973b, Fominykh 1974, Ionov et al. 1987). Apatites are considered to be highly resistant to secondary loss of many elements, including fluorine (Latil and Maury 1977). Resorption of halogens by an aqueous fluid more strongly affects hornblende (Blattner and Black 1980) and biotite (Stormer and Carmichael 1971, Nash 1976) than apatite. This explains why apatites may be used as indicators of halogen fugacities in magmatic (Candela 1986) and metamorphic systems (Yardley 1985), since the experiments by Korzhinskiy (1981).

Biotite and muscovite have also been calibrated to measure halogen fugacities in metamorphic-hydrothermal fluids (Munoz and Ludington 1974, 1978, Munoz 1984). The incorporation of halogens in silicates strongly depends on their crystal chemistry. A negative correlation between fluorine and divalent iron, the so-called "Fe²⁺-F avoidance rule" (Rosenberg and Foit 1977), is commonly observed. Substitution of fluorine for hydroxyl in micas, amphiboles and other silicates generally stabilizes these minerals to higher temperatures, i.e. granulite facies conditions (Kearns et al. 1980, Petersen et al. 1982, Valley et al. 1982). The breakdown temperature of amphibole is increased by as much as 150°C, depending on the amount of F substituting for OH (Fedoseev et al. 1970, Holloway and Ford 1975). Similar values apply for phlogopite (Peterson et al. 1991).

Titanites may also incorporate OH and F, due to the coupled substitution (Al,Fe³⁺) + (OH, F) = Ti + O (Zabavnikova 1957, Černý and Riva di Sanseverino 1972, Higgins and Ribbe 1976). Minor amounts of Cl have also been reported (Zabavnikova 1957). The influence of these substitutions on the titanite stability field is unknown. Substitutions of both F and OH are thought to be temperature and pressure dependent (Oberti et al. 1991).

The transition from upper-amphibolite facies to granulite facies rocks is essentially a matter of H₂O-loss. The causes of this change have recently been reviewed by Newton (1990). They are: (1) the scavenging of water, either due to the introduction of other species, notably carbon dioxide, or due to removal of H₂O by anatectic melts, (2) metamorphism of already partly dried rocks, (3) dehydration due to heat released by underplating magmas. The role of halogens and implications for the behaviour of halogens have not been considered so far.

Detailed study of the halogen distribution in and between minerals may provide clues. As fluorine is strongly partitioned into mineral phases, the interstitial fluid in a closed system becomes progressively depleted in fluorine; hence equilibration between apatite and fluid in a closed system will result in rimward decreasing fluorine contents, provided that conditions remained isothermal. In contrast, rimward increasing or even constant fluorine contents must imply addition of fluorine, provided that the constant contents are not due to homogenization, like homogeneous Mg-distributions in garnets. Diffusion of halogens parallel to the c-axis in apatite may also cause zoning patterns (Brenan 1992).

Variations of halogen fugacities have been documented around granites (Gunow et al.

1980, Sisson 1987) as well as in regional granulite facies terrains associated with anorthositic magmatism like Rogaland, SW Norway (Jansen and Maijer 1987), where the highest amounts of fluorine are observed in granulite facies biotites and amphiboles. On the other hand, fluorine contents of phlogopite, tremolite and talc decrease towards the migmatitic core of the amphibolite facies complex at Naxos, Greece (H. van der Rijst pers. com.), due to a loss of water released from the central core. Burton and O'Nions (1990) observed an enrichment of fluorine in retrograde biotite grown from orthopyroxene relative to primary biotite in Sri Lankan granulites.

4.1.2

The Bamble Sector

The high grade Proterozoic terrain around Arendal in the Bamble Sector, southern Norway, is one of the classic amphibolite to granulite facies transition zones. Metamorphism during the Gothian (Kongsbergian, 1.75–1.5 Ga) and Sveconorwegian (Grenvillian, 1.25–0.9 Ga) orogenies resulted in the regional increase in metamorphic grade from upper-amphibolite to LILE-depleted granulite facies (Touret 1971a, Field et al. 1980, Lamb et al. 1986, Nijland and Maijer 1992, 1993). For detailed descriptions of the geology of the area, the reader is referred to Starmer (1985a, 1990a, 1991). The P-T path of the Froland area of the Bamble Sector was established by Visser and Senior (1990). They interpret the high grade metamorphism to be exclusively of Gothian age. Recent age determinations, however, indicated that granulite facies metamorphism around Arendal had ceased around 1.1 Ga (Kullerud and Dahlgren 1990). Combined petrological-structural studies also indicate high grade conditions during the Sveconorwegian at least in parts of the Bamble Sector (Nijland et al. 1991, Nijland and Senior 1991). Studies regarding the metamorphic fluid evolution were limited to the elaborate fluid inclusion work of Touret (1971b, 1972, 1985).

The aims of this study are: (1) to contribute to the understanding of the incorporation of halogens in apatites during high grade metamorphism and their behaviour under amphibolite–granulite facies conditions, (2) to estimate the realm of fluid control during regional metamorphism in the Bamble Sector with respect to the ceasing water activity and the scale of mineral-fluid equilibration, and (3) to elucidate late hydrothermal and retrograde influences.

To achieve these goals, we concentrated on metabasic rocks, because they generally contain many OH-bearing minerals, have a relatively uniform composition, provide reasonably good field control and occur across the entire transition zone. Four basic rock types occur in the area: (1) Concordant amphibolite bands intercalated with gneisses (Bugge 1940, Starmer 1985a), (2) Entirely metamorphosed but discordant plutons like the Vimme amphibolite (Nijland 1989), (3) Composite bodies ("hyperites") with cores of coronitic gabbro and amphibolitized margins (Brøgger 1934b, Bugge 1940, Brickwood and Craig 1987), which were emplaced during both the Gothian and Sveconorwegian orogenies (de Haas and Verschure 1990, de Haas 1992, de Haas et al. 1993a), (4) Discordant Sveconorwegian basic dikes (Nijland et al. 1991, Nijland and Senior 1991). Samples have been collected of types 1–3 (Fig. 4.1).

Amphibolites usually have a foam texture of plagioclase, hornblende with occasionally large garnets. Granulite facies samples may in addition contain ortho- and clinopyroxene. Biotite and quartz are present in minor amounts in most samples; only four samples contain K-feldspar. Common accessories are apatite, zircon, ilmenite, titanite and sulphides (chalcopyrite, pyrite, pyrrhotite). Some samples show a preferred orientation of biotite and hornblende crystals. While apatite has been recrystallized and is clean in many cases, apatites in several samples contain both fluid and unidentified solid inclusions. Inclusions that could be identified include hornblende, zircon and opaque minerals. A description of the samples is given in the appendix.

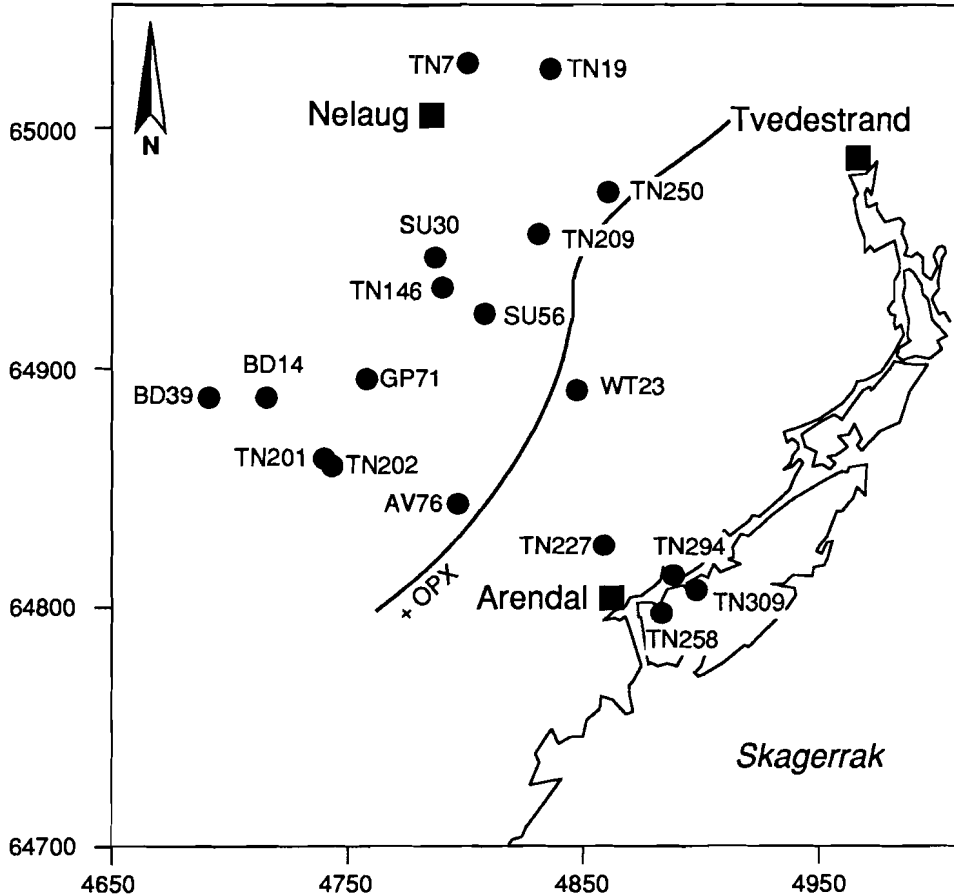


Fig. 4.1 Map of the area with sample locations. The orthopyroxene-in isograd shown is the one for metabasic rocks. The isograd is shifted at expense of the isograds of Touret (1971a) and Field et al. (1980) according to a new set of isograds for this part of the Bamble Sector (Nijland and Majer 1992, 1993).

Minerals were analyzed by a full stage automated Jeol JXA 8600 Superprobe controlled by a Tracor Northern TASK operation system at the Department of Geochemistry, Utrecht University. Running conditions were 15 keV, 10 nA and 30-60 sec. counting time. All minerals were analyzed for Si, Ti, Al, Fe, Mn, Mg, Ca, Na, K, P, Cl and F. The first batch was also analyzed for S or Cr. Cl, F, Na K and Mn were analyzed by WDS, the other elements by EDS. Cl and F were analyzed with the PET and TAP crystals respectively. Halite, lithiumfluoride and topaz standards were used for the halogens. Natural silicates and oxides were used for the other elements; a pyrite standard was used for sulphur. To obtain reliable fluorine analyses, peak height discrimination was applied over 1 to 7 V. The beam was not rastered. Data were corrected with a Tracor Northern PROZA correction programme.

After the first reconnaissance batch, seven samples were selected for detailed investigation. Rim to core scans were analyzed in apatites from these samples. Element distribution diagrams were obtained for apatites from TN19 and WT23 at 128 x 128 pixels and 400x magnification.

Apatite was normalized to 25 oxygens, biotite and hornblende to 22 and 23 respectively. Titanite was normalized to three cations. The OH-content of apatite was calculated from stoichiometry, i.e. $OH = 2 - F - Cl$ for apatites with $F + Cl \leq 2$, and are considered to be zero for apatites with $F + Cl > 2$. The latter are termed apatites with excess halogens. The variation in F-contents is expressed as $(F_{max} - F_{min}) / F_{max}$, with F as atoms per formula unit (a.f.). The mean Ca/P ratios have $\sigma \leq 0.03$, except for WT23 ($\sigma = 0.06$). The Mg-ratio has been calculated as $Mg\# = Mg / (Fe + Mg)$. Selected analyses are presented in table 4.1.

4.3

Results

4.3.1

Apatite

The apatites fall apart in three groups: I). F-OH apatites with more than 50 mole % F and almost no Cl, II). Essentially F-OH apatites with more than 35 mole % F and a minor amount of Cl, and III). Cl-rich apatites with a variable F-content. This is clearly illustrated in a F-OH-Cl plot (Fig. 4.2). The apatite chemistry in each sample is summarized in table 4.2. The threefold division is independent of the basic rocks types which the samples represent. Although the Cl-rich apatites from group III tend to be anhedral, no clear relationship between apatite morphology and chemistry could be detected.

Group I. The Cl-content of the apatites is ≤ 0.20 a.f. and the OH-contents varies from nil to nearly 1 a.f. (Fig. 4.2a). The variation in F-content may be as much as 65 % in one sample. Apatites containing excess halogens occur in several samples. The Ca/P ratio ranges

Table 4.1a Selected mineral analyses for group I.

Mineral Sample	Ap BD14	Ap TN227	Bt BD14	Bt TN294	Hbl TN309	Hbl TN294	Ttn TN7
SiO2	0.00	0.00	37.41	35.66	43.04	41.05	30.11
TiO2	0.00	0.00	2.21	4.95	2.02	2.20	38.06
Al2O3	0.00	0.17	16.07	14.21	10.26	12.68	1.48
FeO	0.00	0.00	18.42	18.54	16.16	16.74	0.91
MnO	0.01	0.00	0.19	0.04	0.35	0.21	0.00
MgO	0.00	0.12	12.49	12.14	11.26	10.01	0.00
CaO	55.11	55.80	0.00	0.00	11.19	11.67	27.94
Na2O	0.00	0.00	0.00	0.08	1.77	1.51	0.00
K2O	0.00	0.00	9.59	9.84	1.35	2.01	0.00
P2O5	42.00	42.05	0.00	0.00	0.00	0.00	0.00
SO3	0.06	0.22	0.06	0.00	0.00	0.20	0.00
Cl	0.46	0.00	0.25	0.05	0.02	0.05	0.00
F	2.84	2.64	0.20	0.22	0.18	0.22	0.36

Total	100.48	101.00	96.89	95.73	97.60	98.55	98.86
--------------	---------------	---------------	--------------	--------------	--------------	--------------	--------------

Table 4.1b Idem, group II.

Ap TN19	Ap TN202	Bt TN19	Hbl TN19
0.00	0.01	34.53	42.74
0.02	0.01	1.47	1.50
0.00	0.01	16.14	11.56
0.00	0.39	21.16	18.45
0.06	0.16	0.06	0.27
0.00	0.01	10.51	9.15
55.38	54.37	0.01	10.62
0.00	0.04	0.34	1.70
0.10	0.01	9.12	0.67
41.96	41.80	0.01	0.01
0.45	nd	nd	nd
0.76	1.16	0.51	0.13
3.43	2.30	0.34	0.33

102.16	100.27	96.42	97.13
---------------	---------------	--------------	--------------

Si	0.00	0.00	5.60	5.45	6.49	6.19	0.99	0.00	0.00	5.45	6.52
Ti	0.00	0.00	0.25	0.57	0.23	0.25	0.94	0.01	0.00	0.18	0.17
Al	0.00	0.03	2.84	2.56	1.83	2.25	0.06	0.00	0.00	3.00	2.08
Fe	0.00	0.00	2.30	2.37	2.04	2.11	0.03	0.00	0.05	2.80	2.35
Mn	0.00	0.00	0.03	0.01	0.05	0.03	0.00	0.01	0.02	0.01	0.04
Mg	0.00	0.03	2.79	2.77	2.53	2.25	0.00	0.00	0.00	2.47	2.08
Ca	9.97	9.98	0.00	0.00	1.81	1.89	0.99	9.94	9.89	0.00	1.73
Na	0.00	0.00	0.00	0.02	0.53	0.44	0.00	0.00	0.02	0.10	0.49
K	0.00	0.00	1.84	1.91	0.24	0.38	0.00	0.02	0.00	1.84	0.13
P	6.00	6.00	0.00	0.00	0.00	0.00	0.00	5.95	6.01	0.00	0.00
S	0.01	0.03	0.01	0.00	0.00	0.02	0.00	0.06	nd	nd	nd
Cl	0.13	0.00	0.06	0.01	0.01	0.01	0.00	0.21	0.34	0.13	0.04
F	1.51	1.39	0.10	0.11	0.08	0.11	0.04	1.82	1.23	0.17	0.16

Table 4.1c Selected mineral analyses for group III.

Mineral Sample	Ap TN250	Ap WT23	Bt WT23	Hbl TN250	Hbl TN250	Hbl WT23
SiO ₂	0.22	0.00	39.50	41.78	37.67	48.40
TiO ₂	0.04	0.00	3.41	1.07	0.28	1.91
Al ₂ O ₃	0.11	0.00	13.88	13.13	16.00	6.73
FeO	0.49	0.00	14.02	17.55	20.12	10.60
MnO	0.01	0.03	0.01	0.22	0.24	0.00
MgO	0.01	0.00	17.39	9.67	8.12	16.15
CaO	52.53	53.81	0.00	10.38	9.88	11.33
Na ₂ O	0.04	0.00	0.00	1.89	1.89	1.96
K ₂ O	0.08	0.00	10.31	0.57	0.53	0.74
P ₂ O ₅	40.12	40.14	0.00	0.01	0.01	0.00
SO ₃	nd	0.23	0.04	nd	nd	0.00
Cl	6.73	4.76	0.54	0.59	1.16	0.22
F	0.55	1.11	0.31	0.33	0.10	0.20
Total	100.93	100.08	99.41	97.19	96.00	98.24
Si	0.04	0.00	5.69	6.37	5.94	7.00
Ti	0.01	0.00	0.37	0.12	0.03	0.21
Al	0.02	0.00	2.35	2.37	2.97	1.15
Fe	0.07	0.00	1.69	2.23	2.65	1.29
Mn	0.00	0.00	0.00	0.03	0.03	0.00
Mg	0.00	0.00	3.73	2.20	1.90	3.48
Ca	9.88	10.07	0.00	1.69	1.67	1.76
Na	0.02	0.00	0.00	0.55	0.57	0.56
K	0.02	0.00	1.89	0.11	0.11	0.14
P	5.96	5.93	0.00	0.00	0.00	0.00
S	nd	0.03	0.00	nd	nd	0.00
Cl	2.00	1.41	0.13	0.16	0.31	0.05
F	0.31	0.61	0.14	0.16	0.05	0.10

from 1.67 to 1.70, indicating that a few apatites are slightly P-deficient. The SO₃-content is ≤ 0.42 wt.%, and typically much lower. MnO and FeO are less than 0.31 and 0.82 wt.% respectively. The apatites may contain traces of Si, Ti, Al, Mg, Na and K. Cr is below detection limit.

Group II. The Cl-content ranges from 0.17 to 0.37 a.f. and F between 0.65 and 1.82 a.f. (Fig. 4.2b). The F-content may vary as much as 64 % in one sample. The calculated OH-content varies between nil and 0.90 a.f. Apatites of this group do not contain excess halogens. The Ca/P ratio of 1.65 for TN202 indicates slight Ca-deficiency in these apatites; the ratio in TN19 is 1.68. SO₃-content of this sample is ≤ 0.57 wt.%. The apatites contain Si, Ti, Al, Mg, Na and K in trace amounts. MnO and FeO are lower than 0.12 and 0.42 wt.% respectively.

Group III. The apatites contain up to 2.00 a.f. Cl, while F varies between 0.31 and 1.20 a.f. The OH-content is low for TN250, but significant for WT23 (Fig. 2c). The highest Cl-content is 6.73 wt.% (TN250). The variation in F-content is large. Ca/P ratios are 1.66 for TN250, which contains some excess halogens, and 1.70 for WT23. SO₃ is less than 1.3 wt.% in the latter. The apatites contain less than 0.09 wt.% MnO and less than 0.66 wt.% FeO, and may contain traces of Si, Ti, Al, Mg, Na and K.

In order to gain insight in fluid evolution during growth of the apatites and in the effects of subsequent resorption and related phenomena, rim to core tracks have been analyzed.

Significant Cl-patterns have only been obtained for WT23 of group III (Fig. 4.3). F-patterns

Fig. 4.2 Volatile composition of apatites plotted in the OH-Cl-F triangle. In the case of excess halogens, X_F and X_{Cl} were calculated at base of the sum of $F + Cl$. In case of $F + Cl \leq 2$, ideal stoichiometry was assumed and they were calculated at base of 2. **a** The OH-F basal part of the triangle (with $Cl < 15\%$) showing the Group I apatites. **b** The OH-F basal part of the triangle (with $Cl < 25\%$) displaying the Group II apatites. Note that only TN19 apatites cross the OH:F = 1:1 divide. **c** Triangle plots of Group III apatites.

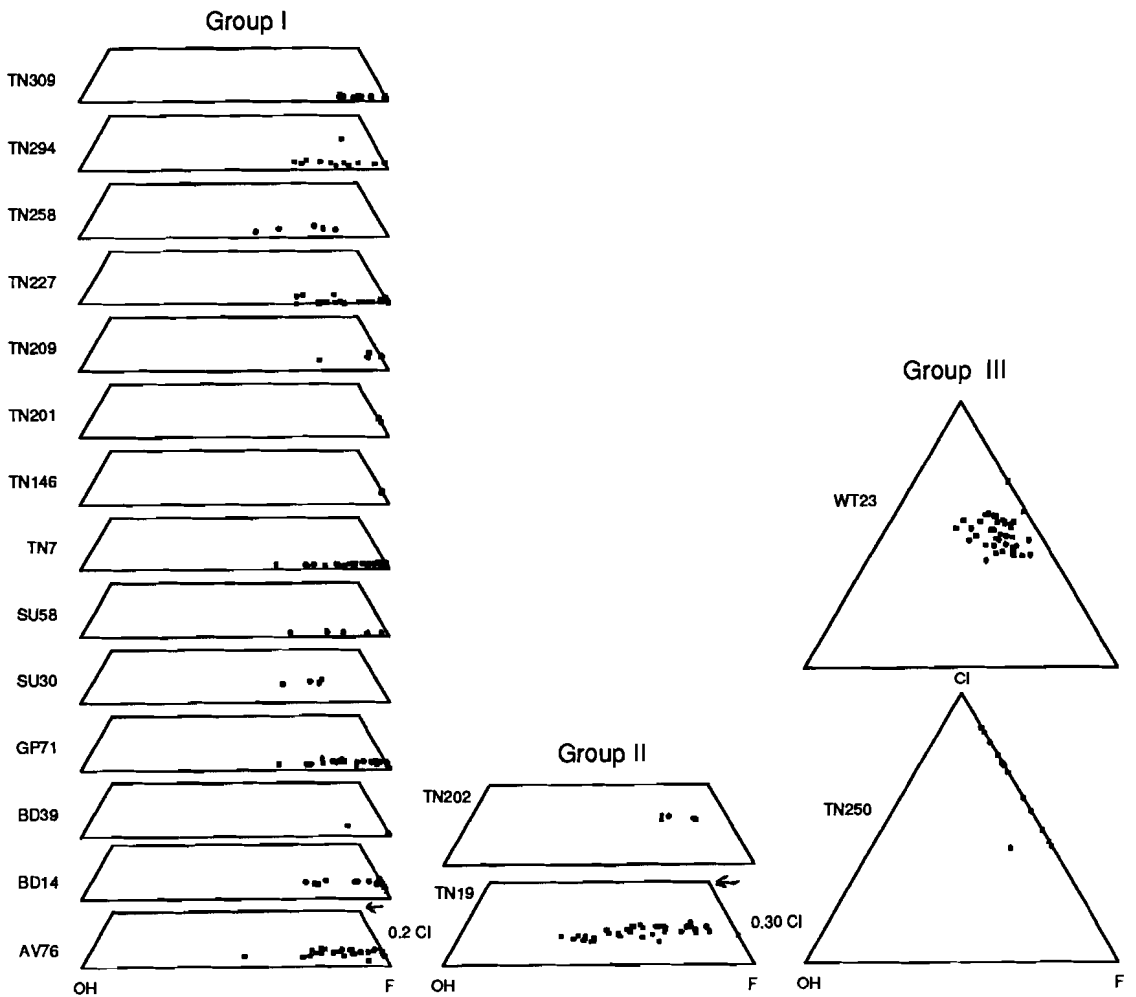


Table 4.2 Summarized apatite chemistry. F, Cl in a.f., SO₃ in wt.%. Fvar denotes variation in F.

Nr	Fvar	F	Cl	SO ₃	Ca/P	Traces
Group I						
AV76	61.7	1.01-2.63	≤0.14	≤0.08	1.69	Al, Fe, Mn, K
BD14	38.1	1.38-2.23	≤0.15	≤0.06	1.68	Ti, Al, Fe, Mn, K
BD39	20.0	2.04-2.55	≤0.08	≤0.15	1.67	
GP71	64.6	1.25-3.53	≤0.08	≤0.08	1.69	Ti, Al, Fe, K
SU30	19.5	1.23-1.47	≤0.17	≤0.07	1.70	
SU56	30.9	1.34-1.94	≤0.04	≤0.09	1.68	Fe
TN7	46.8	1.24-2.33	≤0.05	≤0.09	1.69	Si, Al, Fe, K
TN146	7.7	1.91-2.07	≤0.10	-	1.67	Si, Ti, Al, Fe, Mg, Na, K
TN201	1.6	1.89-1.92	≤0.14	-	1.67	Fe, Mg, Na, K
TN209	34.0	1.51-2.29	≤0.13	-	1.67	Si, Ti, Al, Fe, Mg, Na, K
TN227	45.9	1.39-2.57	≤0.07	≤0.32	1.67	Si, Ti, Al, Fe, Mg, Na, K
TN258	31.5	1.11-1.62	≤0.08	≤0.27	1.67	Si, Fe, Mg, Na, K
TN294	38.6	1.35-2.20	≤0.07	≤0.42	1.67	Si, Ti, Al, Fe, Mg, K
TN309	23.5	1.66-2.17	≤0.04	≤0.32	1.68	Si, Ti, Al, Fe, Na, K
Group II						
TN19	64.3	0.65-1.82	0.17-0.30	≤0.57	1.68	Si, Fe, Mg, K
TN202	16.4	1.22-1.46	0.33-0.37	-	1.65	Si, Ti, Al, Fe, Mg, Na, K
Group III						
TN250	74.2	0.31-1.62	0.84-2.00	-	1.66	Si, Ti, Al, Fe, Mg, Na, K
WT23	55.9	0.45-1.02	0.80-1.41	≤1.30	1.70	Si, Ti, Al, Fe, Mg, Na, K

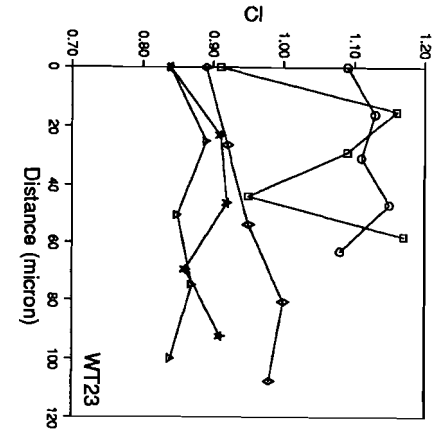
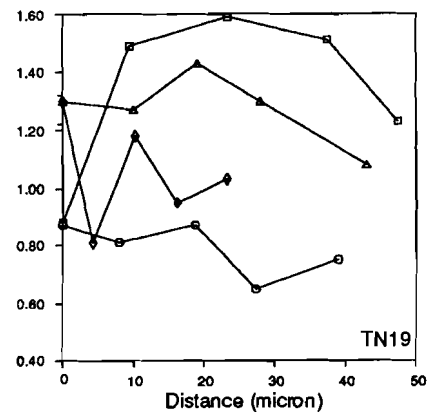
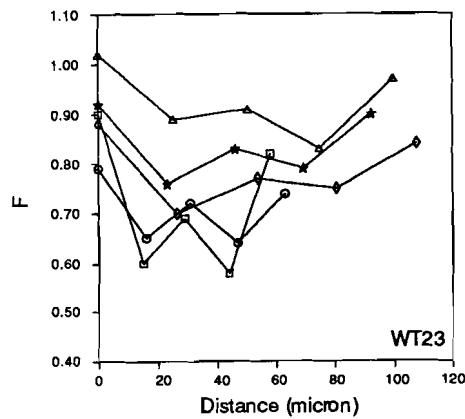
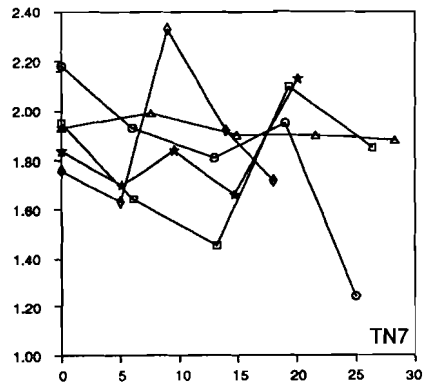
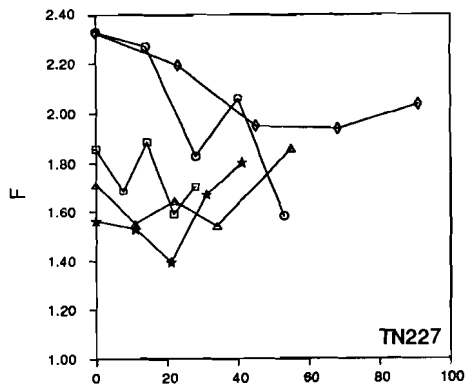
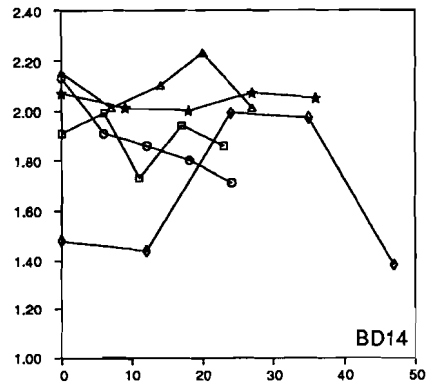
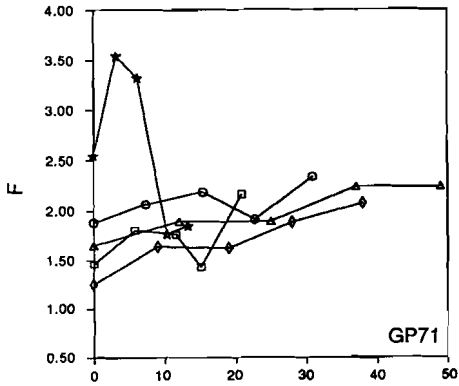
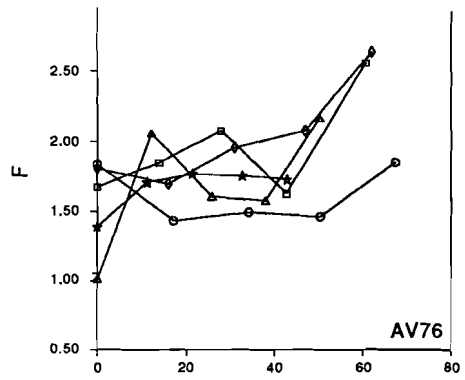


Fig. 4.3 Cl-pattern for group III's WT23. The rim is taken as zero.

Fig. 4.4 F-patterns for apatites from six selected samples. The rim is taken as zero. a AV76 (group I). b BD14 (group I). c GP71 (group I). d TN7 (group I). e TN19 (group II). f TN227 (group I). g WT23 (group III).



obtained from the tracks are shown in fig. 4.4. In each sample, the magnitude of the F-patterns varies from apatite to apatite, regardless whether the samples show a homogeneous set of patterns or not. Samples AV76 (Fig. 4.4a), GP71 (Fig. 4.4c), TN7 (Fig. 4.4d) and WT23 (Fig. 4.4g) show relatively homogeneous sets of F-patterns, while the patterns from BD14 (Fig. 4.4b), TN19 (Fig. 4.4e) and TN227 (Fig. 4.4f) are more heterogeneous.

Partly, the patterns and anomalies may be either obscured or exaggerated by variations in grain size and absolute halogen contents of the apatites. Variations in grain size may be due to different growth rates or different times of nucleation. In the first case, the patterns will be essentially comparable but have been stretched or shortened depending on the size of the apatite crystals. In the second case, patterns will have been displaced with respect to each other. On the other hand, the scale of fluid control will influence the magnitude of the patterns, and it is to be expected that the range of magnitudes will be larger when the fluid is more locally controlled. To minimize these effects, the patterns have been normalized. The distance to the rim is divided by half the diameter (the core), where the rim is arbitrarily taken zero. The halogen content is normalized to the maximum amount in each grain. In the samples AV76, BD14, GP71 and TN19, one grain still displays a completely deviant F-pattern after normalization; these patterns have been omitted.

The shape of the rim to core halogen patterns are not bound to one specific group. In WT23 apatites, Cl decreases slightly from core to rim, but not all patterns have the same shape (Fig. 4.5). Two of the patterns are M-shaped. The same sample shows a homogenous set of normalized F-patterns (Fig. 4.6g). These are all W-shaped, and thus inversely correlated with the two M-shaped normalized Cl-patterns.

The normalized F-patterns of other samples are not so homogeneously shaped as those from WT23. W-shaped patterns are present in group I's AV76 (Fig. 4.6a), TN7 (Fig. 4.6d), and TN227 (Fig. 4.6f), and in group II's TN19 (Fig. 4.6e). The first (core) half of all patterns in AV76, GP71 and TN19 is similar to the first part of this W-shaped base pattern.

Fig. 4.5 Normalized Cl-pattern from rim ($x = 0$) to core ($x = 1$) for group III's WT23. For explanation, see text.

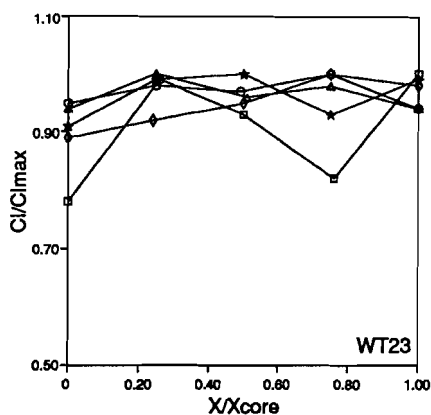


Fig. 4.6 F-patterns from rim ($x = 0$) to core ($x = 1$) for apatites from selected samples. For explanation, see text. a AV76 (group I). b BD14 (group I). c GP71 (group I). d TN7 (group I). e TN19 (group II). f TN227 (group I). g WT23 (group III).

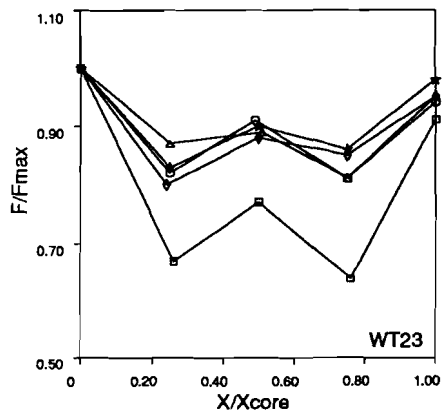
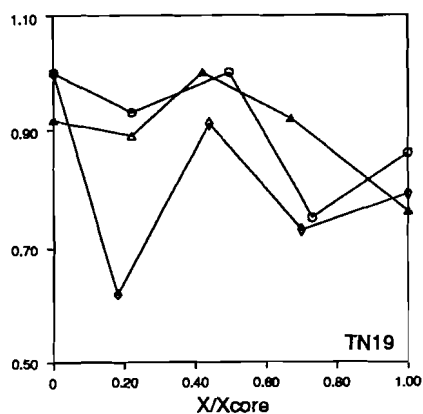
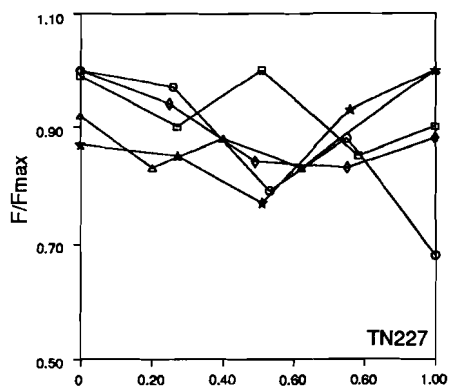
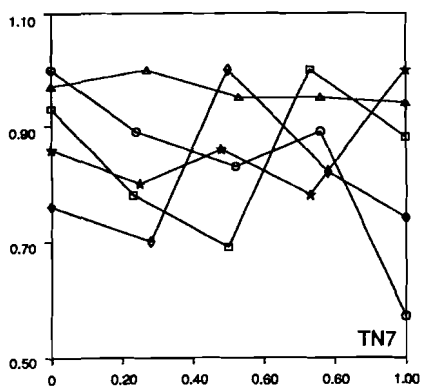
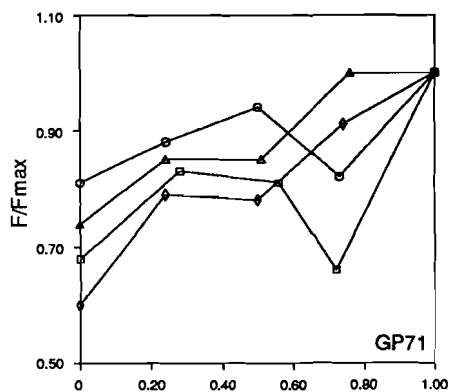
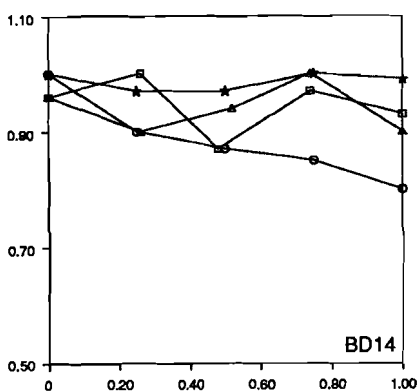
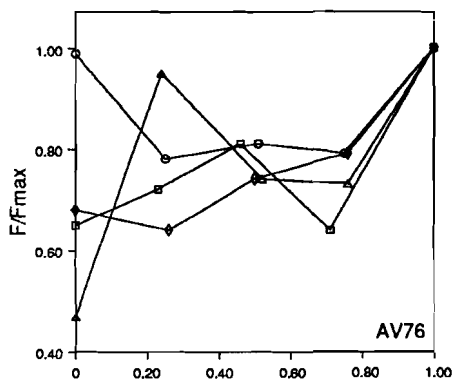


Table 4.3 Summarized biotite chemistry. F, Cl. in a.f., SO₃ and TiO₂ in wt.%. Fvar denotes variation in F. Mg# is Mg-ratio.

Nr	Fvar	F	Cl	SO ₃	TiO ₂	Mg#
Group I						
AV76	36.4	0.14-0.22	0.02-0.04	0.04-0.06	1.66-2.99	0.58-0.63
BD14	53.8	0.06-0.13	0.06-0.07	0.06-0.12	2.11-2.49	0.52-0.55
GP71	84.6	0.02-0.13	0.03-0.06	0.06-0.11	2.13-2.77	0.44-0.45
SU30	46.2	0.07-0.13	0.03-0.04	0.04-0.08	2.30-2.58	0.58-0.59
SU56	15.4	0.11-0.13	0.01-0.02	0.13-0.15	4.58-5.33	0.38-0.39
TN7	0	0.10	0.03	0.12-0.13	1.94-2.10	0.51-0.53
TN146	94.7	0.01-0.19	0.03-0.05	-	1.57-1.83	0.49-0.53
TN201	68.8	0.05-0.16	0.02-0.04	-	0.96-1.49	0.52-0.56
TN209	78.3	0.05-0.23	0.02-0.04	-	2.65-3.37	0.49-0.52
TN294	100	0.00-0.17	0.01-0.02	0.00-0.37	4.39-4.95	0.51-0.54
TN309	100	0.00-0.29	0.01-0.02	0.00-0.25	4.09-5.09	0.64-0.67
Group II						
TN19	85.2	0.04-0.27	0.09-0.14	0.05-0.10	0.79-2.79	0.45-0.49
TN202	95.5	0.01-0.22	0.05-0.06	-	0.95-1.28	0.54-0.55
Group III						
WT23	76.5	0.04-0.17	0.12-0.13	0.02-0.04	3.13-3.41	0.69-0.71

Table 4.4 Summarized amphibole chemistry. F, Cl in a.f. Fvar denotes variation in F. TiO₂ in wt.%. Mg# is Mg-ratio.

Nr	Fvar	F	Cl	TiO ₂	Mg#
Group I					
AV76	25.0	0.09-0.12	≤0.01	1.09-1.56	0.61-0.62
BD14	100	0.00-0.14	0.11-0.16	0.71-1.48	0.42-0.47
BD39	42.9	0.08-0.14	≤0.03	0.43-0.79	0.64-0.68
GP71	100	0.00-0.10	≤0.06	0.85-1.20	0.39
SU30	55.6	0.04-0.09	0.01	0.85-0.91	0.62-0.63
SU56	69.2	0.04-0.13	0.01-0.02	1.61-1.85	0.36-0.38
TN7	44.4	0.10-0.18	0.03-0.22	1.00-1.59	0.44-0.47
TN146	50.0	0.10-0.20	0.01-0.03	0.88-1.17	0.46-0.51
TN201	61.1	0.07-0.18	0.02-0.04	0.44-1.15	0.42-0.57
TN209	95.0	0.01-0.20	0.02-0.03	0.82-1.60	0.46-0.51
TN227	76.9	0.06-0.26	≤0.02	2.32-2.78	0.39-0.42
TN258	94.1	0.01-0.17	≤0.02	2.26-2.60	0.44-0.48
TN294	100	0.00-0.11	0.01-0.03	2.10-2.37	0.49-0.51
TN309	100	0.00-0.14	0.01-0.02	1.78-1.91	0.54-0.60
Group II					
TN19	100	0.00-0.22	0.00-0.04	1.42-1.93	0.44-0.49
TN202	64.3	0.05-0.14	0.01-0.06	0.65-1.35	0.47-0.53
Group III					
TN250	94.1	0.01-0.17	0.12-0.31	0.98-1.60	0.42-0.56
WT23	50.0	0.06-0.12	0.00-0.08	1.77-1.91	0.72-0.76

Table 4.5 Summarized titanite chemistry. F, Cl in wt%. Al and Fe in a.f.

Nr	F	Cl	Al	Fe
Group I				
BD14	0.18-0.25	0.01-0.02	0.05	0.01
BD39	0.17-0.52	0.01-0.03	0.02-0.04	0.01-0.04
GP71	0.36	0.02	0.07	0.05
TN7	0.00-0.45	≤0.03	0.03-0.06	0.01-0.03

F-patterns from group I's AV76 and GP71 show an overall decrease in F from the core towards the rim (Fig. 4.6ac). The F-patterns for BD14 and TN19 show an slight overall increase toward the rim (Fig. 4.6be). In TN227, the apatites show an initial decrease toward the rim, followed by an increase (Fig. 4.6f) The overall pattern in TN227 is rimward increasing. F-patterns for TN7 (Fig. 4.6d) are rather irregular, but more detailed inspection reveals a slight overall increase toward the rim.

Element diagrams for TN19 apatites show an irregular, spotted distribution of Cl. Apatites of WT23 are relatively homogeneous regarding their Cl-distribution, but Cl is clearly absent along cracks and some of the margins.

4.3.2

Biotite

The three groups which could be established for the apatites are not evident in the biotites (Table 4.3), nor is there any relationship between biotite composition and rock types. Nevertheless, we will use the same division as made for the apatites for the purpose of comparison.

Biotites do not clearly differ in F and Cl-contents, but group III biotites tend to have slightly more chlorine than those from group I and II. Biotites generally contain more fluorine than chlorine, except those of group III, in which both are present in roughly equal amounts (Table 4.3). The maximum Cl and F-content is 0.28 and 0.47 wt.% for group I, 0.54 and 0.55 wt.% for group II, and 0.54 and 0.38 wt.% for group III respectively. With the exception of three samples (AV76, SU56 and TN7), the variation in F-content is much larger for biotites than for coexisting apatites. Plots of F and Cl contents of apatite versus those of biotite indicate that F is highly fractionated into apatite. The same, but to a lesser degree, holds for Cl.

Group III biotites have the highest Mg-ratio (0.69-0.71), but equally Cl-rich biotites from TN19 (Group II) however have much lower Mg-ratios (0.45-0.49). No systematic relationship exists between the Cl- and F-contents of the biotites and their Mg-ratio (Mg#), neither in one sample, nor within a whole group. TiO₂ varies between the samples, and may be up to 5 wt.%. No relation between Ti and the halogens could be established. The biotites do not show significant substitution of Na or Ca for K. They contain minor amounts of sulphur (up to 0.37 wt.% SO₃).

4.3.3

Amphibole

The halogen contents are generally low (Table 4.4). As with biotites, the subdivision made for the apatites could not clearly be recognized in the amphiboles. But the highest Cl-content occurs in amphiboles from group III's TN250 (≤ 0.31 a.f., 1.16 wt.%). However amphiboles in sample WT23 from the same group are low in chlorine. F is present up to 0.26

a.f. The variation in fluorine in the amphiboles from one sample tends to be larger than in biotites and apatites. No relation between the F or Cl-contents and the Mg-ratio could be established.

4.3.4

Titanite

As titanites may also incorporate OH or F due to coupled substitution with Al and Fe, they have also been investigated (Table 4.5). All analyzed titanites belong to samples from group I. They contain minor amounts of Al and Fe, and considerable amounts of F (≤ 0.52 wt.%). This is relatively high, but not unusual for titanites, for which values of 1.3–2.3 wt.% have been reported (Zabavnikova 1957, Černý and Povondra 1972). In the Bamble Sector, values comparable to ours have been previously reported for titanites from skarns near Arendal (0.35 wt.%, Jaffe 1947). Cl is almost absent.

4.4

Discussion

4.4.1

Halogen behaviour in apatite

Fluorine (group I) as well as chlorine-rich apatites (group III) show an excess of halogens. The presence of halogens in excess to the 2 stoichiometric atoms has been reported for natural carbonate apatites (McConnell 1970, Binder and Troll 1989) as well as synthetic, foreign ion free apatites (Prener 1971, Mackie and Young 1974). The investigated apatites are not, or only slightly P-deficient, which is occasionally compensated for by small amounts of sulphur. Therefore, the excess halogens can not be attributed to coupled substitution with carbonate for P + O. Interference between the 1st order $K\alpha$ peak of F and the 3rd order $K\alpha$ peak of P may be supposed to be the cause of excess halogens. If this were true, then it might be expected that the amount of F roughly increases with the amount of P. This is not the case. The sum of F + Cl shows a negative correlation with the sum of P + S + Si + Al. From almost F-free, Cl-rich apatite (Boudreau and Kruger 1990, 7.17 wt.% Cl, 0.10 wt.% F; D. Visser unpubl. data: 6.99–7.44 wt.% Cl, 0.00–0.26 wt.% F), it appears that excess halogens also occur in Cl-apatites, and consequently may be a real feature of apatite and not an analytical artefact.

The transition from ordered monoclinic to disordered hexagonal state in OH as well as Cl-apatite end members occurs at c. 210°C (Hitmi et al. 1984, 1986). As the amphibolite to granulite facies apatites were grown above this temperature, the measured excess halogens may be related to a scattered distribution in the disordered state. Such a distribution has been observed in tooth enamel apatite (Young and Mackie 1980). A relationship between the presence of excess halogens or the Cl-content of apatite, and the optical axial angle of apatite might be expected, but has not been observed.

In contrast to older views that a miscibility gap was present between the F and Cl-apatite end members (Walter and Luth 1969, Taborszky 1972, McConnell 1973, Hogarth 1988), recent structure refinements (Hughes et al. 1989, 1990, Tacker and Stormer 1989) indicated the existence of (near) ideal solid solution. Group III apatites support the existence of miscibility, at least from 10 to 60 and from 80 to 100% F-apatite (Fig. 4.2). Group III apatites, notably those from TN250 (≤ 6.73 wt.% Cl) are among the Cl-richest apatites reported. They are comparable to those reported from layered intrusions like the Bushveld complex (6.85, 7.17 wt.%, Boudreau et al. 1986, Boudreau and Kruger 1990) and late magmatic veins like Ødegårdens Verk, South Norway (6.24 wt.% Morton and Catanzaro 1964; 6.74 wt.%, Lieftink and Nijland 1992). To our knowledge, the highest Cl-content reported from metamorphic rocks is 6.2 wt% for vein apatite in Ontarian marbles (Hounslow and Chao 1970).

Apatites from several samples, including these from the intrusions BD39 and WT23, contain minute inclusions of hornblende (See appendix), that is probably metamorphic. Therefore, the halogen distribution of the apatite may be regarded as a metamorphic feature. Chlorine distribution diagrams for apatites from sample TN19 indicate that this distribution is rather inhomogeneous. This shows that even under high grade metamorphic conditions, homogenization is not guaranteed, and may have significant implications for fission track analyses of apatite, as track retention depends on the composition of the OH-site (Green et al. 1986).

4.4.2 Halogen distribution among apatite and hydrous silicates

In all samples, the F-content is much higher in apatite than in coexisting biotites or amphiboles, as is commonly observed (e.g. Ekström 1973b, Sisson 1987). The F-contents of biotite are usually higher than those of amphibole. Titanites (Table 4.5) contain significant amounts of F. The distribution of F between titanite and other silicates has rarely been studied, but Ekström (1973b) observed a preference for biotite. In our samples, the F-contents of titanite are comparable to those in biotite, but maxima tend to be higher in titanite than in biotite (BD14: 0.25 and 0.26 wt.%, GP71: 0.36 and 0.26 wt.%, TN7: 0.45 and 0.20 wt.% respectively). With the exception of BD14, the same holds for titanite and amphibole (BD14: 0.25 and 0.30 wt.%, BD39: 0.52 and 0.31 wt.%, GP71: 0.36 and 0.21 wt.%, TN7: 0.45 and 0.38 wt.% respectively). For fluorine, the partitioning may be described by the series apatites > titanite > biotite \geq amphibole.

As with fluorine, chlorine is strongly partitioned in apatite with respect to biotite. Relationships between biotite and amphibole are less evident due to the low chlorine levels, but Cl tends to favour biotite. In a few samples however (BD14, TN7), Cl is more abundant in amphibole than in biotite. Chlorine is almost absent in titanite. Partitioning of Cl may be described by the series apatite > amphibole \geq biotite > titanite.

In contrast to many other granulite facies areas (e.g. Adirondacks, Petersen et al. 1982; Rogaland, SW Norway, Jansen and Maijer 1987; southern Sri Lanka, de Maesschalck et al. 1991), amphiboles and biotites in granulite facies samples in the Bamble Sector do not show

systematically higher fluorine and/or chlorine contents than those from amphibolite facies samples. This is likely to be due to different behaviour of different rock types; the observations quoted above apply for marbles (Petersen et al. 1982) and felsic rocks (Jansen and Maijer 1987, de Maesschalk et al. 1991), whereas our observations hold for amphibolites. Dekker (1978) did not observe a significant increase in fluorine content of granulite facies calcic amphiboles relative to amphibolite facies ones in Rogaland, SW Norway, albeit that the highest absolute values were recorded in the granulite facies samples.

4.4.3

Halogen fugacities

Relative HF and HCl fugacities of the coexisting fluid were calculated from apatite using the thermodynamic data of Zhu and Sverjensky (1991), and from biotite according to the method of Munoz (1984). Fugacities for the amphibolite and granulite facies have been calculated at the average temperatures for these areas, which are 752°C and 836°C respectively (Nijland and Maijer 1992, 1993).

The scatter in Cl data for group I and II apatites is quite small (Fig. 4.2), and consequently does not largely influence the calculated fugacity ratios. The spread in F data is large, and propagates into the fugacity ratios. However, as they are accompanied by regular F-patterns, and match well with the results derived from biotite, they are considered to represent metamorphic conditions. The scatter in Cl data for group III apatites is larger. However, these also are accompanied by regular Cl-patterns. The scatter in F-data is smaller. The variation in obtained fugacity ratios may reflect different growth stadia.

Apatite (Table 4.6) and biotite (Table 4.7) cores gave comparable results for $\log(f_{\text{HF}}/f_{\text{H}_2\text{O}})$, albeit that values for biotite tend to be slightly lower. Relative HF fugacities for apatite cores range from $\log(f_{\text{HF}}/f_{\text{H}_2\text{O}}) = -4.1$ to -5.3 on average, with the exception two samples (TN146: -2.9 , and TN209: -3.7). Biotite cores range from -4.1 to -4.7 on average. The slightly lower biotite values may be explained by the fact that biotites easily lose fluorine during cooling or alteration.

$\log(f_{\text{HCl}}/f_{\text{H}_2\text{O}})$ values are always two orders of magnitude higher for biotite than for apatite. $\log(f_{\text{HCl}}/f_{\text{H}_2\text{O}})$ for biotite cores ranges from -0.3 to -1.8 on average in group I, from -0.3 to -0.6 in group II and are -0.3 on average in group III (Table 6). Averages for apatite cores vary from -3.7 to -4.9 in group I, from -3.9 to -4.3 in group II and from -3.0 in group III.

Relative HCl fugacities calculated from biotite should be taken with care, as the calibration is partly based on Mg-Cl avoidance, which is not shown by many natural biotites (Munoz 1990) including ours, and assumes ideal mixing between Cl and OH in biotites, whereas recent crystal structure refinements indicate that this is most likely untrue (Swope et al. 1991).

In the metapelitic from the same area, biotite belongs to the assemblage corresponding to the thermal peak of metamorphism of Visser and Senior (1990), and coexists with sillimanite, plagioclase etc. Textural features of biotites in both amphibolite and granulite

facies amphibolites indicate a peak metamorphic origin of the biotite. Therefore, the obtained relative fugacities are considered to represent peak metamorphic conditions. The influence of retrograde re-equilibration will be discussed below.

The question arises what is the cause of the elevated relative HCl fugacities in group III apatites. Apatites from sample WT23 are associated with Cl-rich scapolite. This scapolite replaces plagioclase along the grain boundaries, indicating that it is a relatively late phase. Elsewhere in the Bamble Sector, Cl-rich scapolite occurs as grain boundary replacement of plagioclase in metagabbroic intrusions due to interaction with either late stage magmatic fluids (Frodesen 1968, Glaveris 1970) or with brines derived from neighbouring quartzites (J.L.R. Touret pers. com. 1992), together with andalusite in retrograde aggregates replacing cordierite (D. Visser pers. com. 1991), and as late alteration phase associated with prehnite-pumpellyite facies mineral assemblages. This offers three origins for the chlorine: (1) late stage magmatic, (2) interaction with fluids derived from country rocks during synmetamorphic intrusion, or 3) hydrothermal fluids introduced under retrograde conditions.

Experimental studies indicate that apatite re-equilibration is sluggish below 600°C (Ekström 1973a, Latil and Maury 1977), although this should not be a problem at geological time scales. Thus a retrograde origin for the chlorine, notably in group III samples, may be possible. However, relative HF fugacities calculated for apatites and biotites from WT23 are fairly similar, with average $\log(f_{\text{HF}}/f_{\text{H}_2\text{O}})$ values for the cores of -4.88 and -4.72 respectively. These values fall in the range of peak metamorphic values for biotite, indicating that fluorine in both biotite and apatite equilibrated during peak metamorphism.

It is unlikely that fluorine would not be affected by the retrograde introduction of chlorine into the apatite, as both halogens tend to change the crystal lattice in opposite directions and usually occupy the same site. F- and Cl-patterns are, at least partly, inversely correlated, and were therefore probably simultaneously incorporated in the apatite during peak metamorphism. This can be explained if Cl-rich apatite and scapolite were grown during the same event. If the magmas were synmetamorphic, they may have interacted with Cl-rich fluids that have been derived from the surrounding metasediments, especially quartzites. These generally contain highly saline fluid inclusions (Touret 1972, 1985). Such fluids may have been remobilized due to intrusion. The occurrence of both TN250 and WT23 in quartzites (and in case of WT23 also gneisses) supports this notion.

4.4.4

Fluorine and chlorine patterns

The apatites exhibit roughly three patterns of fluorine distributions: 1) the W-shaped pattern of WT23 (Fig. 4.6g), which is less developed in apatites from AV76, TN7, TN19 and TN227 (Figs. 4.6adef), 2) a decreasing pattern from core to rim in AV76 and GP71 (Figs. 4.6ac), and 3) increasing patterns from core to rim in BD14, TN7 and TN19 (Figs. 4.6bde). Element distribution diagrams for TN19 support an irregular Cl distribution in these samples.

Before trying to interpret the halogen patterns, it should be decided whether they were generated during post-growth diffusion (cf. Brenan 1992) or metamorphism, and, if the

Table 4.6 Relative HCl and HF fugacities calculated from apatite at 752°C for amphibolite facies samples, and at 836°C for granulite facies samples. Samples are ordered relative to a reference line perpendicular to the metamorphic gradient.

Nr	Log ($f_{\text{HCl}}/f_{\text{H}_2\text{O}}$)						Log ($f_{\text{HF}}/f_{\text{H}_2\text{O}}$)					
	Max	Rim Mean	Min	Max	Core Mean	Min	Max	Rim Mean	Min	Max	Core Mean	Min
TN7	-3.79	-4.38	-4.75	-3.99	-4.77	-5.27	-3.07	-3.77	-4.21	-3.41	-4.14	-4.87
BD39					-4.47						-4.26	
BD14		-4.63		-3.37	-4.15	-4.61		-4.57		-3.25	-4.13	-4.66
TN19	-3.95	-4.49	-4.77	-3.80	-4.33	-4.76	-4.37	-4.87	-5.16	-4.15	-4.79	-5.35
GP71	-3.99	-4.76	-5.24	-4.02	-4.53	-4.75	-3.61	-4.37	-4.86	-3.56	-4.19	-4.54
SU30				-4.34	-4.47	-4.67				-4.50	-4.62	-4.82
TN146					-3.18						-2.91	
TN202	-3.81	-4.00	-4.07	-3.81	-3.91	-4.02	-4.26	-4.52	-4.65	-4.29	-4.43	-4.57
TN209	-4.01	-4.37	-4.73		-3.71		-3.81	-4.18	-4.55		-3.66	
SU56				-4.36	-4.94	-5.34				-3.45	-4.26	-4.79
TN250					-3.52						-4.59	
AV76	-3.97	-4.61	-5.06	-3.52	-4.31	-4.64	-3.82	-4.48	-5.07	-3.45	-4.20	-4.61
WT23	-2.73	-3.05	-3.29	-1.77	-2.95	-3.43	-4.63	-4.95	-5.38	-3.73	-4.88	-5.55
TN227	-4.35	-4.76	-5.32	-3.84	-4.79	-5.30						
TN294	-4.42	-4.60	-4.73	-3.92	-4.38	-4.68	-4.64	-4.83	-5.08	-4.05	-4.67	-5.13
TN309	-3.36	-4.23	-4.57	-4.29	-4.40	-4.51	-3.35	-4.35	-4.76	-4.34	-4.57	-4.71
TN258	-4.44	-4.48	-4.50	-4.75	-4.88	-5.02	-4.80	-4.90	-4.98	-5.23	-5.30	-5.37

Table 4.7 Relative HCl and HF fugacities calculated from biotite at 752°C for amphibolite facies samples, and at 836°C for granulite facies samples. Samples are ordered relative to a reference line perpendicular to the metamorphic gradient.

Nr	Rim			Core			Max	Rim			Core		
	Max	Mean	Min	Max	Mean	Min		Max	Mean	Min	Max	Mean	Min
Log($f_{\text{HCl}}/f_{\text{H}_2\text{O}}$)							Log($f_{\text{HF}}/f_{\text{H}_2\text{O}}$)						
TN7				-0.88	-0.89	-0.90					-4.33	-4.34	-4.34
BD14				-0.46	-0.51	-0.53					-4.22	-4.36	-4.54
TN19	-0.29	-0.44	-0.90	-0.29	-0.34	-0.42	-3.87	-4.17	-4.65	-3.79	-4.19	-4.72	
GP71				-0.73	-0.84	-1.04					-4.11	-4.49	-4.95
SU30				-0.67	-0.77	-0.80					-4.28	-4.39	-4.55
TN146	-0.65	-0.77	-0.83	-0.68	-0.75	-0.82	-4.03	-4.13	-4.22	-4.04	-4.32	-5.42	
TN202	-0.53	-0.60	-0.67	-0.34	-0.53	-0.66	-4.21	-4.91	-5.45	-4.14	-4.46	-4.79	
TN209	-0.90	-0.94	-0.99	-0.80	-0.90	-1.09	-4.06	-4.28	-4.65	-3.93	-4.04	-4.18	
SU56				-1.29	-1.40	-1.68					-4.06	-4.09	-4.14
AV76				-0.50	-0.67	-0.97					-4.07	-4.18	-4.25
WT23				-0.27	-0.29	-0.32					-4.48	-4.72	-5.14
TN294	-1.82	-1.83	-1.85	-1.40	-1.60	-1.81	-4.27	-4.45	-4.75	-4.36	-4.55	-4.85	
TN309	-1.60	-1.61	-1.65	-1.18	-1.50	-1.63		-4.53		-4.13	-4.34	-4.66	

latter was the case, if they were generated under isothermal conditions. Diffusion will tend to minimize compositional gradients, and consequently flatten the halogen patterns. Especially the W-shaped pattern, but also the in- and decreasing patterns show that this did not happen. The patterns are therefore considered to be metamorphic. Whether the patterns were generated under isothermal conditions is difficult to establish. But Visser and Senior (1990) concluded that the area remained a deep crustal levels and under roughly constant conditions for a long time. In addition, orthopyroxene-clinopyroxene and hornblende-plagioclase geothermometry does not show significant differences between cores and rims of coexisting mineral pairs (Nijland and Majjer 1992). For this reasons, we will assume near isothermal growth.

It is tempting to consider the F-pattern of sample WT23, which constantly displays the same pattern, as the only one which remained undisturbed during subsequent events. The patterns seem to be rather smooth (Fig. 4.4g), but fit exactly after normalization (Fig. 4.6g). This indicates that the apatites in WT23 equilibrated with the same fluids but that their growth rate locally differed.

To consider the W-shaped pattern as a regional base pattern is supported by occurrence of such patterns in AV76, TN7, TN19 and TN227. Based on comparison with relative HF fugacities and mineral relations, the fluorine in WT23 was considered to represent peak metamorphism (See above). Samples which show W-shaped patterns in some of their apatites, show two different overall patterns: AV76 (Fig. 4.6a) and TN227 (Fig. 4.6f) have rimward decreasing patterns, whereas TN7 (Fig. 4.6d) and TN19 (Fig. 4.6e) have rimward increasing patterns. Of the samples lacking the W-shaped pattern, BD14 shows overall rimward increasing patterns (Fig. 4.6b) whereas GP71 shows decreasing ones (Fig. 4.6c). This shows, that whatever origin of the W-shaped patterns, two general trends in fluid evolution may be distinguished: the one resulting in rimward decreasing F-patterns, and the one producing rimward increasing F-patterns.

Equilibration of a rock with a metamorphic fluid in a closed system will result in the progressive depletion of the fluid in fluorine as it is refractory into minerals like apatite, biotite and amphibole. This will result in a rimward decreasing F-pattern. In contrast, chlorine will preferably be partitioned into the fluid, which will result in progressively chlorine rich fluids. In its struggle to be incorporated in apatites and biotites, it will face the competition of both fluorine and hydroxyl; both fit better in the crystal lattices of apatite and biotite. This effect will act to counter the progressive chlorine-richness of the fluid, and may result in rather smooth or even slightly decreasing Cl-patterns. These occur in WT23 (Fig. 4.5).

Roughly stable or rimward increasing F-patterns require progressively fluorine-enriched fluids. This may be effected in three ways: 1). The introduction of F-enriched fluids, 2). The preferent removal of other species from the coexisting fluid, and 3) The retrograde growth of hydrous minerals, consuming water and leaving a halogen enriched fluid. Options 1) and 2) would imply open system behaviour, whereas 3) would imply that the system remained closed during retrograde metamorphism. It is difficult to choose between these mechanisms. We will consider retrograde effects first.

Studies on experimental (Elliot and Young 1967, Latil and Maury 1977) and natural (Morton and Catanzaro 1964, Boudreau and McCallum 1990, Liefink and Nijland 1992, Liefink et al. 1992) apatites indicate that Cl is easily exchanged for water. Indeed, element

distribution diagrams for apatites from WT23 show replacement of chlorine along cracks and part of the margins. The fact that some of the Cl-patterns do not correlate with the F-patterns may be due to this retrograde loss of chlorine.

To explain the rimward decreasing F-patterns by retrograde re-equilibration, chlorine or hydroxyl would have to be introduced into the system and into the apatites. Apatites with rimward decreasing F-patterns occur in AV76, GP71 and TN227. They have lower average $\text{Log}(f_{\text{HCl}}/f_{\text{H}_2\text{O}})$ values for their rims than corresponding cores. If the decreasing patterns are due to late exchange, it should be hydroxyl for fluorine. This is unlikely because it would not result in a set of gradual rimward decreasing patterns starting in the core, and because F-apatite is the most stable end member.

The question remains whether the rimward increasing patterns in BD14, TN7 and TN19 can be explained by retrograde influences. This seems to be a real possibility as fluorine fits better in the apatite lattice than hydroxyl. However, relative HF fugacities calculated for apatite cores and rims are in fair agreement with those from biotite cores (Tables 4.6 and 4.7). As argued above, these values are considered to represent (near) peak metamorphic conditions. Biotite rims provide lower values (Table 4.7), which indicates that they may have lost fluorine to post peak metamorphic fluids. Therefore the rimward increasing F-patterns in apatite are most likely not due to retrograde re-equilibration, but have to be explained by open system behaviour.

Summarizing, all regular F-patterns, whatever their shape is, are explained by variation from open to closed system behaviour of the respective rocks. Only those F-patterns which are totally deviating (Compare figs. 4.4 and 4.6) are considered to be of (partly) retrograde origin.

4.4.5 Implications for amphibolite-granulite transition

The considerations discussed above have several implications for the nature of amphibolite-granulite facies metamorphism in the area. The halogen patterns revealed that the rock systems did not evolve in one general way. While some behaved as closed systems, others evolved as open systems in which new fluids were introduced. The coexistence of both types of behaviour, as well as the varying magnitude of the patterns (Fig. 4.4) stresses the very local scale of fluid control during metamorphism. This is in good agreement with the results from saline fluid inclusions (Touret 1985). Group III apatites, in which both fluorine and chlorine are prominently present, indicate that synmetamorphic basic intrusions and their country rocks influence each others fluid budgets to a great extent. The introduction of halogen bearing aqueous fluids into the intrusions may have resulted in the expulsion of originally magmatic fluids (cf. Frost et al. 1989).

The transition from amphibolite to granulite facies rocks requires that water fugacities become lower, which might be due to both its own removal and the introduction of new volatile species. In this case, the fugacity of HF relative to water might be expected to increase with increasing metamorphic gradient. In tables 4.6 and 4.7, the relative fugacities of both HF

and HCl are ordered according to increasing metamorphic gradient. No systematic variation is present. This implies that the increasing metamorphic grade can not be coupled to simple changes in the fluid system, but that the relationship between both is much more complex.

It has already been noted that whereas in metapelites from other areas the halogen contents of biotites and amphiboles increase with metamorphic grade, this is not the case in the Bamble amphibolites. Although we did not investigate the Bamble metapelites, it may be concluded that both rock systems behaved differently. Combining the observations from this study with those of fluid inclusion studies (Touret 1971b, 1972, 1985), it may now safely be concluded that the aqueous fluid budget of during metamorphism was to a great extent determined by the fluids present before metamorphism; these may have been both sedimentary and magmatic. The absence of regional compositional gradients indicates that changes in this fluid budget were effectuated by local sources, likely synmetamorphic intrusions. The occurrence of several small granulite facies islands within the amphibolite facies area (e.g. Nijland and Maijer 1992, 1993), might be explained this way.

4.5

Conclusions

1. The presented data for high-grade metamorphic apatites indicate that the F- and Cl-end members are miscible under these conditions, at least in the ranges from 10 to 60 and from 80 to 100% F-apatite.
2. Apatites preserved two types of F-patterns. One group evolved as a closed system, which is reflected by overall rimward decreasing F-patterns. A second group evolved as open systems in which water may have been removed by melts, resulting in overall rimward increasing F-patterns.
3. Correlation with the P-T path of the Bamble Sector shows that the relative HF fugacities represent peak metamorphic conditions.
4. No simple relationship is present between the transition from amphibolite to granulite facies conditions, and the halogen evolution of the fluid.
5. The current calibration to calculate relative HCl fugacities from biotite yields results inconsistent with those from apatite, and probably needs revision.
6. In contrast to other granulite facies terrains, amphiboles and biotites in granulite facies samples from the Bamble Sector do not show elevated halogen contents relative to their amphibolite facies counterparts.
7. Apatites suffered sporadically from resorption and retrograde equilibration at sub grain size scale.

8. The apatites prove that even under high-grade conditions whole grain equilibration is not guaranteed.

Acknowledgements - H. Anijs, B.P. Dam, G.P. van Ditshuizen, W. Theulings and A. Vons provided some of the samples. R.P.E. Poorter and T. Bouten assisted microprobe analyses. Financial support by AWON (NWO 751.353.023, TGN) and the hospitality of the Blakstad Yrkesskole during fieldwork is gratefully acknowledged. M. Röhrman and D. Visser critically read an earlier version of the manuscript. Constructive reviews by J.L.R. Touret and P. Candela helped to improve the paper. P. Piccoli kindly provided information about F-P interference.

CRYSTAL CHEMISTRY OF HORNBLENDES AND BIOTITES AS INDICATORS OF METAMORPHIC CONDITIONS IN THE BAMBLE SECTOR, SOUTH NORWAY.

Abstract - The crystal chemistry of hornblendes and biotites in amphibolites and metapelites has been studied in order to constrain changing metamorphic conditions over the amphibolite to granulite facies transition zone in the Nelaug - Arendal area of the Bamble Sector, South Norway. Hornblendes can be divided in three areas: 1) Nelaug-Froland amphibolite facies area; 2) Arendal-Tromøya-Merdøya granulite facies area; 3) Hisøya granulite facies area. Published analyses from the Kragerø amphibolite facies area define another distinct group. They indicate pressure increases toward the east (Kragerø). Both hornblendes and biotites indicate higher temperatures in the Arendal-Tromøya-Merdøya granulite facies area with respect to both the Hisøya granulite facies area and the Nelaug-Froland amphibolite facies area.

Ferrous iron estimates for both hornblendes and biotites from amphibolites indicate increasing oxidation state towards the Porsgrunn-Kristiansand Fault, i.e. with decreasing metamorphic grade. This is in fair agreement with previous whole rock studies. However, estimates for biotites from metapelites do not show any regional distribution in ferrous iron at all. Ti in hornblende and biotite from amphibolite steadily increases with metamorphic grade. Isopleths indicate a threefold division.

Comparison between hornblende, biotite, and whole rock chemistry of the amphibolites demonstrates that Al^{Tot} and Al^{IV}-contents of both minerals are no suitable indicators of metamorphic conditions as they are mainly controlled by whole rock composition. This does not hold for Ti, and its distribution between hornblende and biotite may provide a possible geothermometer.

5.1

Introduction

5.1.1

Amphibole and biotite

The transition from amphibolite to granulite facies involves a general reduction in the water content of the rocks. This change is most evident in the appearance of the nominally anhydrous mineral orthopyroxene. In the Bamble Sector, Tromøya and Hisøya were

traditionally regarded as its most high grade part (Zone D of Smalley et al. 1983a), and considered to be virtually devoid of hornblende and biotite (Field et al. 1980, 1985), an observation that was righteously disputed by Touret (1985).

Several studies tried to correlate the crystal chemistry of amphiboles with metamorphic conditions. It has been widely shown that Ti increases with temperature (Binns 1965, Bard 1970, Raase 1974, Jackson 1976, Albat 1984); $(\text{Na} + \text{K})^{\text{A}}$ also increases with metamorphic grade (Binns 1965, Jackson 1976, Albat 1984, Schlegel 1991); Albat (1984) observed elevated K-contents in granulite facies hornblendes relative to amphibolite facies ones. Al^{VI} generally increases with decreasing temperature (Albat 1984, O'Beirne-Ryan et al. 1990), whereas Al^{Tot} is thought to be pressure dependent (Raase 1974). These observations led to geothermobarometric calibrations based on single hornblende (Ti (T) - Otten (1984); Al^{IV} (T) - Nabelek and Lindsley (1985); Al^{Tot} (P) - Hammarstrom and Zen (1986), Hollister et al. (1987), Johnson and Rutherford (1989), Rutter et al. (1989)) and in exchange with other minerals (e.g. Na-Al (T) with plagioclase - Blundy and Holland 1990). No broad agreement exists on to what extent hornblende chemistry changes with amphibolite to granulite facies transition (Compare for example Engel and Engel 1962, Binns 1965, Kostyuk and Sobolev 1969, Raase 1974, Dekker 1978, Albat 1984). Apart from different whole rock compositions, this may also be ascribed to different metamorphic conditions. Nevertheless, it has been reasonably well established that the breakdown of hornblende involves the extraction of edenite and, to a lesser degree, tschermakite components with increasing metamorphism (Binns 1965, Glassley and Sørensen 1980).

The changing crystal chemistry of biotite led to its manifold use as Fe-Mg exchange geothermometer in combination with garnet, orthopyroxene etc. Al^{IV} and Ti in biotite have been suggested to increase with metamorphic grade (Binns 1969, Laird and Albee 1981). Many studies also indicate an increase in halogen (notably fluorine) content of biotite, especially in acidic gneisses (e.g. Jansen and Maijer 1987, de Maesschalck et al. 1991). Nijland et al. (1992b, 1993b, ch. 4), however, demonstrated that this is lithology dependent, and does not hold for metabasic rocks in the Bamble Sector.

5.1.2

The Bamble Sector

The Bamble Sector is part of the Southwest Scandinavian Domain (Gaál and Gorbatshev 1987). In the central part of the sector, an amphibolite to granulite facies transition zone has been developed in the Nelaug-Arendal area, in response to metamorphism during the Mid-Proterozoic Gothian and Sveconorwegian orogenies (Bugge 1940, Touret 1971a, Lamb et al. 1986, Nijland and Maijer 1992, 1993, ch. 3). Lithologies and structures of the Bamble Sector have been extensively described by Starmer (1990a, 1991).

As the various exchange geothermobarometers tend to suffer from closure effects and retrograde re-equilibration, this study will try to deduce metamorphic conditions from the changes in crystal chemistry of hornblende and biotite. Hornblendes and biotites in amphibolites from all over the area have been investigated. They will be compared with

biotites in metapelites from the same area, and with amphibolite facies hornblendes from Kragerø, c. 65 km to the northeast (O'Nions et al. 1969b).

5.2

Method

Analyses of coexisting hornblende and biotite from amphibolites, and biotite from metapelites, were obtained with a Jeol JXA 8600 Superprobe at the Department of Geochemistry, Utrecht University. Operating conditions were 15 keV, 10 nA and counting times of 30–60 seconds. Data were checked against synthetic and natural standards, and corrected with a Tracor Northern PROZA correction program. Calculation of amphibole formulas from microprobe analyses is still a problem, because of lack of data about water and ferric iron. Comparison of electron microprobe analyses and wet chemical analyses of the same separates of metamorphic hornblende indicate, that normalization of calcic amphiboles to the sum of cations minus Ca, Na and K equal to 13 is the most satisfying (Cosca et al. 1991). This normalization procedure is used here. Amphibole analyses from literature used in this paper (Shidô 1958, Shidô and Miyashiro 1959, Iwasaki 1963, O'Nions et al. 1969b, Cooper and Lovering 1970, Graham 1974) have been normalized in the same way. In case of wet chemical analyses or microprobe analyses with wet chemically determined iron (First four references), the ferric/ferrous iron ratio was not recalculated.

Calculation of ferric iron in biotites is even a greater problem, if not impossible (Schumacher 1991). Nevertheless, biotites were recalculated according to the iterative method of Dymek (1983a), to enable comparison between amphibole and biotite data.

The Fe^{2+} -ratio, $Fe\#$, is defined as $Fe^{2+} / (Fe^{2+} + Fe^{3+})$, the Mg -ratio, $Mg\#$, as $Mg / (Fe^{2+} + Mn + Mg)$. $Kd(Fe^{2+}-Mg)$ is defined as $(X_{Fe^{2+}}^{Bt} X_{Mg}^{Hbl}) / (X_{Mg}^{Bt} X_{Fe^{2+}}^{Hbl})$, $Kd(Ti)$ as Ti^{Hbl} / Ti^{Bt} , and $Kd(Ti)^*$ as $(Ti / \Sigma \text{ octahedral cations})^{Hbl} / (Ti / \Sigma \text{ octahedral cations})^{Bt}$.

Whole rock analyses were obtained using standard XRF techniques at the Department of Geochemistry, Utrecht University. Ignited splits of rock powder were mixed with $LiBO_2/LiB_4O_7$ (66/34) spectroflux in a ratio of 1:10 and fused at 1000°C in a Herzog HAG 1200 automated furnace. The glass beads were analyzed for major elements with a Philips PW 1400 spectrometer.

5.3

Results

5.3.1

Hornblende chemistry

In accordance with Leake (1978), the amphiboles are formulated as $A_{0-1}B_2C_5T_8O_{22}(OH,F,Cl)_2$. All amphiboles, for which the general term "hornblende" is used in

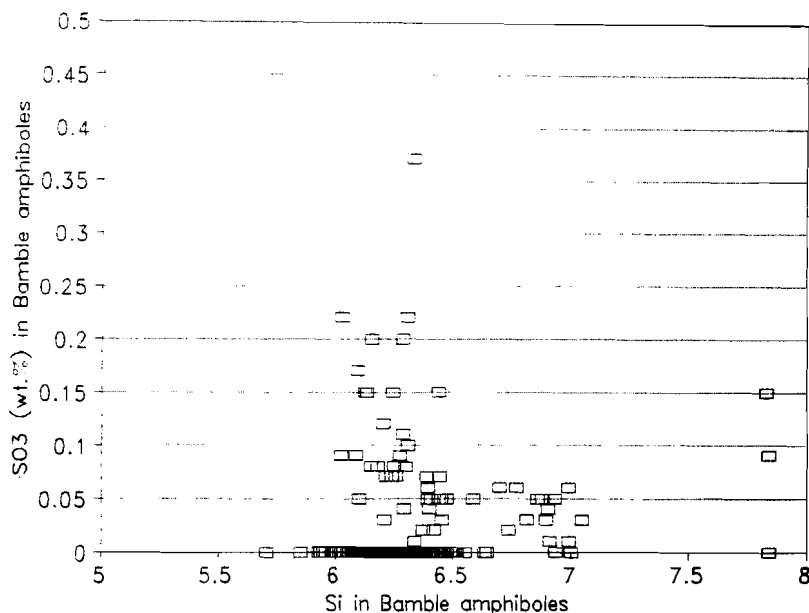
this paper, are calcic amphiboles in the terminology of Leake (1978).

Normalization to 13 cations results in significant Fe^{3+} in all Bamble hornblendes, which is a maximum estimate (cf. Stout 1972). Si and Al together are enough to fill the tetrahedral sites in nearly all hornblendes, and consequently all Fe^{3+} and Ti are assigned to the octahedral sites. As expected from the used normalization, Bamble hornblendes show a clear positive correlation between the sum of high valent octahedral cations, and Al^{IV} . The sum of $(\text{Al} + \text{Fe}^{3+} + \text{Ti})^{\text{VI}}$ shows clear negative correlations with the sum of $(\text{Na} + \text{K})^{\text{A}}$ and Na^{A} , and a positive correlation with Na^{M4} .

Al, Ti and alkalis. Ti does not show any correlation with Na^{A} or Na^{M4} ; a positive correlation exists with Fe#, and a negative one with Mg#. Al^{V} shows weak negative correlations with Na^{A} , $(\text{Na} + \text{K})^{\text{A}}$, and Mg#. Al^{VI} tends to show slightly negative correlation with Na^{M4} and $(\text{Na} + \text{K})^{\text{A}}$, and a more distinctly negative correlation with Mg#. Na^{A} and K^{A} clearly display positive correlations with Fe# and negative correlations with Mg#. Na^{M4} shows inverse relationships.

F and Cl. No relationships between one of the halogens and $(\text{Na} + \text{K})^{\text{A}}$, Na^{A} , or Na^{M4} could be established. Both halogens show a weak positive correlation with Fe#. F is expected to show a positive relationship with Mg# (Rosenberg and Foit 1977), but does not show any correlation at all.

SO_3 . Sulphur is usually not measured in silicates, but seems to be a common minor
Fig. 5.1 Plot of SO_3 (wt.%) vs. Si in hornblendes.



constituent of hornblende. SO_3 shows a weak negative correlations with Si (Fig. 5.1). Other correlations are very weak and probably not significant. Those with $\text{Mg}\#$, $(\text{Al} + \text{Fe}^{3+} + \text{Ti})^{\text{VI}}$, and Na^{M4} seem to be negative, and those with $\text{Fe}\#$, Al^{IV} , and Na^{A} positive. The correlation with Cl seems to be negative, whereas no distinct relationship with F could be established.

5.3.2 Hornblende chemistry versus metamorphic grade

As mentioned above, substitutions in hornblende may serve as indicators of metamorphic gradients. Average Ti-contents of Bamble hornblendes increase from the northwest toward the coastal area around Arendal (Table 5.1, Fig. 5.2). The Ti isopleths confirm the findings of the P-T study (Ch. 3), that the highest grade area, indicated by the highest average Ti-contents (0.30), is situated on the mainland, and not on Tromøya and Hisøya. Average Ti-contents of hornblendes from Hisøy are even similar to those from the amphibolite facies area.

The lowest oxidation levels, as indicated by $\text{Fe}\#$, are observed in the highest grade area (Table 5.1, Fig. 5.3). In the area around Arendal, $\text{Fe}\#$ exceeds 0.70. This $\text{Fe}\#$ isopleth roughly coincides with the isopleth for $\text{Ti} > 0.20$. This area is bordered by a zone in which $0.48 \leq \text{Fe}\# < 0.70$. In contrast to Ti, $\text{Fe}\#$ does not keep decreasing toward the northwest. In the northwesternmost part of the studied area, $\text{Fe}\#$ reaches values as high as in the coastal area.

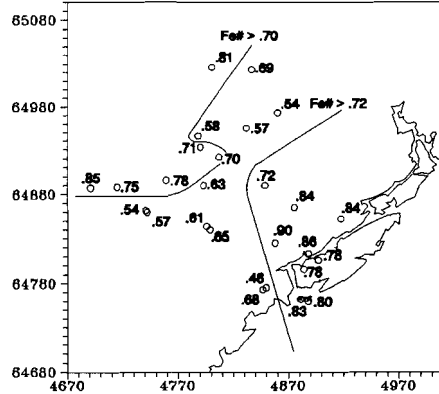
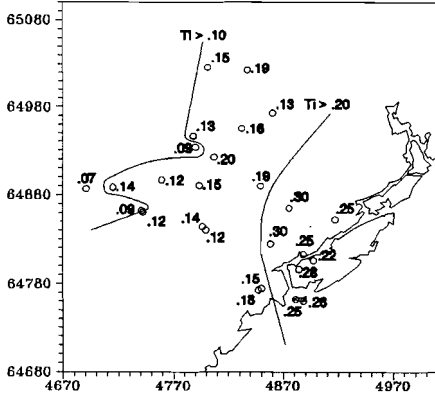


Fig. 5.2 (Left) Map of the investigated area with Ti-isopleths for hornblendes. Zones: I $\text{Ti} < 0.10$, II $0.10 \leq \text{Ti} \leq 0.20$, III $\text{Ti} > 0.20$.

Fig. 5.3 (Right) Map of the investigated area with $\text{Fe}\#$ -isopleths for hornblendes. Zones: I $\text{Fe}\# > 0.70$, II $0.48 \leq \text{Fe}\# < 0.70$, III $\text{Fe}\# > 0.70$.

Table 5.1 Average amphibole chemistry. Elements p.f.u. Averages $\pm 1 \sigma$.

Sample	Ti	Fe#	Mg#	(Na + K) _A	Al tot.	Al(vi)	Al(iv)
AV 76	0.14 \pm 0.02	0.61 \pm 0.04	0.72 \pm 0.01	0.32 \pm 0.02	2.02 \pm 0.05	0.50 \pm 0.03	1.52 \pm 0.08
BD 14	0.14 \pm 0.04	0.75 \pm 0.06	0.51 \pm 0.03	0.63 \pm 0.06	2.35 \pm 0.07	0.46 \pm 0.09	1.89 \pm 0.05
BD 39	0.07 \pm 0.02	0.85 \pm 0.06	0.70 \pm 0.01	0.67 \pm 0.06	1.24 \pm 0.16	0.17 \pm 0.06	1.07 \pm 0.12
GP 4	0.05 \pm 0.01	0.62 \pm 0.02	0.68 \pm 0.01	0.39 \pm 0.05	2.37 \pm 0.09	0.74 \pm 0.04	1.63 \pm 0.06
GP 71	0.12 \pm 0.02	0.78 \pm 0.04	0.45 \pm 0.01	0.60 \pm 0.01	2.14 \pm 0.04	0.40 \pm 0.01	1.75 \pm 0.09
SU 30	0.09 \pm 0.00	0.71 \pm 0.05	0.70 \pm 0.01	0.29 \pm 0.04	1.86 \pm 0.17	0.47 \pm 0.04	1.23 \pm 0.03
SU 56	0.20 \pm 0.01	0.79 \pm 0.03	0.43 \pm 0.01	0.56 \pm 0.02	2.16 \pm 0.03	0.42 \pm 0.03	1.74 \pm 0.04
TN 7	0.15 \pm 0.02	0.81 \pm 0.05	0.51 \pm 0.02	0.67 \pm 0.07	2.11 \pm 0.21	0.40 \pm 0.10	1.71 \pm 0.14
TN 19	0.19 \pm 0.02	0.69 \pm 0.08	0.56 \pm 0.04	0.41 \pm 0.08	2.02 \pm 0.11	0.42 \pm 0.10	1.60 \pm 0.04
TN 142	0.15 \pm 0.06	0.63 \pm 0.07	0.56 \pm 0.05	0.34 \pm 0.07	2.23 \pm 0.28	0.44 \pm 0.19	1.79 \pm 0.10
TN 146	0.13 \pm 0.03	0.58 \pm 0.08	0.62 \pm 0.03	0.24 \pm 0.07	2.19 \pm 0.15	0.48 \pm 0.11	1.71 \pm 0.01
TN 201	0.09 \pm 0.03	0.54 \pm 0.05	0.63 \pm 0.05	0.32 \pm 0.08	2.58 \pm 0.35	0.70 \pm 0.21	1.89 \pm 0.16
		0.30 \pm 0.05	0.81 \pm 0.02	0.12 \pm 0.06			
TN 202	0.12 \pm 0.03	0.57 \pm 0.08	0.62 \pm 0.03	0.25 \pm 0.04	2.18 \pm 0.21	0.50 \pm 0.18	1.68 \pm 0.05
TN 204	0.12 \pm 0.06	0.65 \pm 0.12	0.55 \pm 0.13	0.36 \pm 0.10	2.40 \pm 0.41	0.61 \pm 0.27	1.79 \pm 0.14
		0.25 \pm 0.11	0.80 \pm 0.06	0.11 \pm 0.02			
TN 209	0.16 \pm 0.01	0.57 \pm 0.11	0.62 \pm 0.06	0.30 \pm 0.10	2.15 \pm 0.09	0.45 \pm 0.08	1.70 \pm 0.06
TN 226	0.30 \pm 0.02	0.84 \pm 0.06	0.51 \pm 0.02	0.65 \pm 0.05	2.20 \pm 0.08	0.37 \pm 0.05	1.83 \pm 0.09
TN 227	0.30 \pm 0.02	0.90 \pm 0.05	0.44 \pm 0.02	0.66 \pm 0.07	2.22 \pm 0.09	0.41 \pm 0.05	1.82 \pm 0.07
TN 250	0.13 \pm 0.04	0.54 \pm 0.06	0.63 \pm 0.04	0.38 \pm 0.08	2.37 \pm 0.50	0.51 \pm 0.10	1.87 \pm 0.11
		0.26 \pm 0.08	0.78 \pm 0.07	0.18 \pm 0.09			
TN 258	0.28 \pm 0.01	0.78 \pm 0.06	0.51 \pm 0.02	0.56 \pm 0.07	2.10 \pm 0.05	0.33 \pm 0.07	1.77 \pm 0.05
		0.67 \pm 0.01	0.56 \pm 0.01	0.48 \pm 0.03			
TN 291	0.18 \pm 0.02	0.68 \pm 0.04	0.57 \pm 0.02	0.41 \pm 0.04	2.09 \pm 0.07	0.38 \pm 0.06	1.71 \pm 0.05
		0.49 \pm 0.06	0.65 \pm 0.02	0.21 \pm 0.06			
TN 294	0.25 \pm 0.01	0.86 \pm 0.05	0.54 \pm 0.02	0.74 \pm 0.04	2.20 \pm 0.04	0.35 \pm 0.05	1.85 \pm 0.04
TN 309	0.22 \pm 0.01	0.78 \pm 0.05	0.62 \pm 0.02	0.62 \pm 0.06	1.80 \pm 0.07	0.22 \pm 0.08	1.57 \pm 0.06
		0.68 \pm 0.01	0.65 \pm 0.02	0.56 \pm 0.06			
TN 402	0.25 \pm 0.01	0.84 \pm 0.04	0.39 \pm 0.01	0.72 \pm 0.03	1.97 \pm 0.06	0.25 \pm 0.05	1.72 \pm 0.06
TN 420	0.15 \pm 0.01	0.48 \pm 0.07	0.68 \pm 0.03	0.18 \pm 0.05	1.98 \pm 0.05	0.33 \pm 0.06	1.65 \pm 0.05
		0.32 \pm 0.05	0.75 \pm 0.03	0.05 \pm 0.02			
TN 430	0.26 \pm 0.02	0.80 \pm 0.04	0.45 \pm 0.02	0.56 \pm 0.03	1.91 \pm 0.04	0.23 \pm 0.06	1.67 \pm 0.05
TN 431	0.25 \pm 0.01	0.82 \pm 0.05	0.45 \pm 0.02	0.59 \pm 0.04	2.12 \pm 0.03	0.36 \pm 0.05	1.76 \pm 0.05
WT 23	0.19 \pm 0.02	0.72 \pm 0.06	0.78 \pm 0.02	0.54 \pm 0.08	1.19 \pm 0.06	0.35 \pm 0.08	1.09 \pm 0.04

No systematic regional distribution exists in $Mg\#$, and the Al^{Tot} , $(Na + K)^A$, F and Cl-contents of hornblendes (Table 5.1). Average Al^{VI} -contents tend to decrease from the northwest to the coastal area. In the amphibolite facies northwest, average Al^{VI} values vary between 0.40 and 0.51, with two higher values for samples AV 76 (0.61) and TN 201 (0.70), and an exceptional low average of 0.17 in sample BD 39 (Table 5.1). Samples from Tromøya, Hisøya and the mainland around Arendal have average values between 0.22 and 0.38, with one exception (0.41; sample TN 227).

Laird and Albee (1981) introduced several diagrams to evaluate the Na^{M4} (Al, Fe^{3+}, Ti, Cr)^{VI} = Ca (Fe^{2+}, Mn, Mg)^{VI} glaucophane substitution, the $(Na, K)^A$ Al^{IV} = □ Si edenite substitution, and the (Al, Fe^{3+}, Ti, Cr) ^{VI} Al^{IV} = (Fe^{2+}, Mn, Mg)^{IV} Si Tschermak substitution in amphiboles, by comparing them with amphiboles from well known LP (Abukuma), MP (Dalradian and Haast River) and HP (Sanbagawa) metamorphic series. In these diagrams (Figs. 5.4-7), increasing pressure is represented by an increase in the parameter on the y-axis, whereas increasing temperature is indicated by an increase in the x-parameter. It may be thought that variations in such parameters are an artefact of the used normalization procedure. The $100Na / (Ca + Na)$ vs. $100Al / (Si + Al)$ plot (Fig. 5.4) however does not depend on normalization, and proves the variations to be real.

Four regional groups may be recognized in the Bamble hornblendes: 1) Nelaug-Froland amphibolite facies area, 2) Arendal-Tromøya-Merdøya granulite facies area, 3) Hisøya

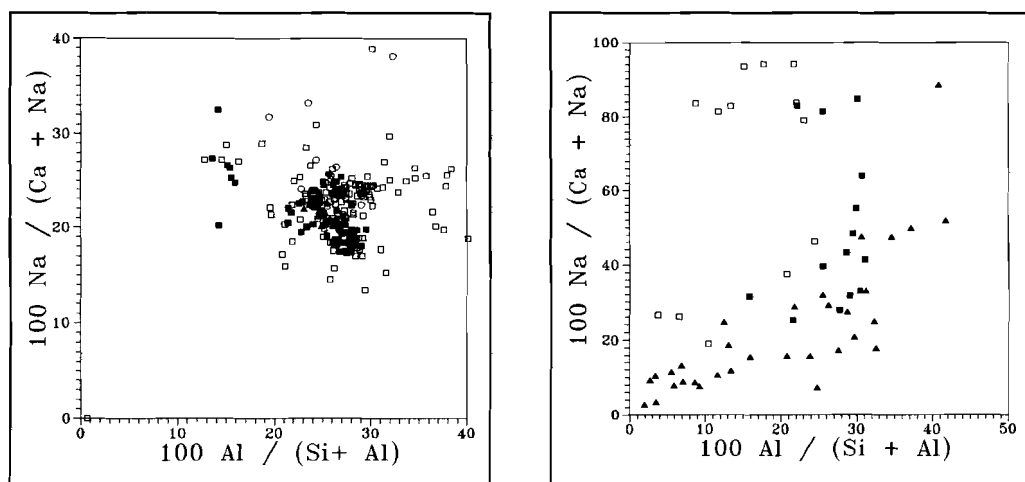


Fig. 5.4 $100Na / (Ca + Na)$ vs. $100Al / (Si + Al)$ plot for Bamble hornblendes compared with literature data. **Left** Bamble - Open squares: Nelaug-Froland amphibolite facies area; filled squares: Arendal-Tromøya-Merdøya granulite facies area; filled triangles: Hisøya granulite facies area; circles: Kragerø amphibolite facies area (O'Nions et al. 1969b). **Right** Literature - Open squares: Sanbagawa HP series (Iwasaki 1963); filled squares: Abukuma LP series (Shidô 1958, Shidô and Miyashiro 1959); filled triangle: Dalradian (Shidô and Miyashiro 1959, Graham 1974) and Haast River MP series (Cooper and Lovering 1970).

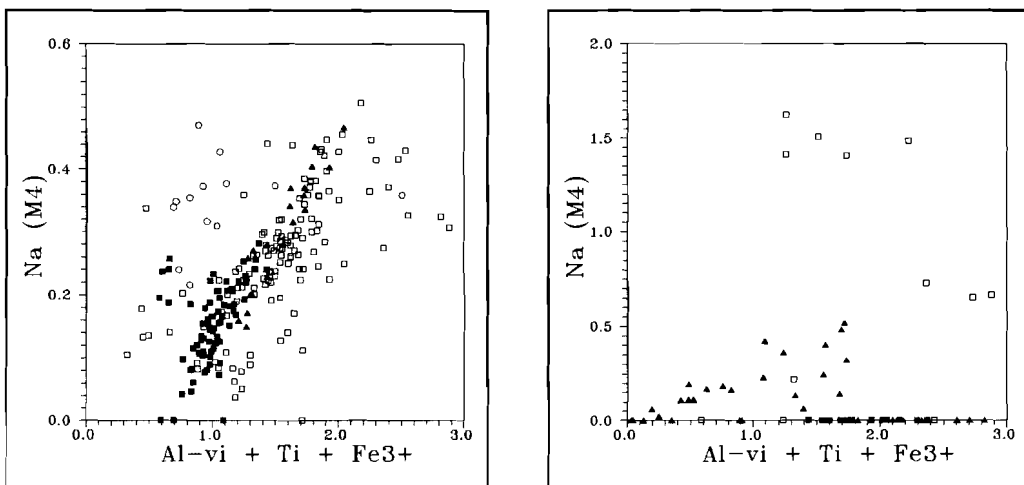


Fig. 5.5 Na^{M4} vs. $(\text{Al} + \text{Fe}^{3+} + \text{Ti})^{\text{VI}}$ plot for Bamble hornblendes compared with literature. Symbols as in fig. 5.4.

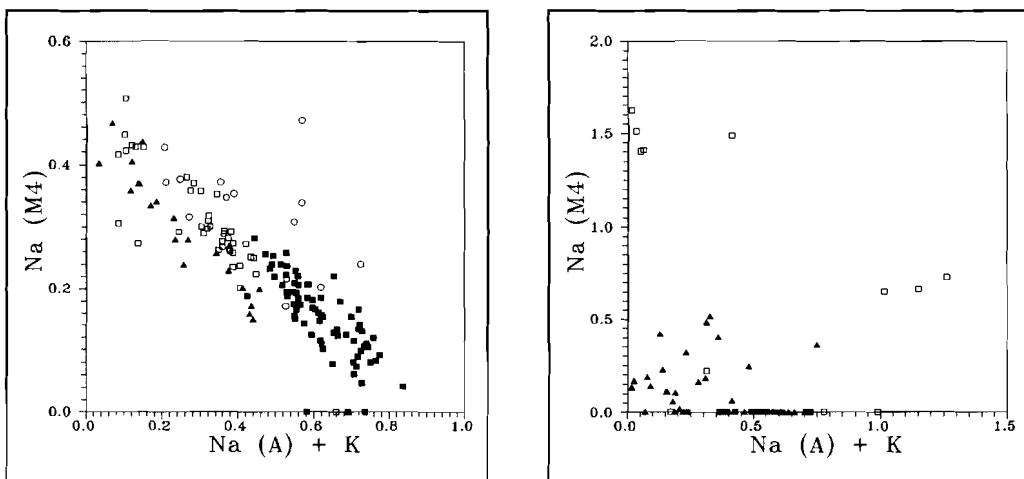


Fig. 5.6 Na^{M4} vs. $(\text{Na} + \text{K})^{\text{A}}$ plot for Bamble hornblendes compared with literature. Symbols as in fig. 5.4.

granulite facies area, and 4) Kragerø amphibolite facies area (O'Nions et al. 1969b), although in this diagram, the first group shows a spread overlapping the others. All Bamble hornblendes essentially plot in the field of medium pressure metamorphic series. However, in the $100\text{Na} / (\text{Ca} + \text{Na})$ vs. $100\text{Al} / (\text{Si} + \text{Al})$ diagram (Fig. 5.11), Kragerø hornblendes and a few of the Nelaug-Froland amphibolite facies hornblendes plot toward higher pressures than Arendal-Tromøya-Merdøya granulite facies hornblendes and most amphibolite facies hornblendes. In the Na^{M4} vs. $(\text{Al} + \text{Fe}^{3+} + \text{Ti})^{\text{VI}}$ diagram (Fig. 5.5), Hisøya and Kragerø show relatively higher Na^{M4} contents than the two other groups at comparable $(\text{Al} + \text{Fe}^{3+} + \text{Ti})^{\text{VI}}$.

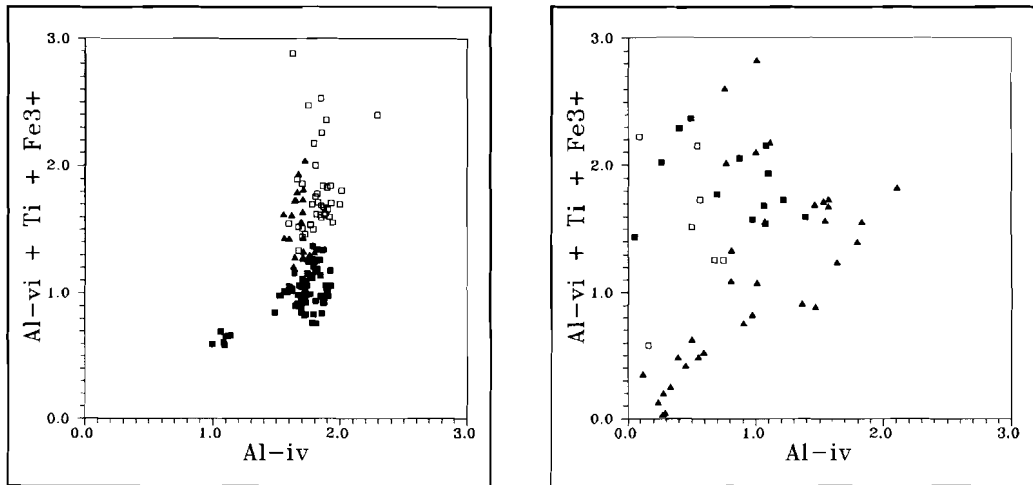


Fig. 5.7 $(Al + Fe^{3+} + Ti)^{VI}$ vs. Al^{IV} plot for Bamble hornblendes compared with literature. Symbols as in fig. 5.4.

Nelaug-Froland amphibolite facies hornblendes show a clearly positive trend; their Na^{M4} -contents tend to be lower than in Arendal-Tromøya-Merdøya granulite facies hornblendes for similar $(Al + Fe^{3+} + Ti)^{VI}$.

In the Na^{M4} vs. $(Na + K)^A$ plot (Fig. 5.6), Hisøya, Kragerø and Nelaug-Froland hornblendes tend to have high Na^{M4} at low $(Na + K)^A$, whereas Na^{M4} in Arendal-Tromøya-Merdøya granulite facies hornblendes is relatively low with respect to $(Na + K)^A$. Kragerø hornblendes seem to have slightly higher Na^{M4} at comparable $(Na + K)^A$. $(Al + Fe^{3+} + Ti)^{VI}$ shows a weakly positive correlation with Al^{IV} (Fig. 5.7), which is most clear within the Arendal-Tromøya-Merdøya group. Nelaug-Froland and Kragerø amphibolite facies, and Hisøya granulite facies hornblendes show relatively high $(Al + Fe^{3+} + Ti)^{VI}$ with low Al^{IV} in comparison with the Arendal-Tromøya-Merdøya granulite facies hornblendes. The largest spread occurs in the Nelaug-Froland hornblendes.

5.3.3

Biotite chemistry

Recalculation of biotite analyses according to the iterative procedure of Dymek (1983) yields considerable Fe^{3+} for most Bamble biotites. However, one biotite from amphibolite TN294, and various biotites from metapelites EJ10, MR35, MR73, AV44, AV106 and all biotites from metapelites CM40 and SU62 have excess positive charge if all iron is considered to be ferrous (Tables 5.2,3). This implies that the sum of the charge of other elements is overestimated, which may be due to 1) presence of octahedral vacancies, 2) deficiency in H^+ , or 3) the presence of Ti^{3+} instead of Ti^{4+} . The used normalization procedure accounts for octahedral vacancies; therefore possibility 1) is unlikely. Fe^{3+} is negatively correlated with

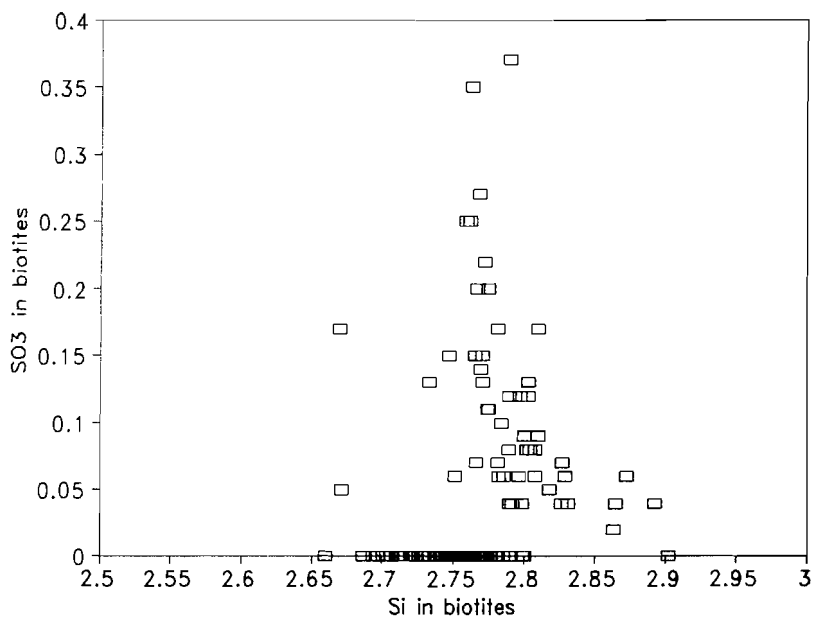


Fig. 5.8 Plot of SO_3 (wt.%) vs. Si in biotites from amphibolites.

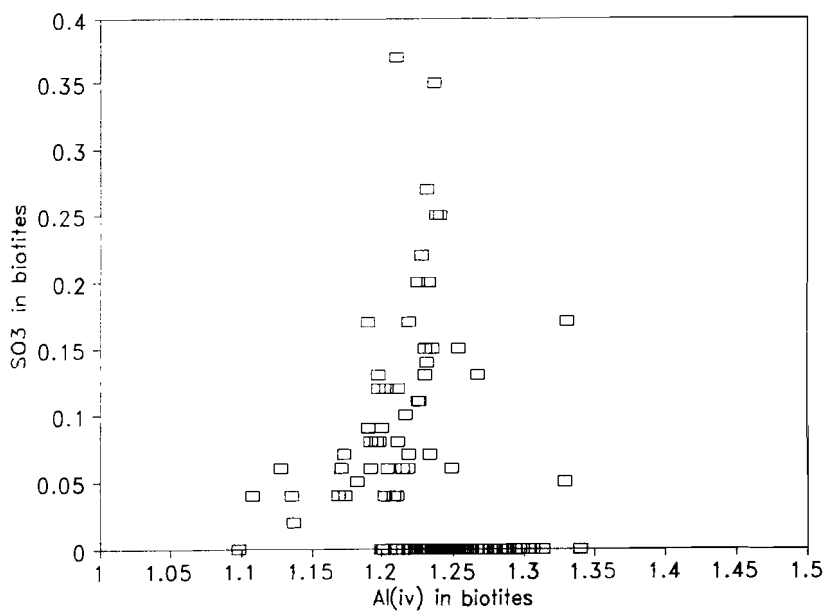


Fig. 5.9 Plot of SO_3 (wt.%) vs. Al^{IV} in biotites from amphibolites.

Mg# in biotites from both amphibolites (steeply) and metapelites (slightly).

Al and Ti. The relation between Ti and Al in biotite has not equivocally been established. Saxena (1967) found negative correlations between Ti and Al^{Tot} in biotites coexisting with calcic pyroxenes. In biotites coexisting with calcic amphiboles, Ekström (1973c) found that Ti and Al^{VI} are often negatively correlated, whereas Laird and Albee (1981) found a Ti increase with increasing Al^{IV}. In the Bamble amphibolites (Table 5.2), Ti correlates negatively with Al^{IV}, Al^{VI} and Al^{Tot}. Biotites from Bamble metapelites (Table 5.3) do not show any clear correlation.

Increasing Al^{VI} with increasing Al^{IV} and temperature has been observed by Laird and Albee (1981) for biotites coexisting with calcic amphiboles. The relationship between Al^{VI} and Al^{IV} is obscure in the investigated Bamble biotites from both amphibolites and metapelites, but tends to be slightly positive. Kretz (1990) found a decrease of Al^{VI} and Ti with increasing Mg# in biotites from Grenvillian metapelites. Ti and Mg# are not well correlated. Al^{VI} in biotites from Bamble metapelites tends to increase slightly from 0 to 0.5 with Mg#, whereas biotites from Bamble amphibolites do not show any relationship. Al^{IV} is independent of Mg# in both rock types, and varies between 1.0 and 1.4 in amphibolites, and between 1.2 and 1.4 in metapelites.

F and Cl. As in the hornblendes, F and Cl do not show any distinct relationship with Mg# in biotites from metapelites and amphibolites.

SO₃. As in the hornblendes, sulphur is systematically present in biotites. Correlations are very weak, but seem to be negative with Si (Fig. 5.8) and positive with (Al + Fe³⁺ + Ti)^{VI} and Al^{IV} (Fig. 5.9). No clear relationships are present with F, Cl or Ti.

5.3.4 Biotite chemistry versus metamorphic grade

Like hornblendes, coexisting biotites in the amphibolites show a Ti increase with metamorphic grade (Table 5.2, Fig. 5.10). Biotites also show decreasing average Fe# with decreasing grade (Table 5.2, Fig. 5.11), but average Fe# for biotites is much lower (0.30 - 0.45) in the highest zone, than for hornblendes (≥ 0.78). An increase in Fe# in the utmost northwest, near the Porsgrunn-Kristiansand Fault, as has been observed for hornblende, has not been found for coexisting biotite. Surprisingly, biotites from metapelites do not show any clear variation of Fe# (Table 5.3, Fig. 5.12). With exception of two more eastern samples (NS10 and NS19), average Fe# in all samples ranges from 0.8 to 1.0.

5.3.5 Fe²⁺-Mg and Ti distribution between hornblende and biotite

Distribution coefficients for Fe²⁺-Mg and Ti between coexisting hornblende and biotite are presented in table 4. Kd(Fe²⁺-Mg) shows a large variation, between 0.65 and 13.37, although the majority ranges from 1 to 3. In plutonic rocks, 1/Kd(Fe²⁺-Mg) tends to increase

Table 5.2 Average biotite chemistry in amphibolites. Elements p.f.u. Averages $\pm 1 \sigma$. In case of two values for Fe#, the first one is without, the second one with an outlier.

Sample	Al(iv)	Ti	Fe#	Mg#
AV 76	1.19 \pm 0.02	0.12 \pm 0.03	0.28 \pm 0.05	0.32 \pm 0.03
BD 14	1.20 \pm 0.01	0.13 \pm 0.01	0.13 \pm 0.05	0.43 \pm 0.01
GP 4	1.21 \pm 0.03	0.10 \pm 0.00	0.22 \pm 0.03	0.33 \pm 0.01
GP 71	1.23 \pm 0.01	0.14 \pm 0.01	0.15 \pm 0.03 0.12 \pm 0.06	0.52 \pm 0.02
SU 30	1.20 \pm 0.01	0.14 \pm 0.01	0.20 \pm 0.02	0.36 \pm 0.01
SU 56	1.25 \pm 0.02	0.28 \pm 0.02	0.26 \pm 0.04	0.54 \pm 0.01
TN 7	1.20 \pm 0.00	0.11 \pm 0.01	0.16 \pm 0.01	0.44 \pm 0.01
TN 19	1.25 \pm 0.04	0.10 \pm 0.03	0.13 \pm 0.06	0.50 \pm 0.02
TN 142	1.25 \pm 0.03	0.09 \pm 0.04	0.15 \pm 0.05	0.45 \pm 0.01
TN 146	1.24 \pm 0.01	0.10 \pm 0.01	0.17 \pm 0.03	0.45 \pm 0.02
TN 201	1.30 \pm 0.02	0.08 \pm 0.01	0.11 \pm 0.03 0.19 \pm 0.12	0.41 \pm 0.04
TN 202	1.26 \pm 0.02	0.07 \pm 0.01	0.17 \pm 0.07	0.41 \pm 0.02
TN 204	1.24 \pm 0.01	0.15 \pm 0.03	0.17 \pm 0.03	0.44 \pm 0.01
TN 209	1.24 \pm 0.03	0.18 \pm 0.01	0.30 \pm 0.10	0.40 \pm 0.04
TN 226	1.23 \pm 0.04	0.31 \pm 0.02	0.35 \pm 0.03	0.41 \pm 0.02
TN 294	1.23 \pm 0.03	0.28 \pm 0.01	0.33 \pm 0.06	0.37 \pm 0.02
TN 309	1.21 \pm 0.01	0.27 \pm 0.02	0.45 \pm 0.04	0.22 \pm 0.02
TN 431	1.24 \pm 0.01	0.27 \pm 0.04	0.30 \pm 0.03 0.25 \pm 0.07	0.52 \pm 0.02
WT 23	1.13 \pm 0.01	0.18 \pm 0.01	0.38 \pm 0.04	0.21 \pm 0.02

Table 5.3 Average biotite chemistry in metapelites. Elements p.f.u. Averages $\pm 1 \sigma$. Fe# values are for the cores.

Sample	Al(iv)	Ti	Fe#	Mg#
AV 44	1.27 \pm 0.02	0.26 \pm 0.02	0.92 \pm 0.05	0.45 \pm 0.01
AV 106	1.22 \pm 0.01	0.21 \pm 0.21	0.99 \pm 0.02	0.53 \pm 0.01
CM 40	1.28 \pm 0.02	0.08 \pm 0.02	1.00 \pm 0.00	0.59 \pm 0.01
CM 407	1.28 \pm 0.01	0.25 \pm 0.04	0.91 \pm 0.06	0.33 \pm 0.03
CM 454	1.33 \pm 0.02	0.27 \pm 0.01	0.80 \pm 0.06	0.39 \pm 0.05
EJ 10	1.28 \pm 0.03	0.30 \pm 0.05	0.82 \pm 0.11	0.28 \pm 0.03
MR 35	1.30 \pm 0.01	0.18 \pm 0.03	0.95 \pm 0.04	0.45 \pm 0.05
MR 73	1.30 \pm 0.01	0.12 \pm 0.04	0.96 \pm 0.04	0.39 \pm 0.02
NS 10	1.20 \pm 0.02	0.33 \pm 0.04	0.42 \pm 0.13	0.13 \pm 0.05
NS 19	1.28 \pm 0.02	0.32 \pm 0.02	0.64 \pm 0.02	0.30 \pm 0.03
RV 108	1.38 \pm 0.02	0.12 \pm 0.02	0.99 \pm 0.02	0.44 \pm 0.01
SU 62	1.21 \pm 0.03	0.20 \pm 0.01	1.00 \pm 0.00	0.48 \pm 0.02
TN 366	1.31 \pm 0.01	0.13 \pm 0.01	0.98 \pm 0.03	0.23 \pm 0.01
WT 66	1.30 \pm 0.02	0.19 \pm 0.02	0.85 \pm 0.02	0.39 \pm 0.02

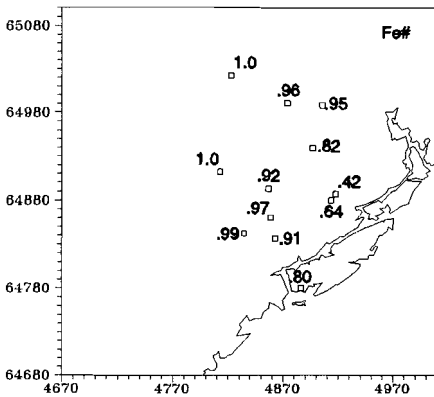
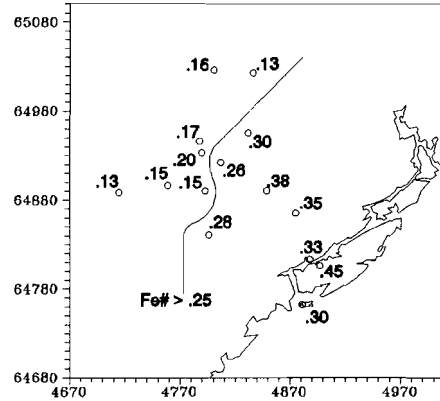
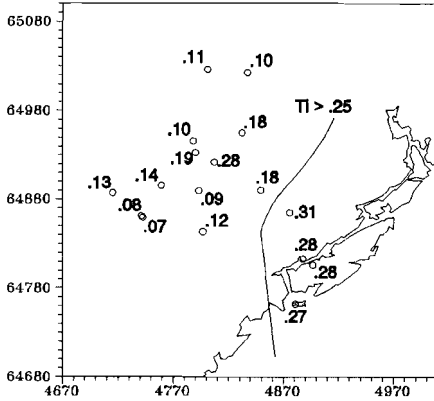


Fig. 5.10 Upper left Map of the investigated area and Ti-isopleth (0.25) for biotites from amphibolites. Note exception of sample SU 56 (0.28 northwest of the isopleth).

Fig. 5.11 Upper right Map of the investigated area with Fe#-isopleth for biotites from amphibolites.

Fig. 5.12 Left Map of the investigated area with Fe# for biotites from metapelites.

with the crystallization temperature of the magma (Hietanen 1971). In granitic rocks from both plutonic (Gorbatshev 1969, 1977, Hietanen 1971) and metamorphic environments (Kretz 1959, Saxena 1966), the Kd is typically 1, although a range of 0.5 to 2.5 is common (e.g. Gorbatshev 1969: 0.54 - 2.40; Hietanen 1971: 0.93 - 1.64). This may indicate that in samples with deviant Kd's (AV 76, GP 4, SU 30, TN 309 and WT 23), equilibrium has not been achieved between biotite and hornblende (cf. Glassley and Sørensen 1980). No relationship with the metamorphic grade is present.

Kd(Ti) ranges from 0.5 to 1.9, but is typically between 0.8 and 1.7 (Table 5.4). Nodirect relationship with the metamorphic grade could be established. Kd(Ti) in granulite facies samples never exceeds 1.0, but values lower than 1 also occur in amphibolite facies samples. This may indicate that a preferred incorporation of Ti in biotite with respect to hornblende as observed in plutonic rocks (Gorbatshev 1969, Hietanen 1971), holds for

Table 5.4 Kd for (Fe²⁺ - Mg) and (Ti) between coexisting hornblende and biotite in amphibolites.

Sample	Kd(Fe ²⁺ -Mg)	Kd(Ti)	Kd(Ti)*
AV 76	5.46	1.17	1.40
BD 14	1.38	1.08	1.65
GP 4	4.31	0.50	2.79
GP 71	0.76	0.86	1.74
SU 30	4.15	0.62	2.38
SU 56	0.65	0.71	2.32
TN 7	1.32	1.36	1.40
TN 19	1.27	1.90	0.88
TN 142	1.56	1.67	1.04
TN 146	1.99	1.30	1.32
TN 201	2.45	1.13	1.30
TN 202	2.35	1.71	0.86
TN 204	1.56	0.80	1.95
TN 209	2.45	0.89	1.82
TN 226	1.50	0.97	1.79
TN 294	2.00	0.89	1.93
TN 309	3.76	0.81	1.87
TN 431	0.76	0.93	2.22
WT 23	13.34	1.06	1.52

Table 5.5 Whole rock analyses of selected amphibolites in wt.%.

	TN19	TN142	TN146	TN201	TN202	TN204	TN227	TN258
SiO ₂	44.56	46.75	44.45	47.33	44.26	43.64	48.35	46.49
TiO ₂	2.80	2.86	3.15	1.18	1.64	2.24	2.57	2.00
Al ₂ O ₃	14.82	19.01	15.97	19.98	14.48	16.03	15.37	14.90
Fe ₂ O ₃	16.17	12.80	16.67	10.39	16.91	16.04	14.89	15.53
MnO	0.30	0.21	0.36	0.22	0.35	0.35	0.26	0.32
MgO	7.63	4.23	6.35	6.60	8.91	7.82	4.91	6.83
CaO	8.91	8.05	7.37	9.16	8.43	7.38	11.92	9.81
Na ₂ O	3.03	3.85	2.29	3.66	2.22	2.68	2.78	2.86
K ₂ O	0.85	0.85	1.34	0.46	0.65	1.34	0.74	0.33
P ₂ O ₅	0.35	0.45	0.73	0.18	0.20	0.34	0.48	0.24
Total	99.42	99.06	98.68	99.16	98.09	97.86	102.27	99.31

Table 5.6 Comparison of whole rock chemistry of the amphibolites and crystal chemistry of hornblende and biotite. Whole rock contents in wt.%, mineral contents in atoms p.f.u.

Sample	Al ₂ O ₃ WR	Altot Hbl	Alvi Hbl	Aliv Hbl	Aliv Bt	Sample	TiO ₂ WR	Ti Hbl	Ti Bt
TN 201	19.98	2.58	0.70	1.89	1.30	TN 146	3.15	0.13	0.10
TN 142	19.01	2.23	0.44	1.79	1.25	TN 142	2.86	0.15	0.09
TN 204	16.03	2.48	0.61	1.79	1.24	TN 19	2.80	0.19	0.10
TN 146	15.97	2.19	0.48	1.71	1.24	TN 227	2.57	0.30	-
TN 227	15.37	2.22	0.41	1.82	-	TN 204	2.24	0.12	0.15
TN 258	14.90	2.10	0.33	1.77	-	TN 258	2.00	0.28	-
TN 19	14.82	2.02	0.42	1.60	1.25	TN 202	1.64	0.12	0.07
TN 202	14.48	2.18	0.50	1.68	1.26	TN 201	1.18	0.09	0.08

granulite facies samples, but may be reversed in the amphibolite facies.

However, if the K_d is defined as $K_d(Ti)^*$, with Ti divided by the total amount of octahedral cations, then any systematic distribution is absent (Table 5.4). Amphibolite facies samples have $K_d(Ti)^*$ ranging from 0.86 to 2.79, whereas $K_d(Ti)^*$ in granulite facies samples varies between 1.79 and 2.22. For comparison, $K_d(Ti)^*$ in epidote-amphibolite facies gneisses ranges from 1.3 (Moxham 1965) to 1.8 (Saxena 1966), whereas granulite facies gneisses have values of 2.0 (Kretz 1959).

5.4

Discussion

Ti-contents of both hornblende and biotite increase with metamorphic grade. This implies a temperature gradient over the amphibolite to granulite facies transition zone, thus contradicting the conclusion of Lamb et al. (1986), and confirming the results of Nijland and Maijer (1992, 1993 ch. 3), which were both based on geothermobarometry. Ti-isopleths (Figs. 5.2 and 5.10) indicate that different thermal regimes prevailed on Hisøya, in the Arendal-Tromøy-Merdøy granulite facies area, and the Nelaug-Froland amphibolite facies area.

Since the Ti-increase in hornblende and biotite with metamorphic grade is independent of the whole rock composition (Table 5.6) and opaque minerals are present in all samples, the Ti-contents of hornblende and biotite appear to be controlled by other parameters than the whole rock TiO_2 -content. The $K_d(Ti)$ is always lower than 1 in the granulite facies samples, whereas it is usually higher than 1 in amphibolite facies samples. These two aspects indicate that distribution of Ti between coexisting hornblende and biotite, given that it is buffered by another Ti-bearing phase, might provide a possible geothermometer.

In contrast, the Al-content of hornblende (Al^{Tot} and Al^{IV} , and to a lesser degree also Al^{VI}) roughly increases with whole rock Al_2O_3 -content (Table 5.6). This indicates that the variation of Al^{VI} in hornblende with metamorphic gradient is not a very useful indicator of changing conditions. The Al-content of coexisting biotites in amphibolites does not vary significantly with either metamorphic gradient or whole rock composition.

In diagrams evaluating the glaucophane, edenite and Tschermak substitutions in amphibole (Figs. 5.4-7), hornblendes from the more eastern Kragerø area (O'Nions et al. 1969b), and a few Hisøya hornblendes tend to have a higher degree of pressure dependent substitutions. An eastward pressure increase was already suggested by Touret and Falkum (1987). Although the basis of this suggestion, the presence of kyanite in the east and not in the west, is unsound (Nijland and Maijer 1992, 1993, ch. 3), the hornblende chemistry supports such a slight pressure increase. The amount of temperature dependent substitution is larger in granulite facies hornblendes from the Arendal-Tromøy-Merdøy area than in those from the Hisøya granulite facies area.

A larger amount of pressure dependent substitutions occurred in some of the amphibolite facies hornblendes. This may correlate with the pressure increase from core to rim in samples from the northern part of the amphibolite facies area, which was deduced from

garnet-hornblende-plagioclase-quartz geobarometry (Nijland and Maijer 1992, 1993, ch. 3).

The regional patterns of Fe# in hornblende (Fig. 5.3) and biotite (Fig. 5.11) show an increase in oxidation with decreasing metamorphic grade, although Fe# in hornblende increases in the utmost northwest. Fe# is considerably lower for biotite than for coexisting hornblende. The large difference in ferric iron estimates for coexisting amphibole and biotite may indicate that the absolute values obtained by one or both normalization procedures is in error. Many of the amphibolites contain garnet in their peak metamorphic assemblage, indicating that oxidation levels should have been relatively low. Therefore, it is likely that the Dymek procedure overestimates Fe³⁺ in biotite.

The concurrent trends, however, indicate that these are probably correct. The decrease of Fe# with decreasing metamorphic grade coincides with the pattern shown by whole rock chemistry of garnetiferous gneisses (Field 1969, Beeson 1972). It may simply reflect the increasingly oxidizing nature of cooling fluids. No regional pattern is displayed by Fe# in biotites from metapelites (Fig. 5.12). This indicates that there existed no single fluid that communicated between the various lithologies.

Sulphur is usually not analyzed in amphiboles and micas, so little is known about the amounts in which it is present or its position in the silicate lattice (cf. Hawthorne 1981, Robinson et al. 1981, Bailey 1983). Low amounts of sulphur have, however, been reported from Cl-rich hastingsites from Dashkessan (0.11 wt.% SO₃; Krutov 1936) and East Antarctica (0.02 wt.% SO₃; Suwa et al. 1987), and from anthophyllites of the Bamble Sector (0.01 wt.% S; Bugge 1943) and the Outer Hebrides (0.18 wt.% S; Guppy 1956), while Sundius (1945) reported 0.19 wt.% SO₃ in a richterite from Långban, Sweden. Jacobsen et al. (1958) reported sulphur in biotite from Nigerian granites and greisens (0.02–0.03 wt.% S). In addition, Giuseppetti and Tadini (1972) reported substitution of (S_{0.85}Cl_{0.15}) for OH in the brittle mica anandite.

The investigation of hornblende and biotite from amphibolites shows that sulphur is not an uncommon trace component. The major sulphur reservoirs in the lower crust are generally thought to be formed by sulphide minerals and scapolite. The presence in silicates like biotite and hornblende may provide a third reservoir. Due to the fact that both minerals are fairly common in lower crustal rocks, this reservoir may significantly contribute to the sulphur budget of the lower crust. The question arises where sulphur is incorporated in the crystal structure of both silicates. This has not been investigated in detail, but element plots hint to the answer. It may be expected that sulphur substitutes for OH⁻ as HS⁻ or S²⁻. However, SO₃ shows no or negative correlations with fluorine in hornblende and biotite, and a negative correlation with chlorine in hornblende. This does not exclude substitution for OH, but it does not indicate competition for it between sulphur and the halogens. A very weak negative correlation has been observed between SO₃ and Si in both biotite and hornblende. This may indicate substitution of SO₄ for SiO₄ in both silicates. The positive correlation between Al^{IV} and SO₃ in both silicates suggests the substitution S⁶⁺ + 2Al³⁺ = 3Si⁴⁺, thus maintaining charge balance.

1. Different peak metamorphic thermal regimes existed in the Nelaug-Froland amphibolite facies area, Hisøya granulite facies area, and Arendal-Tromøya-Merdøya granulite facies area.
2. Pressure likely have increased towards the east (Kragere) and west (Hisø). Minor change also occurred in the Nelaug-Froland amphibolite facies area.
3. Distribution of Ti between coexisting hornblende and biotite may provide a possible geothermometer, as granulite samples have Kd's always lower than one, whereas those in the amphibolite facies samples are usually higher than one.
4. Al-content of hornblende and biotite in metabasic rocks is only a doubtful indicator of changing metamorphic conditions.
5. Oxidation generally increases with decreasing metamorphic grade in amphibolites, but remains constant in metapelites.
6. Different lithologies behaved as independent systems.
7. Hydrous silicates like hornblende and biotite provide a third sulphur reservoir in the lower crust, besides sulphide minerals and scapolite.

Acknowledgements - Samples were kindly provided by H. Anijs, B.P. Dam, G.P. van Ditshuizen, E.J. Kornman, C. Maijer, M. Röhrman, A. Senior, N. Hulzebos-Sijen, W. Theulings, R.J.M.J. Vogels and A. Vons. R.P.E. Poorter and T. Bouten assisted in the microprobe analyses. Most microprobe analyses of biotites from metapelites were performed by E.J. Kornman, A. Moerenhout and A. Vons. W.H.M. Eussen performed the XRF analyses. This paper benefitted from discussions with C. Maijer and the constructive criticism on an earlier draft by G.J.L.M. de Haas, C. Maijer, R.D. Schuiling and D. Visser. Financial support was provided by AWON (NWO 751.353.023).

**METAMORPHIC PETROLOGY OF THE FROLAND CORUNDUM-BEARING ROCKS:
THE COOLING AND UPLIFT HISTORY OF THE BAMBLE SECTOR, SOUTH NORWAY.**

Abstract - Corundum-bearing rocks from Kleggåsen, Froland, preserve metamorphic textures which reflect the cooling and uplift path of the Bamble Sector. The P-T path may be correlated with a T-t path constructed from published ages. The P-T path starts at the thermal climax of prograde metamorphism, M I (c. 750°C, 7 kb), characterized by Sil, Pl, Bt, Rt and Crn. Subsequent near isobaric cooling results in M II, characterized by Ky + Ms ± Chl veinlets (600-700°C, 7 kb). This marks the onset of rehydration. M III assemblages of Mrg ± Crn formed around 500-570°C and 3-7 Kb, and are followed by M IV (c. 400°C, 2-4 kb) characterized by Ms, Bt and Ep. The trajectory from M II via M III to M IV is believed to reflect the uplift of the area in response to Sveconorwegian upthrusting. The uplift was completed before c. 940 Ma, which is the age of post-tectonic granites and K-Ar biotite cooling ages. The latest episode recorded by the Froland rocks, M V (175-280°C, 2-3 kb), is characterized by Prh, Pmp, Scp and Tur, indicating local influx of B- and Cl-bearing hydrous fluids. M V is interpreted as adaption to upper crustal conditions between c. 920 and 760 Ma.

6.1

Introduction

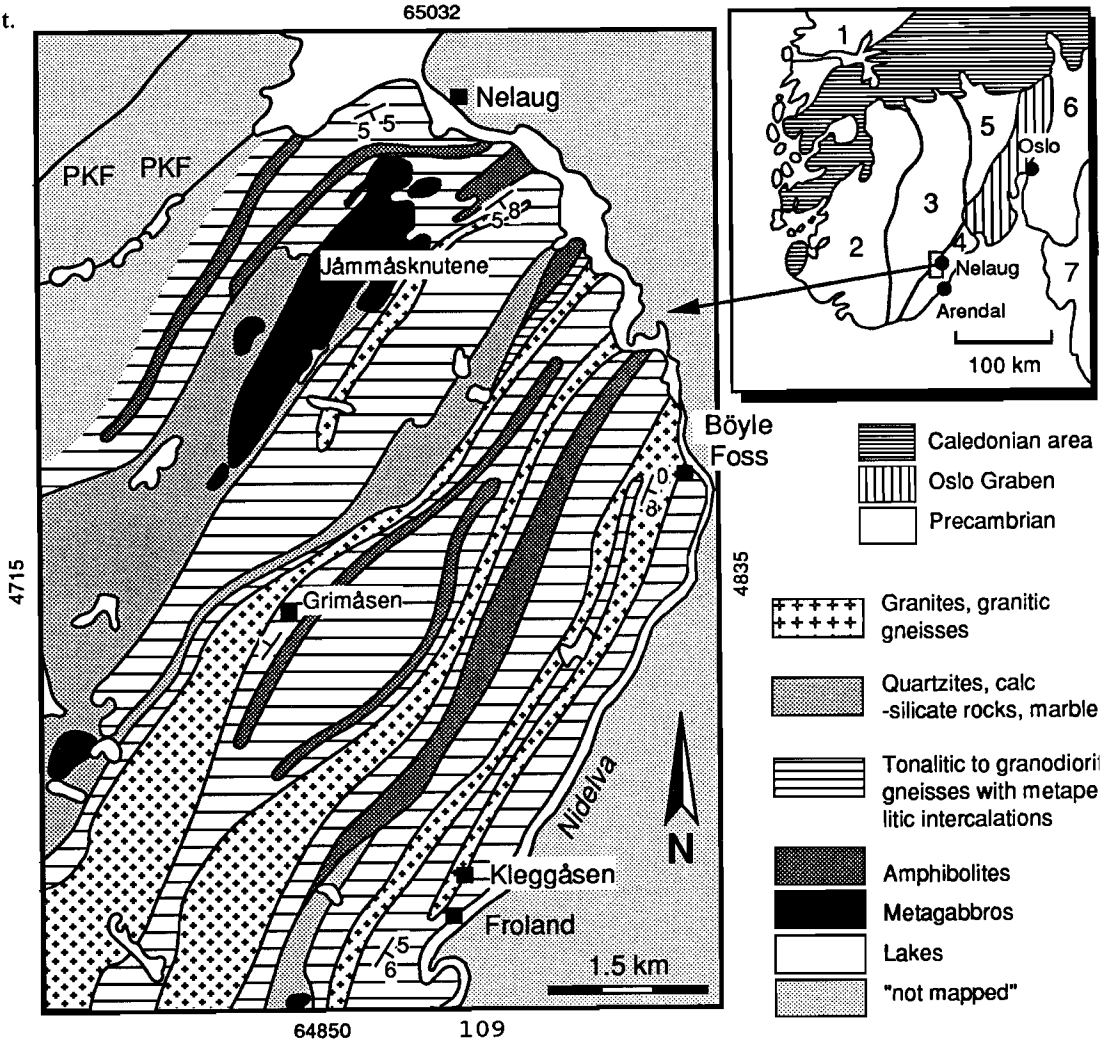
The Bamble Sector (Fig. 6.1) is part of the Southwest Scandinavian Domain of the Fennoscandian Shield (Gaál and Gorbatshev 1987). It is composed of a Proterozoic supracrustal suite that was metamorphosed and intruded by acidic and basic magmas during the Gothian (1750-1500 Ma) and Sveconorwegian (1250-950 Ma) orogenies. For a detailed description of the lithologies and structural geology of the area, the reader is referred to Starmer (1985a, 1991).

In the Nelaug-Froland-Arendal area (Fig. 6.1), the grade of metamorphism ranges from upper-amphibolite facies in the north up to granulite facies in the area around Arendal in the south (Bugge 1940, Touret 1971a, Lamb et al. 1986). P-T estimates range from c. 836°C, 7.7 kb in the core of the granulite facies area to c. 752°, 7.1 kb in the amphibolite facies area (Nijland and Maijer 1992, 1993).

Corundum-bearing rocks occur at Kleggåsen, Froland, 11 km. northwest of Arendal, and were first described by Oftedahl (1963). The rocks have been interpreted as metamorphosed kaolinite-bauxite weathering crusts (Serdyuchenko 1968). They are

leucocratic, and gneissic in their biotite-rich parts. The rocks are mainly composed of plagioclase, corundum, biotite and sillimanite, and cut by veinlets of green mica and kyanite. They occur in a two metres wide, concordant lense, which is separated from steeply dipping banded and granitic gneisses by a 20 cm. thick biotitite. A small, intensively altered part of the outcrop features large brown tourmaline and a rare chromian montmorillonite, volkonskoite (Nilssen and Raade 1973). The rocks provide information about the successive stages of post-peak metamorphism and will be studied to unravel the cooling and uplift history of the Bamble Sector.

Fig. 6.1 Geological sketch map of the Froland area west of the Nidelva river with relevant localities (Modified after Visser and Senior 1990). Coordinates along the margins of the map are according to the grid of Norges geografiske oppmåling. PKF = Porsgrunn-Kristiansand Fault. Inset: Division of the Southwest Scandinavian Domain (Modified after Verschure 1985). Numbers denote: 1 - Western Gneiss Region, 2 - Rogaland / Vest-Agder Sector, 3 - Telemark Sector, 4 - Bamble Sector, 5 - Kongsberg Sector, 6 - Østfold Sector, 7 - Stora Le-Marstrand Belt.



The distribution of the mineral assemblages in the samples is shown in table 6.1.

6.2.1

Oldest mineral assemblages (M I)

The oldest mineral assemblage, M Ia, consists of plagioclase, biotite, fibrolitic and euhedral sillimanite, and rutile, with accessory zircon, allanite and apatite. Microfolds of fibrolite are enclosed by large plagioclase crystals. Plagioclase is occasionally antiperthitic. Large subhedral brown biotites, which often contain small sagenite needles, constitute the foliation together with fibrolite. Younger euhedral sillimanite generally also follows this foliation, but its crystal faces truncate the fibrolite (Fig. 6.2). Large bronze rutile occurs intergrown with euhedral sillimanite. Rutile shows lamellar twinning and has often been accumulated in the hinges of microfolds.

Large colourless to pink pleochroic corundum crystals enclose both fibrolite and euhedral sillimanite, biotite, rutile and plagioclase, and are therefore denoted as M Ib. Boundaries between corundum and the other minerals are usually sharp, and show no signs of reaction; only sillimanite reaction textures are sporadically observed, as evidenced by bottle neck textures, i.e. the thinning of sillimanite prisms at the place where they are overgrown by corundum. The M Ib corundum occurs in two different microstructures: either as large sub- to euhedral crystals (up to several cm.) grown in the centre of sigmoidal thickenings of the fibrolite foliation, or as large archipelago-like crystals (Fig. 6.3). Corundum shows lamellar twinning, and displays slight colour zoning with a bluish tinge, especially along the margins and according to crystallographic planes; the blue colour becomes more intense along altered margins.

6.2.2

Kyanite-bearing veinlets (M II)

Veinlets of kyanite and muscovite with minor chlorite cut through the M I assemblages (Fig. 6.4). Kyanite occurs in the centre of the veinlets, and is weakly bluish pleochroic and twinned. Muscovite and chlorite occur along the margins of the veinlets. Both display a pale green pleochroism. They form relatively large subhedral grains. Rare relics of biotite and fibrolite occur in the veinlets. Although M II minerals are mainly restricted to veinlets, green muscovite and chlorite also occur dispersed throughout the rocks. Here too, they form relatively large, subhedral grains, in contrast to M IV muscovite and chlorite, which usually occur as rims and fine-grained aggregates around older phases. M II Muscovite outside the veinlets has been found to enclose microfolds of fibrolite.

Table 6.1 Distribution of the successive metamorphic assemblages in the different samples. Mineral abbreviations according to Kretz (1983), except Fib - fibrolite.

	M I									M II			M III		M IV					M V							
	S i l	F i l	P l	B t	C r n	R t	Z r n	A l	A p	T u r	K y	M s	C h l	M r g	C r n	P l	B t	M s	C h l	C a l	E p	P h	P p	S c p	T u r		
TN75	x	x	x	x	x	x	x			x		x						x	x		x	x					
TN76	x	x	x	x	x	x	x					x	x	x					x	x	x	x					
TN77	x	x	x	x	x	x	x	x	x		x	x	x		x	x		x	x		x		x	x	x	x	
TN78	x	x	x	x	x	x		x	x		x	x	x		x	x			x	x	x	x					
TN79		x	x			x	x								x				x				x				x
TN81	x	x	x	x	x	x	x					x						x	x	x							
TN82	x	x	x	x		x					x	x							x	x	x		x		x		
TN83	x	x	x	x	x	x	x					x							x		x						
TN84	x	x	x	x	x	x					x	x							x								
MA993	x	x	x	x	x	x	x					x	x	x	x			x	x								
FL143			x	x	x	x						x	x	x					x	x	x	x					
FL144			x		x	x	x					x	x	x	x	x			x			x					
FL145	x	x	x	x	x	x			x										x			x					
FL146	x	x	x	x	x	x					x	x	x	x					x						x		
FL147	x	x	x	x	x	x	x												x	x							
FL148			x	x		x					x	x	x	x					x	x	x	x					
FL149	x	x	x	x	x	x	x				x	x	x	x	x				x	x	x						
FL150	x	x	x	x	x	x					x	x	x		x				x		x	x					
FL151		x	x			x	x	x							x				x			x	x				x

Fig. 6.2 M Ia fibrolite truncated by M Ia euhedral sillimanite. Microphotograph of sample TN84.

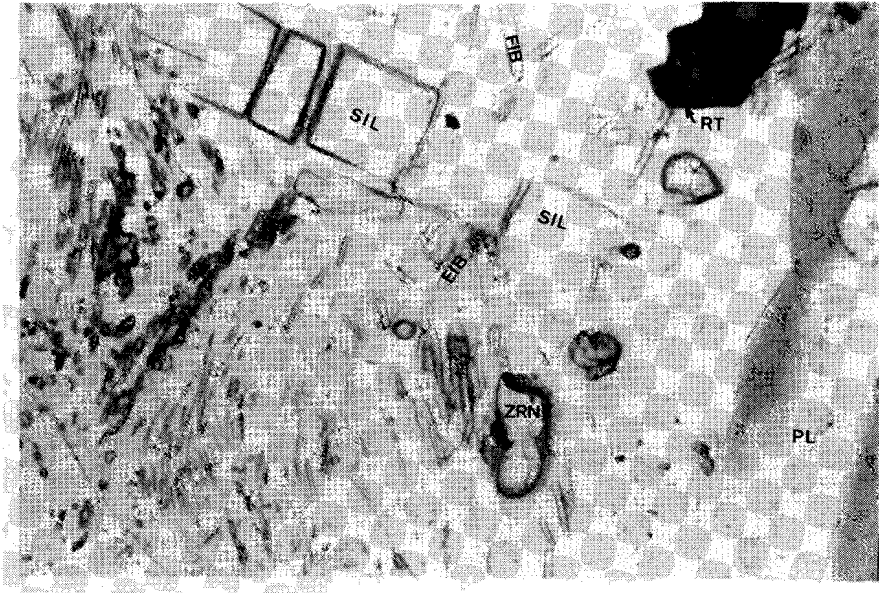


Fig. 6.3 Archipelago crystal of M Ib corundum with enclosed by plagioclase. Microphotograph of sample TN81.



6.2.3

Margaritization reactions (M III)

In the M I assemblage, aggregates of sheaf-like bundles of margarite locally replaced M Ia plagioclase. These aggregates are usually present in the vicinity of M Ib corundum crystals, but the grain boundaries of corundum are virtually unaffected. Sporadically, small corundum grains occur in the margarite aggregates; these may represent relics. Rutile and biotite occur unaffected in these aggregates.

In the M II veinlets, kyanite is partially replaced by fine-grained aggregates and rosettes of margarite. This replacement has preferentially taken place along cracks, cleavage planes and grain boundaries. The margarite is usually accompanied by small cloudy grains of corundum (Fig. 6.5), which are situated in the centre of the cracks. Traces of muscovite occur in the margarite aggregates.

6.2.4

Low grade assemblages (M IV)

Several low grade minerals developed after the margaritization reactions. A rim of anorthite-rich plagioclase is locally present around both M Ib and M III corundum. Small M III corundum is occasionally entirely replaced by aggregates of anorthite-rich plagioclase and micas. Anorthite-rich plagioclase and M Ia matrix plagioclase have never been observed in contact. Previous grain boundaries and characteristic cleavage planes of M Ib corundum can be retraced in the anorthite-rich plagioclase. Plagioclase, biotite and aluminum silicates are locally altered to sericite / muscovite ± calcite. Some pseudomorphs of fine-grained muscovite after kyanite occur. Margarite is sometimes altered to chlorite and calcite. Fine grained brown biotite occurs in small veinlets.

Both anorthite-rich plagioclase and the other phases are grouped in M IV because they clearly postdate M III and predate even lower grade phases. Their mutual relationships are unclear, but anorthite-rich plagioclase is likely to be slightly older, as it has locally been altered to sericite.

6.2.5

Lowest grade alteration (M V)

Prehnite and potash feldspar occur together with chlorite as small lenses along the cleavage planes of biotite. Scapolite with a birefringence of 0.020, has replaced plagioclase in a patchy way, and encloses M II kyanite and M IV pseudomorphs of muscovite after kyanite. Rare pumpellyite occurs, but not in the same aggregates as prehnite. In the intensively altered part of the outcrop (cf. Nilssen and Raade 1973), the main replacing mineral is euhedral prehnite. Prehnite encloses fibrolite, margarite, rutile and fine grained white mica pseudomorphs after kyanite. It occurs together with large

Fig. 6.4 M II veinlet of muscovite and chlorite, with kyanite in the centre, cutting the M I assemblage and foliation. Drawn after thin section of sample MA993.

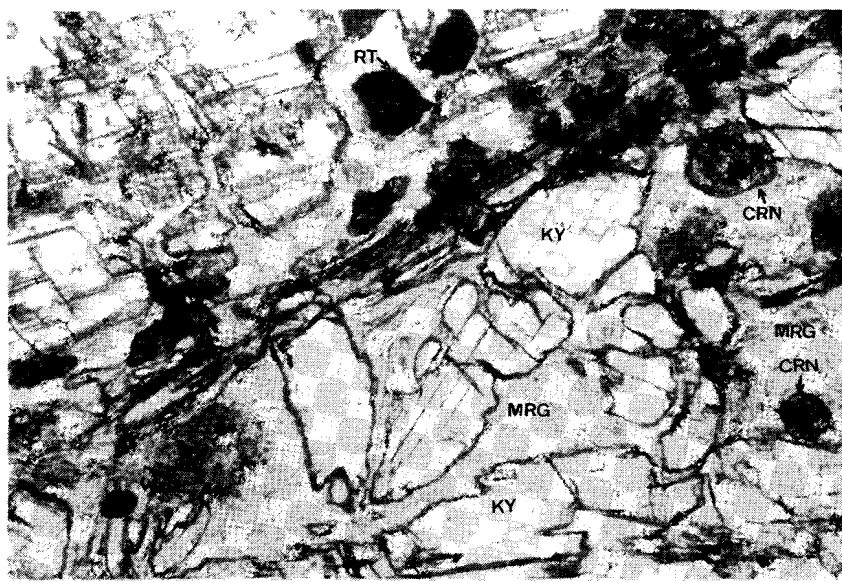
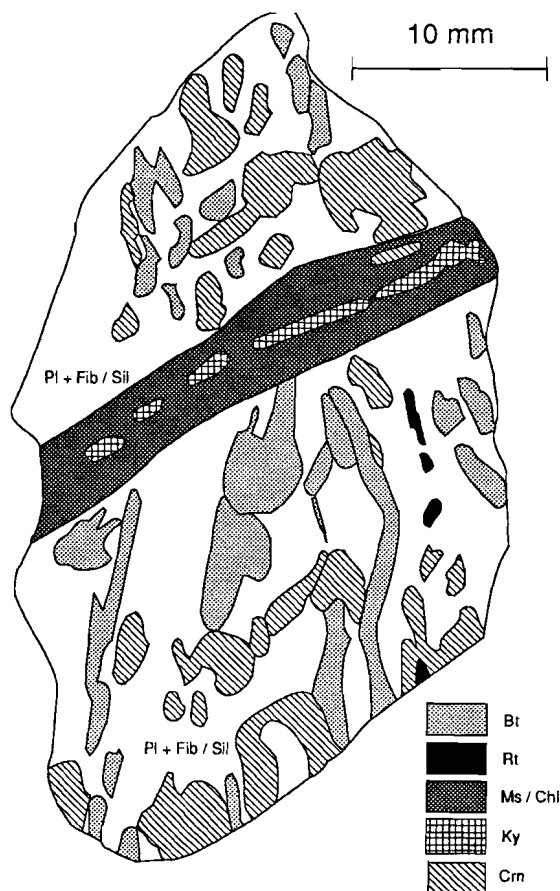


Fig. 6.5 Replacement of M II kyanite by M III margarite and corundum. Microphotograph of sample TN77.

olive-green to blue-green zoned tourmaline. Beryl, which was reported by Oftedahl (1963), has not been found in our samples.

Relations between scapolite and prehnite, pumpellyite and tourmaline could not be established. As they are the youngest minerals present in the samples, they are grouped in the same metamorphic phase.

6.3 Mineral chemistry

Analyses were performed using a Jeol JXA 8600 Superprobe and an automated TPD microprobe at the Dept. of Geochemistry, Utrecht. Operating conditions were 15 keV, 10 nA, and 40 keV, 15 nA for the Jeol and TPD respectively. Analyses were corrected using Tracor Northern PROZA and ZAF correction programs respectively. Selected analyses are presented in table 6.2.

6.3.1 Aluminum silicates

All aluminum silicates have a near ideal stoichiometrical composition. Fe is present in minor amounts only, but Cr-contents are high. M Ia fibrolite contains 0.72 ± 0.05 wt.% Cr_2O_3 (mean $\pm 1\sigma$), M Ia euhedral sillimanite 0.69 ± 0.07 wt.%, and M II kyanite 0.70 ± 0.09 wt.% in samples TN77, 78, 84 and FL144. The Cr-content of the aluminum silicates is much lower in sample MA993: Kyanites contain only 0.24 ± 0.07 wt.% Cr_2O_3 and sillimanites 0.50 ± 0.04 wt%. No systematic difference in Cr_2O_3 -content is shown by aluminum silicates from the successive metamorphic phases. The Cr-contents of Froland sillimanite and kyanite are high for metapelites, which both typically contains less than 0.20 wt.% Cr_2O_3 (Kerrick 1991, and references therein).

6.3.2 Corundum

Both M Ib and M III corundum contain small amounts of Fe and Cr. In spite of its colour zoning, M Ia corundum does not show any detectable chemical zoning. M III corundum has a lower Cr_2O_3 content than the M Ib corundum, respectively 0.78 ± 0.28 wt.% and 1.07 ± 0.10 wt.%.

Table 6.2 Selected mineral analyses. Fib, Sil, Ky normalized to 5 O, Bt, Mrg, Ms to 22 O, Chl to 28 O, Pl to 8 O, Crn to 3 O, Scp to Si + Al = 12.

Phase	Fib	Sil	Pl	Bt	Crn	Ky	Chl	Ms	Mrg	Crn	Ms	Pl	Scp
M	Ia	Ia	Ia	Ia	Ib	II	II	II	III	III	IV	IV	V
SiO2	36.48	36.84	57.70	36.97	.	37.01	26.38	45.55	32.60	.	44.82	55.70	51.82
TiO2	.	.	.	1.82	.	.12	.05	.98	.15	.	.85	.	.
Al2O3	62.66	61.67	25.98	20.03	98.22	61.82	21.90	35.20	47.94	97.93	34.82	28.86	24.94
Cr2O3	.69	.64	.04	.82	.99	.66	nd	.47	.18	.88	.89	nd	nd
FeO	.	.32	.	9.71	.	.	16.61	.44	.37	.26	1.10	.	.
MnO	.03	.	.	.13	.	.01	.06
MgO	.18	.	.	15.06	.	.	20.78	.48	.71	.	.89	.	.
CaO	.	.	8.26	.	.	.08	.	.	8.94	.	.	10.47	11.22
Na2O	.	.	6.96	.36	.	.	.	1.12	1.93	1.25	5.89	6.81	.
K2O	.08	.	.16	9.11	.	.	.	9.71	.69	.	9.55	.	.28
P2O5	nd	.	.
SO3	nd	nd	nd	nd	nd	nd	.	nd	nd	nd	nd	.	.42
Cl	.01	.	.02	.12	.	.	.03	.01	.01	.	nd	.	2.07
F32	.	.	.07	.	.	.	nd	.	.
Total	100.12	99.47	99.12	94.45	99.21	99.70	85.88	93.96	93.52	99.51	94.17	100.82	97.56
Si	.99	1.00	2.61	5.43	.	1.00	5.41	6.12	4.38	.	6.05	2.48	7.66
Ti20	.	.00	.01	.10	.02	.	.09	.	.
Al	2.00	1.98	1.38	3.46	1.99	1.98	5.29	5.58	7.60	1.98	5.54	1.52	4.34
Cr	.02	.01	.00	.09	.01	.01	.	.05	.02	.01	.10	.	.
Fe	.	.01	.	1.19	.	.	2.85	.05	.04	.00	.13	.	.
Mn	.00	.	.	.02	.	.00	.01
Mg	.01	.	.	3.30	.	.	6.34	.10	.15	.	.18	.	.
Ca	.	.	.40	.	.	.00	.	.	1.28	.	.	.50	1.78
Na	.	.	.61	.1129	.50	.	.33	.51	1.95
K	.00	.	.01	1.71	.	.	.	1.66	.11	.	1.64	.	.05
P00	.	.	.
S
Cl	.00	.	.00	.03	.	.	.01	.00	.0052
F15	.	.	.04

6.3.3

Biotite

Only M I biotites have been analyzed. X_{Mg} , defined as $Mg/(Fe+Mn+Mg)$, ranges from 0.69 to 0.73. TiO_2 is present in the range 1.80–2.55 wt.%. Ti shows negative correlations with Al^{IV} and X_{Mg} . The biotites contain 0.64 to 0.99 wt.% Cr_2O_3 . The Cr-content of biotites from MA993 is much lower (0.30–0.42 wt.%). The biotites contain trace amounts of Cl (≤ 0.04 at =22), whereas F ranges from 0 to 0.15 atoms per 22 oxygens (≤ 0.32 wt.%). The F-content of the biotites increases towards their core.

6.3.4

Margarite

M III margarites contain substantial quantities of Na_2O (Table 6.2). In some margarites, Si is higher than the ideal stoichiometric 4 atoms, suggesting that the presence of Na is due to the plagioclase substitution $NaSiCa_{-1}Al_{-1}$ (Frey et al. 1982), giving paragonite solid solution. In other margarites, the number of Ca atoms is low, but Si normal, as has been observed at other localities where margarite has grown out of aluminum silicates (e.g. Guidotti and Cheney 1976, Gibson 1979, Baltatzis and Katagas 1981). Froland margarites have $Ca/(Ca+Na)$ ratios between 0.72 and 0.79. $Ca/(Ca+Na)$ ratios in margarite are considerably higher than those of coexisting plagioclase (0.38 – 0.43), as is commonly observed (Ackermann and Morteani 1973, Gibson 1979, Frey et al., 1982). The amount of K_2O in the margarites shows a weak positive correlation with the amount of Na_2O .

Cr_2O_3 -contents (≤ 0.59 wt%) are higher than usual, and even higher than in the Cr-rich margarites reported by Morand (1990) from New South Wales, Australia, which contain up to 0.37 wt%. The highest Cr-contents (≤ 1.93 wt.%) recorded in retrograde margarites are from the New Zealand Alps (Cooper 1980). The Cr_2O_3 -contents in the Froland margarites reflect the whole rock composition, and are lower for MA993 margarites than those from other samples. The FeO-content (≤ 0.45 wt%) is normal for margarites. TiO_2 in the Froland margarites is less than 0.35 wt.%. Only traces of Mg, Cl and F have been detected.

6.3.5

Muscovite s.l.

Chemically, no distinction could be made between M II and M IV muscovites. The muscovites show limited solid solution with paragonite, and minor Ca-substitution. All muscovites contain FeO (0.37–1.29 wt.%), Cr_2O_3 (≤ 0.90 wt.%) and TiO_2 (0.30–1.42 wt.%). The muscovites contain no Cl and only traces of F (≤ 0.13 wt.%).

6.3.6

Plagioclase and scapolite

Both M Ia and M IV plagioclase are almost orthoclase free. M Ia plagioclase has an anorthite content of 38–43 %. M IV anorthite-rich plagioclase has 48–51 An%. The scapolites are Cl-rich (1.78–2.10 wt%) and SO₃-poor (≤ 0.42 wt%), with trace amounts of fluorine (≤ 0.14 wt%). The meionite percentage ranges from 45 to 47%.

6.3.7

Rutile

Cr is the only element substituting significantly in rutile. Cr₂O₃ is present in moderately high amounts (0.70–1.05 wt%).

6.3.8

Chlorite

X_{Mg} of the chlorites ranges from 0.64 to 0.70. Al^{IV} varies between 1.85 and 2.72. TiO₂ occurs in considerable amounts, up to 1.02 wt%, and traces of Mn, Ca, Na, K, and S may be present.

6.4

Reaction history and P-T path

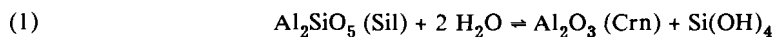
6.4.1

Thermal climax (M I)

The oldest mineral assemblage, M Ia, is represented by plagioclase, sillimanite, biotite and rutile. The observed textures do not directly reveal the relationship between fibrolite and the euhedral sillimanite. However, the euhedral sillimanite truncates the fibrolite foliation (Fig. 6.2). This is interpreted as evidence that euhedral sillimanite replaces the fibrolite (cf. Vernon 1987).

M Ib corundum encloses both types of sillimanite, but mainly grew at expense of the fibrolite, as indicated by the occurrence of large corundum crystals in the centres of fibrolite aggregates. This may be explained by the larger effective reaction surface of the fibrolite aggregates with respect to the euhedral sillimanite, whereas removal of silica will have been much easier along the grain boundary networks in fibrolite aggregates than from massive euhedral sillimanite. Contacts between corundum and the euhedral sillimanite are usually sharp crystal faces. However, bottle necking textures involving this sillimanite indicate that it was also partially consumed by corundum. Neither quartz nor other silica-bearing reactions

products are present. Therefore, the growth of corundum must have involved removal of silica by a fluid phase:

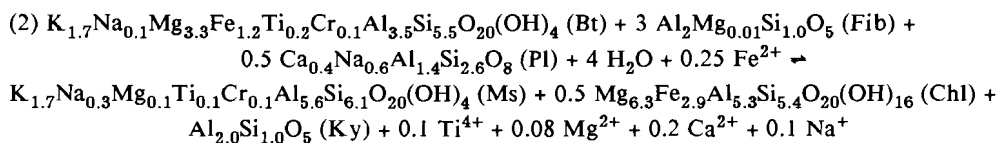


This reaction is not restricted to a narrow P-T space, but mainly depends on the activity of SiO_2 in the coexisting fluid, and may have occurred at temperatures higher than c. 450-500°C (cf. Hemley et al. 1980) for the pressures recorded in the Bamble Sector (7-8 kb).

With exception of the replacement of fibrolite by euhedral sillimanite, no trace of the prograde P-T history has been found in the Froland rocks. Neither early mineral inclusions nor chemical zonations have been observed. Nevertheless, M I is interpreted to represent the thermal climax of metamorphism, because sillimanite is the ubiquitous aluminum silicate in the Bamble Sector (Starmer 1976, Touret and Falkum 1987). From the M I assemblage, it is impossible to estimate peak metamorphic P-T conditions. However, as M I phases sillimanite, biotite and plagioclase are peak metamorphic minerals in this part of the Bamble Sector, we will adopt the peak metamorphic P-T estimates for the Froland area. Nijland and Maijer (1992, 1993) estimated P-T conditions at $752 \pm 34^\circ\text{C}$ and 7.1 ± 0.4 kb based on mineral pairs in amphibolites. Visser and Senior (1990) obtained nearly identical results of $740 \pm 60^\circ\text{C}$, 7 kb, from aluminous enclaves in cordierite-orthoamphibole rocks.

6.4.2 Initial cooling (M II)

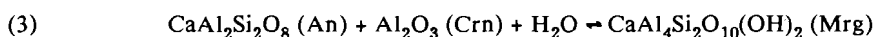
The M I assemblage is replaced by M II kyanite, muscovite and minor chlorite along veinlets. As relics of biotite and sillimanite are still present in these veinlets, the replacement probably took place by the generalized reaction:



As in many terrains, the occurrence of the M II assemblage in veinlets shows that kyanite developed not directly from sillimanite, but by a "transport reaction", i.e. by means of an intermediary fluid phase. The development of the M II assemblage is the first response of the rocks to re-introduction of aqueous fluids after the metamorphic climax. A small drop in temperature at nearly constant pressure might have been sufficient to effectuate the growth of kyanite and hydrous phyllosilicates. M II is constrained by the kyanite-sillimanite phase boundary and reaction (3) which marks the dawn of M III. This implies that M II took place at temperatures of about 600-700°C (Fig. 6.6a), or slightly lower (See below).

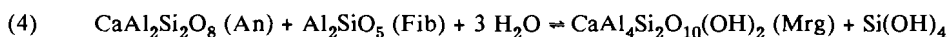
Rehydration progressed by the margaritization of plagioclase and kyanite during M III. As outlined above, margarite formed both in the host rock and in the M II kyanite-bearing veinlets. Textural relations of margarite with respect to corundum are different in both environments. In the host rock (M I assemblage), corundum remains unaffected or occurs as reaction relics within margarite aggregates. In the M II veinlets, corundum occurs, and was most likely formed together with margarite in cracks in kyanite. We will first discuss the reactions in the host rock (reactions 3-4), and subsequently consider the M II veinlets (reactions 5-8).

In the host rock, margarite may have been produced by the following reaction:



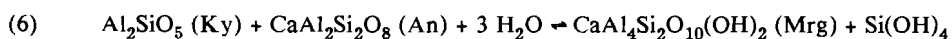
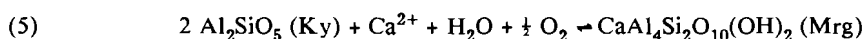
(Gibson 1979, Dymek 1983b). This reaction has been calibrated experimentally, and provides an upper temperature limit of c. 650°C at 7 kb (Chatterjee et al. 1984). However, in case of $P_{\text{H}_2\text{O}} < P_{\text{Total}}$, reaction (3) will be shifted to lower temperatures. The addition of Na to the CASH system will stabilize plagioclase over margarite (as indicated by Ca/(Ca+Na) ratios) and consequently also shift reaction (3) to lower temperatures. Cr is likely to favour corundum. Concluding, reaction (3) will in reality be situated at somewhat lower temperatures than its ideal position in the CASH system (Fig. 6.6a).

Another possible reaction resulting in the growth of margarite in the Froland rocks, which involves the consumption of plagioclase with fibrolite inclusions (which were already metastable as the rocks had passed into the kyanite field), may be reaction (4):

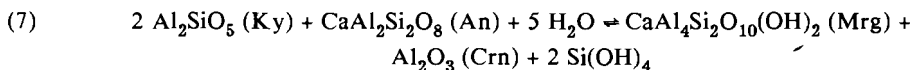


In this reaction, silica again has to be removed by a fluid phase. In a silica saturated environment, the reaction would occur between 3 and 7 kb ($P_{\text{Total}} = P_{\text{H}_2\text{O}}$) and in the temperature range 500-570°C (Chatterjee et al. 1984). Fibrolite is already metastable, which enhances the growth of margarite. The undersaturation of silica will also favour margarite, and shifts the reaction (4) to higher temperatures. This will be opposed, however, by the effect of Na.

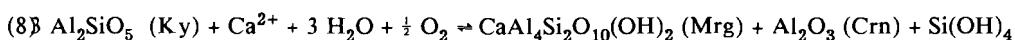
In the M II veinlets, margarite formed within cracks in kyanite. Retrograde reactions (5) (Guidotti et al. 1979, Cooper 1980, Feenstra 1985) and (6) (Yardley and Baltatzis 1985) have been proposed to explain the growth of margarite at the expense of kyanite in other rocks:



Quartz is not present in any of the Froland samples, which excludes the possibility of reaction (6), unless all silica has been removed by a fluid phase. Reaction (5) may have proceeded in the Froland rocks, but does not account for the occurrence of small grains of corundum in the centre of the margarite-filled cracks in kyanite. The latter also holds for (6). Therefore, other reactions have to be considered for the margaritization of kyanite. A possible reaction, involving the consumption of anorthite, is:



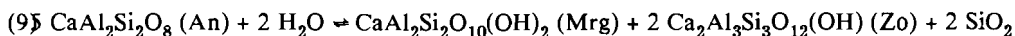
However, there is no textural evidence in the Froland rocks for the involvement of plagioclase in the breakdown of kyanite. Kyanite and plagioclase have not been found in contact with each other, but late scapolite (probably replacing plagioclase) has been found enclosing kyanite. This indicates that plagioclase and kyanite may have coexisted in the M II veins. The reaction may have taken place by a fluid phase:



To our knowledge, reactions producing margarite plus corundum out of aluminum silicates have not been reported until now. The only reaction published so far resulting in the growth of both minerals is: $8 \text{Dsp} + \text{PrI} + 2 \text{Cal} = 2 \text{Mrg} + \text{Crn} + 2 \text{CO}_2 + 3 \text{H}_2\text{O}$, occurring prograde in marbles (Okrusch et al. 1976).

Rosing et al. (1987) calculated equilibria between aqueous solutions and minerals in the CASH and NCFASH systems. Their $\log(a_{\text{Ca}^{2+}}/a_{\text{H}^+}^2)$ vs. temperature and $\log(a_{\text{SiO}_2(\text{aq})})$ vs. temperature diagrams show that margarite and corundum are stable with respect to anorthite and corundum below a maximum temperature of 583°C at $P_{\text{Total}} = P_{\text{H}_2\text{O}} = 5 \text{ kb}$, provided that the silica activity in the coexisting fluid is lower than 0.1. This temperature is in fair agreement with conditions for reaction (6) in the silica saturated system (Chatterjee et al. 1984). The stability of margarite plus corundum with respect to aluminum silicates depends entirely on the silica and lime saturation of the coexisting fluid. Moderately low $\log(a_{\text{SiO}_2(\text{aq})})$ and relatively high $\log(a_{\text{Ca}^{2+}}/a_{\text{H}^+}^2)$ stabilize the assemblage margarite plus corundum, whereas lower silica and higher Ca^{2+} activities favour the forming of clinozoisite / epidote plus corundum. Addition of Na and Fe to the systems tends to narrow the stability field of margarite plus corundum in favour of epidote plus corundum.

Margarite and an epidote group mineral have not been observed together, indicating that reaction (9) did not take place.



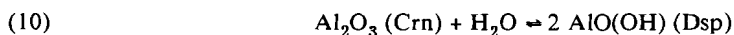
(Chatterjee et al. 1984). This constrains the lower temperature side of M III. The reaction line may slightly deviate from its ideal position. Addition of Na will stabilize plagioclase; regarding the anorthite-content of M I plagioclase (38-48%), this is likely to have occurred. $P_{\text{H}_2\text{O}} < P_{\text{Total}}$ will have the same effect. Addition of Fe to the CASH system will favour zoisite + margarite,

and, under silica-undersaturated conditions zoisite (epidote) over margarite.

6.4.4 Late stage cooling (M IV & M V)

The growth of M IV minerals, i.e. muscovite, new biotite, epidote etc. indicates adaptation to greenschist facies conditions. No mineral reactions could be deduced, so M IV is not well constrained. However, its P-T conditions are indicated by the following: 1). The new growth of biotite, indicating that the rocks were still in the biotite stability field, 2). The absence of diaspore, and 3). The nearby occurrence of late andalusite.

The absence of diaspore indicates that reaction (10) did not occur:



This constrains the lower temperature limit to 400°C. At $P_{\text{H}_2\text{O}} < P_{\text{Total}}$, reaction (10) will be shifted to lower temperatures.

Metapelites at Grimåsen (Fig. 6.1), in the direct vicinity of the Froland locality (c. 4.5 km) contain late blasts of andalusite and staurolite, which overgrow the old biotite foliation. Cordierite-orthoamphibole rocks from the nearby Bøylefoss locality (Fig. 6.1) contain both late stage andalusite and kyanite (Visser and Senior 1990). This indicates equilibration at or below the andalusite-kyanite join.

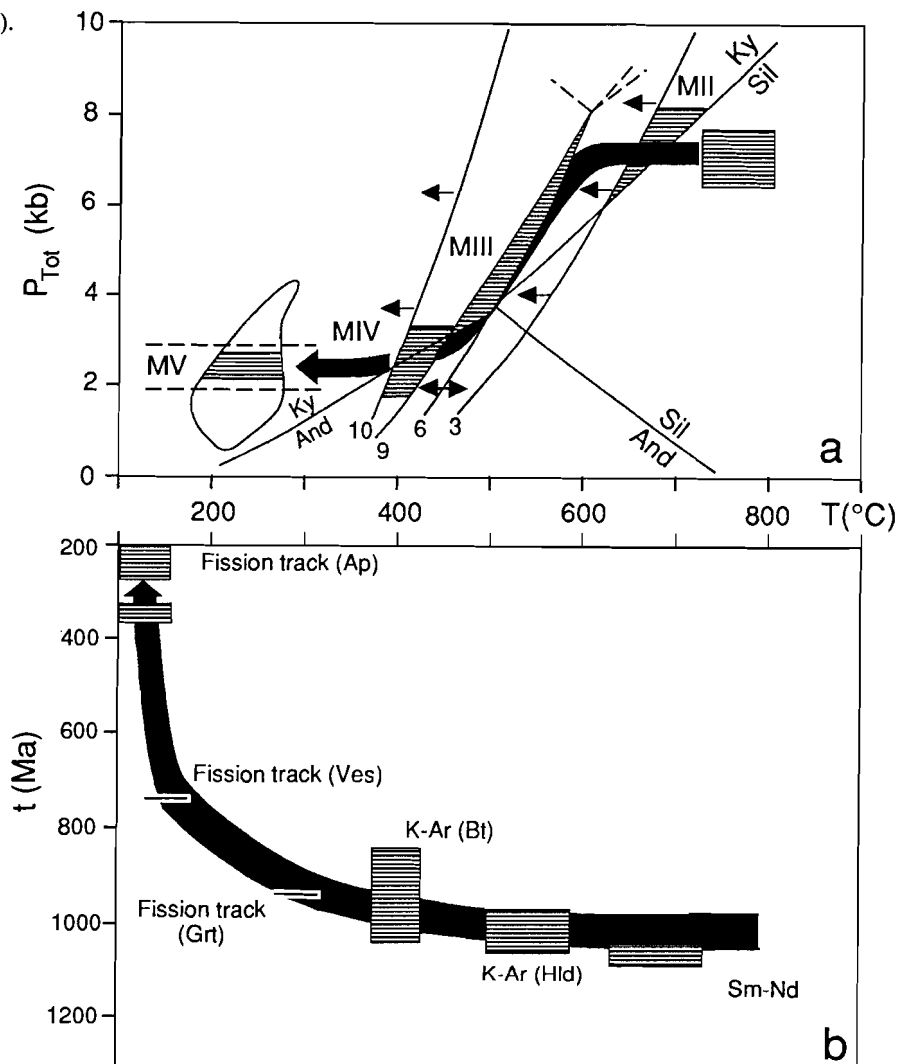
M V is constrained by the coexistence of prehnite and pumpellyite (Fig. 6.6a), which limits the temperature to 175–280°C and pressure from 0.5 to 4.5 kb (Frey et al. 1991). Pressure is more narrowly constrained to 2–3 kb by the fluid inclusion data of Touret and Olsen (1985), who observed that H₂O-rich inclusions were spatially associated with prehnite and pumpellyite. Growth of M V hydrous minerals like prehnite, pumpellyite, Cl-rich scapolite and tourmaline record the local influx of Cl- and B-bearing hydrous fluids.

6.4.5 Retrograde P-T path

The cooling and uplift path of the Froland rocks starts at M I, for which we adopt P-T estimates from the same area (Fig. 6.6a). To form the M II veinlets, while anorthite + corundum + vapour remain stable, limited cooling must have occurred. As discussed above, addition of Na and Cr to the CASH system will shift reaction (3) to lower temperatures than indicated in fig. 6.6a. The field of M II will have been larger, and the rocks may have experienced a slight uplift.

The formation of margarite from M II kyanite implicates that the rocks passed reaction line (6), which constrains the upper limit of M III. The lower temperature limit of M III is less well constrained. Reaction (9) has not been observed in the Froland rocks, but may be situated at slightly lower temperatures than indicated on fig. 6.6a.

Fig. 6.6 The cooling and uplift history of the Bamble Sector. **a** The P-T path as deduced from the Froland rocks. Mineral abbreviations are after Kretz (1983). Indicated are: the aluminum silicates after Holdaway (1971), the peak metamorphic P-T box after Nijland and Maijer (1992), the fields of metamorphic episodes M I-V, relevant reaction lines 3, 6, 9, and 10 as discussed in the text, the prehnite-pumpellyite facies field of Frey et al. (1991) with 2 and 3 kb isobars (See text). **b** The T-t path as constructed from separately published mineral ages. The T-t path was constructed with the mean \pm one sigma of the following published mineral ages (All data recalculated to current decay constants): Sm-Nd - Mineral ages of Kullerud and Dahlgren (1993). K-Ar (Hbl) - O'Nions et al. (1969a). K-Ar (Bt) - Kulp and Neumann (1961), O'Nions et al. (1969a), de Haas et al. (1992a). Fission tracks (Grt) and (Ves) - Haack (1975). Fission tracks (Ap) - Van Haren & Röhman (1988). The following closure temperatures were used: Sm-Nd (Grt) - Mezger et al. (1992). K-Ar (Hbl) - Harrison (1981). K-Ar (Bt) - Verschure et al. (1980). Fission tracks (Grt) and (Ves) - Haack (1977). Fission tracks (Ap) - Sharma et al. (1980).



The M IV stability field must have been along the andalusite-kyanite reaction line (Fig. 6.6a). Its upper temperature limit is constrained by the lower limit of M III. The M V stability field is well constrained by the occurrence of prehnite + pumpellyite (Fig. 6.6a). However, rocks from the alteration zone contain an overwhelming amount of prehnite with respect to pumpellyite. Therefore, it is likely that M V started at slightly higher temperatures than those of the prehnite-pumpellyite facies.

Summarizing, the retrograde P-T path (Fig. 6.6a) starts with near isobaric cooling (M I-II), followed by near isothermal decompression (M III), and is concluded by slight decompression during cooling from greenschist to prehnite-pumpellyite facies conditions (M IV-V). From the discussion above, however, it appears that especially the latest stages indicate gradual changes rather than discrete episodes.

The first part of the deduced retrograde P-T path (Fig. 6.6a) essentially confirms the paths proposed by Touret and Olsen (1985) and Visser and Senior (1990). However, the stability fields of the margarite-bearing assemblages require a P_{H_2O} considerably higher than the $\frac{1}{2}P_{Total}$ suggested by Visser and Senior (1990) for the same metamorphic stage (their M4). The retrograde P-T path of the Froland rocks also agrees with the cooling path of the Modum Complex of the Kongsberg Sector (Munz 1990), which at that time may have constituted one continuous terrain with the Bamble Sector (Bugge 1936, Starmer 1985a). A small increase in pressure between M I and M II, as suggested in the Modum Complex, is not found in the Bamble Sector.

6.5

Time constraints

M I in the Froland rocks is most likely equivalent to the M 3b of Visser and Senior (1990), which is the thermal climax of their prograde P-T path, and the sole sillimanite producing stage in their rocks. These authors considered this stage to be related to Gothian continental collision. This interpretation may be supported by the fact that sillimanite occurs in the foliation cut by the basic intrusions of the Jämmåsknutene Gabbro (Fig. 6.1), which have been dated at 1766 ± 190 Ma (Sm-Nd whole rock, de Haas et al. 1993a).

However, Kullerud and Dahlgren (1992) recently obtained Sm-Nd mineral ages between 1068 and 1107 Ma for granulite facies assemblages near Arendal. Sm-Nd mineral isotopic systems are still poorly understood, and blocking temperatures not defined for most minerals. Recently, Mezger et al. (1992) concluded that the blocking temperature of granulite facies garnets is ca. $600 \pm 30^\circ\text{C}$ for the Sm-Nd system. This is ca. 150°C below our peak metamorphic conditions, and would reflect M II rather than M I temperatures. Consequently, M I will have occurred during or before the Early Sveconorwegian.

Early Sveconorwegian gabbroic intrusions in the Froland area (1.2 ± 0.1 Ga, Sm-Nd whole rock + minerals; de Haas et al. 1992a) still enjoyed amphibolite facies metamorphism (de Haas et al. 1992b). Garnet-hornblende thermometry yields temperatures of ca. 720°C for this metamorphism (G.J.L.M. de Haas pers. com. 1991), indicating that high temperature conditions prevailed at this time. Therefore, the onset of cooling is likely to be Early to Mid

Sveconorwegian (Fig. 6.6b). The end of uplift (Fig. 6.6b) is constrained by K-Ar biotite cooling ages that average 940 Ma (Kulp and Neumann 1961, O'Nions et al. 1969a, de Haas et al. 1992a).

The timing of the latest metamorphic phase, M V, is less evident. Prehnite, pumpellyite and scapolite are also present in several post-tectonic microdolerite dikes in the area, and have been reported from other rocks as well (e.g. Field and Rodwell 1968). The dikes are generally considered to be of Permian age, but may partly be contemporaneous with basic dike swarms in the Rogaland Sector, that were dated by Sundvoll (1990) as Late Proterozoic. Preliminary results from radiometric studies in the Arendal area seem to confirm this (M.M. Moree pers. com. 1992). Correlation of M V with Caledonian activity (Verschure 1982) is unlikely because of the large distance from the Caledonian front. Sauter et al. (1983) suggest that the growth of prehnite was due to Permian thermal disturbance. Available fission track ages from the Bamble Sector are illustrated in fig. 6.6b. Apatite fission track ages c. 240 Ma (van Haren and Röhrman 1988) indicate that temperatures were too low to produce prehnite and pumpellyite during the Permian. Haack (1975) obtained fission track ages on garnet (924 Ma) and vesuvianite (761 Ma) from the Arendal skarns. Andriessen (pers. com. 1991) obtained slightly younger ages for garnet (c. 900 Ma) and slightly older ages for vesuvianite. Both mineral ages suffer from not well established annealing temperatures (P.A.M. Andriessen pers. com. 1991). Haack (1977) estimated annealing temperatures of 135-155°C and 280-300°C for vesuvianite and garnet, respectively, although the latter may actually be a little too low. This indicates that M V, which equilibrated between 175 and 280°C, should have equilibrated between c. 760 and 920 Ma.

6.6

Tectonic history

The combined P-T and T-t paths show that after 1150 Ma the Sveconorwegian was dominantly a cooling and uplift event. The slow uplift points to prolonged residence at lower crustal levels after M I, and indicates a crust thickened by overthrusting, probably with magmatic addition and slow erosion. Evidence for magmatic addition is provided by the evolution of gabbroic intrusions perforating this crust (Frost et al. 1989, de Haas et al. 1992b, 1993a).

The drop in pressure after initial cooling, reflected by the M III and M IV, represents upthrusting of the Bamble Sector, probably accompanied by erosion or tectonic unroofing. The intrusion of undeformed granites between 990-950 Ma throughout the Southwest Scandinavian Domain (Priem et al. 1973, Pedersen and Maaløe 1990, Kullerud and Machado 1991; among others) and slightly younger K-Ar biotite cooling ages of 940 Ma (Kulp and Neumann 1961, O'Nions et al. 1969a, de Haas et al. 1992b) indicate that the process of upthrusting was completed before this time. Sveconorwegian upward movement is likely to have occurred along deeply penetrating, low-angle, shear zones. The imbricated structure of the Sveconorwegian terrain in southern Norway is not as clearly demonstrated as in SW Sweden (Eugeno-S Working Group 1988, Park et al. 1991), but the deep, gently dipping, seismic reflectors cutting the

Moho below southern Norway and the Skagerrak (Husebye et al. 1988, Lie et al. 1990, Pedersen et al. 1990, Kinck et al. 1991) may be remnants of the zones along which upthrusting occurred. After upthrusting, the formerly lower crustal rocks adapted to their new upper crustal environment. Therefore, M V was probably not related to a separate thermal event, but just reflects the adaptation of lower crustal rocks at their new upper crustal environment.

Acknowledgements - R.P.E. Poorter and T. Bouten assisted in the microprobe analyses. J.B.H. Jansen and G.J.L.M. de Haas critically read earlier versions of this paper. Blakstad Yrkesskole provided lodging during field work. This study was made possible by financial support of AWON (NWO grant 751-353-023, TGN). The paper benefitted from the constructive reviews by I.A. Munz and an anonymous reviewer.

**NATURE AND HEAT SOURCE OF METAMORPHISM IN THE BAMBLE SECTOR,
SOUTH NORWAY, AND IMPLICATIONS FOR THE GEODYNAMIC EVOLUTION OF
THE SOUTHWEST SCANDINAVIAN DOMAIN.**

This paper evaluates the constraints on regional granulite facies metamorphism in the Bamble Sector, South Norway, in order to clarify its nature and to try to identify its heat source. Subsequently, the implications for the geodynamic evolution of this part of the Baltic Shield will be discussed. Together, all terranes that were affected by metamorphism, deformation and magmatism during the Gothian and Sveconorwegian orogenies will be termed the **Southwest Scandinavian Orogen**.

7.1 Nature and heat source of metamorphism in Bamble

Dispelling the "myth" of high grade Sveconorwegian metamorphism by Field and coworkers (Field and Råheim 1979, 1980, Field et al. 1985) gave rise to the so-called "Grenville Controversy", i.e. the question whether one or two high grade metamorphic events were responsible for the presently observed metamorphic features of the Precambrian terrain in southern Norway. Whereas in the most western segment of the Southwest Scandinavian Orogen (Rogaland / Vest-Agder Sector) the answer to this question was given almost immediately (Weis and Demaiffe 1983), the controversy had a longer life in the Bamble Sector. Several authors indicated high grade metamorphic conditions for the Bamble Sector during the Sveconorwegian Orogeny (Hagelia 1989, Kullerud and Dahlgren 1990), but questioned the nature of the Gothian orogeny. Recently, it has been shown that both the Gothian and Sveconorwegian orogenies involved medium to high grade metamorphism (Starmer 1990a, 1991, Kullerud and Machado 1991, Nijland and Senior 1991, Nijland et al. 1991). This evolution, involving two major metamorphic episodes, is rather similar to the evolution of the Østfold-Stora Le-Marstrand segment in SE Norway - SW Sweden (Park et al. 1987).

Both the Gothian and Sveconorwegian orogenies were major events in the evolution of the Southwest Scandinavian Domain, and involved major phases of gabbroic and tonalitic/enderbitic magmatism in the Bamble (Verschure 1985, Field et al. 1985, de Haas and Verschure 1990, de Haas et al. 1993a) and Østfold-Stora Le-Marstrand Sectors (Park et al. 1987, Åhäll et al. 1990). Alkaline granitic-monzonitic magmatism occurred at the onset of the Sveconorwegian Orogeny in the Bamble and Telemark Sectors (Smalley et al. 1983b, 1988,

Hagelia 1989). This magmatism also affected older terrains that were not directly involved in the metamorphic–deformational events in the Southwest Scandinavian Domain (e.g. southern Sweden; Johansson 1990).

Although medium to high grade metamorphism occurred during both orogenies, granulites in the area around Arendal show evidence for only one granulite facies event. Recent Sm–Nd mineral age determinations on granulite facies assemblages (Kullerud and Dahlgren 1990, 1993, J. Kihle pers. com. 1991) and U–Pb age determinations of overgrowths on zircon in granulite facies rocks (Kullerud and Machado 1991) indicate closure of these systems at c. 1.15–1.10 Ga. This is significantly older than closure of isotopic systems after granulite facies metamorphism in the more western (0.97 Ga, Rogaland / Vest-Agder Sector; Maijer et al. 1981) and eastern (0.91 Ga, Protogine Zone, SW Sweden; Johansson et al. 1991) segments of the Southwest Scandinavian Orogen. The onset of the peak thermal metamorphism in the Arendal area is unclear. It may have started during the late Gothian Orogeny, as claimed by Visser and Senior (1990), but this would require an unrealistically long period of elevated heat flows. Certainly, no new, prograde metamorphic event affected the area after 1.15 Ga. Therefore the observations on metamorphism in the Bamble Sector discussed below, are considered to be related to this granulite facies event.

The following observations serve to constrain a model for the regional transition from amphibolite to granulite facies metamorphism in the Nelaug–Arendal area:

- (1) A roughly southeast–northwest temperature gradient existed over the amphibolite to granulite facies transition zone in the Nelaug–Arendal area (Nijland and Maijer 1992, 1993, ch. 3).
- (2) In contrast to traditional views, the peak thermal area was not situated on Tromøy and Hisøy, but on the mainland around Arendal (Nijland and Maijer 1992, 1993, ch. 3).
- (3) Different thermal regimes existed in the Tromøy–Merdøy and the Hisøy granulite facies areas (ch. 5).
- (4) Pressure estimates do not show clear gradients (Nijland and Maijer 1992, 1993, ch. 3), but amphibole chemistry indicates higher pressures toward the northeast (Kragerø) and possibly west (Hisøy), with lower temperatures (ch. 5).
- (5) Granulite facies assemblages indicate an essentially static type of metamorphism (ch. 3).
- (6) The majority of mylonitic deformation is situated at the margin of the Bamble Sector (Nijland and Senior 1991, Nijland and Maijer 1992, 1993, ch. 2 and 3).
- (7) No pervasive fluid flow occurred during granulite facies metamorphism, and different lithologies did not communicate (Touret 1985, Nijland et al. 1992b, 1993b, Broekmans et al. 1992, 1993, ch. 4 and 5).
- (8) Cooling after peak metamorphism was almost isobaric (Touret and Olsen 1985, Visser and Senior 1990, Nijland et al. 1993a, ch. 6).

Based on the structural trend and isograd pattern in the Bamble Sector, and (1), (2) and (5), Nijland and Maijer (1992, 1993, ch. 3) have tentatively suggested that granulite facies metamorphism in the area was related to thermal doming. As this hypothesis already fulfils

three constraints, it will be adopted here, and checked against the other constraints.

In case of a thermal dome, the Nelaug-Arendal section would essentially reflect the distance of the amphibolite and granulite facies areas to an elevated mantle, as heat source of the dome. Therefore it might be envisaged that the Nelaug-Arendal section is essentially a vertical crustal section. However, sedimentary structures in the area univocally indicate one

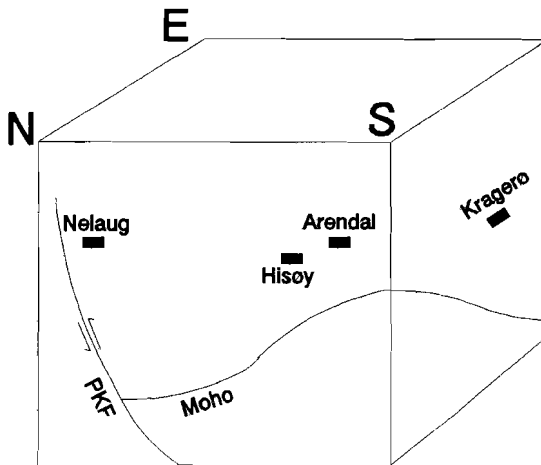


Fig. 7.1 Schematic positions of the different thermal areas in the central part of the Bamble Sector with respect to the elevated asthenosphere.

single younging direction (T.G. Nijland and C. Maijer unpubl. data, P. Padget pers. com. 1991). The younging direction is the same as the upward direction of small layered magma chambers like the Flosta Gabbro (de Haas et al. 1993b). All point to the southeast. Hence a vertical section would require a rotation of almost 180° of the sedimentary-magmatic pile before the peak of thermal metamorphism with respect to its original Gothian position. In addition, geobarometric estimates do not indicate the difference in pressure that would be the result of lithostatic pressure in case of a vertical section (Nijland and Maijer 1992, 1993, ch. 3). A (sub) horizontal section seems to be more probable.

Amphibole chemistry (4) indicates slightly higher pressures but lower temperatures in the east (Kragerø) and on Hisøy. This may be explained by a position further away from the centre of the dome, inherent with lower temperatures, but slightly deeper in the crust, which explains the slightly higher lithostatic pressures (Fig. 7.1). It may be objected that Hisøy, Tromøy and the mainland around Arendal are too near to each other to make the above explanation likely in the case of Hisøy. However, it should be reminded that these three areas are separated by faults (Lamb 1981b, Starmer 1985b).

The nature of the amphibolite to granulite facies transition in the Nelaug- Arendal

geothermometry on samples from the granulite facies areas only, led Lamb et al. (1986) to propose that no temperature gradient exists, and that the transition was entirely due to a flushing of carbon dioxide. Since, the Bamble Sector has been viewed as an example characteristic of this type of metamorphism (e.g. Newton 1990). The established temperature gradient (Nijland and Maijer 1992, 1993, ch. 3 and 5) shows the hypothesis of Lamb et al. (1986) to be invalid. The established temperature gradient is not the only argument against that hypothesis. Touret (1985) concluded that no pervasive fluid flow existed. Recent stable isotopic data (Broekmans et al. 1992, 1993, Van den Kerkhof et al. 1992) and data on halogen geochemistry (Nijland et al. 1992b, 1993b, ch. 4) indicate very limited (sub hand specimen scale) scale of fluid control. This makes heating through circulation of a fluid improbable, regardless its composition.

The origin of the carbon dioxide - rich fluid that should have caused the granulitization is still disputed. Recently, Van den Kerkhof et al. (1992) proposed that the CO₂ was introduced together with charno-enderbitic magmas in the Tromøy-Arendal area. The magmatic nature of these rock is however disputable (e.g. Moine et al. 1972, Visser et al. 1991). Recent U-Pb zircon ages for these rocks vary from 1.59 ± 0.01 Ga on Tromøy (Råheim unpubl. data in Lamb et al. 1986) to 1.54 ± 0.01 Ga on Flostå (Kullerud and Machado 1991). Rb-Sr whole rock ages of c. 1.54 and accompanying low Sr_i of 0.703 indicate that at least some of these rocks intruded during the Gothian (Field and Råheim 1979, 1980, Field et al. 1985). It has been shown above, that the onset of granulite facies metamorphism is unknown, but that it ceased at c. 1.15 Ga. So, any hypothesis that considers the charno-enderbitic carbon dioxide as direct cause of the granulite facies metamorphism, implies that it lasted for 400 million years. However, even if this was not the case, the presence of this carbon dioxide will have facilitated subsequent granulitization enormously.

From the above considerations, it may be concluded that fluids alone are an improbable heat source during granulite facies metamorphism in the Nelaug-Arendal area. An alternative heat source that has been invoked to explain granulite facies metamorphism, is underplating of basic magmas, which has been proposed to play a role in the Bamble Sector (Touret 1969, Visser and Senior 1990). It might be expected that such a basic layer ponding below the crust would be detected by geophysical methods. Neither gravity observations (Smithson 1963, Ramberg et al. 1978), nor extensive recent deep seismic profiling in the Skagerrak (Husebye et al. 1988, Pedersen et al. 1990, Lie et al. 1990, Lie and Husebye 1991, Kinck et al. 1991, Larson and Husebye 1991), indicate the presence of such a layer. However, the evolution of gabbroic intrusions provides some evidence for this hypothesis (de Haas 1992), and the many small intrusions will certainly have increased the heat budget. In addition, elevation of the asthenosphere resulting in thermal doming and magma generation may provide a heat source of metamorphism.

Mylonitic deformation was concentrated at the margin of the Bamble Sector (6). Seismic studies (Lie and Husebye 1991) indicate that some of these structures continue into the mantle, and offset the Moho. The major alkaline augen gneiss complexes, the Hovdefjell-Vegårshei Augen Gneiss, the Gjerstad Augen Gneiss and the Morkheia Monzonite Suite, intruded this mylonitic zone. Although their exact age may be disputed (cf. Nijland and Senior 1991), an age around 1.25 Ga is most likely (Smalley et al. 1983b, 1988). This implies that

mylonitic deformation at the margin of the Bamble Sector can not have been caused by collapse of the dome due to thermally induced gravitational instability (cf. Sandiford and Powell 1986), as the thermal regime evidently lasted until 1.15 Ga. Alternatively, these structures might have originated during the formation of the dome. In that case, the dome would have come into existence at c. 1.3 - 1.25 Ga.

It might be expected that formation of the dome would result in the sliding of crustal slices off its flanks. In this case, mylonitic zones might occur parallel to the flanks of the dome. It follows from the positioning of the dome as depicted in fig. 7.1, that the mylonitic zone at its northern flank would dip away from the Bamble Sector. However, the Kristiansand-Bang Shear Zone dips toward the dome, in stead of away from it. Therefore, it remains unclear how these structures were related to the formation of the dome.

7.2 The Bamble Sector in relation to the geodynamic evolution of the Southwest Scandinavian Domain

Attempts to unveil the geodynamic evolution of southern Scandinavia have led to the speculative location of subduction and continental collision zones at the sites of almost all major tectonic lines in this part of the Baltic Shield. Often, the inferred geodynamic nature of an event was only based on whole rock chemistry of a few intrusions.

The Southwest Scandinavian Domain has been extensively imbricated. This holds especially for the area east of the Oslo Rift. Going from east to west, this area is segmented by the following tectonic lineaments: 1) the Protogine Zone (Sveconorwegian Front, Schistosity Zone, Gothian Front, Småland Suture), which separates the Southwest Scandinavian Domain from the Svecofennian craton and the Transscandinavian Igneous Belt, 2) the Mylonite Zone, and 3) the aligning Dalsland Boundary Thrust - Lerdal Zone - Göta Älv Zone (Gorbatschev 1980, 1988, Park et al. 1991). These north-south trending thrust zones are truncated by the Phanerozoic Tornquist-Teisseyre Line (Zwart and Dornsiepen 1978). To a lesser extent, the western part of the Southwest Scandinavian Domain is also imbricated. Here, the major thrust zone is the Kristiansand-Bang Shear Zone (Great Friction Breccia, Porsgrunn-Kristiansand Fault, Saggrenda-Prestfoss Mylonite Zone, Prestfoss-Sokna Mylonite Zone; Bugge 1928, Starmer 1985ab). A second smaller zone, the Hokksund-Solumsmo Mylonite Zone, has been mapped in the Kongsberg Sector (Starmer 1980). The nature of the roughly north-south trending Mandal-Ustaoset Line (Sigmond 1985) is still disputed, but it coincides with several faulted zones on the Mandel (Falkum 1982) and Sauda (Sigmond 1978) map sheets. At least some of the shear zones in South Norway were already operative as early as 1.6 Ga (Starmer 1985a). The most important tectonic lineaments are shown in fig. 7.2.

Palaeomagnetic data indicate that during Sveconorwegian times, Scotland was positioned northwest of Stavanger (e.g. Poorter 1981, Pesonen and Torsvik 1990). Therefore, Scotland - Rogaland / Vest-Agder - Telemark - Bamble may represent one lateral sequence, albeit not necessarily at the same crustal levels. The relation with the Østfold-Stora Le-Marstrand Sector is less clear.

Models for the geodynamic evolution of the Southwest Scandinavian Domain often implicated that the present imbricated sequence was identical to the original west-east sequence (e.g. Berthelsen 1980, 1987). This however, poses many problems. For example, how could the Bamble Sector and the Østfold-Stora Le-Marstrand Sector be in similar plate tectonic positions at the onset of Gothian subduction, as is indicated by recent age determinations, if they were arranged behind each other (cf. de Haas 1992)? An alternative hypothesis

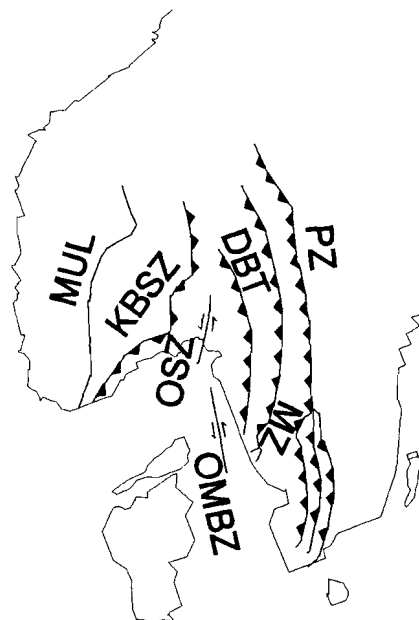


Fig. 7.2 Most important tectonic lineaments in the Southwest Scandinavian Domain. MUL: Mandal-Ustaoet Line. KBSZ: Kristiansand-Bang Shear Zone. OSZ: Oslofjord Shear Zone. OMBZ: Østfold-Marstrand Boundary Zone. DBT: Dalsland Boundary Thrust (and aligning Lerdal Zone and Göta Alv Zone). MZ: Mylonite Zone. PZ: Protogine Zone. For discussion and references, see text.

maintains that the imbricated sequence west of the Oslo Rift was originally the northern analog of the sequence nowadays situated east of the Oslo Rift, that was sinistrally displaced southwards along north-south trending shear zones during the Sveconorwegian (Torske 1985, Park et al. 1991). These shear zones may have been the aligning Østfold-Marstrand Boundary zone (Park et al. 1991) - Oslofjord Shear Zone (Hageskov 1978) - Nesodden Fault (Swensson 1990). Evidence that such a mechanism may be operative in the assemblage of orogens has recently been demonstrated in the Canadian Cordillera (Umhoefer 1987, Samson and Patchett 1991). This latter hypothesis is the basis of the following reconstruction.

7.2.1 Pre-Gothian to Early Gothian (1.7 Ga): Deposition and subduction

The oldest geological event in the entire Southwest Scandinavian Domain is the deposition of the various supracrustal suites. Indications for the depositional ages are often conflicting. Deposition of the Rjukan Group in Telemark occurred between 1.6 and 1.5 Ga (Priem et al. 1973, Dahlgren et al. 1990, Dahlgren and Heaman 1991), and evidently before 1.5 Ga, when they were intruded by porphyries (S. Dahlgren pers. com. 1990, cf. Dahlgren et al. 1990). Pasteels and Michot (1975) indicated similar ages for some of the Rogaland / Vest-Agder supracrustals, and Weis (1986) concluded from extensive Pb-Pb studies that no rocks older than 1.5 Ga exist. However, Sm-Nd systematics led Menuge (1988) to the conclusion that crustal accretion may have started as early as 1.85 Ga.

In the basement of the Bergen Arc / Hardanger-Ryfylke, the Kvitenuit granitoids were emplaced at 1.61 Ga (Andresen et al. 1974), and deposition of supracrustals consequently occurred earlier. In the Bamble Sector, several supracrustal suites, among them the continental Nidelva Quartzite Complex (Nijland and Maijer 1991, Nijland et al. 1992a) and the flysch like Selås Banded Gneisses (Touret 1966) were deposited before 1.77 - 1.64 Ga, at which time they were intruded by gabbroic intrusions (de Haas and Verschure 1990, de Haas et al. 1993a). However, it can not be precluded that the real age of deposition was more or less equal to that in the Telemark and Rogaland / Vest-Agder Sectors, because of the large error of c. 0.2 Ga in the gabbro ages. But at about the same age, 1.76 ± 0.08 Ga, a subduction related supracrustal suite was deposited in the southern segment of the Southwest Scandinavian Orogen, the Østfold-Stora Le-Marstrand Sector (Åhäll and Daly 1989), and O'Nions and Heier (1972) obtained a 1.76 Ga Rb-Sr whole rock reference isochron for the metasedimentary-metavolcanic rocks of the Knute and Håv Groups in Kongsberg.

Hence it is concluded that subduction related supracrustal suites were deposited between c. 1.75 and 1.7 Ga in Bamble and Østfold-Stora Le-Marstrand, and possibly in the Bergen Arc / Hardanger-Ryfylke (Fig. 7.3). In Bamble, the relation between this suite (the Selås Banded Gneisses) and the continental suite is unclear. But as both rocks underwent metamorphism after this time, it is tentatively suggested that the Nidelva Quartzite Complex was deposited before the Selås Banded Gneisses. This would imply that in the Southwest Scandinavian Domain, continental crust was partially formed before c. 1.75 Ga, which conflicts with earlier assumptions that pre-Gothian continental crust existed nowhere in southern Norway (e.g. Jacobsen and Heier 1978, Falkum 1985). Torske (1976) also proposed the presence of reworked pre-Gothian crust in the Southwest Scandinavian Orogen. Åmål tonalites near Stora Busjön in the Swedish part of the Southwest Scandinavian Orogen contain xenoliths of a polymict conglomerate of possibly 2.0 Ga (Wahlgren 1981), supporting the idea of older crust.

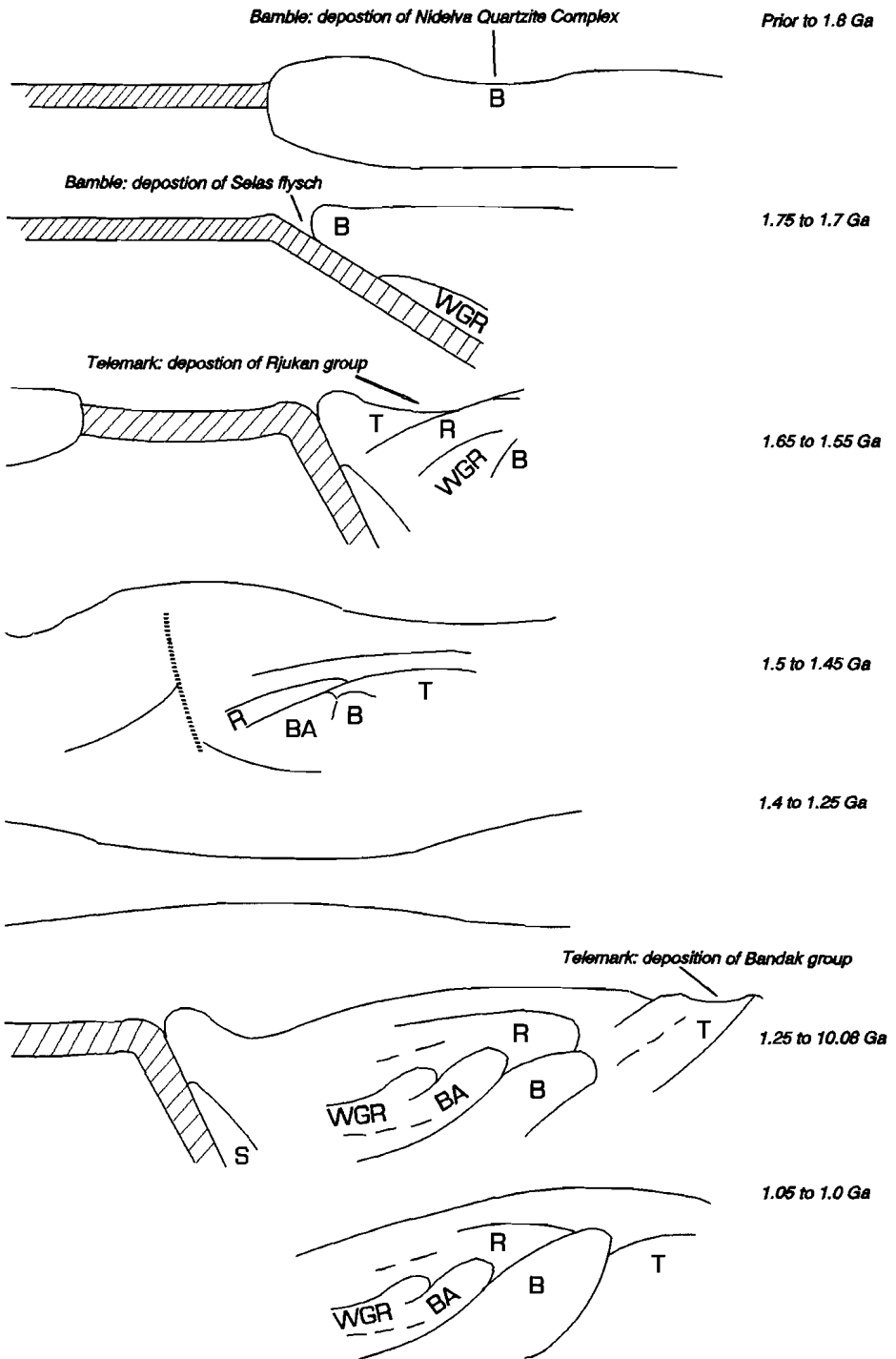


Fig. 7.3 Simplified cartoon of the geodynamic evolution of the northern part of the Southwest Scandinavian Orogen. Ages are in Ga. Schematic P-T paths are shown for Bamble and Rogaland. Sectors - B: Bamble. BA: Bergen Arc/Hardanger-Ryfylke. R: Rogaland. S: Scotland. T: Telemark. WGR: Western Gneiss Region.

Early Gothian subduction probably involved oceanic crust, as indicated by the presence of pillow lavas in the southern part of the subduction belt (Østfold-Stora Le-Marstrand; Åhäll 1984). Ongoing subduction resulted in the transfer of the Western Gneiss Region, Bergen Arc / Hardanger-Ryfylke, Bamble, and Østfold-Stora Le-Marstrand Sectors in the south to deeper crustal levels. The subduction zone was probably situated to the present west of the Western Gneiss Region, as eclogite facies assemblages developed in this segment (Not to be confused with younger Caledonian eclogite facies assemblages in the same rocks; Jamtveit et al. 1991), and mantle peridotite slices were emplaced in the Western Gneiss Region (Mearns 1986).

7.2.2 Mid to Late Gothian (c. 1.7-1.5 Ga): Metamorphism below and deposition above

In the deeper seated segments, extensive magmatism and metamorphism occurred. In the southern part of the belt, Åmål granitoids and the Tjörn tonalite were emplaced in the Østfold-Stora Le-Marstrand Sector between 1.7 - 1.65 Ga (Welin and Gorbatshev 1978, Welin et al. 1982, Hansen et al. 1989), followed by calc-alkaline and trondheimitic rocks between 1.57 - 1.55 Ga and gabbros around 1.51 Ga (Åhäll et al. 1990). During this period amphibolite facies metamorphism occurred.

In the northern part of the belt, between 1.6 and 1.5 Ga, intrusion of granitoid magmas, migmatization and amphibolite facies metamorphism occurred in the Western Gneiss Region (Gorbatshev 1985). In Bamble, granodioritic-tonalitic magmas were emplaced between 1.58-1.54 Ga (Field and Råheim 1979, 1980, Råheim unpubl. data in Lamb et al. 1986, Kullerud and Machado 1991), and amphibolite facies metamorphism, involving wide spread migmatization (Nijland and Senior 1991) occurred possibly between 1.5 and 1.45 Ga (Kullerud and Machado 1991). The Rogaland / Vest-Agder and Telemark Sectors were obviously situated in the upper crust during this time (Fig. 7.2), as various supracrustal suites were deposited in this period (See above).

7.2.3 Late to Post Gothian (c. 1.5-1.45 Ga): Metamorphism in sunken upper crustal segments

The segments that formed part of the upper crust during the Mid to Late Gothian, were transferred to lower levels during the Late Gothian, and metamorphosed (Fig. 7.3). Migmatization and formation of anatectic granites occurred in the Rogaland / Vest-Agder Sector between 1.48 and 1.42 Ga (Pasteels and Michot 1975, Van der Wel unpubl. data in

Sigmond (1978), Verstevee 1975). In the crustal segments that were already deep seated, metamorphism and anatexis continued to 1.45–1.44 Ga (respectively Bamble (Kullerud and Machado 1991) and Bergen Arc / Hardanger-Ryfylke (Gorbatshev 1985)).

7.2.4 Gothian - Sveconorwegian Interlude (c. 1.45-1.2 Ga)

The period between 1.45 to 1.2 Ga is the "Dark Middle Age" in the evolution of the Southwest Scandinavian Domain. In several segments (e.g. Bamble), there is no evidence that they were uplifted during this period; other crustal segments were certainly uplifted during this period (e.g. Telemark and Østfold-Stora Le-Marstrand), as supracrustal rocks were deposited here during the Early Sveconorwegian (See below). Rifting is likely to have attempted during this interval, and may have been responsible for the emplacement of lherzolitic rock that in the Bamble Sector are discordant with respect to the main foliation, but have been metamorphosed. Paleomagnetic evidence demonstrates that the plate tectonic drift velocity was enormously increased (Pesonen and Torsvik 1990), which fits better in an extensional than a compressional tectonic regime. In the Østfold-Stora Le-Marstrand Sector, elaborate emplacement of dykes occurred at 1.42 (Koster-Kattsund dyke swarm; Hageskov and Pedersen 1988) and 1.22 Ga (Orust dykes; Daly et al. 1983). Chemistry of the 1.22 Ga Central Swedish Dolerites may be interpreted as related to continental break-up (Solyom et al. 1992). During this interlude, tholeiitic dykes swarms also intruded the North American continuation of the Southwest Scandinavian Orogen (e.g. Emslie et al. 1983).

Intrusions with anorogenic affinities, like alkaline granitic-charnockitic-monzonitic suites in Bamble and syenites in Rogaland / Vest-Agder, were emplaced at c. 1.25 Ga (Smalley et al. 1983b, 1988, Field et al. 1985) and 1.2 Ga (Wielens et al. 1980) respectively. Granitic intrusion also occurred in this southern part of the belt (Østfold-Stora Le-Marstrand; Åhäll et al. 1990). Gabbroic magmas were emplaced between 1.3 and 1.2 Ga in the Western Gneiss Region (Mearns 1984, Mørk and Mearns 1986). Gower (1990) interpreted anorogenic magmatism during this interlude in both Laurentia and Baltica to be rift related. The alkaline magmatism in the North Atlantic region has been considered as indicative of wide spread continental fracturing (Patchett 1978).

7.2.5 in Sveconorwegian (c. 1.2-1.0 Ga): renewed subduction, deposition and metamorphism.

At the onset of the Sveconorwegian, the Telemark Sector in the northern segment of the Southwest Scandinavian Orogen and the Østfold-Stora Le-Marstrand Sector in its southern segment were situated in the upper crust, as the Bandak and Dalsland supracrustals were deposited at c. 1.16 (Dahlgren and Heaman 1991) and 1.2 Ga (Zeck and Hansen 1988) respectively (Fig. 7.3). It is noteworthy, that events in the northern segments (southern

Norway) of the Southwest Scandinavian Orogen seem consequently 0.04 to 0.05 Ga delayed with respect to the southern segment of the Southwest Scandinavian Orogen (Østfold-Stora Le-Marstrand).

The main evidence for renewed subduction is found in northern Scotland (Fig. 7.3), which indicates that the subduction zone was again situated in the present day west. Here, eclogites were formed (16.5 kb, 730°C; Sanders 1989), whose Sm–Nd system closed at 1.08 Ga (Sanders et al. 1984). These eclogites were uplifted before 1.0 Ga, because the Moines sediments were deposited on the eclogites at that time (Brewer et al. 1979, Sanders 1989). Related to this subduction, metamorphism and reworking also occurred in other segments. Telemark in the north and Østfold-Stora Le-Marstrand in the south were transferred to deeper crustal levels. Telemark was intruded by gabbroic magmas at 1.15 Ga (Dahlgren and Heaman 1991), and metamorphosed under greenschist to amphibolite facies conditions between 1.12 and 1.03 Ga (Pedersen 1981). Around 1.09 Ga, amphibolite facies metamorphism also occurred in the Østfold-Stora Le-Marstrand (Daly et al. 1983).

In Rogaland / Vest-Agder, no evidence exists that this segment was entirely uplifted, but it was situated relatively high in the crust, as metamorphism was essentially of low pressure (Tobi et al. 1985, Jansen et al. 1985). At 1.04 Ga, alkaline augen gneisses were emplaced (Bingen et al. 1990), and between 1.04 and 0.99 Ga, HT-LP metamorphism related to the emplacement of the Egersund-Ogna anorthosite and Bjerkreim-Sokndal lopolith occurred (Wielens et al. 1980, Maijer et al. 1981).

Deeper in the crust, metamorphism also occurred. As argued above, granulite facies metamorphism in Bamble ceased at 1.15 Ga. Amphibolite facies conditions prevailed until c. 1.05 Ga. Metamorphism was accompanied by gabbroic magmatism (Jacobsen and Heier 1978, Dahlgren et al. 1990, Munz and Mørvik 1991, de Haas et al. 1992ab, 1993a). In the Western Gneiss Region, isotopic systems were disturbed at 1.04 Ga, probably due to metamorphism (Mearns 1986). This metamorphism may have been related to thermal doming (Fig. 7.3). After the dome ceased to be active, the South Norwegian segments maintained their crustal position for some time, as the uplift paths for most segments are initially isobaric until c. 1.03 Ga (Rietmeijer 1984, Touret and Olsen 1985, Visser and Senior 1990, Munz 1990, Nijland et al. 1993a, ch. 6). At this time, ultrapotassic magmatism occurred in Bamble (Dahlgren 1991). In the Bergen Arc / Hardanger-Ryfylke, granulite facies metamorphism continued until 0.91 Ga (Cohen et al. 1988).

7.2.6 Late Sveconorwegian (1.0–0.85 Ga): post tectonic intrusions

Post tectonic granitic intrusions were emplaced between 0.99 and 0.87 Ga in the entire Southwest Scandinavian Orogen: Bergen Arc / Hardanger-Ryfylke (0.91 Ga; Priem et al. 1976), Telemark (0.95–0.87 Ga; Priem et al. 1973, Killeen and Heier 1975a, Pedersen 1981), Bamble (0.99–0.96 Ga; Brueckner 1972, Killeen and Heier 1975a, Kullerud and Machado 1991), and Østfold-Stora Le-Marstrand (0.92–0.89 Ga; Killeen and Heier 1975ab, Skiöld 1976, Pedersen and Maaløe 1990, Eliasson and Schöberg 1991). For long, it was thought that late

Sveconorwegian basic magmatism only occurred in the Western Gneiss Region (0.93 Ga; Mørk and Mearns 1986), but recent age determinations indicate the presence of late Sveconorwegian basic dikes in the Bamble Sector (M. M. Moree pers. com. 21-09-1992).

Acknowledgements - This paper benefitted from constructive criticism by G.J.L.M. de Haas, C. Maijer and R.H. Verschure. This work was financially supported by AWON (NWO 751.353.023).

References

- Ackermann, D. & Morteani, G.** 1973. Occurrence and breakdown of paragonite and margarite in the Greiner Schiefer Series (Zillertal Alps, Tyrol). *CMP* 40:293-304.
- Ahall, K.I.** 1984. Pillow lava in the Stora Le-Marstrand formation, south-western Sweden. *GFF* 106:105-107.
- 1990. An investigation of the Proterozoic Stenungsund granitoid intrusion, Southwest Sweden; conflicting geochronological and field evidence. In: Gower, C. F., Rivers, T. & Ryan, B., eds., Mid-Proterozoic Laurentia-Baltica. *Geol. Ass. Can. Spec. Pap.* 38:117-129.
- & **Daly, J.S.** 1989. Age, tectonic setting and provenance of Ostfold-Marstrand belt supracrustals: westward growth of the Baltic Shield at 1760 Ma. *PR* 45:45-61.
- , ——— & **Schöberg, H.** 1990. Geochronological constraints on Mid-Proterozoic magmatism in the Ostfold-Marstrand belt; implications for the crustal evolution in Southwest Sweden. In: Gower, C.F., Rivers, T. & Ryan, B., eds., Mid-Proterozoic Laurentia-Baltica. *Geol. Ass. Can. Spec. Pap.* 38:97-115.
- Albat, H.M.** 1984. The Proterozoic granulite facies terrane around Kliprand, Namaqualand metamorphic complex. *Univ. of Cape Town, Cham. of Mines Precam. Res. Unit Bul.* 33:1-382.
- Andrae, M.O.** 1974. Chemical and stable isotope composition of the high grade metamorphic rocks from the Arendal area, Southern Norway. *CMP* 47:299-316.
- Andresen, A., Heier, K.S., Jorde, K. & Naterstad, J.** 1974. A preliminary Rb/Sr geochronological study of the Hardangervidda-Ryfylke nappe system in the Røldal area, South Norway. *NGT* 54:35-47.
- Ashwal, L.D., Morgan, P. & Hoisch, T.D.** 1992. Tectonics and heat sources for granulite metamorphism of supracrustal-bearing terranes. *PR* 55:525-538.
- Atkin, B.P. & Brewer, T.S.** 1990. The tectonic setting of basaltic magmatism in the Kongsberg, Bamble and Telemark Sectors, southern Norway. In: Gower, C.F., Rivers, T. & Ryan, B., eds., Mid-Proterozoic Laurentia-Baltica. *Geol. Ass. Can. Spec. Pap.* 38:471-483.
- Baadsgaard, H., Chaplin, C. & Griffin, W.L.** 1984. Geochronology of the Gloserheia pegmatite, Froland, southern Norway. *NGT* 54:111-119.
- Baer, A.J.** 1981. A Grenvillian model of Proterozoic plate tectonics. In: Kröner, A., ed., *Precambrian plate tectonics*. Elsevier, Amsterdam, *Dev. in Precam. Geol.* 4:353-385.
- Bailey, S.W.** 1983. Crystal chemistry of the true micas. In: Bailey, S.W., ed., *Micas*. *Rev. Min.* 13:13-60.
- Bakken, R. & Gleditsch, E.** 1938. Analyses in layers of a single crystal of cleveite, Auselmyren, Norway. *AJS* 236:95-106.
- Baltatzis, E. & Katagas, C.** 1981. Margarite pseudomorphs after kyanite in Glen Esk, Scotland. *AM* 66:213-216.
- Bard, J.P.** 1970. Composition of hornblendes formed during the Hercynian progressive metamorphism of the Aracena metamorphic belt (SW Spain). *CMP* 28:117-134.
- Barrow, G.** 1893. On an intrusion of muscovite-biotite gneiss in the SE Highlands, and its accompanying metamorphism. *Quart. J. Geol. Soc.* London 49:330-358.
- Barth, T.F.W.** 1925. On contact minerals from Precambrian limestones in southern Norway. *NGT* 8:93-114.
- 1928. Kalk und Skarngesteine im Urgebirge bei Kristiansand. *NJM, Beil.* 57A:1069-1108.
- 1947. The Birkeland granite a case of petroblastesis. *Compt. Rend. Soc. Geol. Finl.* 20:173-179.
- 1963. Vesuvianite from Kristiansand, other occurrences in Norway, the general formula of vesuvianite. *NGT* 43:457-472.
- & **Dons, J.A.** 1960. Precambrian of Southern Norway. *NGU* 208:6-66.
- Baumer, A. & Argiolas, R.** 1981. Synthèses hydrothermales et déterminations RX d'apatites chlorée, fluoree ou hydroxylée. *NJM, Mh.* 344-348.
- Beeson, R.** 1972. The geology of the country between Songe and Ubergsmoen, Southern Norway. Unpubl. PhD thesis, Univ. of Nottingham.
- 1976. The orthoamphibole-bearing rocks of the Sønedeled-Tvedestrand area, Aust-Agder, South Norway. *NGT* 56:125-139.
- 1988. Identification of cordierite-anthophyllite rock types associated with sulphide deposits of copper, lead and zinc. *Tr. Inst. Mining Metal.* 97B:108-115.
- Berthelsen, A.** 1980. Towards a palinspastic tectonic analysis of the Baltic Shield. *BRGM Memoir* 108:5-21.
- 1987. A tectonic model for the crustal evolution of the Baltic Shield.

- In: Schaer, J.P. & Rodgers, J., eds., The anatomy of mountain ranges. Princeton Univ. Press, Princeton, 31-57.
- Binder, G. & Troll, G.** 1989. Coupled anion substitution in natural carbon-bearing apatites. *CMP* 101:394-401.
- Bingen, B.** 1988. Origine magmatique et evolution metamorphique de la serie des gneiss oeilles de Norvege meridionale. Unpubl. PhD thesis, Free Univ. Brussels, 308 pp.
- 1989. Geochemistry of Sveconorwegian augen gneisses from SW Norway at the amphibolite-granulite transition. *NGT* 69:177-189.
- , **Demaiffe, D. & Hertogen, J.** 1990. Evolution of feldspars at the amphibolite-granulite-facies transition in augen gneisses (SW Norway): geochemistry and Sr isotopes. *CMP* 105:275-288.
- Binns, R.A.** 1965. The mineralogy of metamorphosed basic rocks from the Willyama Complex, Broken Hill district, New South Wales. Part I. Hornblendes. *MM* 35:306-326.
- 1969. Ferromagnesian minerals in high-grade metamorphic rocks. *Geol. Soc. Austr. Spec. Publ.* 2:323-332.
- Blattner, P. & Black, P.M.** 1980. Apatite and scapolite as petrogenetic indicators in granulites of Milford Sound, New Zealand. *CMP* 74:339-348.
- Blundy, J.D. & Holland, T.J.B.** 1990. Calcic amphibole equilibria and a new amphibole - plagioclase geothermometer. *CMP* 104:208-224.
- Bohlen, S.R.** 1987. Pressure-temperature-time paths and a tectonic model for the evolution of granulites. *JG* 95:617-632.
- On the formation of granulites. *JMG* 9:223-229.
- Bos, A.J. & Andriessen, P.A.M.** 1985. Fission-track dating in Norway: An interim report. *Terra Cogn.* 4:191.
- Boudreau, A.E. & Kruger, F.J.** 1990. Variation in the composition of apatite through the Merensky cyclic unit in the Western Bushveld Complex. *Ec. Geol.* 85:737-745.
- , **Mathez, E.A. & McCallum, I.S.** 1986. Halogen geochemistry of the Stillwater and Bushveld Complexes: Evidence for transport of the platinum-group elements by Cl-rich fluids. *J. Petr.* 27:967-986.
- & **McCallum, I.S.** 1990. Low temperature alteration of REE-rich chlorapatite from the Stillwater Complex, Montana. *AM* 75:687-693.
- Bradshaw, J.Y.** 1989. Early Cretaceous vein-related garnet granulite in Fiordland, Southwest New Zealand: A case for infiltration of mantle-derived CO₂-rich fluids. *JG* 97:697-717.
- Breemen, O. van, Halliday, A.N., Johnson, M.R.W. & Bowes, D.R.** 1978. Crustal addition in late Precambrian times. In: Bowes, D.R. & Leake, B.E., eds., Crustal evolution in northwestern Britain and adjacent regions. Seal House Press, Liverpool, 81-106.
- Brenan, J.M.** 1992. Diffusion of fluorine and chlorine in fluorapatite. *Progr. Abstr. V.M. Goldschmidt Conf.*, A13.
- Brewer, M.S., Brook, M. & Powell, D.** 1979. Dating of the tectono-metamorphic history of the southwestern Moine, Scotland. In: Harris, A.L., Holland, H.C. & Leake, B.E., eds., The Caledonides of the British Isles - Reviewed. *Geol. Soc. Spec. Publ.* 8:129-137.
- Brickwood, J.D. & Craig, J.W.** 1987. Primary and reequilibrated mineral assemblages from the Sveconorwegian mafic intrusions of the Kongsberg and Bamble areas, Norway. *NGU* 410:1-23.
- Broch, O.A.** 1926. Ein suprakrustaler gneisscomplex auf der halbinsel Nesodden bei Oslo. *NGT* 9:81-224.
- Broekmans, M.A.T.M., Nijland, T.G. & Jansen, J.B.H.** 1992. Lower crustal transitions: III. Stable isotopic trends in carbonic rocks during amphibolite to granulite facies transition - Survival of diagenetic features (Bamble, Norway). *Vol. Abstr. 1st Neth. Earth Sci. Congr.*, Veldhoven, 115.
- & ——— 1993. Are stable isotopic trends in amphibolite to granulite facies transitions metamorphic or diagenetic? - An answer for the Arendal area (Bamble Sector, SE Norway) from Mid-Proterozoic carbon-bearing rocks. *AJS* in press.
- Brogger, W.C.** 1906. Die Mineralen der sudnorwegischen Granit-Pegmatitgänge. *Det Nor. Vid.-Ak. Skr. Mat.-Nat. Kl.* 1906-6 and 1934-1.
- 1934a. On several Archean rocks from the south coast of Norway. I. Nodular granites from the environs of Kragerø. *Det Nor. Vid.-Ak. Skr., Mat.-Nat. Kl.* 8.
- 1934b. On several Archæan rocks from the south coast of Norway. II. The South Norwegian hyperites and their metamorphism. *Det Nor. Vid.-Ak. Skr., Mat.-Nat. Kl.* 1:1-421.
- & **Reusch, H.H.** 1875. Vorkommen des Apatit in Norwegen. *Z. Deuts. Geol. Ges.* 27:646-702.
- Brook, M., Brewer, M.S. & Powell, D.** 1976. Grenville age for rocks in the Moine of north-western Scotland. *Nature* 260:515-517.

- , **Powell, D. & Brewer, M.S.** 1977. Grenville events in Moine rocks of the northern Highlands, Scotland. *J. Geol. Soc. London* 133:489-496.
- Brueckner, H.K.** 1972. Interpretation of Rb-Sr ages from the Precambrian and Paleozoic rocks of southern Norway. *AJS* 272:334-358.
- Bugge, A.** 1922. Nikkelgruber i Bamble. *NGU* 87:12-42.
- 1928. En forkastning i det syd-norske grunnfjell. *NGU* 130:1-124.
- 1936. Kongsberg - Bamble formationen. *NGU* 146:1-160.
- Bugge, C.** 1922. Statens apatitdrift i rationeringstiden. *NGU* 110:1-34.
- 1934. Gullforekomster i Norge. *NGT* 14:319-320.
- Bugge, J.A.W.** 1940. Geological and petrological investigations in the Arendal district. *NGT* 20:71-120.
- 1943. Geological and petrological investigations in the Kongsberg-Bamble formations. *NGU* 160:1-150.
- 1945. Lødesøl skarn forekomst. *NGT* 25:35-47.
- 1978. Kongsberg-Bamble complex. In: **Bowie, S.H.V., Kvalheim, A. & Haslam, M.W.**, eds., *Mineral deposits of Europe. Vol. 1: Northwest Europe*, 213-217.
- Burrell, D.C.** 1966. Garnets from upper amphibolite lithologies of the Bamble series, Kragerø, South Norway. *NGT* 46:3-19.
- Burton, K.W. & O'Nions, R.K.** 1990. The timescale and mechanism of granulite formation at Kurunegala, Sri Lanka. *CMP* 106:66-89.
- Candela, P.A.** 1986. Towards a thermodynamic model for the halogens in magmatic systems: an application to melt-vapour-apatite equilibria. *Chem. Geol.* 57:289-301.
- Černý, P. & Povondra, P.** 1972. An Al, F rich metamict titanite from Czechoslovakia. *NJM, Mh.* 400-406.
- & **Riva di Sanseverino, L.** 1972. Comments on crystal chemistry of titanite. *NJM, Mh.*, 97-103.
- Chatterjee, N.D., Johannes, W. & Leistner, H.** 1984. The system CaO-Al₂O₃-SiO₂-H₂O: new phase equilibria data, some calculated phase relations, and their petrological applications. *CMP* 88:1-13.
- Chesner, C.A. & Ettliger, A.D.** 1989. Composition of volcanic allanite from the Toba Tuffs, Sumatra, Indonesia. *AM* 74:750-758.
- Claesson, S., Huhma, H., Kinny, P. & Williams, I.S.** 1991. Provenance of Svecofennian metasediments: U-Pb dating of detrital zircons. *Terra Abstr.* 3:505.
- Clough, P.W.L. & Field, D.** 1980. Chemical variation in metabasites from a Proterozoic amphibolite-granulite transition zone, South Norway. *CMP* 73:277-286.
- Cohen, A.S., O'Nions, R.K., Siegenhaller, R. & Griffin, W.L.** 1988. Chronology of the pressure-temperature history recorded by a granulite terrain. *CMP* 98:303-311.
- Comin Chiaramonti, P.** 1974. Iron titanium minerals in the Tromøy island (South Norway). *Atti Mem. Acc. Patavina Sci. Lett. Arti* 86:243-247.
- Comin Chiaramonti, P. & Frangipane, M.** 1974. The amphyclasite of Bråt (Tromøy, southern Norway). *Tscherm. Mitt. Petr. Min.* 21:280-290.
- Cooper, A.F.** 1980. Retrograde alteration of chromian kyanite in metachert and amphibolite whiteschist from the Southern Alps, New Zealand, with implications for uplift on the Alpine Fault. *CMP* 75:153-164.
- & **Lovering, J.F.** 1970. Greenschist amphiboles from Haast River, New Zealand. *CMP* 27:11-24.
- Cooper, D.C. & Field, D.** 1977. The chemistry and origins of Proterozoic low potash high iron charnockitic gneisses from Tromøy, South Norway. *EPSL* 35:105-115.
- Cosca, M.A., Essene, E.J. & Bowman, J.R.** 1991. Complete chemical analyses of metamorphic hornblendes: implications for normalizations, calculates H₂O activities, and thermobarometry. *CMP* 109:472-484.
- Dahl, P.S.** 1980. The thermal-compositional dependence of Fe²⁺-Mg distributions between coexisting garnet and pyroxene: application to geothermometry. *AM* 65:852-866.
- Dahlgren, S.** 1991. Lamproite dikes at Tromøy - The first record of ultrapotassic magmatism in the Sveconorwegian Province. *Exc. log* 2nd SNF Workshop, Bamble, 48-51.
- & **Heaman, L.** 1991. U-Pb constraints for the timing of Middle Proterozoic magmatism in the Telemark region, southern Norway. *Geol. Ass. Can. Progr. Abstr.* 16:28.
- , ——— & **Krogh, T.** 1990. Geological evolution and U-Pb geochronology of the Proterozoic Central Telemark area, Norway. *Geonytt* 17:38-39.
- Dallmeyer, R.D., Mitchell, J.G., Pharaoh, T.C., Reuter, A. & Andresen, A.** 1988. K-Ar and ⁴⁰Ar/³⁹Ar whole-rock ages of slate/phyllite from allochthon basement and cover in the tectonic windows of Finnmark, Norway: Evaluating the extent and timing of

- Caledonian tectonothermal activity. *Geol. Soc. Am. Bul.* 100:1493-1501.
- Daly, J.S., Aitchison, S.J., Cliff, R.A., Gayes, R.A. & Rice, A.H.N.** 1991. Geochronological evidence from discordant plutons for a late Proterozoic orogen in the Caledonides of Finnmark, northern Norway. *J. Geol. Soc. London* 148:29-40.
- , **Park, R.G. & Cliff, R.A.** 1983. Rb-Sr isotopic equilibrium during Sveconorwegian (= Grenville) deformation and metamorphism of the Orust dykes, S.W. Sweden. *Lithos* 16:307-318.
- Daubree, M.A.** 1843. Mémoire sur les dépôts métallifères de la Suede et de la Norvege. *Ann. Mines* 4:199-282.
- Davis, F.B. & Windley, B.F.** 1976. Significance of major Proterozoic high-grade linear belts in continental evolution. *Nature* 263:383-385.
- Dekker, A.G.C.** 1978. Amphiboles and their host rocks in the high-grade metamorphic Precambrian of Rogaland/Vest-Agder, SW. Norway. *Geol. Ultraiectina* 17:1-277.
- Demaiffe, D. & Michot, J.** 1985. Isotope geochronology of the Proterozoic crustal segment of southern Norway: A review. In: Tobi, A.C. & Touret, J.L.R., eds., *The deep Proterozoic crust in the North Atlantic provinces*. Reidel, Dordrecht, 411-433.
- Dewey, J.F. & Burke, K.C.A.** 1973. Tibetan, Variscan and Precambrian basement reactivation: products of continental collision. *JG* 81:683-692.
- Dobretsov, N.L., Konnikov, E.G. & Dobretsov, N.N.** 1992. Precambrian ophiolite belts of southern Siberia, Russia, and their metallogeny. *PR* 58:427-446.
- Dymek, R.F.** 1983a. Titanium, aluminum and interlayer cation substitutions in biotite from high-grade gneisses, West Greenland. *AM* 68:880-899.
- 1983b. Margarite pseudomorphs after corundum, Qorqut, Gothåbsfjord, West Greenland. *Grönl. Geol. Unders. Rep.* 112:95-99.
- Eckert, J.O., Newton, R.C. & Kleppa, O.J.** 1989. Recalibration of the garnet-anorthite-diopside-quartz (GADS) geobarometry oxide-melt solution calorimetry of stoichiometric mineral mixes. *Eos* 70:1392.
- Ekström, T.K.** 1973a. Synthetic and natural chlorine-bearing apatite. *CMP* 38:329-338.
- 1973b. The distribution of fluorine among some coexisting minerals. *CMP* 34:192-200.
- 1973c. Principal component analyses of biotites and coexisting Ca-amphiboles. *NJM, Mh.* 34-43.
- Eliasson, T. & Schoberg, H.** 1991. U-Pb dating of the post-kinematic Sveconorwegian (Grenvillian) Bohus granite, SW Sweden: evidence of restite zircon. *PR* 51:337-350.
- Elliott, J.C. & Young, R.A.** 1967. Conversion of single crystals of chlorapatite into single crystals of hydroxyapatite. *Nature* 214:904-906.
- Emslie, R.F. & Hunt, P.A.** 1990. Ages and petrogenetic significance of igneous mangerite-charnockite suites associated with massif anorthosites, Grenville Province. *J. Geol.* 98:213-231.
- , **Loveridge, W.D. & Stevens, R.D.** 1983. The Mealy dykes, Labrador: petrology, age, and tectonic significance. *Can. J. Earth Sci.* 21:437-446.
- Engel, A.E.J. & Engel, C.G.** 1962. Hornblendes formed during progressive metamorphism, of amphibolites, northwest Adirondack Mountains, New York. *Geol. Soc. Am. Bul.* 73:1499-1514.
- Etheridge, M.A., Rutland, R.W.R. & Wyborn, L.A.J.** 1987. Orogenesis and tectonic processes in the early to middle Proterozoic of northern Australia. In: Kröner, A., ed., *Proterozoic lithospheric evolution*. AGU, 131-147.
- Eugeno-S Working Group** 1988. Crustal structure and tectonic evolution of the transition between the Baltic Shield and the North German Caledonides (the Eugeno-S project). *Tectonoph.* 150:253-348.
- Falkum, T.** 1982. Berggrunnskart Mandal, 1:250,000. NGU.
- & **Petersen, J.S.** 1980. The Sveconorwegian orogenic belt, a case of Late-Proterozoic plate collision. *Geol. Rundsch.* 69:622-647.
- Fedoseev, A.D., Grigoreva, L.F., Chigareva, O.G. & Romanov, D.P.** 1970. Synthetic fibrous fluoramphiboles and their properties. *AM* 55:854-863.
- Feenstra, A.** 1985. Metamorphism of bauxites on Naxos, Greece. *Geol. Ultraiectina* 39:1-206.
- Field, D.** 1969. The geology of the country around Tvedestrand, South Norway. Unpubl. PhD thesis, Univ. of Nottingham.
- & **Clough, P.W.L.** 1976. K/Rb ratios and metasomatism in metabasites from a Precambrian amphibolite-granulite transition zone. *J. Geol. Soc. London* 132:277-288.
- , **Drury, S.A. & Cooper, D.C.** 1980. Rare-earth and LIL element fractionation in high grade charnockitic gneisses, south Norway.

- Lithos 13:281-289.
- & **Råheim, A.** 1979. Rb-Sr total rock isotope studies on Precambrian charnockitic gneisses from South Norway: evidence for isochron resetting during a low-grade metamorphic-deformational event. *EPSL* 45:32-44.
- & ——— 1980. Age relationships in the Proterozoic high-grade gneiss regions of Southern Norway. *PR* 14:261-275.
- & ——— 1983. Age relationships in the Proterozoic high-grade gneiss regions of southern Norway: Reply to "Discussion and comment" by Weis and Demaiffe. *PR* 22:157-161.
- & **Rodwell, J.R.** 1968. The occurrence of prehnite in a high-grade metamorphic sequence from South Norway. *NGT* 48:58-61.
- , **Smalley, P.C., Lamb, R.C. & Råheim, A.** 1985. Geochemical evolution of the 1.6-1.5 GA-old amphibolite-granulite facies terrain, Bamble sector, Norway: dispelling the myth of Grenvillian high-grade reworking. In: **Tobi, A.C. & Touret, J.L.R.**, eds., *The deep Proterozoic crust in the North Atlantic provinces*. Dordrecht, Reidel, 567-578.
- Fominykh, V.G.** 1974. Fluorine and chlorine in the coexisting apatites and amphiboles in the rocks and ores of the titanomagnetite deposits of the Urals. *Geochem. Int.* 11:354-356.
- Fonarev, V.I. & Graphikov, A.A.** 1987. Two-pyroxene geothermometry (critical analyses). *Contr. Physio-chem. Petr.* 14:118-137 (In Russian).
- & ——— 1990. Two-pyroxene thermometry: a critical evaluation. In: **Perchuk, L.L.**, ed., *Progress in metamorphic and magmatic petrology*. Cambridge Univ. Press, Cambridge, 65-92.
- Forbes, D.** 1857. Gæologiske undersøgelser over det metamorfiske territorium ved Norges Sydkyst. *Nyt Mag. Naturvid.* 9:165-184.
- Fossen, H. & Nissen, A.L.** 1991. Rb-Sr age of the Blåfjellhatten granite in the Olden Window, Central Norway. *NGU* 420:51-56.
- Frey, M., Bucher, K., Frank, E. & Schwander, H.** 1982. Margarite in the Central Alps. *Schweiz. Min. Petr. Mitt.* 62:21-45.
- , **Capitani, C. de & Liou, J.G.** 1991. A new petrogenetic grid for low-grade metabasites. *JMG* 9:497-509.
- Frodesen, S.** 1968. Petrographical and chemical investigations of a Precambrian gabbro intrusion, Hiåsen, Bamble area, South Norway. *NGT* 48:281-306.
- Frost, B.R. & Chacko, T.** 1989. The granulite uncertainty principle: Limitations on thermobarometry in granulites. *JG* 97:435-450.
- , **Frost, C.D. & Touret, J.L.R.** 1989. Magmas as a source of heat and fluids in granulite metamorphism. In: **Bridgwater, D.**, ed., *Fluid movements, element transport and the composition of the deep crust*. Kluwer, Dordrecht, 1-18.
- Fujimori, S. & Fyfe, W.S.** 1984. Almanditic garnet-rich metamorphic rocks as an original soil developed during the Precambrian. *Rev. Brasil. Geoci.* 14:194-202.
- Gaal, G. & Gorbatshev, R.** 1987. An outline of the Precambrian evolution of the Baltic shield. *PR* 35:15-52.
- Gibert, F., Moine, B. & Gibert, P.** 1990. Titanites (sphènes) alumineuses formées a basse/moyenne pression dans les gneiss a silicates calciques de la Montagne Noire. *Compt. Rend. Ac. Sci. Paris* 311:657-663.
- Gibson, G.M.** 1979. Margarite in kyanite- and corundum-bearing anorthosite, amphibolite and hornblende from Central Fiordland, New Zealand. *CMP* 68:171-179.
- Giuseppetti, G. & Tadini, C.** 1972. The crystal structure of 2D brittle mica: anandite. *Tscherm. Min. Petr. Mitt.* 18:169-184.
- Glassley, W.E. & Sørensen, K.** 1980. Constant $P_{\text{H}_2\text{O}}$ -T amphibolite to granulite facies transition in Agto (West Greenland) metadolerites: Implications and applications. *J. Petr.* 21:69-105.
- Glaveris, M.** 1970. The occurrence of olivine hyperite at Ødegårdens Verk, Bamble, South Norway. *NGT* 50:15-17.
- Gorbatshev, R.** 1969. Element distribution between biotite and Ca-amphibole in some igneous and pseudo-igneous plutonic rocks. *NJM, Abh.* 111:314-342.
- 1977. The influence of some compositional relations on the partition of Fe and Mg between biotite and Ca-amphibole. *NJM, Abh.* 130:3-11.
- 1980. The Precambrian development of southern Sweden. *GFF* 102:129-136.
- 1985. Precambrian basement of the Scandinavian Caledonides. In: **Gee, D.G. & Sturt, B.A.**, eds., *The Caledonide orogen-Scandinavia and related areas*. John Wiley, New York, 197-212.
- 1988. Sveconorwegian thrusting in southwestern Sweden. *GFF* 110:392-397.
- & **Gaal, G.** 1987. The Precambrian

- history of the Baltic Shield. In: Kröner, A., ed., Proterozoic lithospheric evolution. AGU Geodyn. Ser. 17:149-159.
- Gower, C.F.** 1985. Correlations between the Grenville Province and Sveconorwegian orogenic belt—Implications for Proterozoic evolution of the southern margins of the Canadian and Baltic Shields. In: Tobi, A.C. & Touret, J.L.R., eds., The deep Proterozoic crust in the North Atlantic provinces. Reidel, Dordrecht, 247-257.
- 1990. Mid-Proterozoic evolution of the eastern Grenville Province, Canada. GFF 112:127-139.
- & **Owen, V.** 1984. Pre-Grenvillian and Grenvillian lithotectonic regions in eastern Labrador—correlations with the Sveconorwegian Orogenic Belt in Sweden. Can. J. Earth Sci. 21:678-693.
- , **Ryan, A.B. & Rivers, T.** 1990. Mid-Proterozoic Laurentia-Baltica: an overview of its geological evolution and a summary of the contributions made by this volume. In: Gower, C.F., Rivers, T. & Ryan, A.B., eds., Mid Proterozoic Laurentia-Baltica. Geol. Ass. Can. Spec. Pap. 38:1-21.
- Graham, C.M.** 1974. Metabasite amphiboles of the Scottish Dalradian. CMP 47:165-185.
- Grant, S.M.** 1989. Tectonic implications from sapphirine-bearing lithologies, south-west Grenville Province, Canada. JMG 7:583-598.
- Green, P.F., Duddy, I.R., Gleadow, A.J.W., Tingate, P.R. & Laslett, G.M.** 1986. Thermal annealing of fission tracks in apatite. Chem. Geol. 59:237-253.
- Guidotti, C.V. & Cheney, J.T.** 1976. Margarite pseudomorphs after chialstolite in the Rangeley area, Maine. AM 61:431-434.
- , **Post, J.L. & Cheney, J.T.** 1979. Margarite pseudomorphs after chialstolite in the Georgetown area, California. AM 64:728-732.
- Gunow, A.J., Ludington, S. & Munoz, J.L.** 1980. Fluorine in micas from the Henderson molybdenite deposit, Colorado. Ec. Geol. 75:1127-1137.
- Guppy, E.M.** 1956. Chemical analyses of igneous rocks, metamorphic rocks and minerals, 1931-1954. Mem. Geol. Surv. Great Britain.
- Gupta, L.N. & Johannes, W.** 1982. Petrogenesis of a stromatic migmatite (Nelaug, Southern Norway). J. Petr. 23:548-567.
- Haack, U.** 1975. Aussagemöglichkeiten der Spaltspurenmethode und Spaltspuren-Geochronologie des Damara-Orogens in S.W. Afrika. Habil.schr., Univ. of Göttingen.
- 1977. The closing temperature for fission track retention in minerals. AJS 277:459-464.
- Haas, G.J.L.M. de** 1992. Source, evolution and age of coronitic gabbros from the Arendal-Nelaug area, Bamble, Southeast Norway. Geol. Ultraiectina 86:1-129.
- , **Huijsmans, J.P.P. & Verschure, R.H.** 1990. The magmatic evolution of the Vestre Dale gabbro, Bamble, South Norway, and the Sm-Nd systematics of two hyperites. Geonytt 17:51-52.
- , **Nijland, T.G., Huijsmans, J.P.P., Maijer, C. & Dam, B.P.** 1992b. The magmatic history of a gabbroic intrusion in the Bamble Sector, Vestre Dale, Norway. NJM, Mh 221-240.
- , **Senior, A. & Dam, B.P.** 1993b. Preservation of igneous structure and whole rock chemical profiles during multiple high grade metamorphism (Flostå Gabbro, Bamble, Norway). Proc. Kon. Ned. Ak. Wetensch. submitted.
- & **Verschure, R.H.** 1990. Isotopic variations in gabbroic intrusions perforating the Proterozoic continental crust, Bamble, South Norway: Implications for the evolution of the underlying mantle. Geol. Soc. Austr. Abstr. 27:42.
- , **Maijer, C.** 1993a. Isotope constraints on the timing of the crustal accretion of the Bamble area, as evidenced by coronitic gabbros. PR in press.
- , **Senior, A. & Valbracht, P.J.** 1992a. Isotopic age determinations in South Norway. III. Rb-Sr isotope systematics of the coronitic Vestre Dale gabbro and its country rocks, Bamble, Norway. GFF 114:417-422.
- Hagelia, P.** 1989. Structure, metamorphism and geochronology of the Skagerrak shear belt, as revealed by studies in the Hovdefjell-Ubergsmoen area, South Norway. Unpubl. Cand. Sci. thesis, Univ. of Oslo, 236 pp.
- Hageskov, B.** 1978. On the Precambrian structures of the Sandbukta-Mølen inlier in the Oslo graben, SE Norway. NGT 58:69-80.
- 1980. The Sveconorwegian structures of the Norwegian part of the Kongsberg-Bamble-Østfold segment. GFF 102:150-155.
- & **Pedersen, S.** 1988. Rb/Sr age determination in the Kattsund-Koster dyke swarm in the Østfold-Marstrand belt of the Sveconorwegian Province, W. Sweden-S.E. Norway. Bul. Geol. Soc. Denm. 37:51-61.
- Hammarstrom, J.M. & Zen, E-an** 1986.

- Aluminum in hornblende: an empirical igneous geobarometer. *AM* 64:953-965.
- Halvorsen, E.** 1970. Paleomagnetism and the age of the younger diabasites in the Ny-Hellesund area. *NGT* 50:157-166.
- Hansen, B.T., Persson, P.O., Söllner, F. & Lindh, A.** 1989. The influence of recent lead loss on the interpretation of disturbed U-Pb systems in zircons from metamorphic rocks in southwest Sweden. *Lithos* 23:123-136.
- Haren, J.L.M. van & Röhrman, M.** 1988. Fission track ouderdommen van apatiet in het Bamble gebied (ZW Noorwegen). Unpubl. MSc thesis, Utrecht Univ., 34 pp.
- Harley, S.L.** 1989. The origins of granulites: a metamorphic perspective. *Geol. Mag.* 126:215-247.
- Harrison, T.M.** 1981. Diffusion of Ar in hornblende. *CMP* 78:324-331.
- Haute, P. van den** 1977. Apatite fission track dating of Precambrian intrusive rocks from the southern Rogaland (South-western Norway). *Bul. Soc. belge Geol.* 86:97-110.
- Hawthorne, F.C.** 1981. Crystal chemistry of the amphiboles. In: *Veblen, D.R., ed., Amphiboles. Rev. Min.* 9A:1-102.
- Helland, A.** 1874. Apatit i forekommende i rene stakke og gange i Bamle i Norge. *GFF* 2:148-156.
- Hemley, J.J., Montoya, J.W., Marinenko, J.W. & Luce, R.W.** 1980. Equilibria in the system Al_2O_3 - SiO_2 - H_2O and some general implications for alteration/mineralization processes. *Ec. Geol.* 75:210-228.
- Hietanen, A.** 1971. Distribution of elements in biotite-hornblende pairs and in an orthopyroxene-clinopyroxene pair from zoned plutons, northern Sierra Nevada, California. *CMP* 30:161-176.
- Higgins, J.B. & Ribbe, P.H.** 1976. The crystal chemistry and space groups of natural and synthetic titanites. *AM* 61:878-888.
- Hitmi, N., LaCabanne, C. & Young, R.A.** 1984. TSC study of electric dipole relaxations in chlorapatite. *J. Phys. Chem. Solids* 45:701-708.
- , ——— & ——— 1986. OH^- dipole reorientability in hydroxyapatites: effect of tunnel size. *J. Phys. Chem. Solids* 47:533-546.
- Hoefs, J. & Touret, J.** 1975. Fluid inclusions and carbon isotope study from Bamble granulites (South Norway). *CMP* 52:165-174.
- Hoffman, P.F.** 1988. United plates of America, the birth of a craton: Early Proterozoic assembly and growth of Laurentia. *Ann. Rev. Earth Plan. Sci.* 16:543-603.
- Hogarth, D.D.** 1988. Chemical composition of fluorapatite and associated minerals from skarn near Gatineau, Quebec. *MM* 52:347-358.
- Holbrook, W.S.** 1989. A petrological model of the laminated lower crust in Southwest Germany, based on wide-angle P- and S-wave seismic data. In: *Mereu, R.F., Mueller, S. & Fountain, D.M., eds., Properties and processes of earth's lower crust.* AGU Geophys. Monogr. 51:121-125.
- Holdaway, M.J.** 1971. Stability of andalusite and the aluminum silicate phase diagram. *AJS* 271:97-131.
- Hollister, L.S., Grissom, G.C., Peters, E.K., Stowell, H.H. & Sisson, V.B.** 1987. Confirmation of the empirical correlation of Al in hornblende with products of solidification in calc-alkaline plutons. *AM* 72:231-239.
- Holloway, J.R. & Ford, C.E.** 1975. Fluid-absent melting of the fluoro-hydroxy amphibole pargasite to 35 kilobars. *EPSL* 25:44-48.
- Holmes, A., Shillibeer, H.A. & Wilson, J.T.** 1955. Potassium-argon ages of some Lewisian and Fennoscandian pegmatites. *Nature* 176:390-392.
- Hounslow, A.W. & Chao, G.Y.** 1970. Monoclinic chlorapatite from Ontario. *Can. Min.* 10:522-529.
- Hughes, J.M., Cameron, M. & Crowley, K.D.** 1989. Structural variations in natural F, OH, and Cl apatites. *AM* 74:870-876.
- , ——— & ——— 1990. Crystal structures of natural ternary apatites: Solid solution in the $Ca_5(PO_4)_3X$ (X=F, OH, Cl) system. *AM* 75:295-304.
- Hulzebos-Sijen, N.M.P.E., Visser, D., Maarschalkerweerd, M.H. & Maijer, C.** 1990. Two new kornerupine localities in the Bamble Sector, Norway. *Geonytt* 17:58.
- Hunt, J.A. & Kerrick, D.M.** 1977. The stability of sphene: experimental redetermination and geologic implications. *Geochim. Cosmochim. Acta* 41:279-288.
- Husebye, E.S., Ro, H.E., Kinck, J.J. & Larsson, F.R.** 1988. Tectonic studies in the Skagerrak province: the "Mobil Search" cruise. In: *Kristoffersen, Y., ed., Progress in studies of the lithosphere in Norway.* NGU Spec. Publ. 3:14-20.
- Ihlen, P.M., Ineson, P.R., Mitchell, J.G. & Vokes, F.M.** 1984. K-Ar dating of dolerite dykes in the Kongsberg Fiskum district, Norway, and their relationships with the silver and base metal veins. *NGT* 64:87-96.
- Indares, A.** 1992. Eclogitized gabbros from the central-western Grenville

- Province. *Eos* 73:340.
- Ionov, D.A., Bushlyakov, I.N. & Kovalenko, V.I.** 1987. Fluorine and chlorine content of phlogopite, amphibole and apatite from plutonic xenoliths of the Shavarin Tsaram volcano, Mongolian People's Republic. *Dokl. Ak. Nauk SSSR* 287:174-177.
- Iwasaki, M.** 1963. Metamorphic rocks of the Kotu-Bizan area, eastern Sikoku. *J. Tokyo Univ. Fac. Sci., Ser. II* 15:1-90.
- Jackson, M.P.A.** 1976. High-grade metamorphism and migmatization of the Namaqua metamorphic complex around Aus in the southern Namib desert, South West Africa. *Univ. of Cape Town, Cham. of Mines Precam. Res. Unit Bul.* 18:1-299.
- Jacobsen, R.R.E., Macleod, W.N. & Black, R.** 1958. Ring complexes in the younger granite province of northern Nigeria. *Geol. Soc. Memoir* 1.
- Jacobsen, S. & Heier, K.S.** 1975. Rb-Sr systematics in metamorphic rocks, Kongsberg sector, South Norway. *Lithos* 11:257-276.
- Jaffe, H.W.** 1947. Reexamination of sphene (titanite). *AM* 32:637-642.
- Jahn, B.M., Vidal, P. & Kroner, A.** 1984. High-chronometric ages and origin of Archaean tonalitic gneisses in Finnish Lapland: A case for long crustal residence times. *CMP* 86:398-408.
- Jamtveit, B., Carswell, D.A. & Mearns, E.W.** 1991. Chronology of the high-pressure metamorphism of Norwegian garnet peridotites/pyroxenites. *JMG* 9:125-139.
- Jansen, J.B.H., Blok, R.J.P., Bos, A. & Scheelings, M.** 1985. Geothermometry and geobarometry in Rogaland and preliminary results from the Bamble area, South Norway. In: *Tobi, A.C. & Touret, J.L.R., eds., The deep Proterozoic crust in the North Atlantic provinces.* Reidel, Dordrecht, 499-516.
- & **Maijer, C.** 1987. CO₂ and preferent H₂O depletion in fluid deficient local rock systems during granulite facies metamorphism related to anorthositic magmatism in the Precambrian of Rogaland, SW Norway. In: *Vol. Abstr. NATO ASI "Fluid movements, element transport and the composition of the deep crust."* Lindås.
- & **Schuiling, R.D.** 1976. Metamorphism on Naxos: petrology and geothermal gradients. *AJS* 276:1225-1253.
- Johannes, W.** 1985. The significance of experimental studies for the formation of migmatites. In: *Ashworth, J.R., ed., Migmatites.* Blackie, London, 39-85.
- 1988. What controls partial melting in migmatites? *JMG* 6:431-465.
- Johansson, Å.** 1990. Age of the Önestad syenite and some gneissic granites along the southern part of the Protogine Zone, southern Sweden. In: *Gower, C.F., Rivers, T. & Ryan, B., eds., Mid-Proterozoic Laurentia-Baltica.* *Geol. Ass. Can. Spec. Pap.* 38:131-148.
- & **Larsen, O.** 1989. Radiometric age determinations and Precambrian geochronology of Blekinge, southern Sweden. *GFF* 111:35-50.
- Johansson, L. & Johansson, Å.** 1990. Isotope geochemistry and age relationship of mafic intrusions along the Protogine Zone, southern Sweden. *PR* 48:395-414.
- , **Lindh, A. & Möller, C.** 1991. Late Sveconorwegian (Grenville) high-pressure granulite facies metamorphism in southwest Sweden. *JMG* 9:283-292.
- Johnson, M.C. & Rutherford, M.J.** 1989. Experimental calibration of the aluminum-in-hornblende geobarometer with application to Long Valley caldera (California) volcanic rocks. *Geol.* 17:837-841.
- Kearns, L.E., Kite, L.E., Leavens, P.B. & Nelen, J.A.** 1980. Fluorine distribution in the hydrous silicate minerals of the Franklin marble, Orange county, New York. *AM* 65:557-562.
- Kerkhof, A.M. van den, Touret, J.L.R. & Kreulen, R.** 1993. Evidence for juvenile CO₂ in enderbites of Tromøy (SE Norway): A fluid inclusion and stable isotope study. *JMG* submitted.
- Kerrick, D.M.** 1991. The Al₂SiO₅ polymorphs. *Rev. Min.* 22:1-406.
- Kihle, J.** 1989. Polymetamorf utvikling av cordieritt-førende metapeliter i Bamble-sektoren, Syd-Norge. Unpubl. *Cand. Sci. thesis, Univ. of Oslo*, 360 pp.
- Killeen, P.G. & Heier, K.S.** 1975a. Radioelement distribution and heat production in Precambrian granitic stocks, southern Norway. *Det Nor. Vid.-Ak. Skr., Mat.-Nat. Kl.* 35:1-32.
- & ——— 1975b. A uranium and thorium enriched province of the Fennoscandian shield in southern Norway. *Geoch. Cosmoch. Acta* 39:1515-1524.
- Kinck, J.J., Husebye, E.S. & Lund, C.E.** 1991. The South Scandinavian crust: Structural complexities from seismic reflection and refraction profiling. *Tectonoph.* 189:117-133.
- Kjerulf, T. & Dahll, T.** 1861. Om jernertsener forekomst ved Arendal, Naes og Kragerø. *Nyt Mag. Naturvid.* 11:293-359.
- Kohn, M.J. & Spear, F.S.** 1990. Two new

- geobarometers for garnet-amphibolites, with application to southeastern Vermont. *AM* 75:89-96.
- Kontinen, A.** 1987. An early Proterozoic ophiolite- the Joimua mafic-ultramafic complex, northeastern Finland. *PR* 35:313-342.
- Korzhinskiy, M.A.** 1981. Apatite solid solutions as indicators of the fugacity of HCl and HF in hydrothermal fluids. *Geochem. Int.* 18:44-60.
- Kostyuk, E.A. & Sobolev, V.S.** 1969. Paragenetic types of calciferous amphiboles of metamorphic rocks. *Lithos* 2:67-81.
- Koziol, A.M. & Newton, R.C.** 1988. Redetermination of the anorthite breakdown reaction and improvement of the plagioclase-garnet- Al_2SiO_5 -quartz geobarometer. *AM* 73:216-223.
- Krauss, M. & Lindh, A.** 1990. Der südliche Baltische Schild- seine tektonische Krustenentwicklung und Beziehungen zum mitteleuropäischen Raum. *Z. Geol. Wis.* 18:569-586.
- Kretz, R.** 1959. Chemical study of garnet, biotite, and hornblende from gneisses of southwestern Quebec, with emphasis on distribution of elements in coexisting minerals. *JG* 67:371-402.
- 1983. Symbols for rock-forming minerals. *AM* 68:277-279.
- 1990. Biotite and garnet compositional variation and mineral equilibria in Grenville gneisses of the Otter Lake area, Quebec. *JMG* 8:493-506.
- Krijgsman, A.** 1991a. Geology and ore-genesis of the Ettetdalgrube, a Proterozoic Pb-Zn-Ag deposit in SE Norway. Unpubl. MSc thesis, Utrecht Univ., 34 pp.
- 1991b. Pb-Zn-Ag mineralization at the Ettetdalgrube. *Exc. log 2nd SNF Workshop, Bamble*, 40-41.
- 1991c. (Meta)-ultramafic rocks from Bamble, SE Norway. Unpubl. MSc thesis, Utrecht Univ., 46 pp.
- Kröner, A., Puustinen, K. & Hickman, M.** 1981. Geochronology of an Archean tonalitic gneiss dome in northern Finland and its relations with an unusual overlying volcanic conglomerate and komatiitic greenstone. *CMP* 76:33-41.
- Krutov, G.A.** 1936. Dashkessanite- a new chlorine amphibole of the hastingsite group. *Dokl. Ak. Nauk SSSR*, 341-371 (In Russian).
- Kullerud, L. & Dahlgren, S.** 1990. Timing of the high grade metamorphism in the Bamble sector, South Norway. *Geonytt* 17:68.
- & ——— 1993. Sm-Nd geochronology of Sveconorwegian granulite facies mineral assemblages in the Bamble Shear Belt, South Norway. *PR* in press.
- & **Machado, N.** 1991. End of a controversy: U-Pb geochronological evidence for significant Grenvillian activity in the Bamble area, Norway. *Terra Abstr.* 3:504.
- Kulp, J.L. & Neumann, H.** 1961. Some potassium-argon ages from the Norwegian basement. *Ann. New York Ac. Sci.* 91:469-475.
- Lacroix, A.** 1889. Contribution à l'étude des gneiss à pyroxène et des roches à wernerites. *Bul. Soc. Fr. Min.* 12:83-350.
- Laird, J. & Albee, A.L.** 1981. Pressure, temperature, and time indicators in mafic schist: their application to reconstructing the polymetamorphic history of Vermont. *AJS* 281:127-175.
- Lamb, R.C.** 1981a. Geochemical studies in Proterozoic high-grade gneiss terrain, Bamble Sector, South Norway. Unpubl. PhD thesis, Univ. of Nottingham, ch. 3, 72-120.
- 1981b. Berggrunnskart Arendal 1611 IV map sheet, 1:50,000. Preliminary issue. NGU, Trondheim.
- , **Smalley, P.C. & Field, D.** 1986. P-T conditions for the Arendal granulites, southern Norway: implications for the roles of P, T and CO_2 in deep crustal LILE depletion. *JMG* 4:143-160.
- Larsen, O.** 1971. K/Ar age determinations from the Precambrian of Denmark. *Danm. Geol. Unders. II. Række* 97:1-37.
- Larsson, F.R. & Husebye, E.S.** 1991. Crustal reflectivity in the Skagerrak area. *Tectonoph.* 189:135-148.
- Latil, C. & Maury, R.** 1977. Contribution à l'étude des échanges d'ions OH^- , Cl^- et F^- et leur fixation dans les apatites hydrothermales. *Bul. Soc. Fr. Min. Crist.* 100:246-250.
- Leake, B.** 1978. Nomenclature of amphiboles. *AM* 63:1023-1052.
- Lie, J.E. & Husebye, E.S.** 1991. The structure of the crust below Skagerrak: New results from deep reflection seismic data. *Terra Abstr.* 3:121.
- , **Pedersen, T. & Husebye, E.S.** 1990. Observations of seismic reflectors in the lower lithosphere beneath the Skagerrak. *Nature* 346:165-168.
- Lieftink, D.J. & Nijland, T.G.** 1992. Behaviour of La, Ce, Nd, Dy and Y during the replacement of Cl by OH in apatites from the ancient Ødegårdens Verk Mines (Kragersø, Norway). In: *Vol. Abstr. 1st Neth. Earth Sci. Congr., Veldhoven*, 134.
- , ——— & **Maijer, C.** 1993. The behaviour of REE in high temperature Cl-bearing aqueous fluids: Results

- from the Ødegårdens Verk natural laboratory. Can. Min., submitted.
- Lindahl, I. & Gust, J.** 1987. Registeringskart for malmforekomster, Arendal, 1:250,000. NGU, Trondheim.
- Lindh, A.** 1982. Trends in the Postveco Karelian development of the Baltic Shield. *Geol. Rundsch.* 71:130-140.
- 1987. Westward growth of the Baltic Shield. *PR* 35:53-70.
- & **Schöberg, H.** 1987. U-Pb age of a granitoid in the banded sequence at Grums, SW Sweden. *GFF* 109:165-169.
- & ——— 1988. A tentative study of the U-Pb isotope system in zircons from the Mylonite Zone, south-east Norway. *GFF* 110:15-20.
- Lindsley, D.H.** 1983. Pyroxene thermometry. *AM* 68:477-493.
- Liou, J.G., Marayama, S., Wang, X. & Graham, S.** 1990. Precambrian blueschist terranes of the world. *Tectonoph.* 181:97-111.
- Mackie, P.E. & Young, R.A.** 1974. Fluorine-chlorine interaction in fluor-chlorapatite. *J. Solid State Chem.* 11:319-329.
- Maesschalck, A.A. de, Touret, J.L.R., Maaskant, P. & Dahanayale, K.** 1991. Petrology and fluid inclusions in garnetiferous gneisses and charnockites from Weddagala (Ratnapura district, Sri Lanka). *JG* 99:443-456.
- Maijer, C.** 1990. Metamorphism in the Froland-Nelaug-Tvedestrand-Arendal area, Bamble: Reevaluation of the Sveconorwegian as a high-grade event. *Geonytt* 17:75.
- , **Andriessen, P.A.M., Hebeda, E.H., Jansen, J.B.H. & Verschure, R.H.** 1981. Osumilite, an approximately 970 Ma old high - temperature index mineral of the granulite facies metamorphism in Rogaland, SW Norway. *Geol. Mijnb.* 60:267-272.
- & **Padget, P.** 1987. The geology of southernmost Norway. *NGU Spec. Publ.* 1:1-109.
- Maiti, G.C. & Freund, F.** 1981. Incorporation of chlorine into hydroxy-apatite. *J. Inorgan. Nucl. Chem.* 43:2633-2637.
- Mansfield, J.** 1991. U-Pb age determinations of Småland-Värmland granitoids in Småland, southeastern Sweden. *GFF* 113:113-119.
- McConnell, D.** 1970. Crystal chemistry of bone material: hydrated carbonate apatites. *AM* 55:1659-1669.
- McConnell, D.** 1973. Apatite. Springer, Berlin, 111 pp.
- Mearns, E.W.** 1984. Isotopic studies of crustal evolution in western Norway. Unpubl. PhD thesis, Univ. of Aberdeen.
- 1986. Sm-Nd ages for Norwegian garnet peridotite. *Lithos* 19:269-278.
- Menuge, J.F.** 1988. The petrogenesis of massif anorthosites: a Nd and Sr isotopic investigation of the Proterozoic of Rogaland/Vest Agder, SW Norway. *CMP* 98:363-373.
- Mezger, K., Essene, E.J. & Halliday, A.N.** 1992. Closure temperatures of the Sm-Nd system in metamorphic garnets. *EPSL* 113:397-409.
- Michel-Lévy, M.A.** 1878a. Sur une roche à sphène, amphibole et wernerite granulitique des mines d'apatite de Bamble pres Brevig (Norwege). *Bul. Soc. Fr. Min.* 1:43-46.
- 1878b. Note sur le gisement de l'amphibolite à wernerite granulitique d'Odegaard pres Bamble (Norwege). *Bul. Soc. Fr. Min.* 1:78-81.
- Miller, J.A., Matthews, D.H. & Roberts, D.G.** 1973. Rock of Grenville age from Rockall Bank. *Nature Phys. Sci.* 246:61.
- Milne, K.P. & Starmer, I.C.** 1982. Extreme differentiation in the Proterozoic Gjerstad-Morkheia Complex of South Norway. *CMP* 79:381-393.
- Moine, B., Roche, H. de la & Touret, J.** 1972. Structures geoc zoneographie métamorphique dans le Précambrien catazonal du Sud de la Norvège. *Sci. Terre* 17:131-164.
- Morand, J.V.** 1990. High chromium and vanadium in andalusite, phengite and retrogressive margarite in contact metamorphosed Ba-rich black slate from the Abercrombie Beds, New South Wales, Australia. *MM* 54:381-391.
- Mørk, M.B.E. & Mearns, E.W.** 1986. Sm-Nd isotope systematics of a gabbro-eclogite transition. *Lithos* 19: 255-267.
- Moorbath, S. & Vokes, F.M.** 1963. Lead isotope abundance studies on galena occurrences in Norway. *NGT* 43:283-343.
- Moore, J.M. & Thompson, P.H.** 1980. The Flinton Group: a late Precambrian metasedimentary succession in the Grenville Province of eastern Ontario. *Can. J. Earth Sci.* 17:1685-1707.
- Morton, A.C. & Taylor, P.N.** 1991. Geochemical and isotopic constraints on the nature and age of basement rocks from Rockall Bank, NE Atlantic. *J. Geol. Soc. London* 148:630-634.
- Morton, R.D.** 1961. Synthetic chlorapatites and equilibria in the system calciumorthophosphate-calciumchloride. *NGT* 41:223-234.
- & **Catanzaro, E.J.** 1964. Stable chlorine isotope abundances in apatites from Ødegårdens Verk, Norway. *NGT*

- 44:307-313.
- Morvik, R.** 1987. Tektonometamorf historie for Modum og Kongsberg kompleksene belyst ved aldersbestemmelse og petrologi av Morud og Nakkerud gabbroene. Unpubl. Cand. Sci. thesis, Univ. of Oslo.
- Moxham, R.L.** 1965. Distribution of minor elements in coexisting hornblende and biotite. *Can. Min.* 8:204-235.
- Munoz, J.L.** 1984. F-OH and Cl-OH exchange in micas with application to hydrothermal deposits. In: Bailey, S.W., ed., *Micas. Rev. Min.* 13:469-544.
- 1990. F and Cl contents of hydrothermal biotites: Are-evaluation. *Geol. Soc. Am. Abstr. Progr.* 22:A135.
- & **Ludington, S.D.** 1974. Fluorine-hydroxyl exchange in biotite. *AJS* 274:396-413.
- & ——— 1978. Fluorine-hydroxyl exchange in synthetic muscovite and its application to muscovite-biotite assemblages. *AM* 62:304-308.
- Munz, I.A.** 1990. Whiteschists and orthoamphibole-cordierite rocks and the P-T-t path of the Modum Complex, South Norway. *Lithos* 24:181-200.
- & **Morvik, R.** 1991. Metagabbros in the Modum Complex, southern Norway: an important heat source for Sveconorwegian metamorphism. *PR* 52:97-113.
- Nabelek, C.R. & Lindsley, D.H.** 1985. Tetrahedral Al in amphibole: a potential thermometer for some mafic rocks. *Geol. Soc. Am. Abstr. Progr.* 17:673.
- Nash, W.P.** 1976. Fluorine, chlorine, and OH-bearing minerals in the Skaergaard intrusion. *AJS* 276:546-557.
- 1984. Phosphate minerals in terrestrial igneous and metamorphic rocks. In: Nriagu, J.O. & Moore, P.B., eds., *Phosphate minerals*. Springer, Berlin, 215-241.
- Neumann, H.** 1960. Apparent ages of Norwegian minerals and rocks. *NGT* 40:173-191.
- Neumann, E.R., Pallesen, S. & Andresen, P.** 1986. Mass estimates of cumulates and residues after anatexis in the Oslo Graben. *J. Geophys. Res.* 91:11629-11640.
- Newton, R.C.** 1990. The nature of the orthopyroxene isograd in Precambrian high-grade terrains. In: Naqvi, S.M., ed., *Precambrian continental crust and its economic resources*. Elsevier, Amsterdam, *Dev. Precam. Geol.* 8:13-45.
- & **Haselton, H.T.** 1981. Thermodynamics of the garnet-plagioclase-Al₂SiO₅-quartz geobarometer. In: Newton, R.C., Navrotsky, A. & Wood, B.J., eds., *Thermodynamics of minerals and melts*. Springer, New York, 129-145.
- & **Perkins, D.** 1982. Thermodynamic calibration of geobarometers based on the assemblages garnet-plagioclase-orthopyroxene (clinopyroxene)-quartz. *AM* 67:203-222.
- Nijland, T.G.** 1989. De geologie van het Nelaug gebied, Bamble sector, Zuid Noorwegen. Unpubl. MSc thesis, Utrecht Univ., 85 pp.
- , **Jansen, J.B.H. & Maijer, C.** 1992b. Lower crustal transitions: II. Halogen evolution of apatites and biotites in amphibolite to granulite facies transitional metabasites (Bamble, Norway). Vol. Abstr. 1st Neth. Earth Sci. Congr., Veldhoven, 140.
- , **Jansen, J.B.H. & Maijer, C.** 1993b. Halogen geochemistry of fluid during amphibolite-granulite metamorphism as indicated by apatite and hydrous silicates in basic rocks from the Bamble Sector, South Norway. *Lithos* in press.
- , **Liauw, F., Visser, D., Maijer, C. & Senior, A.** 1993a. Metamorphic petrology of the Froland corundum-bearing rocks: The cooling and uplift history of the Bamble Sector, South Norway. *NGU* in press.
- & **Maijer, C.** 1991. Primary sedimentary structures and infiltration metamorphism in the Håvatn-Bårlindåsen-Tellaugstjern area, Froland. *Exc. log 2nd SNF Workshop, Bamble*, 2-5.
- & ——— 1992. Lower crustal transitions: I. Changing mineral assemblages and thermobarometric estimates over a classic amphibolite to granulite facies transition zone, Bamble, Norway. Vol. Abstr. 1st Neth. Earth Sci. Congr., Veldhoven, 139.
- & ——— 1993. The regional amphibolite to granulite facies transition at Arendal, Norway: Evidence for a thermal dome. *NJM* in press.
- , ———, **Senior, A. & Verschure, R.H.** 1992a. Primary sedimentary structures and composition of the high-grade metamorphic Nidelva Quartzite Complex (Bamble, Norway) and origin of the nodular gneisses. *Proc. Kon. Ned. Ak. Wetensch.* 97, 16 pp.
- & **Senior, A.** 1991. Sveconorwegian granulite facies metamorphism of polyphase migmatites and basic dikes, South Norway. *JG* 99:515-525.
- , ——— & **Maijer, C.** 1991. High-grade Grenvillian metamorphism in

- the Bamble Sector, Norway: Field and petrographic evidence. *Terra Abstr.* 3:444.
- Nilssen, B. & Raade, G.** 1973. On chromian montmorillonite (Volkonskoite) in Norway. *NGT* 53:329-331.
- Noe-Nygaard, A.** 1963. The Precambrian of Denmark. In: Rankama, K., ed., *The Precambrian*. I. Interscience, New York, 1-25.
- O'Beirne-Ryan, A.M., Jamieson, R.A. & Gagnon, Y.D.** 1990. Petrology of garnet-clinopyroxene amphibolites from Mont Albert, Gaspé, Quebec. *Can. J. Earth Sci.* 27:72-86.
- Oberti, R., Smith, D.C., Rossi, G. & Caucia, F.** 1991. The crystal-chemistry of high-aluminium titanites. *Eur. J. Min.* 3:777-792.
- Oftedahl, C.** 1963. Red corundum of Froland at Arendal. *NGT* 43:431-443.
- Okrusch, M., Bunch, T.E. & Bank, H.** 1976. Paragenesis and petrogenesis of a corundum-bearing marble at Hunza (Kashmir). *Min. Dep.* 11:278-297.
- O'Nions, R.K. & Heier, K.S.** 1972. A reconnaissance Rb-Sr geochronological study of the Kongsberg area, South Norway. *NGT* 52:143-150.
- , **Morton, R.D. & Baadsgaard, H.** 1969a. Potassium-argon ages from the Bamble Sector of the Fennoscandian shield in South Norway. *NGT* 49:171-190.
- , **Smith, D.G.W., Baadsgaard, H. & Morton, R.D.** 1969b. Influence of chemical composition on argon retentivity in metamorphic calcic amphiboles from South Norway. *EPSL* 5:339-345.
- Otten, M.T.** 1984. The origin of brown hornblende in the Artfjallet gabbro and dolerites. *CMP* 86:189-199.
- Park, A.F.** 1983. Nature, affinities and significance of metavolcanic rocks in the Outokumpu assemblage, eastern Finland. *Bul. Geol. Soc. Finl.* 56:25-52.
- Park, R.G., Åhäll, K.I. & Boland, M.P.** 1991. The Sveconorwegian shear-zone network of SW Sweden in relation to mid-Proterozoic plate movements. *PR* 49:245-260.
- , **Crane, A. & Daly, J.S.** 1987. The structure and kinematic evolution of the Lysekil-Marstrand area, Ostfold-Marstrand belt, southwest Sweden. *Sver. Geol. Unders.* C816:1-42.
- Pasteels, P. & Michot, J.** 1975. Geochronologic investigations of the metamorphic terrain of southwestern Norway. *NGT* 55:111-134.
- Patchett, P.J.** 1978. Rb/Sr ages of Precambrian dolerites and syenites in southern and central Sweden. *Sver. Geol. Unders.* C747:1-63.
- Pedersen, S.** 1981. Rb/Sr age determinations on late Proterozoic granitoids from the Evje area, South Norway. *Bul. Geol. Soc. Denm.* 29:129-143.
- & **Maaloe, S.** 1990. The Iddefjord granite: geology and age. *NGU* 417:55-64.
- Pedersen, T., Larsson, F.R., Lie, J.E. & Husebye, E.S.** 1990. Deep and ultra-deep seismic studies in the Skagerrak (Scandinavia). In: Piner, B. & Bois, C., eds., *The potential of deep seismic profiling for hydrocarbon exploration*. Technip, Paris, 345-351.
- Perchuk, L.L.** 1981. Correction of the biotite-garnet thermometer for \rightarrow Mg + Fe isomorphism in garnet. *Dokl. Ak. Nauk SSSR* 256:72-73.
- Perkins, D., Westrum, E.F. & Essene, E.J.** 1980. The thermodynamic properties and phase relations of some minerals in the system $\text{CaO-Al}_2\text{O}_3\text{-SiO}_2\text{-H}_2\text{O}$. *Geochim. Cosmochim. Acta* 44:61-84.
- Persson, P.O., Wahlgren, C.H. & Hansen, B.T.** 1983. U-Pb ages of Proterozoic metaplutons in the gneiss complex of southern Värmland, south-western Sweden. *GFF* 105:1-8.
- Pesonen, L.J. & Torsvik, T.H.** 1990. The Fennoscandian palaeomagnetic database: compilation of palaeomagnetic directions and poles from the northern segment of the EGT. In: Freeman, R. & Mueller, S., eds., *Proceedings of the sixth workshop of the European Geotraverse (EGT) project: data compilations and synoptic interpretations*, 389-399.
- Petersen, E.U., Essene, E.J., Peacor, D.R. & Valley, J.W.** 1982. Fluorine end-member micas and amphiboles. *AM* 67:538-544.
- Peterson, D.E. & Valley, J.W.** (In prep.): Garnet-orthopyroxene-plagioclase-quartz geobarometry, Bamble Sector, Norway: The importance of orthopyroxene activity.
- Peterson, J.W., Chacko, T. & Kuehner, S.M.** 1991. The effects of fluorine on the vapor-absent melting of phlogopite + quartz: Implications for deep-crustal processes. *AM* 76:470-476.
- Pineau, F., Javoy, M., Behar, F. & Touret, J.** 1981. La géochimie isotopique du faciès granulite du Bamble (Norvège) et l'origine des fluides carbonés dans la croûte profonde. *Bul. Min.* 104:630-641.
- Piper, J.D.A.** 1982. The Precambrian palaeomagnetic record: the case for the Proterozoic supercontinent. *EPSL* 59:61-89.

- . 1992. The quasi-rigid premise in Precambrian tectonics. *EPSL* 107:559-569.
- Ploegsma, M.** 1991. A pilot Rb-Sr dating of the Suomusjärvi ultramylonite: evidence for major post-Svecofennian deformation in SW Finland. *Bul. Geol. Soc. Finl.* 63:1-13.
- Ploquin, A.** 1980. Etude géochimique et pétrographique du complexe de gneiss, migmatites et granites du Telemark-Aust Agder (Precambrien de Norvège du Sud). Sa place dans l'ensemble épizonal à catazonal profond du Haut Telemark au Bamble. *Sci. Terre Mémoire* 38:1-389.
- Poorter, R.P.E.** 1981. Precambrian paleomagnetism of Europe and the position of the Balto-Russian plate relative to Laurentia. In: Kröner, A., ed., *Precambrian plate tectonics*. Elsevier, Amsterdam, *Dev. Precam. Geol.* 4:599-622.
- Powell, R.** 1985. Regression diagnostics and robust regression in geothermometer/geobarometer calibration: the garnet-clinopyroxene geothermometer revisited. *JMG* 3:231-243.
- Prener, J.S.** 1971. Nonstoichiometry in calcium chlorapatite. *J. Solid State Chem.* 3:49-55.
- Priem, H.N.A., Verschure, R.H., Verdurmen, E.A.T., Hebeda, E.H. & Boelrijk, N.A.I.M.** 1970. Isotopic evidence on the age of the Trysil porphyries and granites in eastern Hedmark, Norway. *NGU* 266:263-276.
- , **Boelrijk, N.A.I.M., Hebeda, E.H., Verdurmen, E.A.T. & Verschure, R.H.** 1973. Rb-Sr investigations on Precambrian granites, granitic gneisses and acidic metavolcanics in central Telemark. *Metamorphic resetting of Rb-Sr whole-rock systems*. *NGU* 289:37-53.
- , ———, ———, ———, & ———. 1976. Isotope geochronology of the Eidfjord granite, Hardangervidda, West Norway. *NGU* 327:35-39.
- Raase, P.** 1974. Al and Ti contents of hornblende, indicators of pressure and temperature of regional metamorphism. *CMP* 45:231-236.
- Ramberg, I.B. & Barth, T.F.W.** 1966. Eocambrian volcanism in southern Norway. *NGT* 46:219-236.
- , **Gabrielsen, R.H., Larsen, B.T. & Solli, A.** 1977. Analysis of the fracture patterns in Southern Norway. *Geol. Mijnb.* 56:295-310.
- Reymer, A.P.S., Boelrijk, N.A.I.M., Hebeda, E.H., Priem, H.N.A., Verdurmen, E.A.T. & Verschure, R.H.** 1980. A note on Rb-Sr whole-rock ages in the Seve Nappe of the central Scandinavian Caledonides. *NGT* 60:139-147.
- Rickard, D.T.** 1978. The Svecofennian anomalous ore lead line. *GFF* 100:19-29.
- Rivers, T. & Nunn, G.A.G.** 1985. A reassessment of the Grenvillian orogeny in western Labrador. In: Tobi, A.C. & Touret, J.L.R., eds., *The deep Proterozoic crust in the North Atlantic provinces*. Reidel, Dordrecht, 163-174.
- Rietmeijer, F.J.M.** 1984. Pyroxene (re-) equilibration in the Precambrian terrain of SW Norway between 1030-990 Ma and reinterpretation of events during regional cooling (M3 stage). *NGT* 64:7-20.
- Roberts, D.G., Ardu, D.A. & Dearnley, R.** 1973. Precambrian rocks drilled on the Rockall Bank. *Nature Phys. Sci.* 244:21-23.
- Robinson, P., Spear, F.S., Schumacher, J.C., Laird, J., Klein, C., Evans, B.W. & Doolan, B.L.** 1981. Phase relations of metamorphic amphiboles: natural occurrence and theory. In: Veblen, D.R. & Ribbe, P.H., eds., *Amphiboles*. *Rev. Min.* 9B:1-228.
- Rosenberg, P.E. & Foit, F.F.** 1977. Fe²⁺-F avoidance in silicates. *Geochim. Cosmochim. Acta* 41:345-346.
- Rosing, M.T., Bird, D.K. & Dymek, R.F.** 1987. Hydration of corundum-bearing xenoliths in the Qôrqt Granite Complex, Godthåbsfjord, West Greenland. *AM* 72:29-38.
- Ruszala, F. & Kostiner, E.** 1975. Preparation and characterization of single crystals in the apatite system Ca₁₀(PO₄)₆(Cl,OH)₂. *J. Crystal Growth* 30:93-95.
- Rutter, M.J., Laan, S.R. van der & Wyllie, P.J.** 1989. Experimental data for a proposed empirical igneous geobarometer: Aluminum in hornblende at 10 kbar pressure. *Geol.* 17:987-900.
- Samson, S.D. & Patchett, P.J.** 1991. The Canadian Cordillera as a modern analogue of Proterozoic crustal growth. *Austr. J. Earth Sciences* 38:595-611.
- Sanders, I.S.** 1989. Phase relations and P-T conditions for eclogite-facies rocks at Glenelg, north-west Scotland. In: Daly, J.S., Cliff, R.A. & Yardley, B.W.D., eds., *Evolution of metamorphic belts*. *Geol. Soc. Spec. Publ.* 43:513-517.
- , **Calsteren, P.W.C. van & Hawkesworth, C.J.** 1984. A Grenville Sm-Nd age for the Glenelg eclogite in northwest Scotland. *Nature* 312:439-440.
- Sandiford, M.A.** 1985. The metamorphic evolution of granulites at Fyfe Hills: implications for Archaean crustal

- thickness in Enderby Land, Antarctica. *JMG* 3:155-178.
- & Powell, R. 1986. Deep crustal metamorphism during continental extension: modern and ancient examples. *EPSL* 79:151-158.
- Sauter, P.C.C., Hermans, G.A.E.M., Jansen, J.B.H., Maijer, C., Spits, P. & Wegelin, A. 1983. Polyphase Caledonian metamorphism in the Precambrian basement of Rogaland/Vest-Agder, Southwest Norway. *NGU* 380:7-22.
- Saxena, S.K. 1966. Distribution of elements between coexisting biotite and hornblende in metamorphic Caledonides, lying to the west and northwest Trondheim, Norway. *NJM*, Mh. 67-80.
- 1967. Intracrystalline chemical variations in certain calcic pyroxenes and biotites. *NJM*, Abh. 107:299-316.
- 1979. Garnet-clinopyroxene geothermometry. *CMP* 70:229-235.
- Scheerer, T. 1843. Geognostische-mineralogische Skizzen, gesammelt auf einer Reise an der Süd-Küste Norwegens. *NJM Geol. Geogn. Petrefakt.* 631-670.
- Schlegel, G.C.J. 1991. The metamorphic and structural evolution of the Kheis tectonic province. Univ. of Cape Town, Cham. of Mines Precam. Res. Unit Bul. 36:1-215.
- Schouenborg, B.E., Johansson, L. & Gorbatshev, R. 1991. U/Pb zircon ages of basement gneisses and discordant felsic dykes from Vestranden, westernmost Baltic Shield and central Norwegian Caledonides. *Geol. Rundsch.* 80:121-134.
- Schuiling, R.D. 1960. Le dôme gneissique de l'Agout (Tarn & Herault). *Mem. Soc. Geol. Fr.* 91, 59 pp.
- & Kreulen, R. 1979. Are thermal domes heated by CO₂-rich fluids from the mantle? *EPSL* 43:298-302.
- & Vink, B.W. 1967. Stability relations of some titanium-minerals (sphene, perovskite, rutile, anatase). *Geochim. Cosmochim. Acta* 31:2399-2411.
- Schumacher, J.C. 1991. Empirical ferric iron corrections: necessity, assumptions, and effects on selected geothermobarometers. *MM* 55:3-18.
- Serdyuchenko, D.P. 1968. Metamorphosed weathering crusts of the Precambrian, their metallogenic and petrographic features. *Proc. XXIII Int. Geol. Congr., Prague*, 4:37-42.
- Sharma, Y.P., Lal, N., Bal, K.D., Parshad, R. & Nagpaul, K.K. 1980. Closing temperatures of different fission track clocks. *CMP* 72:335-336.
- Shido, F. 1958. Plutonic and metamorphic rocks of the Nakoso and Iritono districts in the central Abukuma Plateau. *J. Tokyo Univ. Fac. Sci., Ser. II* 11:131-217.
- & Miyashiro, A. 1959. Hornblendes of basic metamorphic rocks. *J. Tokyo Univ. Fac. Sci., Ser. II*, 12:85-102.
- Sigmond, E.M.O. 1978. Beskrivelse till det berggrunnsgeologiske kartbladet Sauda 1:250,000. *NGU* 341:1-94.
- 1985. The Mandal-Ustaoset line, a newly discovered major fault zone in South Norway. In: Tobi, A.C. & Touret, J.L.R., eds., The deep Proterozoic crust in the North Atlantic provinces. Reidel, Dordrecht, 323-331.
- Sisson, V.B. 1987. Halogen chemistry as an indicator of metamorphic fluid interaction with the Ponder pluton, Coast Plutonic Complex, British Columbia, Canada. *CMP* 95:123-131.
- Sjögren, H. 1883. Om de norska apatitförekomsterna och om sannolikheten att anträffa apatit i Sverige. *GFF* 6:447-498.
- Skiöld, T. 1976. The interpretation of the Rb-Sr and K-Ar ages of late Precambrian rocks in south-western Sweden. *GFF* 98:3-29.
- Skjærnaa, L. & Pedersen, S. 1982. The effects of penetrative Sveconorwegian deformation on Rb-Sr isotope systems in the Rømskog-Aurskog-Höland area, SE Norway. *PR* 17:215-243.
- Smalley, P.C. & Field, D. 1985. Geochemical constraints on the evolution of the Proterozoic continental crust in southern Norway (Telemark Sector). In: Tobi, A.C. & Touret, J.L.R., eds., The deep Proterozoic crust in the North Atlantic provinces. Reidel, Dordrecht, 551-566.
- , Lamb, R.C. & Clough, P.W.L. 1983a. Rare-earth, Th, Hf, Ta and large-ion lithophile element variations in metabasites from the Proterozoic amphibolite-granulite transition zone at Arendal, South Norway. *EPSL* 63:446-458.
- & Råheim, A. 1983b. Resetting of Rb-Sr whole rock isochrons during Sveconorwegian low-grade events in the Gjerstad augen gneiss, Telemark, southern Norway. *Isot. Geosci.* 1:269-282.
- & ——— 1988. Rb-Sr systematics of a Gardar-age layered alkaline monzonite suite in Southern Norway. *JG* 96:17-29.
- Smithson, S.B. 1963. Granite studies: I. A gravity investigation of two Precambrian granites in S. Norway. *NGU* 214:53-140.
- Solås, E.M. 1990. Minner fra de gamle feldspatgruvene i Tvedestrand-

- området. In: *Sørlandets Geol. for.* 20 år, 52-56.
- Solly, R.H.** 1892. Minerals from the apatite-bearing veins at Naerestad near Risør on the SE coast of Norway. *MM* 10:1-7.
- Solyom, Z., Andréasson, P.G., Johansson, I. & Hedvall, R.** 1984. Petrochemistry of late Proterozoic rift volcanism in Scandinavia I: The Blekinge-Dalarna Dolerites (BDD)-volcanism in a failed arm of the Iapetus? *Lund Publ. Geol.* 23:1-56.
- , **Lindqvist, J.E. & Johansson, I.** 1992. The geochemistry, genesis, and geotectonic setting of Proterozoic mafic dyke swarms in southern and central Sweden. *GFF* 114:47-65.
- Spear, F.S.** 1980. NaSi-CaAl exchange equilibria between plagioclase and amphibole. *CMP* 72:71-74.
- Starmer, I.C.** 1969. Basic plutonic intrusions of the Risør-Söndeled area, South Norway: The original lithologies and their metamorphism. *NGT* 49:403-431.
- 1972. Polyphase metamorphism in the granulite facies terrain of the Risør area, South Norway. *NGT* 52:43-71.
- 1972. The Sveconorwegian regeneration and earlier orogenic events in the Bamble series, South Norway. *NGU* 277:37-52.
- 1976. The early major structure and petrology of rocks in the Bamble series Söndeled-Sandnesfjord, Aust-Agder. *NGU* 327:77-97.
- 1980. A Proterozoic mylonite zone in the Kongsberg Series, north of Hokksund, south central Norway. *NGT* 60:189-193.
- 1985a. The evolution of the South Norwegian Proterozoic as revealed by major and mega-tectonics of the Kongsberg and Bamble sectors. In: *Tobi, A.C. & Touret, J.L.R., eds., The Atlantic provinces.* Reidel, Dordrecht, 259-290.
- 1985b. Geological map of the Bamble Sector, South Norway (1:100,000). In: *Maijer, C. & Padget, P., eds., 1987. The geology of southernmost Norway.* *NGU Spec. Publ.* 1.
- 1990a. Mid-Proterozoic evolution of the Kongsberg-Bamble belt and adjacent areas, southern Norway. In: *Gower, C.F., Rivers, T. & Ryan, B., eds., Mid-Proterozoic Laurentia-Baltica.* *Geol. Ass. Can. Spec. Pap.* 38:279-305.
- 1990b. Rb-Sr systematics of a Gardar-age layered alkaline monzonite suite in southern Norway: A discussion. *JG* 98:119-123.
- 1991. The Proterozoic evolution of the Bamble Sector shear belt, southern Norway: correlations across southern Scandinavia and the Grenville controversy. *PR* 49:107-139.
- Stormer, J.C. & Carmichael, I.S.E.** 1971. Fluorine-hydroxyl exchange in apatite and biotite: A potential igneous geothermometer. *CMP* 31:121-131.
- Stout, J.H.** 1972. Phase petrology and mineral chemistry of coexisting amphiboles from Telemark, Norway. *J. Petr.* 13:99-145.
- Sturt, B.A., Pringle, J.R. & Ramsay, D.M.** 1978. The Finnmarkian phase of the Caledonian orogeny. *J. Geol. Soc. London* 135:597-610.
- Sundius, N.** 1945. The position of the richterite in the amphibole group. *GFF* 67:266.
- Sundvoll, B.** 1990. Geochronology and Sr- and Nd-isotopes in the Egersund and Hunnedalen dyke swarms, south-western Norway. In: *Dahlgren, S.H., ed., Nordic research projects on mafic dikes.* *Min.-Geol. Museum, Univ. of Oslo, Interne Skr.* 13:22.
- Suwa, K., Enami, M. and Horiuchi, T.** 1987. Chlorine-rich potassium hastingsite from West Ongul Island, Lutow-Holm Bay, East Antarctica. *MM* 51:709-714.
- Swainbank, I.** 1965. Zircon geochronology of the Norwegian basement. *Ann. Progr. Rep. 11, Contr. AT30-1-1669, Lamont Geological Observatory, App. C,* 22 pp.
- Swenson, E.** 1990. Cataclastic rocks along the Nesodden Fault, Oslo Region, Norway: a reactivated Precambrian Shear Zone. *Tectonoph.* 178:51-65.
- Swope, R.J., Smyth, J.R., Munoz, J.L. & Gundersen, L.C.S.** 1991. Crystal structure refinement of Cl-rich 1M biotite. *Geol. Soc. Am. Abstr. Progr.* 23.
- Taborszky, F.K.** 1972. Chemismus und Optik der Apatite. *NJM, Mh.* 79-91.
- Tacker, R.C. & Stormer, J.C.** 1989. A thermodynamic model for apatite solid solutions, applicable to high-temperature geologic problems. *AM* 74:877-888.
- Teale, G.S.** 1979. Margarite from the Olary Province of South Australia. *MM* 43:433-435.
- Thomas, A., Nunn, G.A.G. & Wardle, R.J.** 1985. A 1650 Ma orogenic belt within the Grenville Province of northeastern Canada. In: *Tobi, A.C. & Touret, J.L.R., eds., The deep Proterozoic crust in the North Atlantic provinces.* Reidel, Dordrecht, 151-161.
- Thompson, A.B.** 1976. Mineral reactions in pelitic rocks: II. Calculation of some P-T-X(Fe-Mg) phase relations. *AJS*

- 276:425-454.
- Tobi, A.C., Hermans, G.A.E.M., Maijer, C. & Jansen, J.B.H.** 1985. Metamorphic zoning in the high-grade Proterozoic of Rogaland-Vest Agder, SW Norway. In: Tobi, A.C. & Touret, J.L.R., eds., *The deep Proterozoic crust in the North Atlantic Provinces*. Reidel, Dordrecht, 477-497.
- Torske, T.** 1976. Metal provinces of a Cordilleran-type orogen in the Precambrian of South Norway. In: Strong, D.F., ed., *Metallogeny and plate tectonics*. Geol. Ass. Can. Spec. Paper 14:597-613.
- 1985. Terrane displacement and Sveconorwegian rotation if the Baltic Shield: a working hypothesis. In: Tobi, A.C. & Touret, J.L.R., eds., *The deep Proterozoic crust in the North Atlantic provinces*. Reidel, Dordrecht, 333-343.
- Touret, J.** 1962. Geological studies in the region of Vegårshei-Gjerstad. NGU 215:120-139.
- 1966. Sur l'origine supracrustale des gneiss rubanés de Selås (formation de Bamble, Norvège méridionale). *Comp. Rend. Ac. Sci. Paris* 262:9-12.
- 1967. Les gneiss oeilés de la région de Vegårshei-Gjerstad (Norvège méridionale). I. Etude pétrographique. NGT 47:131-148.
- 1968. The Precambrian metamorphic rocks around the Lake Vegår (Aust-Agder, southern Norway). NGU 257:1-45.
- 1969. Le socle Précambrien de la Norvège méridionale (Région de Vegårshei-Gjerstad). Unpubl. PhD thesis, Univ. of Nancy, CNRS no.AO 2902, 316 pp.
- 1971a. Le faciès granulite en Norvège méridionale. I Les associations minéralogiques. *Lithos* 4:239-249.
- 1971b. Le faciès granulite en Norvège méridionale. II Les inclusions fluides. *Lithos* 4:423-436.
- 1972. Les faciès granulite en Norvège méridionale et les inclusions fluides: paragneiss et quartzites. *Sci. Terre* 17:179-193.
- 1979. Les roches à tourmaline-cordiérite-disthène de Bjordammen (Norvège méridionale) sont-elles liées à d'anciennes évaporites ? *Sci. Terre* 23:95-97.
- 1985. Fluid regime in Southern Norway: the record of fluid inclusions. In: Tobi, A.C. & Touret, J.L.R., eds., *The deep Proterozoic crust in the North Atlantic provinces*. Reidel, Dordrecht, 517-549.
- & **Falkum, T.** 1987. The high-grade metamorphic Bamble Sector. In: Maijer, C. & Padget, P., eds., *The geology of southernmost Norway*. NGU Spec. Publ. 1:22-24.
- & **Olsen, S.N.** 1985. Fluid inclusions in migmatites. In: Ashworth, J.R., ed., *Migmatites*. Shiva, Glasgow, 265-288.
- & **Roche, H. de la** 1971. Saphirine à Snaresund, près de Tvedestrand (Norvège méridionale). NGT 51:169-175.
- Umhoefer, P.J.** 1987. Northward translation of 'Baja British Colombia' along the Late Cretaceous to Paleocene margin of western North America. *Tectonics* 6:377-394.
- Valley, J.W., Petersen, E.U., Essene, E.J. & Bowman, J.R.** 1982. Fluorophlogopite and fluortremolite in Adirondack marbles and calculated C-O-H-F fluid compositions. *AM* 67:545-557.
- Vernon, R.H.** 1987. Growth and concentration of fibrous sillimanite related to heterogeneous deformation in K-feldspar-sillimanite metapelites. *JMG* 5:51-68.
- , **Clarke, G.L. & Collins, W.J.** 1990. Local, mid-crustal granulite facies metamorphism and melting: an example in the Mount Stafford area, central Australia. In: Ashworth, J.R. & Brown, M., eds., *High temperature metamorphism and crustal anatexis*. Unwin-Hyman, New York, 272-319.
- Verschure, R.H.** 1982. The extent of Sveconorwegian and Caledonian metamorphic imprints in Norway and Sweden. *Terra Cogn.* 2:64-65.
- 1985. Geochronological framework for the late-Proterozoic evolution of the Baltic Shield in south Scandinavia. In: Tobi, A.C. & Touret, J.L.R., eds., *The deep Proterozoic crust in the North Atlantic provinces*. Reidel, Dordrecht, 381-410.
- , **Andriessen, P.A.M., Boelrijk, N.A.I.M., Hebeda, E.H., Maijer, C., Priem, H.N.A. & Verdurmen, E.A.T.** 1980. On the thermal stability of Rb-Sr and K-Ar systems: Evidence from coexisting Sveconorwegian (ca 870 Ma) and Caledonian (ca 400 Ma) biotites in SW Norway. *CMP* 74:245-252.
- , **Maijer, C., Andriessen, P.A.M., Boelrijk, N.A.I.M., Hebeda, E.H., Priem, H.N.A. & Verdurmen, E.A.T.** 1983. Dating explosive volcanism perforating the Precambrian basement in southern Norway. NGU 380:35-49.
- , ——— & ——— 1989. Isotopic age determinations in South Norway. I The Skår volcanic breccia, Greipstad, Vestagder. *Geol. Mijnb.* 68:253-256.
- Verstevee, A.** 1975. Isotope geochronology in the high-grade metamorphic Precambrian of southwestern Norway.

- NGU 318:1-50.
- Visser, D., Nijland, T.G. & Maijer, C.** 1991. Orthopyroxene-cordierite-garnet-kornerupine-albite-bearing metaevaporites intercalated with enderbitic gneisses at Faervik School, Tromøya. Exc. log 2nd SNF Workshop, Bamble, 60-64.
- & **Senior, A.** 1990. Aluminous reaction textures in orthoamphibole bearing rocks: the P-T path of the high grade Proterozoic of the Bamble Sector, South Norway. *JMG* 8:231-246.
- & ——— 1991. Mg-rich dumortierite in cordierite-orthoamphibole-bearing rocks from the high-grade Bamble Sector, south Norway. *MM* 55:563-577.
- Vogels, R.J.M.J. & Nijland, T.G.** 1991. Biotite breakdown to orthopyroxene, spinel-albite±corundum symplectite and sapphirine, Hauglandsvatnet, Norway. Exc. log 2nd SNF Workshop, Bamble, 28-30.
- Vogt, J.H.L.** 1908. De gamle norske jernverk. *NGU* 46:1-83.
- Vuollo, J. & Piirainen, T.** 1989. Mineralogical evidence for an ophiolite from the Outokumpu serpentinites in North Karelia, Finland. *Bul. Geol. Soc. Finl.* 61:95-112.
- Wahlgren, C.H.** 1981. The Stora Busjön conglomerate - an indication of granitoid basement in the gneiss complex of south-western Sweden. *Sver. Geol. Unders.* C781:31-37.
- Walters, L.J. & Luth, W.C.** 1969. Unit-cell dimensions, optical properties, halogen concentrations in several natural apatites. *AM* 54:156-162.
- Weiby, P.C.** 1847. Bemerkungen über die geognostischen Verhältnisse der Küste von Arendal bis Laurvig im südlichen Norwegen. *NJM Geol. Geogn.* Petrefakt. 697-709.
- 1849. Beiträge zur topographischen Mineralogie des Distrikts Brevig. *NJM Geol. Geogn.* Petrefakt. 467-470.
- Weis, D.** 1986. Genetic implications of Pb isotopic geochemistry in the Rogaland anorthositic complex (Southwest Norway). *Chem. Geol.* 57:181-189.
- & **Demaiffe, D.** 1983. Age relationships in the Proterozoic high-grade gneiss regions of Southern Norway: discussion and comment. *PR* 22:149-155.
- Welin, E. & Gorbatshev, R.** 1978. Rb-Sr isotopic relations of a tonalitic intrusion on Tjörn island, south-western Sweden. *GFF* 100:228-230.
- & **Kähr, A.M.** 1982. Zircon dating of polymetamorphic rocks in southern Sweden. *Sver. Geol. Unders.* C797:1-34.
- & **Kähr, A.M.** 1980. The Rb-Sr and U-Pb ages of Proterozoic gneissic granitoids in Central Varmland, western Sweden. *Sver. Geol. Unders.* C777:24-28.
- , **Lundegårdh, P.H. & Kähr, A.M.** 1980. The radiometric age of a Proterozoic hyperite diabase in Varmland, western Sweden. *GFF* 102:49-52.
- Wells, P.R.A.** 1977. Pyroxene thermometry in simple and complex systems. *CMP* 62:129-139.
- 1978. Chemical and thermal evolution of Archean sialic crust, southern West Greenland. *J. Petr.* 20:187-226.
- Wielens, J.B.W., Andriessen, P.A.M., Boelrijk, N.A.I.M., Hebeda, E.H., Verdurmen, E.A.T. & Verschure, R.H.** 1980. Isotope geochronology in the high-grade metamorphic Precambrian of south-western Norway: New data and reinterpretations. *NGU* 359:1-30.
- Wilkerson, A., Carlson, W.D. & Smith, D.** 1988. High-pressure metamorphism during Llano orogeny inferred from Proterozoic eclogite remnants. *Geol.* 16:391-394.
- Wood, B.J. & Banno, S.** 1973. Garnet-orthopyroxene and orthopyroxene-clinopyroxene relationships in simple and complex systems. *CMP* 42:109-124.
- Wynne-Edwards, H.R.** 1976. Proterozoic ensialic orogenies: the millipede model of ductile plate tectonics. *AJS* 276:927-953.
- Yardley, B.W.D.** 1978. Genesis of the Skagit gneiss migmatites, Washington, and the distinction between possible mechanisms of migmatization. *Bul. Geol. Soc. Am.* 89:941-951.
- 1985. Apatite composition and the fugacities of HF and HCl in metamorphic fluids. *MM* 49:77-79.
- & **Baltatzis, E.** 1985. Retrogression of staurolite schists and the sources of infiltration fluids during metamorphism. *CMP* 89:59-68.
- Young, R.A. & Mackie, P.E.** 1980. Crystallography of human tooth enamel: initial structure refinement. *Mat. Res. Bul.* 15:17-29.
- Zabavnikova, I.I.** 1957. Diadochic substitutions in sphene. *Geochem. Int.* 271-278.
- Zeck, H.P., Andriessen, P.A.M., Hansen, K., Jensen, P.K. & Rasmussen, B.L.** 1988. Paleozoic paleo-cover of the southern part of the Fennoscandian shield-fission track constraints. *Tectonoph.* 149:61-66.
- & **Hansen, B.T.** 1988. Rb-Sr mineral ages for the Grenvillian metamorphic development of spilites from the Dalsland Supracrustal Group, SW

- Sweden. Geol. Rundsch. 77:683-692.
- Zhu, C. & Sverjensky, D.A. 1991.
Partitioning of F-Cl-OH between
minerals and hydrothermal fluids.
Geochim. Cosmochim. Acta 55:1837-
1858.
- Zwart, H.J. & Dornsiepen, U.F. 1978. The
tectonic framework of Central and
Western Europe. Geol. Mijnb. 57:627-
654.

The following short abbreviations have been used:

AJS	American Journal of Science
AM	American Mineralogist
CMP	Contributions to Mineralogy and Petrology
EPSL	Earth and Planetary Science Letters
GFF	Geologiska Föreningens i Stockholm Förhandlingar
JG	Journal of Geology
JMG	Journal of Metamorphic Geology
MM	Mineralogical Magazine
NGT	Norsk Geologisk Tidsskrift
NGU	Norges geologiske undersøkelse
NJM	Neues Jahrbuch für Mineralogie
PR	Precambrian Research

APPENDIX

Concise sample description. Coordinates for the localities refer to the 1:50,000 topographic map sheets Nelaug, Mykland and Arendal of Norges Geografiske Oppmåling. Rocktypes refer to those used in chapter 4. Facies indicate the metamorphic grade of the sample area. Mineral abbreviations according to Kretz (1983), except FI: fluid inclusions, Opq: opaque minerals, Ser: sericite, SI: unidentified solid inclusions.

Amphibolites.

- AV76 **Locality:** 4796-64844 **Rocktype:** 1 **Facies:** Amphibolite
Occurrence: Concordant band in quartzites.
Major constituents: Pl (An50), Hbl, Grt, Bt.
Accessoria: Ap, Cum, Ilm, Mag, Qtz, Zrn.
Retrogradation: Minor Act, Chl, Prh, Ser.
Apatite: Rounded, contains FI and SI.
- BD14 **Locality:** 4715-64888 **Rocktype:** 2 **Facies:** Amphibolite
Occurrence: Small discordant body in quartzites.
Major constituents: Pl (An57), Hbl, Bt.
Accessoria: Ap, Cp, Cpx, Po, Ttn, Zrn.
Retrogradation: Minor Act, Chl, Ep, Ms, Ser.
Apatite: Euhedral, contains Hbl and Zrn; more in Hbl than in other minerals.
- BD39 **Locality:** 4691-64887 **Rocktype:** 3 **Facies:** Amphibolite
Occurrence: Amphibolitized margin of the Blengsvatn Gabbro.
Major constituents: Pl (An38), Hbl, Cpx.
Accessoria: Ap, Mag, Ttn, Zrn.
Retrogradation: Minor Chl, Ep, Ser.
Apatite: Subhedral, contains FI, Hbl, Opq, SI.
- GP71 **Locality:** 4759-64896 **Rocktype:** 1 **Facies:** Amphibolite
Occurrence: Lens in tonalitic gneisses.
Major constituents: Pl (An32), Hbl, Bt, Qtz, Ilm.
Accessoria: Aln, Ap, Ttn.
Retrogradation: Minor Act, Ep.
Apatite: Rounded, subhedral, contains Bt, Hbl, Opq, SI.
- SU30 **Locality:** 4790-64933 **Rocktype:** 1 **Facies:** Amphibolite
Occurrence: Alternating amphibolites and amphibole-bearing gneisses.
Major constituents: Pl (An32), Hbl, Bt, Qtz.
Accessoria: Ap, Ath, Opq, Zrn.
Retrogradation: Minor Ep, Ms.
Apatite: Rounded, contains FI, Hbl, SI.
- SU56 **Locality:** 4807-64922 **Rocktype:** 1 **Facies:** Amphibolite
Occurrence: Fine grained concordant amphibolite.
Major constituents: Pl (An31), Hbl, Grt, Bt, Qtz.
Accessoria: Ap, Opq, Zrn.
Retrogradation: None.
Apatite: Subhedral, contains FI and SI.
- TN7 **Locality:** 4801-65026 **Rocktype:** 2 **Facies:** Amphibolite
Occurrence: Discordant Vimme amphibolite (Nijland 1989).
Major constituents: Pl (An27), Hbl, Bt, Qtz, Kfs.
Accessoria: Aln, Ap, Rt, Trm, Ttn, Zrn.
Retrogradation: Minor Chl, Ep, Ser.
Apatite: Subhedral, contains SI.
- TN19 **Locality:** 4837-65023 **Rocktype:** 1 **Facies:** Amphibolite
Occurrence: Intercalated in Selås Banded Gneisses (Touret 1966).
Major constituents: Pl (An31), Hbl, Grt, Bt.
Accessoria: Ap, Cp, Ilm, Mag, Py, Qtz, Rt, Trm, Zrn.
Retrogradation: Minor Act, Cal, Chl, Ms, Prh, Ser.
Apatite: Subhedral, contains Hbl, SI, Zrn.
- TN142 **Locality:** 4793-64890 **Rocktype:** 1 **Facies:** Amphibolite
Occurrence: Garnet-amphibolite separated metagabbro by a c. 1 metre thick band of strongly sheared gneisses.
-

-
- Major constituents:** Pl, Hbl, Grt.
Accessoria: Act, Ap, Bt, Ms, Opq, Zrn.
- TN146 **Locality:** 4788-64946 **Rocktype:** 1 **Facies:** Amphibolite
Occurrence: Foliated amphibolite in sequence of different amphibolites and minor gneisses.
- Major constituents:** Pl (An39), Hbl, Bt, Grt.
Accessoria: Ap, Cp, Ilm, Qtz, Zrn.
Retrogradation: Minor Act, Chl, Kfs, Prh, Ser.
Apatite: Rounded-subhedral, contains FI and Zrn.
- TN201 **Locality:** 4741-64862 **Rocktype:** 1 **Facies:** Amphibolite
Occurrence: Isolated outcrop in gneisses.
- Major constituents:** Pl (An46), Hbl, Grt, Bt.
Accessoria: Ap, Hem, Ilm, Mag, Zrn.
Retrogradation: Minor Chl, Kfs, Prh.
Apatite: Anhedral.
- TN202 **Locality:** 4742-64860 **Rocktype:** 1 **Facies:** Amphibolite
Occurrence: Small concordant band bordered by pegmatite.
- Major constituents:** Pl (An34), Hbl, Grt, Bt.
Accessoria: Ap, Cum, Hem, Mag.
Retrogradation: Minor Act, Chl, Prh, Ser.
Apatite: Rounded, contains FI and Opq.
- TN204 **Locality:** 4799-64840 **Rocktype:** 1 **Facies:** Amphibolite
Occurrence: Isolated outcrop of homogeneous foliated amphibolite.
- Major constituents:** Pl, Hbl, Grt, Bt.
Accessoria: Ap, Chl, Cum, Ms, Opq.
- TN209 **Locality:** 4832-64965 **Rocktype:** 1 **Facies:** Amphibolite
Occurrence: Concordant layer in gneisses.
- Major constituents:** Pl (An34), Hbl, Grt, Bt, Qtz.
Accessoria: Ap, Ilm, Zrn.
Retrogradation: Minor Prh, Ser.
Apatite: Sub/euhedral, contains FI, Hbl, Sl.
- TN226 **Locality:** 4875-64865 **Rocktype:** 1 **Facies:** Granulite
Occurrence: Concordant garnet-amphibolite in charnockitic gneisses.
- Major constituents:** Pl, Hbl, Grt, Opx, Cpx, Bt.
Accessoria: Ap, Opq, Qtz.
- TN227 **Locality:** 4863-64835 **Rocktype:** 1 **Facies:** Granulite
Occurrence: Small amphibolite band in charnockitic gneisses.
- Major constituents:** Pl (An50), Hbl, Grt, Opx, Cpx, Qtz.
Accessoria: Ap, Ilm.
Retrogradation: Minor Cal, Chl.
Apatite: Rounded, contains FI.
- TN250 **Locality:** 4860-64973 **Rocktype:** 1 **Facies:** Amphibolite
Occurrence: Small lens in massive quartzites.
- Major constituents:** Pl (An40), Hbl, Grt.
Accessoria: Ap, Cp, Cum, Hem, Ilm, Py, Qtz, Zrn.
Retrogradation: Minor Act, Chl, Ser.
Apatite: Anhedral, contains FI and Sl.
- TN258 **Locality:** 4884-64796 **Rocktype:** 1 **Facies:** Granulite
Occurrence: Layer intercalated in enderbite gneisses (Visser et al. 1991).
- Major constituents:** Pl (An46), Hbl, Grt, Opx, Cpx.
Accessoria: Ap, Cp, Ilm, Py.
Retrogradation: Minor Chl, Ser.
Apatite: Rounded-subhedral, contains FI and Sl.
- TN291 **Locality:** 4850-64775 **Rocktype:** 1 **Facies:** Granulite
Occurrence: Garnet-amphibolite intercalated with enderbite gneisses.
- Major constituents:** Pl, Hbl, Grt.
Accessoria: Opq, Qtz.
- TN294 **Locality:** 4888-64813 **Rocktype:** 1 **Facies:** Granulite
Occurrence: Layer intercalated in enderbite gneisses.
- Major constituents:** Pl (An63), Hbl, Grt, Opx, Cpx, Bt.
Accessoria: Ap, Cp, Ilm, Py, Zrn.
Retrogradation: Minor Prh.
-

-
- TN309 **Apatite:** Anhedral, contains FI.
Locality: 4897-64806 **Rocktype:** 1 **Facies:** Granulite
Occurrence: Small band in enderbite gneisses.
Major constituents: Pl (An30), Hbl, Bt, Opx, Cpx.
Accessoria: Ap, Cp, Hem, Ilm, Po, Qtz, Zrn.
Retrogradation: Minor Cal, Chl.
- TN402 **Apatite:** Subhedral, contains FI and SI.
Locality: 4917-64852 **Rocktype:** 1 **Facies:** Granulite
Occurrence: One metre thick amphibolite intercalated with massive, quartz-rich charnockitic gneisses.
Major constituents: Pl, Hbl, Opx, Cpx.
Accessoria: Ap, Ilm, Opq.
- TN420 **Locality:** 4847-64773 **Rocktype:** 1 **Facies:** Granulite
Occurrence: Isolated outcrop of garnet-amphibolite.
Major constituents: Pl, Hbl, Grt, Qtz.
Accessoria: Act, Ap, Cal (late veinlet), Ms, Opq.
- TN430 **Locality:** 4888-64760 **Rocktype:** 1 **Facies:** Granulite
Occurrence: Amphibolite alternating with massive quartzites, hornblende gneisses and sillimanite-garnet-biotite gneisses.
Major constituents: Pl, Hbl, Opx, Cpx.
Accessoria: Opx, Zrn.
- TN431 **Locality:** 4881-64762 **Rocktype:** 1 **Facies:** Granulite
Occurrence: Garnet-amphibolite intercalated with garnet-plagioclase-bearing quartzites and charnockitic gneisses.
Major constituents: Pl, Hbl, Grt, Qtz.
Accessoria: Ap, Bt, Chl, Ms, Opq, Opx.
- WT23 **Locality:** 4849-64890 **Rocktype:** 3 **Facies:** Granulite
Occurrence: Amphibolitized margin of gabbro cutting across quartzites, granitic gneisses and biotite gneisses.
Major constituents: Pl (An10), Hbl, Bt, Qtz.
Accessoria: Ap, Cpx, Cum, Opq, Rt, Scp (Me02), Ttn, Zrn.
Retrogradation: Minor Chl, Ep, Kfs, Ser.
Apatite: Large, brownish margin, anhedral, contains FI, Hbl, Rt, SI, Zrn.
-

Amphibolites in contact aureole of the Ubergsmoen Augen Gneiss.

-
- AS2191 **Locality:** 4850-65024 **Rocktype:** 4 **Facies:** Granulite
Occurrence: Garnet-amphibolite dike cross-cutting F2 folds in surrounding migmatitic gneisses (Nijland and Senior 1991).
Major constituents: Cpx, Grt, Hbl, Pl (An49).
Accessoria: Ms, Opq, Qtz.
- TN16 **Locality:** 4850-65024 **Rocktype:** 4 **Facies:** Granulite
Occurrence: Garnet-amphibolite dike cross-cutting F2 folds in surrounding migmatitic gneisses (Nijland and Senior 1991).
Major constituents: Cpx, Hbl, Opx, Pl (An30).
Accessoria: Chl, Cum, Ilm, Mag, Mc, Py, Zrn.
- TN17 **Locality:** 4854-65030 **Rocktype:** 4 **Facies:** Granulite
Occurrence: Amphibolite dike cross-cutting D1/2 fabric in older amphibolite (Nijland and Senior 1991).
Major constituents: Cpx, Hbl, Opx, Pl (An47), Qtz.
Accessoria: Bt, Chl, Cum, Ilm.
-

Metapelites.

-
- AV44 **Locality:** 4859-64860 **Facies:** Amphibolite
Occurrence: Intercalated with biotite gneisses.
Major constituents: Bt, Grt, Mc, Pl, Qtz.
Accessoria: Chl, Ccp, Czo, Ilm, Mag, Ms, Py, Zrn.
- AV106 **Locality:** 4840-64843 **Facies:** Amphibolite
Occurrence: Intercalated with amphibolites.
Major constituents: Bt, Grt, Mc, Pl, Qtz.
Accessoria: Aln, Ap, Chl, Czo, Ms, Zrn.
-

-
- CM40 **Locality:** 4823-65022 **Facies:** Amphibolite
Occurrence: Intercalated with amphibolites, calcisilicate rocks, marbles and banded gneisses.
Major constituents: Bt, Grt, Mc, Pl, Qtz.
Accessoria: Ap, Gr, Opq, Zrn.
- CM407 **Locality:** 4863-64836 **Facies:** Granulite
Occurrence: Intercalated with amphibolites and charno-enderbitic gneisses.
Major constituents: Bt, Grt, Pl, Qtz, Sil.
Accessoria: Ccp, Ilm, Mag, Py, Zrn.
- CM454 **Locality:** 4888-64777 **Facies:** Granulite
Occurrence: Isolated outcrop.
Major constituents: Bt, Grt, Kfs, Pl, Qtz.
Accessoria: Ccp, Po, Rt, Sil.
- EJ10 **Locality:** 4897-64939 **Facies:** Amphibolite
Occurrence: Intercalated with biotite-rich gneisses and minor amphibolites.
Major constituents: Bt, Grt, Kfs, Pl, Qtz, Sil.
Accessoria: Ap, Cal, Ccp, Chl, Gr, Ms, Po, Py, Rt, Zrn.
- MR35 **Locality:** 4906-64988 **Facies:** Amphibolite
Occurrence: Intercalated in quartzites.
Major constituents: Bt, Grt, Kfs, Pl, Qtz, Sil.
Accessoria: Ilm, Ms, Py, Rt, Zrn.
- MR73 **Locality:** 4874-64990 **Facies:** Amphibolite
Occurrence: Intercalated in quartzites.
Major constituents: Bt, Grt, Pl, Qtz.
Accessoria: Cal, Ky, Ms, Zrn.
- NS10 **Locality:** 4918-64887 **Facies:** Granulite
Occurrence: Intercalated with intermediate and granitic gneisses.
Major constituents: Bt, Crd, Grt, Mc, Pl (An32), Qtz, Sil.
Accessoria: Ccp, Po, Py, Rt, Zrn.
- NS19 **Locality:** 4914-64880 **Facies:** Granulite
Occurrence: Intercalated with Hbl-gneisses and granitic gneisses. Bordered at one side by a shear zone.
Major constituents: Bt, Grt, Kfs, Pl, Sil.
Accessoria: Ap, Ilm, Qtz, Zrn.
- RV108 **Locality:** 4903-65066 **Facies:** Amphibolite
Occurrence: Intercalated with metasediments.
Major constituents: Bt, Kfs, Mp, Pl (An06-38), Qtz.
Accessoria: Ap, Crn, Ilm, Mag, Opq, Spl, Zrn.
- SU62 **Locality:** 4813-64912 **Facies:** Amphibolite
Occurrence: Intercalated with granitic gneisses.
Major constituents: Bt, Grt, Pl, Qtz.
Accessoria: Chl, Ep, Sil, Zrn.
- TN366 **Locality:** 4911-65081 **Facies:** Granulite
Occurrence: Concordant band of migmatitic metapelites (Vogels and Nijland 1991).
Major constituents: Bt, Kfs, Mp, Opx, Pl (An05-30), Qtz.
Accessoria: Adr, Ap, Chl, Crn, Ilm, Mag, Mnz, Sil, Spl, Spr, Zrn.
- WT66 **Locality:** 4857-64893 **Facies:** Amphibolite
Occurrence: Band in biotite-rich gneisses.
Major constituents: Bt, Grt, Pl, Qtz, Sil.
Accessoria: Ilm, Kfs, Zrn.
-

SUMMARY

Granulites are likely candidates to be major constituents of the middle to lower continental crust. Whereas we are unable to directly explore the lower levels of the current continents, the root zones of former orogens are exposed in many Precambrian (4.38–0.59 Ga) cratons, that still constitute large parts of the current continents. The present thesis deals with the transition from amphibolite to granulite facies rocks in one of these areas, the Mid-Proterozoic Bamble Sector in southern Norway.

In chapter 1, the reader is introduced to some general aspects of Precambrian geology and of the Fennoscandian (Baltic) Shield. A more detailed introduction is given to the geology, metamorphic petrology and geochemistry of the Bamble Sector, and a retrospective of earth scientific research in that area is provided.

The question whether the present day metamorphic features are the result of one or two high grade events is addressed in chapter 2, using combined structural and petrological criteria. It is shown that both the Gothian (1.75–1.5 Ga) and the Sveconorwegian (1.25–0.9 Ga) orogenies were of major importance in the evolution of the area, and involved amphibolite facies metamorphism, while the emplacement of the Ubergsmoen Augen Gneiss resulted in local granulite facies metamorphism, for which PT estimates are provided.

The classic regional amphibolite to granulite facies transition zone in the Nelaug-Arendal-Tromøy area is studied by the use of metamorphic index minerals and geothermobarometry in chapter 3. A new isograd sequence is established, involving the relocation of old, and the definition of new isograds, and a temperature gradient is shown. From combination of these data with structural criteria, it is tentatively suggested that granulite facies metamorphism was due to thermal doming.

As the transition from amphibolite to granulite facies is essentially a change from wet to dry rocks, the role of $P_{\text{H}_2\text{O}}$ is considered in chapter 4 by the study of Cl and F that substitute for OH in apatite and hydrous silicates. It is shown that aqueous fluids were locally controlled during metamorphism, at least in the amphibolites. No relationship between relative HF and HCl fugacities and metamorphic grade could be detected. In addition, the behaviour of halogens in apatite during metamorphism, which is still poorly understood, is addressed.

Which other crystal chemical changes do and do not occur in the hydrous silicates amphibole and biotite with the transition from amphibolite to granulite facies is investigated in chapter 5. The results support conclusions drawn in chapter 3.

These lower crustal rocks were finally transferred to the levels at which they are currently exposed. In chapter 6, this process of cooling and uplift is studied in the corundum-bearing rocks from Froland. The initially isobaric P–T path derived from their metamorphic petrology is combined with a T–t path constructed from published data.

In chapter 7, relationships between the Bamble Sector and other segments of the Southwest Scandinavian Domain are considered, and a model for the evolution of this part of the Fennoscandian Shield between 1.8 and 0.8 Ga is presented, involving subduction in the west of present day Norway during both the Gothian and Sveconorwegian orogenies.

SAMENVATTING

Het is aannemelijk dat granulieten het hoofdbestanddeel van de midden tot onder korst vormen. Terwijl het voor ons onmogelijk is om de diepere niveaus van de huidige continenten direct te onderzoeken, dagzomen de wortelzones van voormalige gebergten in vele Precambrische (4,38-0,59 miljard jaar) schilden, die nog immer grote delen van de huidige continenten uitmaken. In dit proefschrift wordt de overgang van amfiboliet naar granuliet facies gesteenten in een dergelijk gebied, de Midden Proterozoische Bamble Sector in zuidelijk Noorwegen, onderzocht.

In hoofdstuk 1 wordt de lezer geïntroduceerd in enige algemene aspecten van de geologie van het Precambrium en van het Fennoscandische (Baltische) Schild. Een meer gedetailleerde introductie wordt gegeven in de geologie, metamorfe petrologie en geochemie van de Bamble Sector, alsmede een terugblik betreffende het aardwetenschappelijk onderzoek in dit gebied.

Of de huidige metamorfe karakteristieken het resultaat zijn van één danwel twee hoog gradige gebeurtenissen is een vraag die in hoofdstuk 2 behandeld wordt aan de hand van gecombineerde structurele en petrologische criteria. Aangetoond wordt dat zowel de Gothische (1,75-1,5 miljard jaar) als de Sveconorwegische (1,25-0,9 miljard jaar) gebergtevormingen een belangrijke rol speelden in de ontwikkeling van het gebied en gepaard gingen met amfiboliet facies metamorfose, terwijl het indringen van de Ubergsmoen Ogengneis lokaal granuliet facies metamorfose tot gevolg had, waarvoor druk en temperatuur schattingen gegeven worden.

De klassieke, regionale amfiboliet naar granuliet facies overgang in het Nelaug - Arendal-Tromøy gebied wordt bestudeerd in hoofdstuk 3 m.b.v. metamorfe index mineralen en geothermobarometrie. Een nieuwe volgorde van isograden wordt vastgesteld, waarbij oude isograden verplaatst en nieuwe isograden gedefinieerd worden, en een temperatuursgradient wordt aangetoond. Combinatie van deze gegevens met structurele criteria duidt er op dat de granuliet facies metamorfose het gevolg was van thermische opwelling.

Aangezien de overgang van amfiboliet naar granuliet facies in essentie een verandering is van natte naar droge gesteenten, wordt in hoofdstuk 4 de rol van de waterdruk beschouwd aan de hand van Cl en F, die OH vervangen in apatiet en waterhoudende silicaten. Aangetoond wordt dat, in ieder geval in de amfibolieten, waterige oplossingen lokaal gecontroleerd werden gedurende de metamorfose. Tussen de relatieve fugaciteiten van HF en HCl en de graad van metamorfose is geen relatie aanwezig. Hiernaast wordt het gedrag van halogenen in apatiet, dat nog steeds niet goed begrepen wordt, gedurende metamorfose bestudeerd.

Welke andere kristalchemische veranderingen al dan niet plaatsvinden in de waterhoudende silicaten amfibool en biotiet met de overgang van amfiboliet naar granuliet facies wordt onderzocht in hoofdstuk 5. De resultaten ondersteunen de in hoofdstuk 3 getrokken conclusies.

De onderkorstgesteenten werden uiteindelijk naar het niveau gebracht waarop ze nu dagzomen. In hoofdstuk 6 wordt dit proces van afkoeling en opheffing bestudeerd in de korundhoudende gesteenten uit Froland. Het aanvankelijk isobare druk-temperatuur pad dat

afgeleid werd uit de metamorfe petrologie wordt aangevuld met een tijd-temperatuur pad dat is geconstrueerd m.b.v gepubliceerde gegevens.

In hoofdstuk 7 worden de relaties tussen de Bamble Sector en andere delen van het Zuidwest Scandinavische Domein beschouwd, en wordt een model voor de ontwikkeling van het Fennoscandische Schild tussen 1,8 en 0,8 miljard jaar gepresenteerd met onderschuiving ten westen van het huidige Noorwegen gedurende zowel de Gothische als de Sveconorwegische gebergtevorming.

ACKNOWLEDGEMENTS

Now this project has been finished, I would like to seize the opportunity to thank the many persons who assisted in some way or another:

T. Bouten, for assistance with microprobe analyses.

The *Bunæs Boys* (*A. Krijgsman*, *D.J. Liefstink*, and *R.J.M.J. Vogels*), and *M.A.T.M. Broekmans*, for their cooperation and other activities.

Dr. P. Candela, for reviewing chapter 4.

S. Dahlgren and *L. Kullerud*, for organizing the 1991 SNF Workshop in Bamble.

Drs. B.P. Dam, for discussions.

W.J.H. Eussen, for performing the XRF analyses.

Ing. H.M.V.C. Govers, for performing XRD analyses.

J.W. de Groot, *I. Nussgen*, *O.H. Stiekema* and *W.J. Wildenberg*, for producing all those thin sections.

Dr. G.J.L.M. de Haas, for a great field summer in 1989, many discussions, sharing unpublished data and critically reading several chapters.

Drs. J.L.M. van Haren, for company during the 1990 field summer and discussion.

Dr. J.B.H. Jansen, for co-initiating this study, cooperation in chapter 4, critically reading chapters 2, 3 and 6, and for the many long discussions about many more aspects of petrology and geochemistry than visible in this thesis, also following having been dumped during reorganization.

K.S.K. Kalt, for secretarial assistance.

The deceased *M.H. Maarschalkerweerd*, for his indispensable assistance in so many things.

Dr. C. Maijer, for initiating this study, for his enthusiastic support, for stimulating many other studies that have been or will be published separately, critically reading all manuscripts, and for the lots of time he spent supervising his study, also after 'voluntarily' leaving the institute, and much more.

Dr. I.A. Munz, for reviewing chapter 6.

Dr. P. Padget, for reading a manuscript that has been published separately, but was important in writing chapters 1 and 7.

Dr. P. Piccoli, for his kind discussion about fluorine-phosphorous interference.

Dr. R.P.E. Poorter for his assistance in microprobe work.

Drs. F.G. Postma, for many discussions.

Rektor K. Rausand and his people at Blakstad Yrkesskole for providing lodging during field work in all those years..

Drs. M. Röhrman, for company during the 1991 field summer, discussions and critically reading chapter 4.

Prof. dr. R.D. Schuiling, for being prepared to take care of this project as promotor.

Dr. *A. Senior*, for his aid with several chapters of this thesis, also following having been dumped during reorganization, but especially for one field day during the summer of 1988, without which chapter 2 would never have seen the daylight. All students participating in the *Bamble project*, whose detailed mapping provided the secure field base for this study that is too often disregarded in modern geological research.

Drs. *P.H.M. Thijssen*, for many discussions.

Thor, for keeping at distance during most of the field work.

Prof. dr. *J.L.R. Touret*, for time spent behind the microscope, discussions and reviewing chapters 3 and 4.

Several *U.R.O.'s* (Unidentified Reviewing Object), who reviewed chapters 2 and 6.

Drs. *R.H. Verschure*, for many discussions and critically reading chapter 7.

Drs. *D. Visser*, for many discussions, sharing unpublished data, cooperation, and critically reading chapters 4 and 5.

Dr. *C.F. Woensdregt*, for the use of his printing facilities.

The people of the *AV Dienst and library*, and all those who had to be named, but have not.

This study was financially supported by AWON (NWO 751.353.023). Travel grants were provided by NWO (SIR 14-90.90, SIR 14-288, SIR 14-431).

CURRICULUM VITAE

The author was born on January 11, 1967 in Zwolle, The Netherlands. From autumn 1979 until summer 1985, he was educated at the Praedinius Gymnasium in Groningen. Mid spring 1989, he cum laude finished his study geology at Utrecht University with principals petrology and geochemistry. From mid spring 1989 until now, he did his PhD study at Utrecht University, being employed by the Netherlands Organization for Scientific Research.